WATER AND NUTRIENT BUDGETS AT FIELD AND REGIONAL SCALE

Travel times of drainage water and nutrient loads to surface water

G.A.P.H. van den Eertwegh

WATER AND NUTRIENT BUDGETS AT FIELD AND REGIONAL SCALE

Travel times of drainage water and nutrient loads to surface water

Gerardus Anna Paulus Hendrina van den Eertwegh

PROEFSCHRIFT

ter verkrijging van de graad van doctor

op gezag van de rector magnificus

van Wageningen Universiteit

Prof. dr. ir. L. Speelman

in het openbaar te verdedigen

op woensdag 11 september 2002

des namiddags om 16.00 uur in de Aula

ABSTRACT

Eertwegh, G.A.P.H. van den, 2002: Water and nutrient budgets at field and regional scale: Travel times of drainage water and nutrient loads to surface water. Doctoral thesis, Wageningen University, the Netherlands.

Nitrogen and phosphorus loads to surface waters have caused eutrophication problems in the Netherlands. Linking agricultural nutrient budget surpluses to observed losses of nutrients to the surface water by drainage requires water and nutrient balances as well as a travel time distribution of drainage water. In this research *the travel time of drainage water was estimated by using steady-state flow analysis* as well as *transient modeling i.e., using a 2D dual-porosity water flow and solute transport code*. To analyze and estimate nutrient loads to the surface water, this research covered both *field-scale analyses* as well as *a regional-scale approach*.

At the *Flevoland field experimental site*, arable crops were grown on clay soil. The presence of a non-ripened clay layer in the soil profile appeared to be a key factor in the division of total drainage into tile drainage, drainage through a collecting and draining ditch, and drainage through the regional surface water. Tile drainage in the 1992-1994 period was between 50% and 85% of the total drainage. Nutrient losses by drainage were 55-86 kg ha^{-1} a^{-1} N and less than 0.5 kg ha^{-1} a^{-1} P. The analysis showed that 50-70% of the drainage water had a travel time of less than two years. Taking the travel time distribution into account, the observed N-loads of drainage water could be reasonably predicted. The P-surplus was almost fully adsorbed by the clay soil. The *Hupsel-Assink field experimental site* was located on grassland on a loamy sand. About 70% of total drainage was discharged by tile drains in the 1993-1994 period. N-losses by drainage were 165 kg ha^{-1} a^{-1} N and the calculated P-loads were unreliable. About 50-70% of the drainage water had a travel time of less than two years. Using the travel time distribution, the observed drainage N-loads could be reasonably predicted. The P-surplus was almost fully adsorbed by the loamy sand. The *regional-scale approach* estimated annual water flow and solute loads to the regional surface water. Annual water, salt, nitrogen, and phosphorus budgets were calculated for the *Hoge Afdeling region in the Flevopolder area* (1988-1999) and the *Hupsel brook basin* (1985-1994). A regional-scale travel time distribution of drainage water was estimated. Annual averages of nutrient loads to the regional surface water were well predicted. Nutrient losses by drainage from agricultural land and groundwater seepage were important sources in the Hoge Afdeling region, whereas in the Hupsel brook basin, nutrient losses by drainage from agricultural land were the main source.

Keywords: water and nutrient budget, travel time of drainage water, dual-porosity concept, agricultural nutrient losses, loads to surface water, field-scale experiments, regional-scale approach.

CONTENTS

VOORWOORD - PREFACE

In bepaalde kringen is de betekenis van de zinsnede 'goed werk heeft tijd nodig' niet positief bedoeld. Of het letterlijk in mijn geval waar is blijft de vraag, feit is dat er aan een periode van bruto 10,5 jaar werken aan een proefschrift een einde is gekomen.
Een spreuk op een muur in Haarlem die ik zag in maart 1999 inspireerde me om door te gaan en luidde: 'Beginnen kan ik, Volharden wil ik, Volbrengen zal ik'. Welnu, het kostte me enige tijd om de klus te klaren, maar hij is geklaard! Het ging niet vanzelf, kostte een boel energie en was niet gelukt zonder de mede- en samenwerking van vele (ex-)collega's.

In de periode 1992-1997 heb ik Kees Meinardi altijd en vrijwel dagelijks lastig mogen vallen met vragen, discussies of andere zaken over water, milieu en meststoffen, hydrologie en het Nederlandse landschap en haar ondergrond. Hij heeft me geïnspireerd om met een (geo)hydrologische blik door kleigronden, zandgronden en meer recent ook door veengronden heen te kijken om de oppervlakkige maar ook onderhuidse wegen van het water voor te kunnen stellen. Toerend door de Nederlandse kleigebieden wist hij veel en liefdevol te vertellen hoe dat land tot stand was gekomen en wat voor consequenties dat voor de hydrologie heeft gehad. Niet te beroerd om zelf de laarzen in de klei te zetten beleefden Kees en ik mooie tijden in wind, regen en sneeuw, van ochtend tot schemerduister. Hoewel ook stug en eigenwijs soms, maar altijd tijd en belangstelling om over het werk te praten en plannen te maken hoe problemen op te lossen, zo werkte en werkt dat met Kees uit Groningen. We werken nog steeds samen en ik vind het prima zo, dank je wel Kees.

Reinder Feddes is een gewaardeerde promotor. De manier waarop hij door concept-teksten heen is gegaan heeft mij verbaasd. Details en grote lijn, inhoud en stijl, alles kan hij tegelijkertijd over- en doorzien, daarbij de tekst voorziend van vele pennenstreken. Deze waren qua aantal soms enigszins ontmoedigend, maar nooit overbodig en meestal terecht. Dankbaar ben ik voor het vertrouwen dat hij in me bleef stellen, want het duurde en duurde maar voordat er weer eens een pak papier geschreven was. Iemand anders had het wellicht anders aangepakt, maar Reinder gaf me de ruimte en de tijd om vanuit mijn eigen situatie het proefschrift toch af te ronden. In oktober 1996 heeft hij me nog aanbevolen bij het hoogheemraadschap van Rijnland, met als toevoeging dat het proefschrift wel snel (. . .) af zou kunnen komen. In december 2001, ruim 5 jaar later, stuurde hij me een bericht met 'stug volhouden: alles sal reg kom'. Het is nu 'reg' gekomen, Reinder bedankt. Je inaugurele rede uit september 1990 was getiteld 'Waar blijft het water. . .'. Ik hoop met dit werk, waarbij 'het water' aangevuld is met opgeloste stoffen, een bijdrage geleverd te hebben aan het antwoord.

De Romeinen hadden een gezegde dat luidde 'in aqua scribere'. Hopelijk geldt dat niet voor dit proefschrift.

Gé van den Eertwegh

Leiden, zomer 2002.

De Zee

De zee heeft me verteld dat zij zo moe is
Zij zei dat zij er zeer beroerd aan toe is
Zij zei: wat is daar toch bij jullie allemaal aan de hand?
Wat doen jullie toch tegenwoordig allemaal op dat land?
Zij zei: er komen tegenwoordig steeds meer van die dagen
Dan kan ik alle vuile rotzooi haast niet meer verdragen
Dat zei de zee die me vertelde dat zij moe is
Die zei dat zij er zeer beroerd aan toe is
Zij zei: ik hoor dat er bij jullie af en toe wel een rapport verschijnt
Dat na de eerste onrust dan weer ergens in een la verdwijnt
Van de een of andere waardeloze functionaris
Die vanwege het toerisme niet wil weten dat het waar is
Dat het waar is dat ik er zeer beroerd aan toe ben
Dat het waar is als ik zeg dat ik zo moe ben
Vroeger vond ik het fijn wanneer het zomer was geworden
Met al die mensen en die kinderen, dat was gezellig hoor, maar nú?
Nu heb ik vaak de neiging om te roepen als ze komen:
Blijf maar liever weg, niet te dichtbij want dat is slecht voor me
Dat zei de zee die me vertelde dat zij moe is
Die zei dat zij er zeer beroerd aan toe is
Soms in november en december word ik nog wel es driftig
Maak ik me net als vroeger nog wel weer eens giftig
Dan ram ik op die degelijke nieuwe delta-dijken
En ik hoop dat ik iemand daarachter kan bereiken
Ik hoop dat er een paar mensen daar zullen zijn misschien
Die de reden van mijn radeloze woede willen zien
Maar dat houdt niet op, het gaat maar door, het komt erger telkens terug
En ik denk: dit heeft geen zin, en trek mij maar weer terug
Dat zei de zee die me vertelde dat zij moe is
Die zei dat zij er zeer beroerd aan toe is
Toen zweeg de zee en ik stond daar in de zomernacht
Ik zei: kan ik iets voor je doen misschien?
De zee heeft even nagedacht en toen zei zij
Zo overbodig als het was in vroeger dagen
Zo nodig is het nu om water naar de zee te dragen
Dat zei de zee die me vertelde dat zij moe is
Die zei dat zij er zeer beroerd aan toe is
Die zei dat zij er zeer beroerd aan toe is
Dat zei de zee die me vertelde dat zij moe is
En als de zee zegt dat zij moe is
Wil dat zeggen dat het land er zeer beroerd aan toe is

LIST OF MAIN SYMBOLS

Symbol	Quantity	Dimension
a	Characteristic half-distance between macropores	L
A	Area	L^2
b	Actual soil evaporation coefficient	$L\,T^{-1}$
c	Hydraulic resistance	T
C	Solute concentration	$M\,L^{-3}$
C_{drainage}	Solute concentration in drainage water	$M\,L^{-3}$
C_{meas}	Solute concentration measured	$M\,L^{-3}$
C_{seep}	Solute concentration in seepage water	$M\,L^{-3}$
C_a	Solute concentration adsorbed to soil	$M\,M^{-1}$
d	Depth of local-scale groundwater flow system	L
d_{root}	Depth of root zone	L
D_e	Effective diffusion-dispersion coefficient	$L^2\,T^{-1}$
D_0	Diffusion-dispersion coefficient of solute in bulk water	$L^2\,T^{-1}$
D_l^s	Diffusion-dispersion coefficient of solute in pore liquid	$L^2\,T^{-1}$
D_v^s	Diffusion-dispersion coefficient of water vapor in pore space	$L^2\,T^{-1}$
E_i	Interception evaporation rate	$L\,T^{-1}$
E_a	Actual evaporation rate	$L\,T^{-1}$
E_p	Potential evaporation rate	$L\,T^{-1}$
ET_r	Evapotranspiration rate of reference-crop	$L\,T^{-1}$
ET_p	Potential evapotranspiration rate	$L\,T^{-1}$
ET_a	Actual evapotranspiration rate	$L\,T^{-1}$
f_c	Crop factor	-
f_τ	Fraction of total travel time	-
$f(k_s)_{\text{interface}}$	Reduction factor for saturated hydraulic conductivity at matrix-macropore interface	-
h	Pressure head	L
H	Hydraulic head	L
i_{root}	Root length density	$L\,L^{-3}$
I	Infiltration rate	$L\,T^{-1}$
k	Hydraulic conductivity	$L\,T^{-1}$

Symbol	Quantity	Dimension
k_s	Saturated hydraulic conductivity	$L\,T^{-1}$
k_h	Horizontal hydraulic conductivity	$L\,T^{-1}$
k_v	Vertical hydraulic conductivity	$L\,T^{-1}$
K_d	Distribution coefficient	-
$\boldsymbol{K}\downarrow$	Daily average of global solar radiation flux density	$M\,T^{-3}$
L	Spacing (tile drain, ditch, channel)	L
LAI	Leaf Area Index	$L^2\,L^{-2}$
M	Mass	M
n_d	Decay factor for biological/chemical degradation	T^{-1}
P	Rainfall rate	$L\,T^{-1}$
$\boldsymbol{q}$	Darcy rate or specific discharge	$L\,T^{-1}$
$\boldsymbol{q}_x$	Darcy rate or specific discharge in x-direction	$L\,T^{-1}$
$\boldsymbol{q}_z$	Darcy rate or specific discharge in z-direction	$L\,T^{-1}$
q_m	Mass rate	$M\,L^{-2}\,T^{-1}$
Q_{drainage}	Drainage rate	$L\,T^{-1}$
Q_{meas}	Measured drainage rate	$L\,T^{-1}$
Q_{recharge}	Groundwater recharge rate	$L\,T^{-1}$
Q_{unmeas}	Unmeasured drainage rate	$L\,T^{-1}$
Q_{runoff}	Surface runoff rate	$L\,T^{-1}$
Q_{seep}	Seepage rate	$L\,T^{-1}$
R	Retardation factor	-
s_c	Soil cover	-
S	Degree of saturation	-
$\boldsymbol{S}_a$	Actual root water extraction rate	T^{-1}
$\boldsymbol{S}_p$	Potential root water extraction rate	T^{-1}
t	Time	T
t_r	Residence time in surface water	T
t_τ	Travel time of drainage water	T
T_a	Actual transpiration rate	$L\,T^{-1}$
T_p	Potential transpiration rate	$L\,T^{-1}$
$\boldsymbol{T}$	Temperature	Θ
$\boldsymbol{T}_{\text{air}}$	Air temperature	Θ
V_w	Amount of water stored in soil profile	L
w	Water level above reference level (stage)	L
z	Depth	L

Symbol	Quantity	Dimension
α	Shape parameter soil water retention function	L^{-1}
α_L	Longitudinal dispersivity	L
α_T	Transversal dispersivity	L
β	Soil aggregates geometry coefficient	-
Φ_m	Macropore porosity	-
Φ_μ	Matrix porosity	-
Φ_{tot}	Total porosity	-
Φ_{eff}	Effective porosity	-
γ_w	Scaling factor	-
Γ_W	Mass transfer of water	T^{-1}
κ_w	First-order mass transfer coefficient	$L^{-1} T^{-1}$
λ	Leakage factor	L
η_{rw}	Root water uptake reduction factor	-
ρ	Density	$M L^{-3}$
ρ_s	Density of solid phase	$M L^{-3}$
ρ_w	Density of liquid water at 4^oC	$M L^{-3}$
Υ_C	Mass transfer of solute	$M L^{-3} T^{-1}$
θ	Volumetric soil water content	-
χ	Flow direction coefficient of mass transfer from one flow domain to the other	-

I

INTRODUCTION

1   Nutrients in soil and surface-water systems

1.1   Agriculture and the fate of applied nutrients

Agriculture in the Netherlands is in trouble as far as management practices, public and political acceptance of animal health, and environmental aspects are concerned. There is a lot of pressure on farmers and farm systems from the Dutch public and national government as well as from the European Community (EC) to implement more animal-friendly farming systems and to reduce losses of chemicals to the environment. Since the end of the 1950s, agriculture has been undergoing a strong development, leading to scale enlargement and reconstruction. The distance has increased between the production systems and the natural resources the farmer has to work with. Based on governmental support and EC policy measures in the past, farming technology and high inputs of energy and nutrients have yielded not only an increase of the agricultural production rates, but also resulted in an absolute larger pressure on the environment, air, soil, and water. Presently, large quantities of nitrogen (N) and phosphorus (P) are still used by agriculture in the Netherlands, either as fertilizer or cattle fodder, which are partly imported from abroad. Intensive agricultural practices result in high crop yields, in high animal production rates, and consequently in high manure production.

The agricultural area in the Netherlands is 2.10^6 ha, about 60% of the nation's area. Roughly 40% of this area is covered by sandy soils, 35% by clay soils, and 20% by peat soils. In the southeast of the country, loess soils occur. From an environmental point of view, there is a negative effect of the imbalance in the nation's nutrient budget, leading to soils loaded with nutrients and losses to the aquatic environment (Table I.1.1). The average balance surplus or accumulation term in the national phosphorus balance for soil and groundwater compartments was 79 kg ha^{-1} a^{-1}. This surplus did not decrease between 1986 and 1994 (CBS, 1996). From an environmental point of view, it will take many decades before for example the high soil P levels have been reduced to acceptable values (Schoumans and Groenendijk, 2000). To illustrate the intensity of agricultural practices in the Netherlands, nutrient surplus numbers for Germany, as presented by Bach and Frede (1998), showed an N-surplus of about 110 kg ha^{-1} a^{-1} and a P-surplus of about 11 kg ha^{-1} a^{-1}. Nutrient use and nutrient surpluses in the

Netherlands were about twice as large compared to the next European country on the list of agricultural production states, the Federal Republic of Germany (FAO, 1999). The nutrient surplus is lost to the atmosphere, accumulates in the soil, and is potentially subject to leaching and transfer to groundwater and surface waters.

Table I.1.1
Average nutrient budgets of the Netherlands in 1985-1986.

Nutrient	In $[\text{kg ha}^{-1} \text{ a}^{-1}]$	Out $[\text{kg ha}^{-1} \text{ a}^{-1}]$	Surplus $[\text{kg ha}^{-1} \text{ a}^{-1}]$
Nitrogen (N)	575	145	430
Phosphorus (P)	107	28	79

Sources: Van der Meer (1991), CBS (1991).

To reduce nutrient losses to the environment, information is needed on nutrient application rates and timing, crop yields, and nutrient loss routes to air, soil, and water. Nijland and Schouls (1997) gave an overview on the theory of nutrient application and crop yield, combined with the extent of the agricultural area. Their conclusion is that the crop production model used and the decisive variable chosen, e.g., financial productivity or nutrient surplus per unit surface, determines the result on the most effective measure, either financially or environmentally.

Frouws (1993) reported primarily on political aspects of manure, produced by pig and dairy livestock, and the legislation procedures in the Netherlands. He stated that until the 1990s, the agricultural sector and industries had a lot of power. Until then, policy measures to protect the environment failed as the national agricultural interest prevailed and harsh measures were delayed or merely not implemented. The delay resulted from tactics pursued by the agricultural sector turned toward the same sector as a kind of boomerang back on itself in terms of negative public opinion. The public concern about the impact of agriculture and on the environment grew rapidly, and a discussion on the 'new', future role of agriculture began. The national policy changed as well from the middle of the 1980s onward, with more attention to nature and environmental quality, diminishing the power of the 'Green Front'. Meanwhile, EC policy also changed. For example, the ERC Nitrates Directive (European Community, 1991) was introduced in order to reduce nitrogen losses to the groundwater. Implementation of this directive

should result in compliance with drinking water standard of nitrate in groundwater of 50 mg l^{-1} (11.3 mg l^{-1} as N).

The agricultural sector in the Netherlands recently encountered the classical swine fever from February 1997 through March 1998, foot and mouth disease during the spring of 2001, and the cases of mad cow disease. Agriculture became more and more in trouble in terms of economics and its social and environmental impacts. The sector is now at a crossroads leading toward either more commercialization and scale enlargement, or to an integrated development program for rural areas (Van der Ploeg, 1999). The present agricultural expertise and knowledge system in the Netherlands lacks sufficient knowledge on the relation between low nutrient-input farming systems and environmental losses (Schröder and Corré, 2000). Both authors also remark that more emphasis should be put on the adoption and transfer of knowledge that is already available to practitioners for practical situations. Meanwhile, the soil and the aquatic environment suffer from high nutrient loads.

In his book *The Virtual Farmer*, Van der Ploeg (1999) stated that Dutch policy on agriculture, in its broadest sense, has been based on a virtual farmer, not on the real practicing farmer. As a consequence, the risk is present that policy measures do not relate (enough) to the real farmer's practice, diminishing their potential and actual success. To the farmers, complicated systems of administration and of legislation have been introduced to establish a reduction of nutrient losses to the environment. Many rules have been set, among these are rules to restrict the annual time period for manure application and the method of application. For example: it is forbidden to apply manure to grassland on peat soils from September 15 to February 1. As far as application techniques are concerned, farmers are obliged to either inject manure into the soil at a depth of 0.05-0.15 m or to plough the parcel to which manure is applied within 24 h after application. The expected result is that less nutrients will reach the surface water system by surficial transport routes (e.g., surface runoff), and that less ammonia is lost by volatilization to the atmosphere. A distinction has been made in legislation on the application of manure and soil type, where soil type is distinguished, and on land use, where crop type is distinguished.

The EC Nitrates Directive (European Community, 1991) was introduced to protect groundwater quality across Europe. Oenema et al. (1997) gave an overview of the nitrate (NO_3-N) problem in the Netherlands. N-losses from agriculture were in total 385 kg ha^{-1} a^{-1} in 1986, 322 kg ha^{-1} a^{-1} in 1990, and 317 kg ha^{-1} a^{-1} in 1996. These N-losses led to nitrate concentrations exceeding groundwater quality standards. To implement the EC Nitrates Directive, crop-dependent maximum application levels and a 'nutrient accounting system' called MINAS were introduced to livestock farming in the Netherlands in 1998 and to other farm types in 2000. MINAS-rules imply that

farmers register and report a farm-scale-based nutrient balance, also called 'farm gate' balance, with all incoming and outgoing annual nitrogen and phosphorus mass rates, including exported (from the farm) products like cattle, milk, or crops. Incoming 'farm gate' balance terms are animals, concentrates, fodder, fertilizer, by-products, and manure. Outgoing terms are milk, animals and eggs, fodder, arable products, manure, and NH_3-losses from stables. In MINAS, a certain maximum nutrient surplus is defined as the 'levy-free surplus,' which is lowered stepwise in time from 1998–99 to 2003. If the reported nutrient balances show a surplus larger than allowed, a levy (tax) is charged by the national government (Oenema et al., 1997). Table I.1.2 shows the annual levy-free surpluses per soil type and land use combination as prescribed in the MINAS system.

Table I.1.2
MINAS 'nutrient accounting system'. Annual levy-free N and P-surpluses for grassland and arable land for the time period 1998-2003 are shown.

Surplus applicable to	Soil type	Levy-free surplus [kg ha^{-1} a^{-1}], valid for year				
		1998–99	2000	2001	2002	2003
N, grassland	clay, peat	300	275	250	220	180
	other	300	275	250	220	180
	dry sands, loess	300	275	250	190	140
N, arable land	clay, peat	175	150	150	150	100
	other	175	150	125	110	100
	dry sands, loess	175	150	125	100	60
P, grassland	all	17.5	15	15	11	8.5
P, arable land	all	17.5	15	15	13	8.5

Source: DLV Adviesgroep Helpdesk, personal communication (2001).

The policy program is intended to lead to a 50% reduction in the 1986 level of farm scale nutrient surplus by the year 2003. This expected decrease should lead to a significant reduction of N-losses to the environment (Oenema et al., 1997). Whether the 2003 levy-free surplus level will be reached on Dutch farms on the national scale is still under discussion. In addition, from the soil and water point of view, unfortunately the 2003 levy-free surplus set in 2003 still does not meet environmental loss criteria

(e.g., Bos, 2002). Schröder and Corré (2000) conclude that surface water quality standards will not be met by the implementation of the N- and P-surplus levels for 2003. The EC directive 2000/60/EC (European Community, 2000) has provided the setup of a legal framework in the field of water policy to protect water quality across the EC. To meet present and future objectives to improve surface water quality, it is expected that much effort is still needed. Until then, the nutrient budget surplus of the Netherlands will continue to contribute to the degradation of the atmospheric, land, and aquatic environments.

1.2   Eutrophication of surface waters and its consequences

Eutrophication is defined as the response in surface waters to over-enrichment by nutrients, particularly nitrogen and phosphorus, having a strong impact on a-biotic and biotic factors in aquatic ecosystems. Eutrophication can either be natural or man-made, and human presence and activities like agriculture and wastewater production accelerate the process (Klapwijk, 1988). Excessive nutrient loads to aquatic ecosystems lead to increased biomass production, especially algae growth, and reduced nature conservation quality due to a decrease in the number of plant and animal species (Boers et al., 1995). The negative environmental effects of eutrophication on surface-water systems are potentially visible on every spatial scale in the Netherlands, from ditch and rivulet to lakes, rivers, and the North Sea. As far as aquatic ecosystems in the Netherlands are concerned, nitrogen and phosphorus are growth-limiting factors for algae. In freshwater ecosystems, the growth-limiting factor in the present situation is phosphorus; whereas in marine ecosystems it is likely to be nitrogen.

The problem of eutrophication of surface waters originates from the different sources of nutrients. Examples of point sources are wastewater treatment plants, domestic sewage from isolated houses and farms in sparsely populated regions, fertilizer factories, and the detergent industry. The main diffusive sources are atmospheric deposition and agriculture. Kolenbrander (1971) stated that eutrophication problems in the Netherlands during the 1960s, as far as phosphorus is concerned, were caused by point sources due to the large population increase, the use of polyphosphates in detergents, and by diffuse sources, mainly due to agricultural practices. The large increase in livestock volume and manure production since the 1960s increased the role of agricultural losses of nutrients in eutrophication. Klapwijk (1988) described and analyzed eutrophication problems in lakes and channel systems in the lowland areas in the western part of the Netherlands. He showed that in the basin area of the Rijnland Water Board, extensive phosphate removal from the effluent of wastewater treatment plants during 1979-1982 did not lead to a substantial decrease in algae growth in the lakes. Loads from other point and diffuse P-sources still exceeded the 'reception' capacity of the lakes.

Quality standards for N and P concentrations in groundwater and surface water are given by Willems and Fraters (1995). These objectives originate from water quality standards or aquatic ecosystems, as well as from the functional use of these ecosystems, and they presently focus on stagnant surface-water systems that are sensitive to eutrophication. According to the Dutch 'MILBOWA'-system, two different nutrient concentration levels are under consideration as reference: higher 'allowed values' and lower 'desired values.' For freshwater ecosystems, the reference levels for surface waters are defined in terms of allowed values. The reference levels for fresh surface water are relative to the average summer concentration i.e., average values for the period of April through September. No reference levels are available for salt or brackish-water ecosystems, mainly due to the lack of a clear relationship between nutrient concentration levels and eutrophication parameters. For fresh surface water, solute concentrations are allowed to exceed the total-P reference level as far as 'natural' or background-concentration levels are concerned.

Table I.2.1
Groundwater and surface water composition. General reference levels.

Reference level applicable to	Soil type	Reference level for concentration [mg l^{-1}]			
		Ammonia-N	Nitrate-N	Total-N	Total-P
Groundwater	sand	2.0	11.3	-	0.4
	clay, peat	10	11.3	-	3.0
Fresh surface water, average summer situation	-	-	-	2.2	0.15

Source: Willems and Fraters (1995).

In 1985, policy-makers in the countries within the catchments of the Rhine and Meuse rivers stated that a 50% reduction of nutrient emissions to the North Sea should be achieved in 1995. Between 1985 and 1993, the reduction in nitrogen emission to surface waters in the Netherlands however was only 8% (RIVM, 1995). More recent figures confirmed the insufficiently decreased N-loads (RIVM, 2001). Nitrogen emissions from agriculture due to surface runoff and leaching decreased by 10% during this period. Nitrogen loads of rivers have not changed, and reduction goals have not been met. As far

as phosphorus loads are concerned, a different and more promising trend has been observed with regard to river Rhine: the phosphorus load of the river Rhine decreased 60% between 1985 and 1993, while the loads for the river Meuse only decreased by about 10%.

The phosphorus loads to *surface waters* in the Netherlands decreased by almost 50% due to reduced point-source emissions between 1970 and 1995. Overall reduction goals of the national government have been met, but the reference level for total-P concentrations in surface waters is often still exceeded, both in space and time.
The relative share of diffuse sources of phosphorus in the total load to the surface-water system has increased due to an increased emission of phosphorus from agricultural activities and a decrease in point sources. Wunderink (1996) stated that between 1985 and 1995 a reduction of 60–75% for phosphorus from *point sources* was achieved, while for nitrogen the reduction was 55–75%. However, reductions of emissions from *diffuse sources* of nutrients in surface water systems lagged behind. Oenema and Roest (1997) reported that compared to reductions in agricultural balance surpluses, the reduction in diffuse losses to surface waters was far less and took much more time to become effective and visible. The long-term storage of nutrients in the soil-water system (e.g., in soil organic matter) as well as *travel time of the drainage water* cause a *delay in response* up to decades. In the 1995-1997 period, the nation-wide relative contribution of agricultural nutrient losses to the total loads to surface water systems amounted to 52-56% for nitrogen, and 26-30% for phosphorus (Schröder and Corré, 2000).

To analyze policy measures with respect to their effect on the nutrient losses to groundwater and surface water systems, a modeling approach has been developed by Dutch research institutes since the mid 1990s. This approach is operated on the national scale and is called STONE (in Dutch: Samen Te Ontwikkelen Nutriënten Emissie-model). The approach and the software used is a joint product of several Dutch research institutes (Boers et al., 1996), and it is used for nationwide policy analyses regarding the nutrient and water management practices. The STONE model originates partly from a combination of field-scale models using the SWAP (Kroes et al., 1999) and ANIMO (Groenendijk et al., 1997) approaches. These models are soil-physical and chemical process-oriented and need input parameters on various processes.
The STONE-concept subdivides the country as a whole into unique hydrological units, which are modeled using one-dimensional soil columns. These columns get their bottom boundary information from a regional-scale groundwater model and groundwater composition data. Recently, Kroon et al. (2001) revised the schematization of the Netherlands.

The governmental research institutes initiating STONE have committed themselves to consider the technical approach and the modeling concepts chosen as a common

instrument to support policy measures on fertilizer and manure use in agriculture. The idea behind this so-called 'consensus-modeling' originated mainly from policy and financial considerations, not from a technical or conceptual point of view. Research institute leaders, and later policy makers, apparently disliked the variability in modeling results and advice given in the past, which limited their possibilities to define appropriate policy measures. The financial situation at several research groups implied that is was more efficient to bring forces and sources together. The result is that, at present, the national government is provided with the result of one modeling instrument mainly made to develop and evaluate policy measures on nutrient loads to both groundwater and surface water. However, alternative modeling approaches lack any further support because of this development, thus limiting overall technical developments and scientific discussions. This is not a balanced situation, given the goal to reconcile agricultural practices and the quality of the aquatic environment.

2 Soil regions and hydrological situations in the Netherlands

Nutrient loads to surface water systems cannot be determined without knowing the transport routes of the precipitation excess and the presence of seepage from deep groundwater entering the surface-water system, including the solute concentrations in all contributing sources of water. The driving force behind the nutrient loads is the transport of water, which carries dissolved nutrients along with it. Given the same nutrient budget for an agricultural soil, differences in hydrological situations lead to differences in nutrient loads to surface waters.

The Netherlands is a delta area that lies in a still subsiding basin, dipping from southeast to northwest. Important sedimentation periods were present in the Pleistocene and Holocene Ages. The land-surface elevation ranges from about +320 m to -6 m to MSL. The main drainage system consists of the river Rhine branches Waal, Nederrijn, Lek, and IJssel, and of the river Meuse, as well as of artificial, man-made channels.
The groundwater system consists of sandy aquifers being subdivided by clay and loam layers. Groundwater depths are usually shallow, making for a strong relationship between landscape, surface elevation level, and groundwater system (Meinardi, 1985). The long-term average rainfall is about 800 mm a^{-1}, the potential evapotranspiration about 525 mm a^{-1}. Due to spatial variation of rainfall and evapotranspiration, the annual, average of excess rainfall varies spatially across the country from less than 200 mm a^{-1} in parts of the Friesland province to over 350 mm a^{-1} in the Veluwe area (Dufour, 1998; NHV, 1998). Groundwater recharge basically takes place in the southern, central, eastern, and northeastern sandy areas of the country and in coastal

dunes. Long-term average recharge in these areas varies spatially from 150 to 300 mm a^{-1} (Meinardi et al., 1998a).

The different hydrological situations can be described by dividing the country according to De Bakker (1979) into distinguished districts, based on geohydrological properties and soil parent materials: marine soils, fluviatile soils, drained lakes and peat uplands, cut-over raised bog, anthropogenic soils, Pleistocene sands, and loess soils. Due to the choice of the field experiment locations and hydrological regions under attention in this thesis, marine soils, drained lakes, and Pleistocene sands are of interest and also illustrated here.

The *marine soils* district roughly covers 25% of the total area of the Netherlands, consisting of the coastal polders, the northern and southwestern coastal areas, and the Zuyder Zee polders. The aquifer systems of Pleistocene sand layers are confined by marine deposits. The parent material of the soils, consisting of peat and clay, originates from the Holocene Age. The Zuyder Zee polders, or at present IJsselmeer polders, are the most recent examples of artificial man-made land. Van Duin and De Kaste (1989) give a full overview of man-made polders as a part of the Zuyder Zee project, starting with the Zuyder Zee Act in 1918. Other information can be found in e.g., Schultz (1992) and Van de Ven (1993). They were reclaimed between 1935 and 1968 (Van Duin and De Kaste, 1989). The main polder areas are the Wieringermeer (20 000 ha; 1930), the Noordoostpolder (48 000 ha; 1942), and the Flevoland polder area (97 000 ha), as shown in Fig. I.2.1.

The Flevoland polder area was reclaimed in two stages, eastern (54 000 ha, 1957) and southern Flevoland (43 000 ha, 1968), with the dike called 'Knardijk' separating the two. The boundary of Flevoland differs from the older polder areas. To reduce seepage from the 'old' land, in between the 'old' and 'new' land, boundary lakes were created (Van Duin and De Kaste, 1989; Van de Ven, 1993). A ring dike was built (1950 to 1956) in lake IJssel (IJsselmeer), formerly Zuyder Zee, marking the area of the future polder. Since 1950, construction pits were built for the pumping-stations. In 1956 the ring dike was closed, and about one year and 1600 million m^3 of water later, the eastern Flevoland area ran dry. During the process of pumping out the lake water, the main channels were dredged under water. Good drainage is essential to convert reclaimed land into agricultural land. Soil ripening occurs by removal of water by drainage, evapotranspiration, and soil-chemical and soil-biological processes.

The first step of soil ripening was to grow reed on the reclaimed land. Reed was sown by aircraft to enhance evapotranspiration and drying that introduced physical ripening of the new polder soils. Within the reed land, furrows or trenches were dug at varying distances ranging from 4 m to 48 m, depending on the soil texture; thus physical and

Fig. I.2.1
The Netherlands, central part. Overview of man-made polders as a part of the Zuyder Zee project, showing the Wieringermeer, Noordoostpolder, and Flevoland polder area (by Van Duin and De Kaste, 1989).

chemical ripening of the soils began. The reed was burnt, part-by-part (3000 to 4000 ha) throughout the polder area, and it was replaced by rape seed. After rape seed, cereals were sown. As the soil ripening processes progressed, trenches were refilled and replaced by subsurface tile drains and collection ditches, usually at greater distances. After full implementation of the drainage system, the land was handed over to farmers. This process is still underway in the present situation.

The Flevoland soils are mainly of Holocene parent materials deposited in lakes. These lakes were surrounded by bog peat, and wave erosion of this peat caused high organic matter contents in the clay sediments. After the main part of the bog peat was eroded, mineral material was mainly deposited on top. The sedimentation took place under fresh conditions, and afterwards under increasing brackish conditions. Reworked deposits were again laid down (Groen, 1997). Depending on the clay content, clay type, and drainage situation, both permanent (illite and kaolinite clay) and non-permanent ripening cracks (montmorillonite) may be present in the soil, largely increasing its permeability. The region is extensively drained and well-suitable for agriculture. Soil moisture deficits in the loam and clay soils are almost absent, which is a good starting point for agricultural production. The position of the Flevopolder area within the marine clay areas in the Netherlands is situated so that both the high organic matter content, as well as the pronounced, mostly permanent ripening cracks in the subsoil, are not often found. Therefore, this area's soils are an exception to most other marine soils in the Netherlands.

The *Pleistocene sands* district covers about 40% of the Netherlands. It consists mainly of fine and coarse sand, but sometimes loamy materials are also found. The so-called plaggen and inland-dunes soil pattern is mainly controlled by soil-surface relief. Groundwater levels are sloping less than land surface; therefore, a transition from dry sandy soils to wet peaty soils can be distinguished. The regional heathlands were used as rough grazing grounds and also provided heather sods, which were used as bedding material in stables. The dung-impregnated bedding was used for manure in arable land near the farmyard. The drier parts of the district were susceptible to severe wind erosion, which could cause transformation of agricultural land into active dunes. The groundwater level under the deep sandy soils in the district slopes gradually and about parallel to the soil surface and is between 1 m and over 2 m below soil surface. Its fluctuation is 1 m in summer and less than 1 m in winter. Most of the area is drained by natural brooks, which run in shallow valleys. Ditches are present in depressions and are connected to the brooks. Aquifers in this district can be separated by finer materials, hampering the recharge of the underlying aquifers. In the central part of the Netherlands, ice-pushed ridges with an elevation up to maximum 100 m are important recharge areas, generally without a surficial drainage system. If shallow boulder-clay

deposits are present, perched water tables and surface runoff or shallow lateral drainage may occur.

3   Locations of experimental fields and modeled regions

To provide insight in the field hydrological situations and losses of nutrients by drainage, field experiments were set up Using hydrological measurements and sampling of drainage water as the basic elements of these experiments. The field experiments were carried out on drained agricultural land. Two experimental sites have been set up to study the drainage and nutrient leaching process and to provide data and experimental knowledge for this thesis. The *Flevoland* experimental site was located in eastern Flevoland, the *Hupsel-Assink* experimental site in the eastern Pleistocene sands district. Fig. I.3.1 shows both locations of the experimental sites.
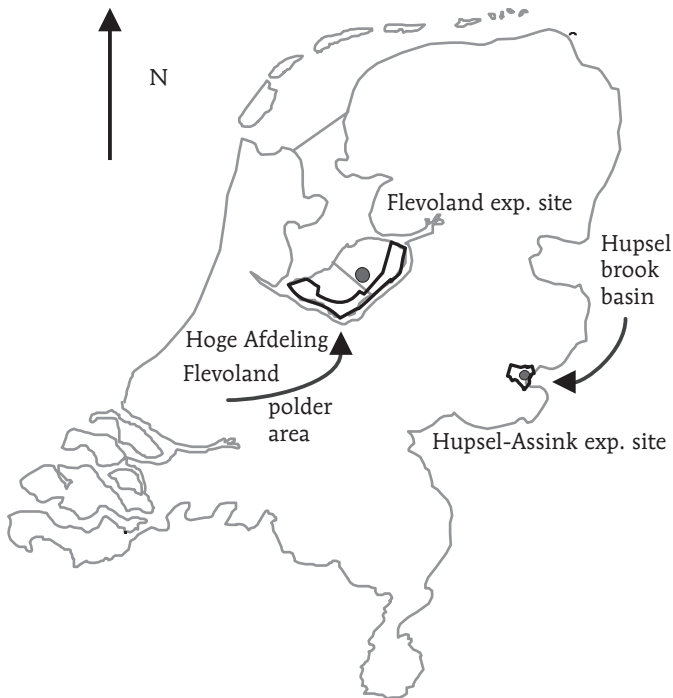
Fig. I.3.1
The Netherlands. Experimental field sites and regions considered. Flevoland polder area with Hoge Afdeling (HA region) and experimental site location (●). Hupsel-Assink experimental site (●)is located within Hupsel brook basin (HB region).

The field experiments were performed at scales ranging from 1 to 30 ha. Both sites were different in soil type, land use, and drainage situation. Table I.3.1 briefly summarizes the experimental sites that were used to determine the temporal variations in hydrology and nutrient leaching.

Given the locations of the experimental sites, regional-scale modeling has been carried out for two regions. The first region is the *Hoge Afdeling* of the Flevoland polder area with an area of about 40 000 ha. In this area, no special measurement program at the polder scale was set up, but data collected by the Zuiderzeeland Water Board were used. The second region is the 650 ha *Hupsel brook basin*, located near the eastern border of the Netherlands (Fig. I.3.1). The soils and land use in this catchment are representative for the eastern Gelderland region. At the basin area, a shallow sandy aquifer overlies an impermeable clay layer of Tertiary, Miocene origin. A measurement program, set up by the Ministry of Transport, Public Works, and Water Management, Rijn & IJssel Water Board, and Wageningen University, generated hydrological data and nutrient concentrations of the local surface water, which were used for this thesis.

Other experimental sites in the Netherlands - Some field experiments were performed to study the hydrology and leaching characteristics of agricultural soils. Van Ommen (1988) analyzed travel times of tile drainage of grassland on a shallow, sandy soil by bromide tracer transport. Bronswijk et al. (1995) conducted field experiments with a bromide tracer on grassland on a heavy, cracked clay river soil. Groen (1997) analyzed breakthrough curves for the Flevoland experimental site within one year after application of a bromide tracer. All these experiments led to the conclusion that 30-40% of the drained precipitation excess had a travel time of drainage of less than one year. In terms of fractions f_τ of the travel time distribution, f_1 was in these cases equal to 0.30 to 0.40. The value of this fraction can be explained by preferential flow processes in the unsaturated zone, induced by unstable wetting fronts and due to the presence of macropores. For situations with drained shallow aquifers, often the case in the Netherlands, the first, second, and maybe third year preceding tile drainage field observations, are likely to play a major role in the interpretation of the solute concentrations measured.

Table I.3.1
Field experimental sites. Overview of continuously monitored experimental sites.

| Experimental site | Soil type | Land use | Tile drains | | Ditch | Monitoring period |
			Distance [m]	Catchment [ha]	Catchment [ha]	
Hupsel-Assink	loamy sand	permanent grassland	14	0.25	no data	Nov 92 - May 94
Flevoland	heavy clay	arable crops	48	2.16	30	Apr 92 - Jun 94

4   Research objectives and thesis structure

The objectives of this study are as follows:

1. To distinguish and to quantify different discharge components of the precipitation excess, drained by *local-scale* drainage systems such as subsurface tile drains and collection ditches.
2. To present a procedure to estimate the amount of nutrients transported from the land surface to surface-water systems at the *regional scale* based on water and nutrient budgets. This procedure must be able to account for differences in soil types, hydrology, and soil surface loads of nutrients. The procedure should be applicable for different hydrological regions in the Netherlands.

The research objectives can be achieved by these methods:

- collecting and analyzing field data on hydrology and nutrient budgets for specific field situations, and
- presenting the travel time distribution of drainage water for different experimental sites and regions across the Netherlands.

In this thesis, the *travel time of drainage water* is defined as the time that it takes for net precipitation to discharge into the surface water from the moment it reaches the land surface and subsequent subsurface flow.

Chapter II begins with steady-state approaches to describe the travel time distribution of drainage water for saturated flow systems. For transient and variably saturated cases, a numerical computer code to simulate transient water flow and solute transport is proposed using a mechanistic description of the dual-porosity concept. The code is used to create models at the field scale; then conclusions are drawn on how to analyze and evaluate the travel time distribution of drainage water at field scale and regional scale. The applicability of different approaches to regional-scale modeling of annual water and nutrient flow and budgets are also concluded.

Chapter III follows with the presentation of a regional modeling approach to calculate the average of annual water flow and solute loads from the land surface to a regional surface water system. The approach also accounts for the influence of atmospheric deposition, regional-scale groundwater seepage or recharge, and point sources on the surface water quantity and quality. Annual budgets of water, chloride, nitrogen, and phosphorus are used to keep track of the calculations. The land and small-scale surface water system in a modeling region is subdivided into several sub-regions. On a sub-regional level, a travel time distribution of drainage water is also implemented in the approach. Differences in annual weather conditions cause this travel time distribution to vary from year to year.

Chapters IV and V show results of two field-scale experiments, performed in Flevoland and in the Hupsel brook basin during the 1992-1994 period. The experimental field, Flevoland, was located on a permanently structured clay soil, and arable crops were grown. The experimental field, Hupsel-Assink, was located on loamy sand with permanent grassland. At both sites, subsurface drains were present, as well as a collection ditch. At the field sites, measurements were performed on hydrology and nutrient concentrations in drainage water. Analysis of the experiments are shown by using field data interpretation and field-scale modeling of transient water flow and solute transport in a variably saturated, dual-porosity medium. Agricultural nutrient balances are compared to solute loads of drainage water, using a travel time distribution of drainage water. The latter is based on a tracer experiment (Flevoland site only) and numerical computer modeling at the field scale. Conclusions are drawn on hydrology of the field sites, including the travel time distribution of drainage water, and on nutrient losses from agricultural land.

Chapters VI and VII follow with the application to two regions of the regional-scale modeling of annual water flow and solute loads to the regional-scale surface water system. Based on the analysis in Chapters IV and V, the average of travel time distribution of drainage water is used, and the experimental methods for the field plots provided field data on hydrology and solute leaching, which characterized the nutrient transport process from soil surface to surface water. The Hoge Afdeling drainage area within the Flevoland polder is the first region presented, followed by the Hupsel brook basin in Chapter VII. Results of the regional model will be compared to regional-scale measurements, especially to field data of calculated solute loads of the regional surface water system. Also, representative parts of the model will be compared to the field data presented in Chapters IV and V. Conclusions will be drawn on the regional-scale travel time distribution of drainage water and on solute loads to the surface water system and their sources. Then, the effects of chemical processes within the surface water itself and the applicability of the approach will be discussed.

Finally, the summary and conclusions of the field measurements, field and regional-scale modeling efforts, and analyses of the travel time distribution of drainage water constitute the finishing part of this thesis.

II

THEORY AND MODELING OF WATER FLOW AND SOLUTE TRANSPORT AT FIELD SCALE

1   Introduction

In this Chapter a theory is presented underlying the modeling of water flow and solute transport in the unsaturated-saturated zone at the plot scale, as well as methods used to interpret the field data. First, steady-state approaches for travel time distribution of drainage water will be shown. In theory, their applicability is limited to fully-saturated flow systems. In case an analysis is needed for a variably-saturated medium under transient flow conditions, the dual-porosity concept is explained. It will be applied to calculate water flow and solute transport using a computer code based on numerical methods. The advantage of using this concept is that flow in permanently structured media can be simulated. The code presented is able to handle two-dimensional (2D) flow situations.

In this thesis the focus is on solute transport by the processes of convection, diffusion, and dispersion in soil and groundwater in the liquid phase, containing dissolved chloride (Cl^-), total-nitrogen (total-N), and total-phosphorus (total-P) components. Chemical and solid-liquid phase exchange processes affect the transportation of dissolved chemicals through the soil matrix, specifically, the transport of N and P-components which is highly influenced by chemical processes. In this thesis, the chemical processes involved will not be modeled in detail and dynamically, but their effects on the solute transport to subsurface drains and surface water systems will be accounted for in the following ways. By using a retardation factor R larger than 1.0, the numerical water flow and solute transport code takes retardation of solutes into account. Moreover, annual chloride and nutrient balances will be set up for the agricultural soil system by applying source and sink terms as a result of chemical processes.

A short overview of the relevant chemical processes involved in chloride and nutrient transport is as follows: Transfer of solutes can occur from the liquid to the gaseous phase. Gaseous nitrogen compounds like ammonia (NH_3) will volatize and escape into the air during applications such as manure and fertilizer. Decomposition or mineralization of organic matter leads to the formation of mineral N-components, which are available to plant roots by uptake. Fixation of air-nitrogen into organic matter

occurs by papilionaceous plants e.g., clover. The process of nitrification turns ammonia into ammonium, a step that is usually followed by the formation of nitrate. Denitrification (chemical and microbial) is the reduction of NO_3-N to N_2, involving intermediates like nitrite (NO_2-N). The bacteria causing bio-chemical denitrification need organic matter as a carbon source (e.g., Klein, 1994). Denitrification can also be caused by a redox reaction due to pyrite-oxidation. Pyrite (FeS_2) is often present in unripened sea clay soils due to the absence of oxygen and the availability of iron and sulfur compounds (Appelo and Postma, 1993). The major soil-chemical process with respect to phosphate transport is sorption. P-sorption can be subdivided into adsorption –directed from the liquid to the solid phase– and desorption –directed from the solid to the liquid phase. Besides sorption, P-diffusion can also occur.

Model simulations are used to interpret the field observations on hydrology and tracer breakthrough, if available, as well as to extrapolate the calculation results in space and time. To calculate field water and nutrient budgets, interpretation of field data in terms of water and solute balances is required. The methods that are used to analyze field registrations and measurements will also be presented. To correctly interpret solute concentrations in drainage water, in terms of solute balances or linking agricultural nutrient losses to drainage water composition, the travel time distribution of drainage water is an essential factor.

2   Travel time distribution of drainage water

2.1   Introduction

The travel time distribution of drainage water is relevant to understand the solute transport process and interpret the measured solute concentrations in drainage water. A point of interest is the time delay between application of a solute at the soil surface and appearance of it in drainage water. The focus in this section is on the travel time distribution of drainage water in the soil and groundwater. The travel time of drainage water is defined as the time that it takes for excess rainfall to discharge into the surface water from the moment of reaching the soil surface and infiltration onwards, followed by subsurface flow. The travel time distribution of drainage water varies in space and time due to differences in soil-physical characteristics, crops, and weather conditions. Temporal variations may occur within a year, and from year to year, but variations are also likely to occur within a day. To begin, several *steady-state* approaches to estimate the travel time distribution of drainage water for *fully saturated flow domains* are shown and discussed.

The depth of the groundwater flow system d and the effective porosity Φ_{eff} of the porous medium are important factors in the steady-state approaches. In the Netherlands, tile drains are usually found at depths between 0.7 and 1.3 m below the soil surface. The thickness of the unsaturated zone varies between 0.5 and 1.5 m. The depth of the groundwater flow systems in drained land is often between 3 m and 10 m. On the average, Φ_{eff} of the flow domain in sandy soils is usually between 0.30 and 0.40 (Meinardi, 1994). In several clay soils, Φ_{eff} was estimated at 0.4 (Meinardi and Van den Eertwegh, 1995). The approaches presented assume steady-state and Darcy-type flow conditions, homogeneous, uniform soils –where examples such as porosity and hydraulic conductivity are concerned, and saturated soil-water systems. They neglect possible diffusion and dispersion influence, plant-root-soil-water interaction, and consequences of unsaturated flow conditions. If the flow situation in the porous medium does not match these conditions, an alternative approach is shown in Section II.3.

2.2   Steady-state approaches to saturated flow systems

Kirkham - Kirkham (1949) theoretically analyzed the velocity potential, stream potential, drain flux, and surface inflow distribution for *ponded water flow* into drain tubes overlying an impervious layer. He concluded that *drain depth primarily controls the rate of water seeping into tube or tile drains*. With decreasing distance of the tile drain depth to the impervious layer, the seepage rate increases. He also concluded that the surface inflow rate immediately above the drains is greater than it is at distances further from the drains. For *water table conditions*, this situation leads to rapid flow rates near the drains and a reduced travel time for water and solutes to pass through the soil from soil surface to drain depth. Kirkham (1958) derived theoretical equations for the arch-shaped groundwater table between tile drains for steady-state flow conditions and homogeneous soils.

Jury - An approach for estimating the travel time distribution of drainage water from *tile-drained fields* was given by Jury (1975a, 1975b) being based on Kirkham (1958). Jury constructed a model for estimating travel times of drainage in the saturated zone, based on convective transport in a steady-state flow situation. He stated that *travel times are a function of cumulative discharge* rather than discharge rate, as long as the relative shape of the streamlines remains more or less the same for different groundwater level heights. Whether the latter assumption is true in practice, it needs to be judged by local observations. Jury (1975a) also states that the geometric and physical assumptions of the method 'rarely if ever are met in practice' and may reduce the applicability of the approach to practical situations.

The average dimensionless travel time τ_{sat} of water in the *saturated zone* is given by (Jury, 1975a)

$$\tau_{\text{sat}} = \frac{I\,t}{\Phi_{\text{tot}}\,L/2} \tag{II.1}$$

where I is the infiltration rate, t is time, Φ_{tot} is the total porosity, and L the drain spacing. Note that only that portion of the total porosity that really takes part in the flow process should be taken into account i.e., the mobile part of the liquid phase. Hence, Φ_{tot} in [II.1] should be replaced by the effective porosity Φ_{eff}. Jury (1975a) estimated the dimensionless delay time, or time lag τ_{unsat}, to traverse the *unsaturated zone* by

$$\tau_{\text{unsat}} = \frac{d_{\text{drain}}}{L/2}\,\vartheta \tag{II.2}$$

where d_{drain} is the depth to the tile drain, L the drain spacing, and ϑ the average saturation degree for the unsaturated zone. τ_{unsat} should be added to τ_{sat} to estimate the total dimensionless travel time from the soil surface to the tile drain.

Ernst-Bruggeman - Another theoretical framework to estimate the travel time distribution of drainage water under fully saturated flow conditions has been given by Ernst (1973) and Bruggeman (1999). Ernst derived an equation for long-term steady-state saturated flow conditions to calculate the travel time distribution of infiltrated water entering a local, symmetrical *ditch* that fully penetrates the soil layer down to the hydrological basis i.e., an impermeable layer (Fig. II.2.1). A Piston-type transport process is assumed, and the influence of possible density or viscosity differences on the groundwater flow are neglected. Groundwater of a different age or residence time does not mix.

The flow paths in soils that are drained by *subsurface drains* are different; they show a radial flow component in a zone near the tile drain. Fig. II.2.2 schematically shows a drainage situation with tile drains installed. It is evident in the region near the tile drain that radial flow components dominate the flow pattern. The deviation of the travel time distribution for the situation shown in Fig. II.2.1 from the situation shown in Fig. II.2.2 is not large for values of d/L smaller than 0.1. For a drainage situation shown in Fig. II.2.2 and with d/L smaller than 0.1, the following equation is valid (Ernst, 1973):

$$t_\tau = \frac{\Phi_{\text{eff}}\,d}{I}\,\ln\left(\frac{d}{d-z}\right) \tag{II.3}$$

where t_τ is the travel time, Φ_{eff} is the effective porosity, d the drained aquifer thickness, I the long-term average infiltration rate, and z the depth considered. I is equal to

$$I = P - ET_a - Q_{\text{surficial}} \tag{II.4}$$
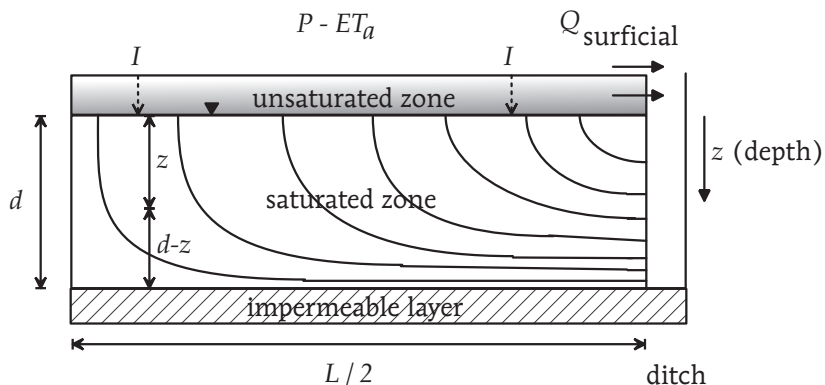
Fig. II.2.1
Travel time distribution of drainage water entering a ditch. Schematic flow paths to a symmetric ditch drainage system down to hydrologic basis i.e., impermeable layer (Ernst, 1973).
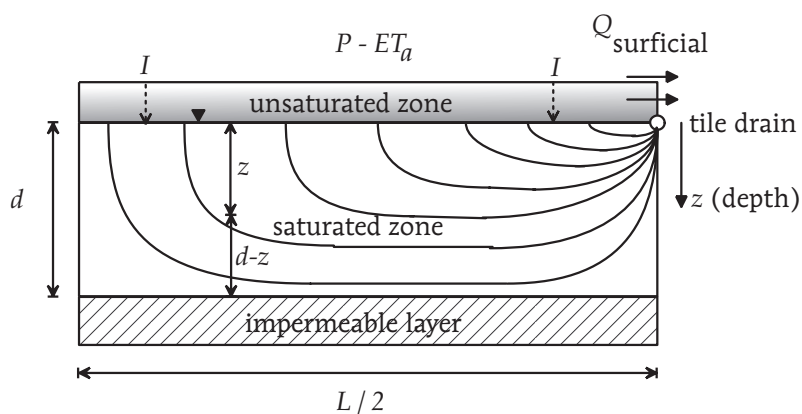
Fig. II.2.2
Travel time distribution of drainage water entering a subsurface drain. Schematic flow paths to a symmetric subsurface drainage system (Ernst, 1973).

where $Q_{surficial}$ is the sum of surficial drainage rates not reaching the saturated zone, such as surface runoff and interflow.

To derive a travel time distribution, Ernst (1973) concluded that the *drained aquifer depth* d is of major importance. The aquifer hydraulic conductivity or drainage resistance factors are not influencing the travel time distribution. [II.3] is suitable for estimating the travel time distribution for field situations, if estimates only for d and Φ_{eff} are available.

Bruggeman (1999) elaborated the travel time distribution approach, as presented by Ernst (1973), to the following equation for a drainage situation under steady-state saturated flow conditions as shown in Fig. II.2.1, reaching the same result:

$$\frac{z}{d}(t) = 1 - e^{\frac{-(I\,t)}{\Phi_{eff}\,d}} \qquad [\text{II.5}]$$

z is the depth below the phreatic groundwater surface and t the time. All units in [II.5] are in [m], [a], or [m a^{-1}]. Application of [II.5] with $d = 2$ m, $I = 0.325$ m a^{-1}, and $\Phi_{eff} = 0.35$, leads to annual travel time fractions f_τ of the total tile drainage water as shown in Table II.2.1.

Table II.2.1
Example of travel time distribution of drainage water. Long-term annual average travel time distribution of drainage with fractions f_τ based on the Ernst (1973) - Bruggeman (1999) approach [II.5], using $d = 2$ m, $I = 0.325$ m a^{-1}, and $\Phi_{eff} = 0.35$.

Fraction	Age-class of travel time [a]	f_τ[-]
f_1	$t \le 1$	0.37
f_2	$1 < t \le 2$	0.23
f_3	$2 < t \le 3$	0.15
f_4	$3 < t \le 4$	0.09
f_5	$t > 4$	0.16

Meinardi and Van den Eertwegh (1995, 1997) elaborated the approach by Ernst (1973) and Bruggeman (1999) for 18 marine clay soil locations, spread across the Netherlands. They expanded the approach with a factor which varied with linear time within one

drainage season in order to allow solute concentrations within a drainage season to also vary with linear time. Van den Eertwegh et al. (1999) used a conceptual model to vary the travel time distribution of drainage water on a daily basis. This model assumed f_τ fractions as a function of daily discharge rates. Van den Eertwegh and Meinardi (1999) used a conceptual model to divide the total discharge into three discharge components: surficial runoff, shallow groundwater discharge, and deep groundwater discharge.

Thunnissen - Thunnissen (1987b) reported on different approaches to estimate the travel time of drainage water. He also elaborated the approach by Ernst (1973) and integrated the *influence of regional-scale seepage or groundwater recharge* on travel times of the drainage water (Fig. II.2.3).

As seen in Fig. II.2.3, the bottom layer is a low-permeable layer as compared to the impermeable layer for the situation drawn in Fig. II.2.2. The actual depth of the flow system d is reduced to an effective depth d^*. Three situations will cause a reduction of d in combination with a possible change in I as compared to the framework described above: the presence of regional-scale groundwater recharge, of regional-scale seepage, and of a radial flow component. In the case regional-scale groundwater recharge occurs, the shallow flow system will lose some water to the aquifer below. On the local scale, this will lead to longer travel times of drainage water because I is reduced to I^* according to

$$I^* = P - ET_a - Q_{\text{surficial}} - Q_{\text{recharge}} \qquad \text{[II.6]}$$

The local-scale flow system will not be as deep as in the previous case due to a regional system that takes part in the flow process, and d is reduced to d^* according to

$$d^* = d\frac{I^*}{I} \qquad \text{[II.7]}$$

If regional-scale seepage enters the local-scale groundwater flow system, travel times of drainage in the latter system will be shorter. This effect can be accounted for the decrease to d because the groundwater seepage 'consumes' part of the flow depth of the local-scale system. The reduced depth d^* can be calculated according to

$$d^* = d\frac{I}{(I + Q_{\text{seep}})} \qquad \text{[II.8]}$$

In this thesis, Q_{seep} is assumed to enter only the surface water system directly, not the local-scale groundwater system. In a tile drained flow situation as shown in Fig. II.2.2 and with d/L smaller than 0.1, d does not need to be reduced. A reduction of d^* to d^{**} in a tile drained flow system is needed in case d/L larger than 0.2 (Thunnissen, 1987b) and can be calculated according to

$$d^{**} = \frac{L}{2\pi} \qquad \text{[II.9]}$$

I^* I^*

unsaturated zone   tile drain

d d^* z (depth)

saturated zone

low-permeable layer

regional-scale groundwater recharge (a)

I^* I^*

unsaturated zone   tile drain

d d^* z (depth)

saturated zone

low-permeable layer

regional-scale groundwater seepage (b)
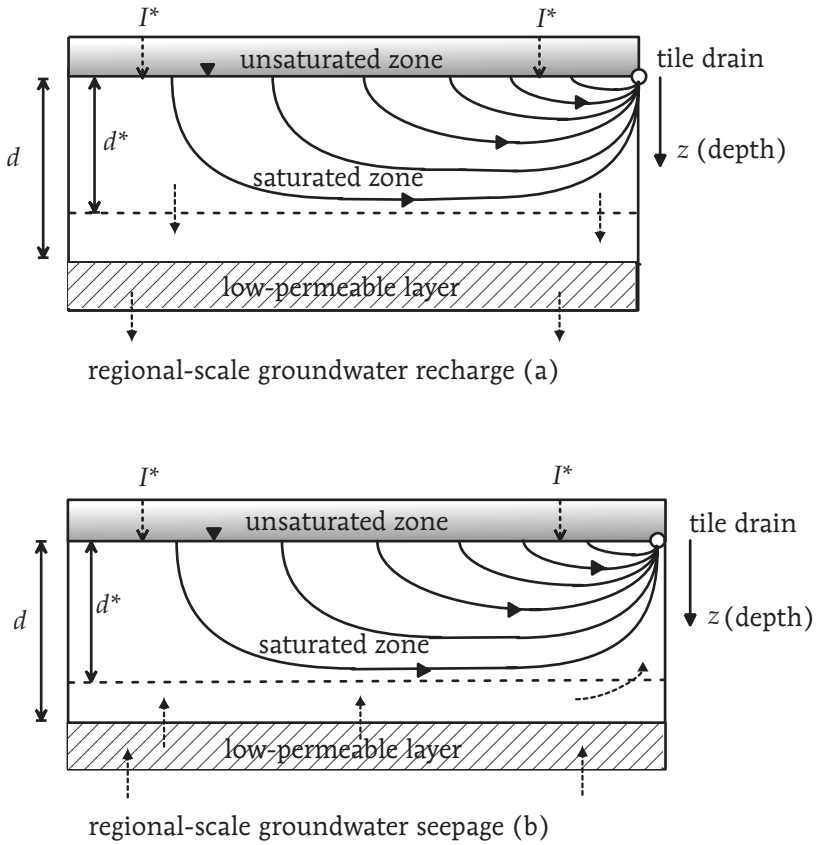
Fig. II.2.3
Travel time distribution of drainage water. Schematic flow paths to a symmetric
subsurface drainage system and the influence of regional-scale groundwater *recharge* (a)
and of regional-scale groundwater *seepage* (b). Dashed line marks lower boundary of
flow domain (Thunnissen, 1987b).

Discussion and conclusions - The approaches presented above assume steady-state and Darcy-type flow conditions, homogeneous and uniform soils, and saturated soil-water systems. These approaches neglect possible diffusion and dispersion influence, plant-root-soil-water interaction, and consequences of unsaturated flow conditions. The references discussed before present mainly theoretical approaches to estimate water and solute travel times from soil surface to tile or ditch drain under steady-state and saturated flow conditions. In the Netherlands, L usually varies between 10 m and 20 m, and d varies between 2 m and 5 m. The typical ratio d/L then lies between 0.1 and 0.5. The theoretical *assumptions are often not met* in practical field situations, and in practice, it is clear that steady-state flow conditions usually do not occur. Also, transport of water and solute in the unsaturated zone needs to be taken into account. Although for most Dutch drainage situations the drained aquifer depth d is a major geometrical factor for the travel time distribution of water and solutes, the approaches presented lack the influence of transport processes in the unsaturated zone.

To interpret the calculated solute loads (e.g., Klavers and De Vries, 1993) of drainage water as, at least partially, a result of agricultural practices, information is needed on the soil route and travel time distribution of drainage water. The travel time of water and solutes entering tile drains and/or ditches is a *combination and superposition of the travel time needed to pass both the unsaturated zone and saturated zone*. The depth of the unsaturated zone in winter is generally less than 0.5 m to 1 m, and in the summer more than 1 m to 2 m in the case of a tile-drained situation under conditions in the Netherlands.

Note that the approaches by Ernst (1973) and Bruggeman (1999) exclude the travel time needed to pass the unsaturated zone above the groundwater table. Applying [II.5] always leads to a f_1 fraction larger than f_2. In *structured soils*, it is likely that all pores do not contribute equally to the flow process. The mobile-immobile water concept (e.g., Jury et al., 1991) is an example of the division of the total wetted pore space into a mobile and immobile, stagnant water content. *Preferential flow processes* in the unsaturated zone are not likely to contribute to the replacement of 'old' water by 'new' water, as opposed to Piston-type flow processes. In the case of structured soils, it is not likely that the precipitation excess will fully replace all water present in the unsaturated zone from the top of the soil downward. It depends on the soil type and hydrological situation, such as groundwater depth, how much water is needed to fully replace the water in the unsaturated zone. When the most recent year is considered, the infiltrated and/or infiltrating water of that year remains mainly in the unsaturated zone, partially replacing the so-called 'f_2'-water. In this example, it is likely that the drainage water f_2 is larger than f_1, at least at the start of the drainage season. At that time, the larger part of the 'f_2'-water will have passed the unsaturated zone, and the upper part of the saturated

groundwater body will consist of 'f_2'-water. Depending on the porous medium characteristics, i.e., soil structure and the weather conditions, f_1 will increase during the drainage season at the expense of f_2, and possibly, but less likely in 'older' fractions as well.

Nitrate concentration measurements by De Vos (1997) showed that as groundwater levels rose, the relative part of the drainage outflow originating from the part of the soil above the tile drain level became greater. This observation denoted a shift in travel times of draining soil water as a function of groundwater level –thus of drainage intensity.

Oostindie and Bronswijk (1995) computed travel times by a combination of crude estimates and numerically modeling hydrological situations in cracking clay soils. For a heavy clay soil they found that about 15% of the precipitation drained rapidly by cracks with a travel time between 75 and 275 days for reaching an aquifer system. The other 85% infiltrated into the soil matrix and percolated toward the aquifer with a travel time of about 800 days. It is obvious that information on travel times is needed for a reasonable interpretation of field data. This information will be provided by field tracer experiments and by numerically modeling water flow and solute transport in the unsaturated-saturated soil-water-system.

It is concluded that in practical situations at the field scale, transient solutions of variably-saturated water flow and solute transport are needed, especially for structured soils. Using a numerical model, the travel time distribution of drainage water can be calculated. After analysis, a comparison of the simulation results with the steady-state solutions will show differences, and the magnitude of these differences is a measure of the possibility and value of the application of simple approaches to complex field-scale situations.

3 Modeling transient water flow

3.1 Dual-porosity concept

Solute losses by drainage are strongly related to water flow. Without the flow of water, only negligible transport of solutes occurs. Without an adequate description of water flow and of the drainage process in a heterogeneous field situation, attempts made to simulate the solute transport process will probably fail due to the major impact of water flow on solute transport. The field-scale modeling focus is mainly on the hydrology of dual-porosity media, and it includes solute transport.

It is generally recognized that in the case of porous media containing large structures such as aggregates, macropores play an important role in the transport of water, solutes,

and energy through the soil profile. Macropores are present in the form of shrinkage cracks, and biological channels such as worm and root holes are also present. Preferential flow processes, as a result of soil structure, have been subject to investigation, mostly since the late 1970s (e.g., Bouma, 1981; Beven and Germann, 1982). Bronswijk (1991) e.g., elaborated on the modeling of swelling and shrinking clay soils and their effects on flow and transport. Field experiments on structured soils performed in the Netherlands include the studies reported by e.g., Booltink (1994), Bronswijk et al. (1995), and Groen (1997). An overview of flow mechanisms and field experiments on preferential flow was given by Jury and Flühler (1992). Different concepts have been developed to model preferential flow processes in structured porous media, i.e., the transfer function concept, the mixing cell-concept, and approaches such as the kinematic wave concept. The dual-porosity concept (e.g., Berkowitz, 1994; Brusseau et al., 1994) is an approach which is useful in the cases where the flow domain is structured, and in those cases where exchange processes between the soil matrix and the macropores are very likely to play an important role in the water flow and solute transport behavior.

The *dual-porosity concept* based on the approach of Gerke and van Genuchten (1993a, 1993b) is used in this thesis to describe transient water flow and solute transport in a variable unsaturated-saturated porous medium. Nieber and Misra (1995), Ray et al. (1996, 1997), Nieber et al. (1998), and Van den Eertwegh et al. (2001) used an identical approach. The porous medium is seen as a rigid system of two interconnected flow domains, i.e., a soil matrix and a macropore flow domain. Flow in both domains is assumed to obey Darcy's law. It is often stated that flow in the macropore domain is mainly gravity-driven (e.g., Germann and DiPietro, 1996). This is probably correct from a mechanistic point of view. The soil-physical parameter values should be chosen such that the response-characteristic of the macropore domain is according to what one might expect, such as a near-zero water retention and fast transport capability due to a large hydraulic conductivity.

To derive the general equations for water flow, the volumetric flux density equation is, according to Darcy's law, combined with the continuity or mass balance equation (conservation of mass). Transport of water by soil vapor movement in the gas phase is taken into account. Assumptions that determined this experimental, macroscopic law are that the density of the fluid involved (water; symbol ρ_w) is constant and equal to 1000 kg m^{-3}, the fluid is incompressible, the viscosity of the fluid is constant, and flow occurs under isothermal conditions. The continuum approach neglects boundaries between phases and assumes that physical properties in any phase can be described at any point within a representative elementary volume (REV). Furthermore, the porous medium is rigid and has a stable geometry. Air in the porous medium is present at

atmospheric pressure. The governing general equations for water flow are

$$\frac{\partial \theta_\mu}{\partial t} = \nabla \cdot \left[\left(k_\mu + \frac{1}{\rho_w} D_v^s \frac{\partial \rho_v}{\partial h} \right) \nabla h_\mu \right] + \frac{\partial k_\mu}{\partial z} - S_p + \Gamma_W \qquad \text{[II.10]}$$

and

$$\frac{\partial \theta_m}{\partial t} = \nabla \cdot \left[\left(k_m + \frac{1}{\rho_w} D_v^s \frac{\partial \rho_v}{\partial h} \right) \nabla h_m \right] + \frac{\partial k_m}{\partial z} - \Gamma_W \qquad \text{[II.11]}$$

where the subscript μ denotes the matrix domain, subscript m the macropore domain, θ the volumetric soil water content, k the hydraulic conductivity, h the soil water pressure head, S_p the sink term for the root water uptake by plants from the matrix domain only, D_v^s the effective diffusion coefficient of water vapor in pore space, ρ_v the water vapor density or vapor concentration in the pore space, ρ_w the density of water at 4°C, and Γ_w the mass transfer or water exchange term from macropore domain to matrix domain (positive sign). The total porosity Φ_{tot} is the sum of matrix and macropore porosity. The vapor diffusion coefficient is assumed to be isotropic at the element scale. D_v^s is calculated according to (Jury et al., 1991)

$$D_v^s = D_v^a \frac{\theta_{\text{air}}^{\frac{10}{3}}}{\Phi_i^2} \qquad \text{[II.12]}$$

where D_v^a is the water vapor diffusion coefficient in free air, θ_{air} is the air-filled porosity, and the subscript i denotes either the matrix or the macropore domain. At standard atmospheric conditions, the value for D_v^a is $2.0 \ 10^{-5} \ \text{m}^2 \ \text{s}^{-1}$ according to Jury et al. (1991). The vapor density ρ_v is calculated according to (Jury et al., 1991)

$$\rho_v = \rho_v^* \exp{\frac{Mgh}{R_M T}} \qquad \text{[II.13]}$$

where ρ_v^* is the saturated water vapor density, M is the molecular mass of water, g is the gravity constant, R_M is the universal gas constant, and T is the temperature. Unless the soil is very dry, i.e., h is smaller than -200 m to -100 m, ρ_v is essentially equal to ρ_v^*, which is a function of T only. The water vapor density gradient can be described as a function of h according to (Philip and De Vries, 1957)

$$\nabla \rho_v = \frac{\partial \rho_v}{\partial h} \nabla h \qquad \text{[II.14]}$$

Rainfall reaching the soil surface will be divided between the two flow domains relative to the porosity of the top layer of each domain, taken as a fraction of the total porosity, $\Phi_\mu / \Phi_{\text{tot}}$ and $\Phi_m / \Phi_{\text{tot}}$, respectively. The infiltration capacity at the soil surface of both domains determines which part of the rainfall will enter the flow domain. The rainfall

intensity can possibly exceed this infiltration capacity, and if the infiltration capacity at the soil surface of the matrix domain is exceeded, the part of the rainfall that cannot infiltrate will be added to the rainfall at the macropore domain. Water will move, like 'runoff' from the soil matrix, into the macropores that are open at the soil surface. Usually, with macropores present at the soil surface, total infiltration capacity is large enough that all rainfall will infiltrate. However, if the sum of the rainfall directly to the macropore domain and the runoff from the matrix domain exceeds the infiltration capacity of the macropore domain, runoff from the macropore domain will occur due to ponding at the soil surface. When this ponding condition occurs, it is assumed that runoff is sufficient to maintain a zero ponding depth. Runoff will also occur if the soil profile is fully saturated from the bottom to the top.

In general, surface runoff is generated by rainfall events of certain intensity and duration, depending on the soil surface slope, infiltration capacity of the topsoil, soil water storage capacity, soil surface storage, and drainage situation. It remains open to question whether actual runoff from the soil surface to an open drain, ditch, or brook can be better modeled by introducing a depth to ponding. Surface runoff will be generated on locations having low-permeable soils, and this may be amplified by top soil compaction by local-scale tractor tracks or by grazing livestock. Once present, it is uncertain whether this generated runoff will reach the surface water. Flow paths can be interrupted by clods or be caught in surface level depressions where water will infiltrate at a later time. Thunnissen (1987a) summarized potential surface runoff events and conditions in the Netherlands. He concluded that for sandy soil cases, surface runoff effects were observed in solute concentration patterns in surface waters. Quantification of surface runoff volumes based on solute concentrations led to rough estimates of percentages of rainfall discharged by surface runoff in wet periods. These percentages varied between 30% and 50% in certain periods of time, but were estimated far lower (not quantified) on an annual basis. To comment on the method of the surface runoff calculation, the method shown provides a rough indication of the potential occurrence of surface runoff from the soil surface to surface waters.

The mass transfer or exchange rate of water Γ_w is calculated according to (Gerke and van Genuchten, 1993b)

$$\Gamma_W = \kappa_w \left(h_m - h_\mu \right) \qquad\qquad \text{[II.15]}$$

and

$$\kappa_w = \frac{\beta}{a^2} k_a \gamma_w \qquad\qquad \text{[II.16]}$$

where κ_w is a first-order mass transfer coefficient, β is a dimensionless coefficient depending on the geometry of the soil structure, a the characteristic distance from the

center of a fictitious matrix block to its edge (half-width of matrix block or half-distance between two macropores), k_a the effective hydraulic conductivity of the soil matrix at or near the matrix-macropore interface, and γ_w an empirical dimensionless scaling factor. Γ_w is larger than 0 when h_m is larger than h_μ. Γ_w is smaller than 0 when h_μ is larger than 0 and h_m is smaller than h_μ. k_a is based on k_μ because the matrix domain characteristics are assumed to limit mass transfer. k_μ is evaluated by using the pressure heads in both the matrix and macropore domain. k_a is calculated according to:

$$k_a = 0.5 \left[k_{\mu,i} \left(h_\mu \right) + k_{\mu,i} \left(h_m \right) \right] \tag{II.17}$$

where the subscript i denotes the hydraulic conductivity at or near the matrix-macropore interface, which can differ by a constant, linear factor $f(k_s)_{\text{interface}}$ from the soil matrix hydraulic conductivity, due to, for example, occurrence of chemical deposits or weathering. The soil water retention function and hydraulic conductivity function for the matrix and macropore domain are described using the Mualem - van Genuchten model. The soil water retention function is described by

$$\theta_i = \theta_{r,i} + \left(\theta_{s,i} - \theta_{r,i} \right) \left(1 + \alpha \left| h_i \right|^n \right)^{-m} \tag{II.18}$$

where the subscript i denotes either the matrix domain $(i = \mu)$ or the macropore domain $(i = m)$, θ_i is the volumetric soil water content, $\theta_{r,i}$ the residual volumetric soil water content, $\theta_{s,i}$ the volumetric soil water content at saturation, h_i the soil water pressure head, and α, n and m are shape parameters. Hysteresis in the soil water retention function is not considered in this example, although the code does have the algorithm for hysteresis described by Mualem (1974).

The hydraulic conductivity function for each domain is described by

$$k_i \left(S_{e,i} \right) = k_{s,i} \, S_{e,i}^l \left[1 - \left(1 - S_{e,i}^{1/m} \right)^m \right]^2 \tag{II.19}$$

where the subscript i denotes either the matrix domain $(i = \mu)$ or the macropore domain $(i = m)$, $k_{s,i}$ is the saturated hydraulic conductivity and $S_{e,i}$ the effective saturation degree, given by

$$S_{e,i} = \frac{\theta_i - \theta_{r,i}}{\theta_{s,i} - \theta_{r,i}} \tag{II.20}$$

Using a value of 0.1 for the α-parameter and of 10 for the n-parameter both given in [II.18], a very steep retention function is created, representing the retention behavior of macropores quite effectively.

3.2   Estimation of actual evapotranspiration

The reference-crop evapotranspiration rate (ET_r) according to Makkink (1957, 1960) is used as a basis for the calculation of the potential evapotranspiration rate (ET_p) during

the actual growing season of crops in the Netherlands. The method to calculate ET_r was tested by Makkink (1957) against lysimeter experiments. ET_r has been calculated by the Royal Dutch Meteorological Institute (KNMI) since the late 1980s for several meteorological stations across the country. ET_r is a good measure for the potential evapotranspiration rate of well-watered, short-cut grass, defined as the reference-crop. This is well correlated with Penman's formulation for the open water evaporation E_0 during the growing season (De Bruin, 1987). ET_r is given by the following empirical relationship (Makkink, 1957; 1960):

$$\lambda_w ET_r = 0.61 \frac{s}{s + \gamma} K \downarrow -0.12 \qquad \text{[II.21]}$$

where λ_w the latent heat of vaporization of water [J kg^{-1}], s is the slope of the saturation water vapor pressure curve at the daily average of air temperature [mbar K^{-1}], γ the psychrometer constant [mbar K^{-1}], $K \downarrow$ the daily average (0-24 h) of global solar radiation flux density [W m^{-2}], and 0.61 and 0.12 are coefficients. De Bruin (1981, 1987) used a slightly adjusted version of [II.21], which is used by the KNMI as calculation standard:

$$\lambda_w ET_r = 0.65 \frac{s}{s + \gamma} K \downarrow \qquad \text{[II.22]}$$

where 0.65 is an empirical constant. To calculate ET_r on a daily basis, only measurements of $K \downarrow$ and air temperature T_{air} are needed. In [II.21] and [II.22] ET_r has the unit [kg m^{-2} s^{-1}]. At 4°C, 1 kg of water on 1 m^2 surface area results in a water layer of 1 mm thickness. ET_r and other evapotranspiration terms in this thesis are expressed in the unit [mm d^{-1}], by multiplying ET_r in [II.21] and [II.22] with 86 400.

ET_r provides an estimate of the evapotranspiration of a theoretical reference-crop i.e., well-watered and short-cut grass. To calculate the potential evapotranspiration rate ET_p for actual crops, ET_r must be multiplied by so-called crop factors f_c (Feddes, 1987). These empirical factors inhibit crop characteristics like height, leaf area, and they were determined from field and lysimeter experiments. ET_p of a specific crop under consideration is calculated according to

$$ET_p = f_c ET_r \qquad \text{[II.23]}$$

Bare soils during the off-crop season are hard to represent by a crop factor (Allen et al., 1998). To represent potential evaporation from bare soil, $f_c = 0.4$ has been applied (Makkink, 1960; Meinardi, 1994).

ET_p as calculated according to [II.23] and is provided as input for the code. The *potential soil evaporation rate* E_p is calculated by

$$E_p = ET_p^{-0.6\,\text{LAI}} \qquad \text{[II.24]}$$

where LAI is the Leaf Area Index which varies with time. LAI-data used for different crops originated from Boons-Prins et al. (1993), Van Dam et al. (1997), and Allen et al. (1998). Soil evaporation is calculated both for the matrix and macropore domain. The actual soil evaporation rate E_a is a function of the $(RH_{surface} - RH_{air})$ gradient where RH_{air} is the relative humidity of the air given as an input variable, and $RH_{surface}$ is the relative humidity of the pore air at the soil surface. $RH_{surface}$ is calculated according to (Jury et al., 1991)

$$RH_{surface} = \exp^{\dfrac{Mgh}{R_M T_{air}}}$$ [II.25]

where h is the soil water pressure head, M is molecular mass of water vapor, g is the gravity constant, R_M is the universal gas constant, and T_{air} is the air temperature at the soil surface. The *actual soil evaporation rate E_a* is calculated by

$$E_{a,i} = b \left(RH_{surface,i} - RH_{air} \right) \frac{\Phi_i}{\Phi_\mu + \Phi_m}$$ [II.26]

where the subscript i denotes either the matrix or the macropore domain, and coefficient b is equal to

$$b = \frac{E_p}{1 - RH_{air}}$$ [II.27]

In the case where RH_{air} exceeds $RH_{surface}$, E_a =0.

When soil moisture is lacking, E_a is smaller than E_p. The energy saved in the soil evaporation process is assumed to become available for plant transpiration. The *potential transpiration rate T_p* is therefore computed as

$$T_p = ET_p - E_a$$ [II.28]

The potential root water extraction rate S_p, integrated over the root zone depth d_{root}, is equal to the potential transpiration rate T_p [II.27]. $S_p(z)$ is calculated by (e.g. Bouten, 1992)

$$S_p(z) = \frac{i_{root}(z)}{\int\limits_{-d_{root}}^{0} i_{root}(z)dz} T_p$$ [II.29]

where $i_{root}(z)$ is the root length density function [$cm^1 \, cm^{-3}$]. Three different types of root length density distribution functions can be used in the model with respect to depth: constant, linearly decreasing, or exponentially decreasing with depth. For each model built and used later in this thesis, the function type will be given. d_{root} varies with

time during the growing season and is computed from a given crop-dependent maximum rooting depth and the development stage of the crop.

Reduction of T_p can be caused by too wet (oxygen deficiency) or too dry conditions. This reduction was described by Feddes et al. (1978), whose approach yielded a reduction factor η_{rw} as a function of h in the root zone. Fig. II.3.1 shows this function for the crop potatoes. Root water uptake is zero when the soil water pressure head of the matrix domain is above pressure head h_1 and below pressure head h_4. Root water uptake increases linearly with soil water pressure heads between h_1 and h_2, and it is optimal (potential) between pressure heads h_2 and h_3. Pressure head h_3 is split into a low ($h_{3,L}$) and high ($h_{3,H}$) variant, where subscript L indicates a low potential evapotranspiration rate of 1 mm d^{-1}, and subscript H a high potential evapotranspiration rate of 5 mm d^{-1}. Where transpiration reduction is computed, the value of h_3 is interpolated linearly as a function of potential evapotranspiration rate. Root water uptake decreases linearly between h_3 and h_4 (wilting point), and stops when h is smaller than h_4. The h_1 to h_4-parameters are crop-dependent.
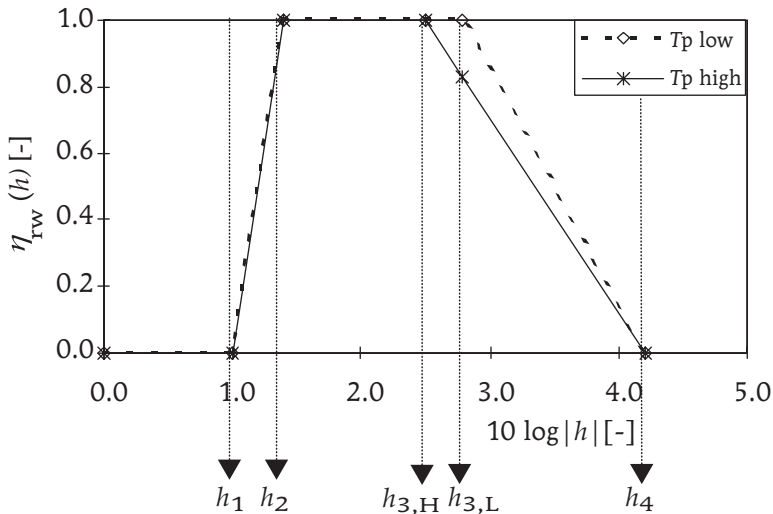
Fig. II.3.1
Plant transpiration. Reduction factor $\eta_{rw}(h)$ to T_p as a function of h in the root zone of the matrix domain after Feddes et al. (1978). Parameters for potatoes: $h_1 = -0.1$ m, $h_2 = -0.25$ m, $h_{3,L} = -6.0$ m, $h_{3,H} = -3.2$ m, and $h_4 = -160.0$ m (wilting point).

Actual root water uptake $S_a(z)$ is computed according to

$$S_a(z) = \eta_{rw}(h)S_p(z)$$

[II.30]

The actual plant transpiration rate T_a is computed according to

$$T_a = \int\limits_{-d_{\text{root}}}^{0} S_a(z)dz \qquad\qquad [\text{II.31}]$$

The actual evapotranspiration rate ET_a is calculated by

$$ET_a = E_a + T_a \qquad\qquad [\text{II.32}]$$

4 Modeling transient solute transport

The solute transport in both flow domains is described by the following coupled convection-dispersion equations with the subscript μ for the matrix domain and m for the macropore domain:

$$\frac{\partial \left(\theta_\mu R_\mu C_\mu\right)}{\partial t} = -\nabla \left(q_\mu C_\mu - \theta_\mu D_{e,\mu}\nabla C_\mu\right) - C_\mu S_p + Y_C \qquad\qquad [\text{II.33}]$$

and

$$\frac{\partial \left(\theta_m R_m C_m\right)}{\partial t} = -\nabla \left(q_m C_m - \theta_m D_{e,m}\nabla C_m\right) - Y_C \qquad\qquad [\text{II.34}]$$

where R is the retardation factor, D_e is the effective diffusion-dispersion coefficient, C is the solute concentration, and q is the specific discharge or Darcy rate. The retardation of chemicals can be seen as an overall net effect of sorption processes. Solute uptake by plant roots is taken into account for the matrix domain only. This uptake can be gradually switched off/on (0-100%). The solutes to be considered are assumed to be non-volatile so that evaporation of the solutes will not occur. In the case where macropores are present at the soil surface and water at the top boundary is moved from the matrix to the macropore domain by surface runoff, the solute concentration of this runoff water is equal to the solute concentration of the water infiltrating at the top boundary.

The non-zero diffusion-dispersion coefficients of tensor D_e (D_{xx}, D_{xz}, D_{zz}) are calculated on an element basis using the Darcy rate q, not the pore velocities. In two dimensions, using the x- and z-direction representing a vertical cross-section of the porous medium, q is calculated by

$$q = \sqrt{\left(q_x^2 + q_z^2\right)} \qquad\qquad [\text{II.35}]$$

where q_x is the Darcy rate in the x-direction and q_z in the z-direction. The coefficients building D_e are usually dominated by hydrodynamic dispersion and calculated by

(Bear and Verruijt, 1987; Jury et al., 1991)

$$D_{xx} = \theta \left[D_0 \xi_l(\theta) + \alpha_T q + \alpha_L \frac{q_x^2}{q} - \alpha_T \frac{q_x^2}{q} \right]$$ [II.36]

$$D_{xz} = \theta \left[\alpha_L \frac{q_x q_z}{q} - \alpha_T \frac{q_x q_z}{q} \right]$$ [II.37]

$$D_{zz} = \theta \left[D_0 \xi_l(\theta) + \alpha_T q + \alpha_L \frac{q_z^2}{q} - \alpha_T \frac{q_z^2}{q} \right]$$ [II.38]

where D_0 is the diffusion coefficient of solute in bulk water, α_L the longitudinal dispersivity, α_T the transversal dispersivity, and $\xi_l(\theta)$ the liquid tortuosity factor given by (Jury et al., 1991)

$$\xi_{l,i}(\theta_i) = \frac{\theta_i^{\frac{10}{3}}}{\Phi_i}$$ [II.39]

where the subscript i denotes either matrix or macropore domain. Values for D_0 were given by e.g. Bowman et al. (2001), for chloride (salt) in bulk water a value of 2.0 cm^{-2} d^{-1} is used here. The value of the dispersivity depends on the geometry of the flow domain structure (Dagan, 1989), and thus on the scale over which the water and solute flux is averaged. The value of the dispersivity is to represent the dispersion at the scale smaller than the scale of the measured heterogeneity. For the numerical method, the smallest scale at which heterogeneity is represented is at the scale of the element or grid cell, where the flow medium is assumed to be homogeneous. Yet, there may be some heterogeneities even at a smaller scale, but these are not simulated by the flow solution. Gelhar et al. (1992) reported values of α_L between 0.1 and 0.2 times the scale of the element as the asymptotic value of dispersivity. The dispersivity is scale dependent i.e., it grows as a solute plume gets larger, and it takes some time i.e., some distance traveled by the solute before the asymptotic value is realized. From experiments and numerical studies, it was found that the asymptotic value of α_L should be about 0.1 times the size of the model region representing the scale of the heterogeneity. In these cases no detailed information is given on heterogeneities for the scale smaller than the element.
To capture the effect of the smaller-than- grid-scale heterogeneities, the longitudinal dispersivity, α_L is set to 0.5 times the minimum length of all grid cells in the mesh representing the flow domain. This value is derived from the smallest grid cell and appears to prevent numerical oscillations in the solution, especially near outflow boundaries. The transversal dispersivity α_T is taken 0.1 times α_L.

Application of a linear adsorption isotherm and the assumption of equilibrium conditions result in a retardation factor R given by

$$R = 1 + \frac{(1 - \Phi) \rho_s K_d}{\Phi}$$ [II.40]

where ρ_s is the solid phase density, and K_d a constant, referred to as the distribution coefficient. This coefficient relates the adsorbed concentration (solid phase) to the concentration in the liquid phase. For a non-reactive solute, K_d equals zero and R equals 1.0. The value of R is identical for both flow domains. The use of K_d originates from a linear Freundlich adsorption isotherm and is calculated according to

$$K_d = \frac{C_a}{C_l} \qquad\qquad [\text{II.41}]$$

where C_a is the solute concentration adsorbed to the soil matrix and C_l the concentration of the solute in the liquid phase (Jury et al., 1991).

Sorption of chemicals is the change in concentration of chemicals in the solid phase as a result of mass transfer from liquid to solid phase. Chemicals are adsorbed to the *surface* of the solid phase, whereas the intake of chemicals *into the solid phase* is called absorption. Exchange of chemicals at the solid phase involves a replacement of one chemical for another one. Desorption is the opposite process of adsorption. The rate of desorption of phosphate is taken 100 times smaller by Schoumans (1997) as compared to the sorption rate. Phosphate and ammonium (NH_4^+) are known to strongly take part in adsorption processes. Sorption processes generally lead to transport velocities of solutes smaller than the transport velocity of the liquid phase itself. López et al. (1992) performed column experiments to determine transport properties of unstructured soils using chloride as a tracer. They found $R = 1.2$ and 1.5 for the two columns they set up. Their explanation of R values larger than 1.0 was that chloride was partially adsorbed by soil organic matter and/or Fe and Al oxides present. This adsorption process was probably reversible. An R value larger than 1.0 for chloride is especially likely to occur at low pH (Appelo and Postma, 1993).

Y_C in [II.33] and [II.34] is the solute mass transfer between the two domains, given by

$$Y_C = \left[(1 - \chi)\, \Gamma_W C_m + \chi \Gamma_W C_\mu \right] + \frac{\beta}{a^2} \overline{D_l^s} \left(C_m - C_\mu \right) \qquad\qquad [\text{II.42}]$$

where D_l^s is the diffusion coefficient of the solute in pore liquid of the matrix domain at or near the interface and calculated as the average of the diffusion coefficient for the matrix domain at matrix and macropore pressure head (a and β according to [II.16]). χ is a dimensionless coefficient which determines the direction of flow between the two domains computed by

$$\chi = 0.5 \left(1 - \frac{\Gamma_W}{|\Gamma_W|} \right), \Gamma_W \neq 0 \qquad\qquad [\text{II.43}]$$

5 Numerical solution of transient water flow and solute transport equations

The governing equations for transient water flow [II.10] and [II.11] and solute transport [II.33] and [II.34] are solved numerically. The water flow equations for the matrix and macropore domains are coupled through the water exchange term. The solute transport equations for the two domains are coupled through the solute mass exchange term. No direct coupling exists between the water flow and solute transport equations; however, the solute transport equations take the water pressure and velocity data from the water flow equation solutions as input to drive the transport of the solute. The flow equations are in the mixed-form of the Richards equation with the unknown variables expressed in both pressure head h and volumetric water content θ. The water flow equations to solve are in the form:

$$\frac{\partial \theta_i}{\partial t} = \nabla \cdot [(k_i + D_{vi}) \nabla h_i] + \frac{\partial k_i}{\partial z} - S_p + \Gamma_{Wi} \qquad \text{[II.44]}$$

The solute transport equations are in the form:

$$\frac{\partial (\theta_i c_i)}{\partial t} = \nabla \cdot (D_i \nabla c_i) - \nabla \cdot (\boldsymbol{q}_i c_i) + Y_{Ci} \qquad \text{[II.45]}$$

where the subscript i denotes either the matrix or macropore domain and subscript v denotes water vapor. Γ_{Wi} and Y_{Ci} are positive if directed from the macropore to the matrix domain.

Initial conditions for water flow are either defined as hydrostatic equilibrium above a given groundwater level, or as prescribed initial nodal pressure heads. The initial condition for the solute transport is provided for by initial nodal concentrations as prescribed, i.e., either uniform or node-by-node. The water flow boundary condition that can be used is either of Dirichlet type (specified pressure head), or Neumann type (specified flux). Also the hydraulic gradient assumption (gravity-driven flow) can be used as boundary condition (specified flux). A model built with the code considers three boundary types of which the system-dependent boundary conditions cannot be defined a priori:

- the air-soil interface at the atmospheric boundary,
- a seepage face dependent on the atmospheric pressure, and
- a seepage face dependent on pressure heads at a so-called far field reference point outside the flow domain.

These three types are simulated by applying either the specified head or prescribed flux boundary condition, possibly switching between iterations. The solute transport

boundary condition is of Dirichlet type i.e., the concentration is specified for the case of diffusion in the absence of convection; Neumann type i.e., the solute mass flux by diffusion is given; or Cauchy type i.e., the solute mass flux by diffusion and flow is given.

When a boundary condition is defined as a seepage face representing a subsurface drain, a conductance factor can be used. This factor allows the user to implement an extra flow resistance at or near the subsurface drain. This extra resistance can be caused by a combination of factors: disturbance of the soil properties during installation, which leads to a decrease of the soil hydraulic conductivity; the characteristics of the drainage material such as the geometry of the tube and the drain envelop (e.g., Bently and Skaggs, 1993). Also, there may be 'back pressure head' applied to the outlet of the drain. In this type of condition, the subsurface drainage does not necessarily flow into the open air at atmospheric pressure conditions, but it may discharge into a ditch that has water at an elevation above the elevation of the drain outlet. Therefore, the drain outlet will have positive 'back pressure head' on the system (Fig. II.5.1). For each model used in this thesis, the 'back pressure head' will be presented at the model section.
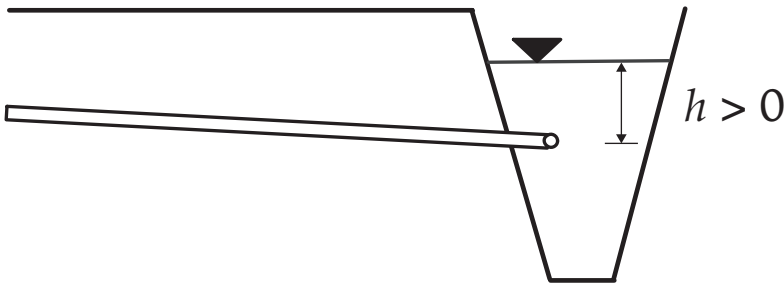
Fig. II.5.1
Field-scale transient modeling. Seepage face boundary condition for subsurface drain with 'back pressure head' h larger than 0 in case the ditch water level is above the subsurface drain outlet.

Leakage i.e., a drainage flux, can occur from any domain boundary below the soil surface. One needs to define the conductance between the domain boundary and the reference point at some distance away from the domain ('far field'; Fig. II.5.2). The conductance is equal to k_s/x, where x is the horizontal distance between the reference point and the boundary. Flow across the boundary is directly proportional to the difference between the boundary pressure and the pressure at the reference point. The flow will be into the domain if the reference pressure is greater than the domain boundary pressure, and the flow will be out of the domain if the far field pressure is less than the boundary pressure. In this thesis the conditions are restricted so that flow occurs only out of the domain.

This restriction was imposed by having an index in the code that would allow flow either in one direction only (out), or would allow flow in either direction. In a sense this boundary type is still a seepage face boundary, but with a resistance to flow at the boundary rather than acting as a free drainage boundary under the usual conditions of seepage.
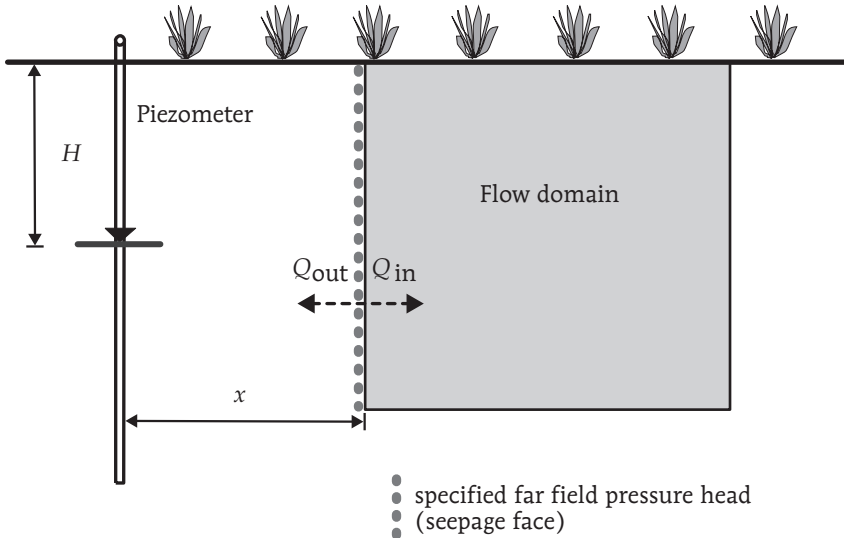
Fig. II.5.2
Field-scale transient modeling. 'Far field' reference point boundary condition for the left side (dotted line) of 2D flow domain represented by the rectangle. 'Far field' pressure head h at distance x from the permeable boundary at the left side of the flow domain is derived from far field hydraulic head H as measured in a piezometer.

The space discretization of the non-linear water flow and linear solute transport equations is accomplished with a general Galerkin finite element formulation (FEM) with linear shape functions. The flow or solution domain is discretized by using a network or mesh of triangular elements, the corners of which are the nodal points. For each element the governing differential equation is approximated using the method of weighted residuals. The contributions of all individual elements are assembled into one global system of algebraic matrix equations. The FEM transformation of [II.44] and [II.45] in space leads to a system of ordinary algebraic differential equations for water flow (symbol W):

$$[A_{Wi}] \left\{ \frac{\partial \theta_i}{\partial t} \right\} + [B_{Wi}] \{h_i\} - \{f_{Wi}\} - \{k_i\} + \{\Gamma_{Wi}\} = \{0\} \qquad \text{[II.46]}$$

where Γ_w is the mass transfer or water exchange term from macropore domain to matrix domain (positive sign), and for solute transport (symbol C):

$$[A_{Ci}] \left\{ \frac{\partial (\theta_i c_i)}{\partial t} \right\} + [B_{Ci}] \{c_i\} - \{f_{Ci}\} + \{Y_{Ci}\} = \{0\} \qquad \text{[II.47]}$$

where the subscript i denotes the flow domain. Integration of equations [II.44] and [II.45] with time is achieved by discretizing the time domain into a sequence of finite intervals, replacing the time derivatives by finite differences. The modified Picard method (Celia et al., 1990), with fully implicit backward differencing for the time derivative (Euler method), was used to express the two unknowns in terms of changes in pressure heads between iterations in the Richards equation.

The implicit scheme leads to the following system of equations for water flow:

$$\begin{aligned}
\left[A'_{Wi}\right]^{k+1,m} & \{h_i\}^{k+1,m+1} + \Delta t \, [B_{Wi}]^{k+1,m} \{h_i\}^{k+1,m+1} \\
&= \left[A'_{Wi}\right]^{k+1,m} \{h_i\}^{k+1,m} + \Delta t \left[\{f_{Wi}\} + \{k_i\} + \{\Gamma_{Wi}\}\right]^{k+1,m} \\
&\quad + [A_{Wi}]^{k+1,m} \{\Delta\theta_i\}^m
\end{aligned} \qquad \text{[II.48]}$$

with

$$\Delta\theta_i = \theta_i^k - \theta_i^{m,k+1} \qquad \text{[II.49]}$$

where subscript i denotes the flow domain, superscript k denotes the time step and superscript m the iteration level. All coefficients are evaluated at time level $k + 1$ and iteration level m. The explicit scheme leads to the following system of equations (no iterations):

$$\begin{aligned}
[A_{Wi}]^k & \{\theta_i\}^{k+1} \\
&= [A_{Wi}]^k \{\theta_i\}^k - \Delta t \, [B_{Wi}]^k \{h_i\}^k + \Delta t \left[\{f_{Wi}\} + \{k_i\} + \{\Gamma_{Wi}\}\right]^k
\end{aligned} \qquad \text{[II.50]}$$

During the simulations, one is allowed to let the code itself switch from a fully implicit scheme to an explicit scheme. The switch point for each node depends on a saturation degree, which is set by the user. One should remember that switching should only occur at low saturation degrees, because the solution of the explicit scheme is conditionally stable ; thereby it constrains the time step to smaller values. If the saturation degree at a given node is lower (drier) than, or equal to, the user-set saturation degree, the code switches to an explicit solution scheme. In this case, modified Picard iteration does not follow –the code handles the 'explicit nodes' first. The results are used for the solution at the 'implicit nodes.' If the saturation degree at a given node is larger than the user-set saturation degree, the implicit solution scheme is used. In this case, the modified Picard iterations follow until convergence is reached for the non-linear equations.

The solution scheme for the solute transport equations leads to the following system of equations:

$$
\begin{aligned}
\left[A'_{Ci}\right]^{k+1} \{c_i\}^{k+1} &+ \omega\Delta t \left[B_{Ci}\right]^{k+1} \{c_i\}^{k+1} \\
&= \left[A'_{Ci}\right]^{k} \{c_i\}^{k} + (\omega - 1)\,\Delta t \left[B_{Ci}\right]^{k} \{c_i\}^{k} \\
&+ \omega\Delta t \left[\{f_{Ci}\}^{k+1} + \{Y_{Ci}\}^{k+1}\right] + (\omega - 1)\,\Delta t \left[\{f_{Ci}\}^{k} + \{Y_{Ci}\}^{k}\right]
\end{aligned}
$$

[II.51]

where ω is the time weighting factor. In case $\omega = 0.0$, the solution scheme is fully explicit. If $\omega = 0.5$, the solution scheme is equal to the Crank-Nicholson scheme; if $\omega = 1.0$, the solution scheme is fully implicit. A value for ω of either 0.5 or 1.0 is used to prevent numerical instabilities. The solution schemes lead to the following form of matrix equations for each flow domain:

$$
[M_W] \{h\}^{k+1,m+1} = \{b_W\}
$$

[II.52]

in case of water flow, and

$$
[M_C] \{c\}^{k+1} = \{b_C\}
$$

[II.53]

for solute transport. The $[M_W]$ matrix is symmetric and sparse, the $[M_C]$ matrix is non-symmetric and sparse. The matrix equations [II.52] are solved for $h^{k+1,m+1}$ using an iterative matrix solver procedure, called the Preconditioned Conjugate Gradient (PCG) method (e.g., Golub and van Loan, 1989) with a modified Picard iteration after each matrix solution. The matrix equations [II.53] are solved for c^{k+1} using a direct sparse matrix solver based on the Gaussian elimination method (e.g., Golub and van Loan, 1989).

Convergence of the numerical solution of the water flow equations is verified by using a relative tolerance and an absolute threshold value for the linear iterations within the same time step and an absolute value for the non-linear iterations between the time steps. All convergence checks are performed simultaneously for both the matrix and macropore domain, using identical values for the convergence parameters indicated. Convergence is reached only if the criteria are met for both domains at the same iteration or time level. Time step control is arranged by the code, which is based on the number of iterations needed to converge and a specified maximum time step. The solute transport time step control is based on the minimum of the Peclet and Courant number.

The distribution of the travel time of drainage water is a result of possible complex water flow and transport processes. If one wants to study transient flow conditions in a structured soil under different weather conditions, the steady-state approaches shown and discussed are likely to fail –to a certain extent. To better understand the hydrological

response in terms of tracer transport in a variably saturated, and possibly structured soil-water system, the numerical model presented in Sections II.2 to II.5 is used to analyze the travel time of drainage water under transient conditions. The model can handle 1D, 2D, and 3D axi-symmetric heterogeneous flow systems and hysteresis in the water retention function. Boundary conditions may vary, as well as input time series of rainfall and potential evapotranspiration; consequences of diffusion and dispersion can also be taken into account, and tracers can be applied at arbitrary amounts, dates, and parts of the upper boundary section.

6   Calculation of water and nutrient budgets

To calculate water and nutrient budgets at the field scale of the experimental field sites, hydrological and agricultural field data were used. The measurement program was often limited to the field-scale experimental site. Larger scale flow and transport processes may have influenced the local situation. Also bottom layers that were considered to be impervious, often appeared to be lowly permeable. Drainage volumes and nutrient loads transported across such boundaries were not detected.

Water budgets - The presence of an unmeasured drainage term can be illustrated by Fig. II.6.1, which shows an example situation. Measured drainage from the tile drains is denoted by Q_{meas}. Part of the local-scale excess rainfall drains directly to the ditch and to the channel, and it may become part of a regional flow component, bypassing the tile drains. These unmeasured drainage routes Q_{ditch}, $Q_{channel}$, and $Q_{regional}$ were, however, not accounted for in the calculation of the field water balance, thus constituting an unmeasured drainage term for the field-scale water budget.

Another possible discharge route is surface runoff. In case of rainfall events of long duration and/or high rainfall rates, the infiltration capacity of the soil at the surface may be exceeded. This may possibly lead to ponding and to surface runoff. Although ponding is likely to occur in short-time periods, it is not clear whether, and if, which part of the surface runoff will actually reach the surface water system. The travel paths of surface runoff to surface waters are possibly long, and they may pass dryer soil surface parts and/or small-scale soil surface depressions. Also, especially at arable land, the edges of parcels are usually sharp due to plough activities, and they function as a barrier to surface runoff. A kind of 'chain' of factors and circumstances indicated needs to be created in order to generate surface runoff that actually reaches the surface water. If even one link is missing, water will not runoff, but after ponding occurs, it will most likely infiltrate into the soil.

In this thesis, no attention is paid to the flow process at or near the soil surface that leads to actual surface runoff. The numerical models used will calculate surface runoff as soon as the infiltration capacity of the soil is exceeded, and this runoff is assumed to be actual surface runoff. If field observations are available and/or if surface runoff is likely to occur, it is taken into account in annual water and solute mass balances.
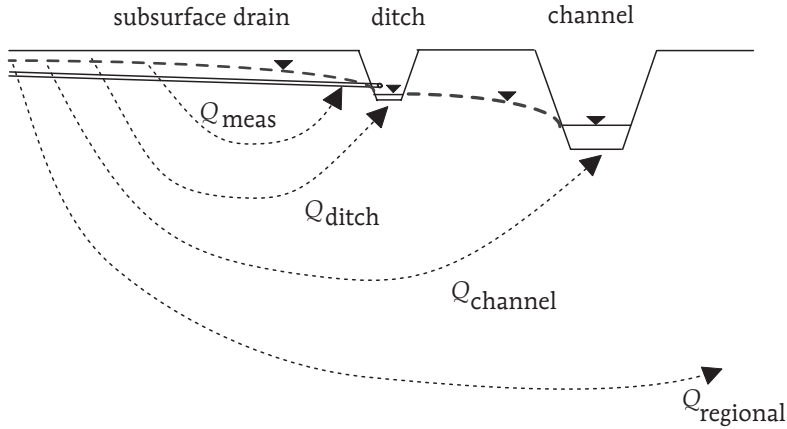
Fig. II.6.1
Calculation of the field water budget. There are four routes of excess rainfall water: the measured flow to tile drains (Q_{meas}), to the collection ditch (Q_{ditch}), to the channel ($Q_{channel}$), and a regional flow component ($Q_{regional}$). In case the latter three flow rates were not measured: $Q_{unmeas} = Q_{ditch} + Q_{channel} + Q_{regional}$.

Depending on data availability, field water budgets were set up for time periods of April through March the following year i.e., hydrologic years, and they were calculated for the experimental sites in three steps:

$$\Delta V_{w,\text{calc}} = \Delta t \left(P - ET_{a,\text{estim}} - Q_{\text{drainage}} \right) \qquad \text{[II.54]}$$

where $V_{w,\text{calc}}$ is the calculated volume of water storage in the soil profile, at the start of the calculation set to the initially measured storage volume, P is measured rainfall rate, $ET_{a,\text{estim}}$ is the estimated actual evapotranspiration rate, Q_{drainage} the measured discharge (tile drains, collection ditch), and Δt the time interval [d]. Using [II.54], the change of storage volume $\Delta V_{w,\text{calc}}$ was calculated at the end of each time step.

$$\text{If} \quad V_{w,\text{calc}} > V_{w,\text{max}} \quad : \quad Q_{\text{unmeas}} = \frac{V_{w,\text{calc}} - V_{w,\text{max}}}{\Delta t} \qquad \text{[II.55]}$$

where V_{max} is the maximum storage volume, calculated from the total porosity of the different soil layers. Using [II.55], an extra, unmeasured drainage term Q_{unmeas} is

introduced in case the calculated volume exceeded the maximum storage capacity. This unmeasured discharge, drained by means other than tile drains (Fig. II.6.1), was calculated because the measured discharge from the tile drains was already accounted for in [II.54]. $V_{w,\text{calc}}$ is adjusted after this second step. $V_{w,\text{meas}}$, determined from field measurements on soil water contents and groundwater levels, then used in the third and last step:

$$\text{If} \quad V_{w,\text{calc}} \neq V_{w,\text{meas}} \quad : \quad Q^*_{\text{unmeas}} = Q_{\text{unmeas}} + \frac{V_{w,\text{calc}} - V_{w,\text{meas}}}{\Delta t} \qquad \text{[II.56]}$$

where Q^*_{unmeas} is the corrected unmeasured drainage, as a result of the calculation method presented.

Rainfall measurements - In the Netherlands, rain gauges are often installed at 0.4 m above the soil, which is the standard measuring height as used by the Royal Dutch Meteorological Institute. At this height, a systematic error ranging from 2% to 8% occurs, due to air turbulence around the gauge. This so-called wind effect leads to an underestimation of the actual rainfall rate (e.g., Braak, 1945; Colenbrander and Stol, 1970; Neff, 1977; Dekker, 1979; Buishand and Velds, 1980). In this thesis, measurements on rainfall rates were retrieved from rain gauges installed at, or as close as possible, to the soil surface to reduce the wind effect.

Nutrient budgets - Nutrient balances can be principally set up for three different systems by accounting for the incoming and outgoing fluxes along with the storage change across the system boundaries. Oenema and Heinen (1999) define three balance systems: 1) The so-called farm gate balance has a virtual boundary i.e., a fence around the farm as a whole, and it is used in the MINAS nutrient accounting system (Chapter I). 2) The so-called soil surface where the incoming and outgoing fluxes across the virtual plane of the soil surface are accounted for. 3) An extension of the soil surface balance, the so-called soil system balance, which also covers the internal processes, sources, and sinks in the soil and groundwater system. The soil system balance provides the most information on nutrient flows within the soil and groundwater system, but it also needs the most field data and knowledge. In this case, estimated annual soil system balances for salt and nutrients i.e., nitrogen N, and phosphorus P are presented for specific field locations. The net term from the soil surface balance is used, combined with estimates for soil chemical processes like sorption and denitrification.

The nutrient budget of the experimental sites was based on a soil system balance as schematically shown in Fig. II.6.2. This figure shows all mass fluxes taken into account, which are applicable to the specific nutrient. The farmer or farm staff registered agricultural practices at the sites. Cultivated crops, harvest, fertilizer and manure used, and nutrient contents of the soil (soil fertility information) were provided for, and based

on these data, annual nutrient budgets could be calculated. During the field experiments specific investigations or measurements were not performed on physical-chemical-biological processes involved in soil nutrient dynamics such as denitrification of NO_3-N or P-adsorption to the solid phase.
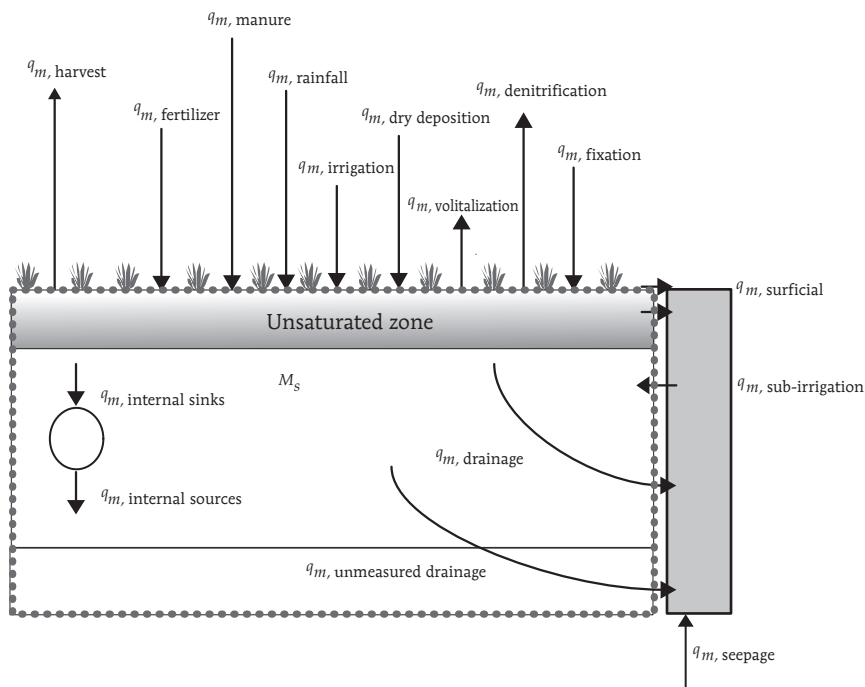
Fig. II.6.2
Nutrient budgets for experimental sites. Schematic nutrient budget of agricultural land based on the soil system balance. Nutrient mass rates q_m across system boundaries (dotted line) and internal sinks and sources of nutrients.

Annual nutrient budgets were calculated from February through January the following year. This balance period deviates somewhat from the water balance period. It was chosen to account for possible early spring applications of fertilizer and manure, which are allowed globally after February. The soil system balance surplus and drainage loads were related by applying the fractions of the travel time distribution of drainage water and the surplus accompanying each fraction. The first year fraction f_1 of the travel time distribution was coupled with the nutrient surplus for the same year; the f_2 fraction was coupled with the nutrient surplus of the previous year, the f_3 fraction with the nutrient surplus of the year before the previous year, etc.

7   Conclusions

Chloride and nutrients applied to the soil surface find their way to groundwater and surface water as a result of drainage in a variably-saturated flow medium. In analyzing agriculture and the use and outcome of nutrients, it is useful to construct soil system balances. Estimated chloride and nutrient surpluses of these soil system balances can be used to estimate losses to the water environment. Solutes in drainage water originate from atmospheric deposition, agriculture, soil material, and history, such as the year and time of application. The travel time distribution of drainage water is a key factor to understand and interpret solute loads of drainage water.

Solute concentrations of tile-drained water vary with time. Variations occur from year to year, and within a single drainage season. Trends might occur in solute concentration time series, as well as in variation around an average concentration. These variations reflect a transient reality as far as the travel time distribution of drainage water is concerned. Analytical approaches do not take the time-variable infiltration into account from day to day, from summer to winter, or from wet to dry years. Also, the flow process in the unsaturated zone, with preferential flow in structured soils as a special and extreme case, is excluded in the steady-state approaches. Consequentially, the Ernst (1973) and Bruggeman (1999) approaches can be further elaborated or replaced by numerical modeling analysis to calculate possible time-variable solute concentrations in tile drainage. Drainage water with short travel times will be especially influenced, whereas 'older' water is likely to contribute more consistently to the total drainage water.

The *steady-state approaches* discussed that calculate the travel time drainage water initiated from a number of assumptions and boundary conditions. The application of these approaches to practical situations is limited, but still possible as Meinardi and Van den Eertwegh (1997) showed. These methods have their shortcomings but they can be useful because they are simple and they need only a small number of parameters. Of major importance are the depth of the local-scale flow system d, the effective porosity of the flow medium Φ_{eff}, and the weather conditions.

When soils with a variably-saturated flow medium are considered and one wants to analyze the effect of short-term weather influence, a *numerical modeling approach* is recommended to calculate travel times of drainage water under transient conditions, especially for structured field soils. A *dual-porosity* flow and transport code is used to perform 2D modeling of transient water flow and tracer transport, focusing on the *field-scale hydrology*. To construct a model, parameter estimates are needed to characterize the structure of the flow medium and the soil-physical and tracer transport behavior. Also parameters are needed for the matrix-macropore interface with respect to mass transfer between domains, the actual crop, and the drainage situation. Independent

parameter estimates are partially available, such as soil-physical parameters for small-scale soil samples. Some other parameter values are, however, hard to determine in the field situation because it is difficult to find a plot-scale representative value.

The soil-chemical processes in the soil and groundwater system are not accounted for by the dual-porosity flow and transport code. An exception is made for adsorption processes, causing retardation effects. The main reason to omit the soil-chemical processes in transient and field-scale modeling is that the focus in this thesis is on the *physical transport process* and on the effect of *travel times of drainage water* on drainage water quality. The information on the physical transport process, as generated by the numerical models, is used to construct solute budgets at the field and regional scale. The effect of soil-chemical processes is taken into account in the mass balances of annual solute at these scales.

III

STEADY-STATE ANNUAL WATER FLOW AND SOLUTE TRANSPORT AT REGIONAL SCALE

1 Introduction

Chapter II was based on a description of the hydrological and solute transport processes at the *field scale*. These modeling efforts, however, do not immediately lead directly to a description that is appropriate to apply at the *regional scale*. The regional approach leads to a method that calculates regional-scale water and solute fluxes to the regional surface water system in an area. *A model approach based on mass balance equations is set up, operating on a regional scale, and calculating water, chloride, and nutrient budgets and, on an annual basis, mass fluxes to the regional surface water*. These annual mass fluxes occur between the two systems i.e., the land area and the regional surface water, and they represent the annual exchange of water and solute mass. The regional approach calculates an annual, regional-scale travel time distribution of drainage water and the mean annual residence time of water in the surface water system. The travel time distribution of drainage water varies from year to year, dependent on the weather conditions. Two systems are defined: 1) The mobile liquid phase of an hydrologically defined soil and groundwater system i.e., land area including the local-scale surface water, and 2) The regional surface water system. The method incorporates the travel time distribution of drainage water from the land area on an annual basis.

2 Conceptual steady-state regional approach

The regions that will be modeled in this thesis are composed of land area, small-scale surface water bodies, and regional surface water bodies. The land area is composed of a complex of farms, natural areas, residential housing, suburban areas and urban areas. Both the small-scale surface water bodies and the regional surface water bodies receive water and solute mass fluxes that leave the land area by drainage. Water is drawn from the regional-scale water system during the occurrence of sub-irrigation for the land area. The small-scale surface water included in the land area is surface water that can be neglected as far as water and solutes storage and residence time is concerned. *The land area of the region is subdivided into sub-regions, whereas the regional surface water system is treated as one single system.* The sub-regions are geographical areas, each having their own

hydrological boundaries. As far as the land area is concerned, sources and sinks of water and solutes originate from mass transfer across the upper and lower system boundaries and they exchange with the solid phase of the soil-groundwater system. The land area and the regional surface water have their own domain boundaries. The system boundaries are the 'Regional surface water system' at the side, and the 'Hydrological divide' at the side and bottom as schematically shown in Fig. III.2.1.
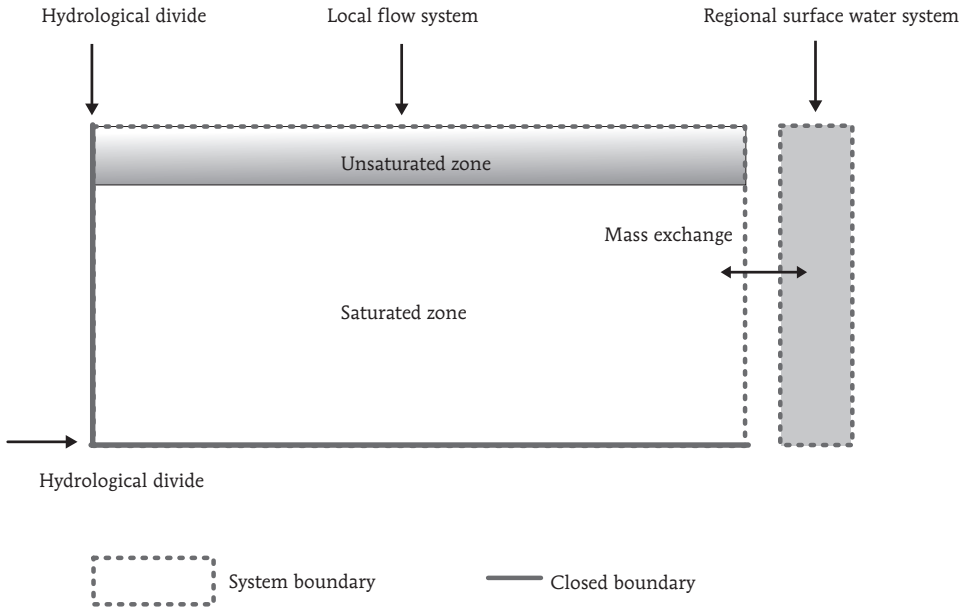
Fig. III.2.1
Regional approach. System boundaries are shown for local flow system and regional surface water system. The left and bottom boundaries of the local flow system are practically impermeable, and they serve as hydrological divide.

The regional approach calculates drainage and solute fluxes from the liquid phase in the unsaturated and saturated zone of a specific and hydrologically-defined region to the regional surface water system on an annual basis, using hydrologic years from April through March. Inflow and outflow across the system boundaries are presented as annual water and solute fluxes, and internal sinks and sources of solutes can be taken into account. The input of solutes across the land surface is based on soil surface balances of chloride, total-N, and total-P. In the model, the regional surface water system has one outlet and one inlet. Possible effects of transport through the surface water or residence time of water and solutes, as well as chemical processes within the surface

water system itself are not taken into account because the approach assumes *steady-state flow conditions* and *chemical equilibria* during the one-year time scale. The approach uses mass balance equations for water and solutes. Storage change of water in soil and surface water are neglected because it is assumed that on, or around April 1, the starting date of a new hydrologic year, identical field capacity conditions prevail throughout the years. Fig. III.2.2 schematically shows a region with six sub-regions and the outlet. The annual boundary fluxes of water and solutes for the region need to be previously known.
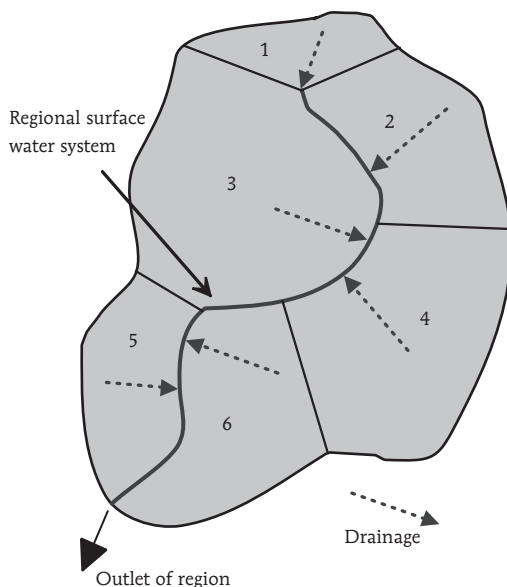
Fig. III.2.2
Regional approach. Schematic model region sub-divided into sub-regions numbered 1 to 6, each showing sub-regional drainage to the regional surface water system and to the regional outlet.

The choice and definition of the (number of) sub-regions depends mainly on geography and hydrology, effective porosity Φ_{eff}, drain spacing L, and depth of local-scale flow system d, taking into account the dominant soil type, dominant Groundwater Table Class (GTC), and type of land use (Appendix C, Table C.1). In the Netherlands, seven major GTCs are defined: GTC I through VII (Table III.2.1). The GTC represents the long-term groundwater regime, indicating seasonal differences. The GTCs were mapped for the Netherlands on a 1:50 000 scale in the period of 1960-1980. Region-wise updates of this mapping are currently carried out. The increase of land drainage activities has caused a general shift in GTCs from wet to drier conditions.

Table III.2.1

Regional approach. Groundwater Table Classes (GTC), used in the Netherlands. *MLG: mean lowest groundwater level. **MHG: mean highest groundwater level; both are shown in [m] below the soil surface.

Groundwater Table Class (GTC)	MLG*	MHG**
I	< 0.50	(< 0.20)
II	$0.50 - 0.80$	(< 0.40)
III	$0.80 - 1.20$	< 0.40
IV	$0.80 - 1.20$	> 0.40
V	> 1.20	< 0.40
VI	> 1.20	$0.40 - 0.80$
VII	(> 1.60)	> 0.80

The last factor is the regional-scale groundwater recharge or seepage rate.
Each sub-region represents a fraction of the total land area of the region. The travel time distribution of drainage water from a sub-region is divided into a maximum of five travel time fractions $f_\tau(\tau = 1, \ldots, 5)$ of the total travel time distribution of drainage water. Mixing of drainage water with different travel times occurs as soon as water leaves the flow domain and enters the surface water system. The travel time fractions are calculated by the model and are derived initially from a steady-state analysis using the Ernst-Bruggeman approach (Section II.2). These fractions are a function of I or I^*, d or d^*, and Φ_{eff}, and vary annually as infiltration I varies annually. Manual adjustments of the f_τ fractions are possible and can be the result of transient analysis as will be shown in Chapters IV and V.

The model is set up to treat major soil types clay, loam, sand, and peat. The GTC may vary from I through VII. The land use types to choose from are:

  – grassland,
  – corn cultivation,
  – arable land, represented by a 1:3 rotation of potatoes, sugar beet, and winter wheat,
  – orchard,
  – rural area, or
  – urban area.

The land use type –'rural area'– is assumed to consist of a mixture of grass, bushes, trees, and farmyards distributed across a rural region.

For each of the soil types, a dominant GTC and land use type are introduced because of differences in

- hydrology, for example, in travel times of drainage water, in discharge routes, and/or in $Q_{\text{surficial}}$ (e.g. Meinardi, 1991),
- agricultural use, for example, in crops and/or nutrient applications, and
- chemical processes in the soil-water-system, for example, denitrification of NO_3-N (e.g. Boumans et al., 1989) or sorption of P (e.g., Schoumans and Groenendijk, 2000).

3 Water budget for sub-regions and regional surface water system

The water budget for a *sub-region* is shown schematically in Fig. III.3.1 and can be calculated as

$$\Delta V_{w,\text{tot}} = P + Q_{\text{irrig}} + Q_{\text{sub}-\text{irrig}} - ET_a - Q_{\text{surficial}} - Q_{\text{drainage}} \qquad \text{[III.1]}$$

On an annual basis, $\Delta V_{w,\text{tot}}$ is assumed zero. If $P - ET_a$, on an annual basis, is calculated as negative, an annual minimal drainage rate of 5 mm a^{-1} is introduced. $Q_{\text{surficial}}$ is the surficial runoff rate from the land (surface runoff and interflow), $Q_{\text{sub-irrig}}$ is the sub-irrigation rate from the regional surface water system to the soil, and Q_{irrig} is the irrigation rate (Fig. III.3.1). ET_p is calculated from ET_r according to [II.24] with an annual average crop factor f_c per land use type, which represents the 'average crop' for a sub-region. Using an estimate of the reduction rate based on soil type, crop, and GTC (Werkgroep HELP-Tabel, 1987), ET_a is calculated (Appendix C, Table C.2). E_i is not specified and is incorporated in ET_a. Annual average values for $Q_{\text{surficial}}, Q_{\text{sub-irrig}}$, and Q_{irrig} need to be specified by the user for each sub-region.

If seepage occurs, it is assumed that on an annual basis, *all seepage water and dissolved solutes end up in the regional surface water system*; therefore, Q_{seep} is not implemented in [III.1]. It seems likely that in practice a fraction of the total groundwater seepage ends up in the soil profile of the land area, thus contributing to ET_a, especially in areas with controlled surface water levels. However, in areas with free drainage and no surface water supply the assumption is most likely suitable. Furthermore, Q_{seep} is assumed to be constant input throughout the years; in practice, year to year variations may occur due to variable weather conditions. To calculate travel time distribution of drainage water, the parameters d and Φ_{eff} need to be known. Depending on the infiltration rate, seepage rate,
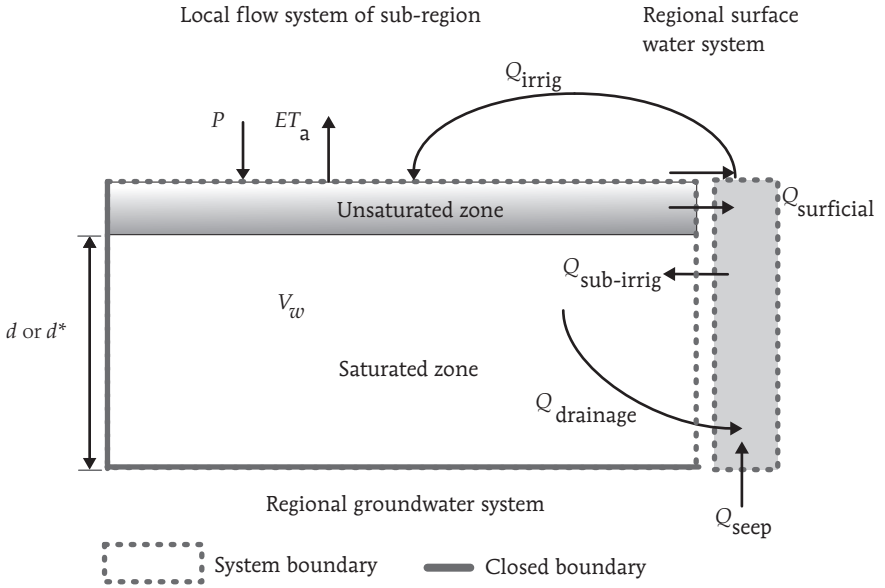
Fig. III.3.1
Regional approach. Water budget for local flow system of sub-region showing mass fluxes. Note: Q_{seep} is used only for the regional surface water system.

and occurrence of radial flow components, the depth of the local-scale flow system d is reduced to d^* or to d^{**} (Section II.2).

The total volume of water per unit of length stored in the soil profile in a sub-region $V_{w,\text{tot}}$ is calculated as

$$V_{w,\text{tot}} = d\,\Phi_{\text{eff}} \qquad \text{[III.2]}$$

$\Delta V_{w,\text{tot}}$ in [III.1] can be calculated from this value. The drainage outflow for a sub-region is divided into travel time fractions (Fig. III.3.2), according to

$$Q_{\text{drainage},\tau} = f_\tau\, Q_{\text{drainage}} \qquad \text{[III.3]}$$

where

$$Q_{\text{drainage}} = \sum_{\tau=1}^{5} Q_{\text{drainage},\tau} \qquad \text{[III.4]}$$

After calculating the water budget for all sub-regions, water balances for the *regional surface water system* are set up. Relevant 'shape factors' for this system are its area A_{sw}, to
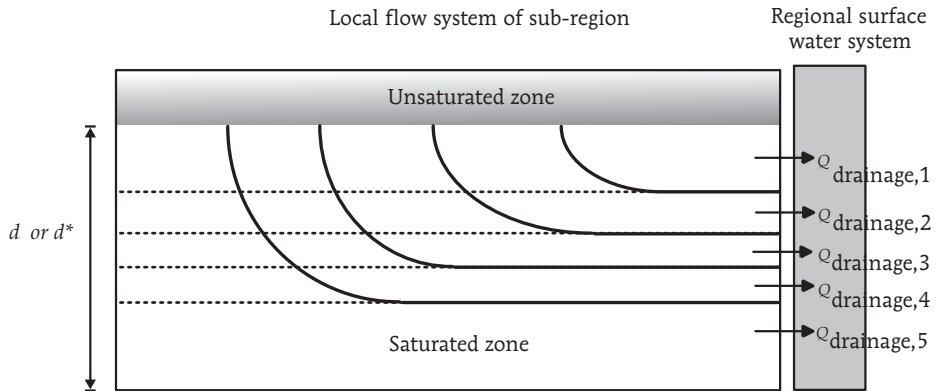
Fig. III.3.2
Regional approach. Schematic overview of the local flow system of sub-region, showing division of total drainage rate Q_{drainage} into drainage rates $Q_{\text{drainage},\tau}$ belonging to travel time t_τ with τ =1 to 5.

calculate the contribution of P and ET_a, and volume $V_{w,sw}$ to calculate the residence time. The water balance for the regional surface water system is schematically shown in Fig. III.3.3 and can be calculated according to

$$\Delta M_{W,sw} = P + Q_{\text{drainage}} + Q_{\text{surficial}} + Q_{\text{inlet}} + Q_{\text{seep}} \\ + Q_{\text{point}} - Q_{\text{irrig}} - Q_{\text{sub-irrig}} - ET_a - Q_{\text{outlet}} \qquad \text{[III.5]}$$

On an annual basis, $\Delta M_{W,sw}$ equals zero. To calculate ET_a from open water, a 'crop factor' $f_c = 1.25$ is used. The field locations, at which inlet and outlet of water into and away from the regional-scale water system takes place, are usually measurement locations for both water quantity and quality. In this case, field data such as discharge measurements are often available; hence, this balance term is used as a final mass balance check for the annual water budget.

A special point of interest is the annual average residence time of water within the surface water system, as calculated by

$$t_r = \frac{V_{w,sw}}{Q_{\text{incoming},t}} \qquad \text{[III.6]}$$

where $Q_{\text{incoming},t}$ is the sum of all mass rates of water entering the regional surface water system. t_r is a factor of influence regarding, for example, chemical processes inside the surface water system like denitrification of nitrate and sorption of phosphate to ditch bottom sediments.
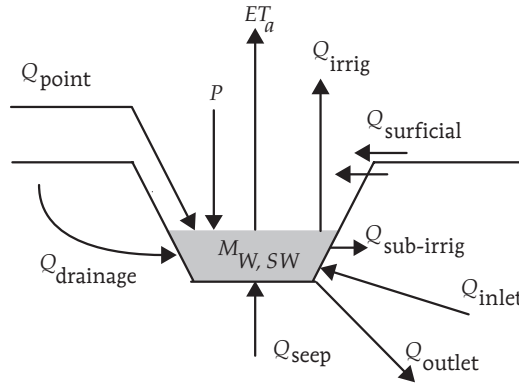
Fig. III.3.3
Regional approach. Water balance terms for regional surface water system.

4 Solute budget for sub-regions and regional surface water system

The solute mass balance terms q_m are shown in Fig. III.4.1. Mass fluxes of internal sinks and sources are the result of processes like mineralization, degradation, diffusion, desorption, and sorption (Section II.6). The data input for the regional model on these processes is region specific and may also differ between sub-regions within a region.

Calculation of the annual solute mass balance is as follows. Starting with a certain solute mass stored M_S in the liquid phase of the flow region, the incoming solute mass in a year is computed as

$$\begin{aligned} \Delta M_S = &\ q_{m,\text{rainfall}} - q_{m,\text{surficial}} + q_{m,\text{irrig}} + q_{m,\text{sub-irrig}} + q_{m,\text{dry deposition}} \\ &+ q_{m,\text{fertilizer}} + q_{m,\text{manure}} + q_{m,\text{grazing}} - q_{m,\text{volatilization}} + q_{m,\text{fixation}} \\ &+ q_{m,\text{mineralization}} - q_{m,\text{degradation}} + q_{m,\text{diffusion}} - q_{m,\text{harvest}} \\ &+ q_{m,\text{desorption}} - q_{m,\text{adsorption}} - q_{m,\text{drainage}} \end{aligned}$$

[III.7]

As far as the total-phosphorus mass balance is concerned, desorption and sorption terms do not appear at the same time in the equation. The net result of both processes returns in [III.7]. Note that the terms considering NH_3-volatilization, N-fixation, for example, by clover, and denitrification only influence the total-N mass balance. The annual NH_3-volatilization is calculated according to (Van Beek and Oenema, 2002)

$$q_{m,\text{volatilization}} = 0.02\, q_{m,\text{fertilizer}} + 0.10\, q_{m,\text{manure}} + 0.08\, q_{m,\text{grazing}}$$

[III.8]
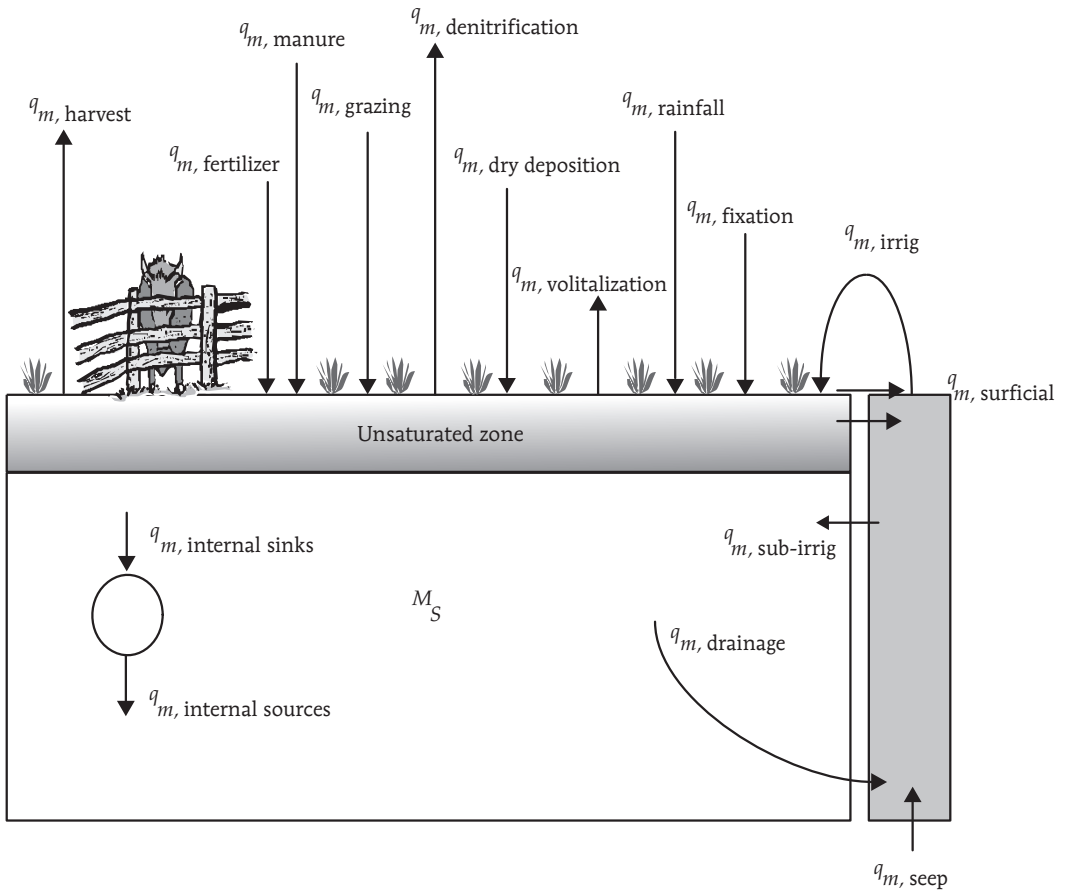
Fig. III.4.1
Regional approach. An illustration showing an overview of solute mass balance terms q_m for a sub-region. Mass fluxes of internal sinks and sources are the result of processes like mineralization, degradation, diffusion, desorption, and sorption. Harvesting includes the grazing of livestock. Note that $q_{m,\text{seep}}$ is used for the regional surface water system only.

The solute mass loss term by harvest and grazing varies annually by

$$q_{m,\text{harvest}} = q_{m,\text{harvest average}} \frac{ET_a}{ET_{p,\text{long-term}}}$$ [III.9]

The values for $q_{m,\text{harvest average}}$ are derived from literature references (e.g., Schröder, 1999; Stouthart and Leferink, 1992; Meurs and Booij, 1999). $ET_{p,\text{long-term}}$ is based on 30-year average data by the Royal Dutch Meteorological Institute at five meteorological stations across the Netherlands.

To calculate q_m for surficial runoff, irrigation, and sub-irrigation, and information is needed on the solute concentrations of these water mass fluxes. $C_{\text{surficial}}$ is needed as model input, and it is a function of soil and land use. Values for C_{irrig} and $C_{\text{sub-irrig}}$ are computed by the model. These concentrations are equal to the annual average solute concentration in the regional water system. The mass flux associated with the sinks and sources terms is a function of soil type, of GTC, and of land use (N only) and are specified for each separate sub-region.

The diffusion of solutes from the solid phase to the liquid phase is defined by a fixed mass flux. Diffusion is proportional to the concentration gradient. Volker and Van der Molen (1991) showed the process of Cl-diffusion in the subsoil of the Noordoostpolder region, northeast of the Flevopolder area (Fig. I.2.1). De Vos (1997) calculated an annual mass rate of 220 kg ha^{-1} a^{-1} for a loamy soil in this region as a result of diffusive upward transport of Cl$^-$. One is able to implement a diffusion component in the solute mass balance for a sub-region separately by setting an annual diffusion mass rate.

Mineralization of organic matter by oxidation of organic matter (e.g., Hassink, 1995) as a source of solutes is treated as a fixed mass flux, a function of soil type and GTC. The soil type is assumed to determine the amount of organic compounds stored in the profile. Peat soils have the largest organic matter mass storage, followed by clay, loamy, and sandy soils. The GTC is a measure of the drainage situation and determines the oxygen presence in the soil profile. The drier the GTC, the more, and to a deeper extent, oxygen is assumed to be present, and the higher the mineralization rate is expected, given the presence and availability of soil organic matter.

Degradation of solutes in this case only applies to nitrogen, with denitrification as the main process. Denitrification of NO$_3$-N into gaseous nitrogen compounds is treated as a sink term. The process is determined by the availability of NO$_3$-N and organic matter, the lack of oxygen, the soil temperature, and/or the presence of pyrite (e.g., De Klein, 1994; Corré, 1995). The denitrification rate is also a function of the fertilizer and manure application level, but this functional relation is omitted in this case. The best circumstances for denitrification to occur are wet conditions with high organic matter contents present in the soil profile. Denitrification at peat soils is assumed to be the

largest compared to other soils, followed by clay soils, loam, and sandy soils. At a drier GTC, the denitrification rate will be smaller.

Desorption and sorption of phosphate are a function of P-surplus at the soil surface, soil P level, P saturation of the soil profile, solid phase characteristics, and drainage situation (e.g., Van der Zee, 1988; Van Riemsdijk, 1990; Schoumans et al., 1991; Van der Salm et al., 1995). Schoumans (1997) concluded that it will take one to several decades for soil P levels to decrease after the identification of a negative soil surface P balance.
The P-desorption rate is small, and here desorption of phosphate is occurring only if the P-surplus from the soil-surface balance is negative. No distinction is made between soil types. At a drier GTC, a smaller desorption rate is used. Iron and aluminum (hydr)oxides at/near the solid phase surface and clay minerals play an important role in the sorption process. The annual mass rate of P-sorption is taken as a fraction of the P-surplus from the soil-surface balance. Again, no distinction is made between soil types. At a drier GTC, a larger fraction of the P-surplus is adsorbed.

The solute concentration in the incoming water for each sub-region is calculated as

$$C_{\text{in},t} = \frac{q_{m,\text{in},t}}{I^*} \qquad\qquad \text{[III.10]}$$

The solute mass load of the drainage water leaving the soil and groundwater system is calculated by

$$q_{m,\text{drainage},t} = \sum_{\tau=1}^{5} Q_{\text{drainage},\tau}\, C_{\text{in},\tau-1} \qquad\qquad \text{[III.11]}$$

The solute concentration in the drainage water is calculated by

$$C_{\text{drainage},t} = \frac{q_{m,\text{drainage},t}}{Q_{\text{drainage}}} \qquad\qquad \text{[III.12]}$$

Finally, the solute mass stored in the liquid phase of a sub-region M_S is adjusted by the difference between incoming and outgoing mass fluxes.

A first order decay function can be used to describe the removal of nitrogen by degradation, for example, the removal of nitrate by bacteria:

$$C(t) = C_0^{-n_d t} \qquad\qquad \text{[III.13]}$$

where n_d is a decay coefficient $[\text{a}^{-1}]$. The idea behind using degradation as a function of time is that time can be translated into a groundwater flow route, connected with a travel time. As time progresses, groundwater remains in the system longer, and a flow route is possibly longer and deeper, increasing the chance of nitrogen removal. Wessel (1987) reported on the maximum relative growth rate of two types of denitrifying bacteria under

anaerobic conditions at $T = 25^oC$. Reported rates were between 0.014 and 0.25 h^{-1}. If the growth rate of these bacteria would be 1:1 and coupled linearly with the degradation rate of NO_3-N, one could derive values for n_d. Whether this is valid or not, in practice the conditions within the soil system also deviate temporally and spatially from those assumed or used in theoretical approaches. Therefore, the value of n_d is roughly estimated, given solute mass balance information on annual denitrification rates for different soil type, groundwater table class, and crop combinations.

On the other hand, denitrification of nitrate can be modeled as a process of NO_3-N removal, either completely or partially, depending on the characteristics of the soil layer. This type of degradation is e.g., likely to occur if groundwater with nitrate passes a soil layer with pyrite FeS_2, which is able to reduce all NO_3-N. This feature can also be used in the approach by specifying the number of years from the moment of infiltration per sub-region after this layer is passed by the groundwater. The nitrate concentration in groundwater, which is older than this pre-set number of years, is set to be equal to zero.
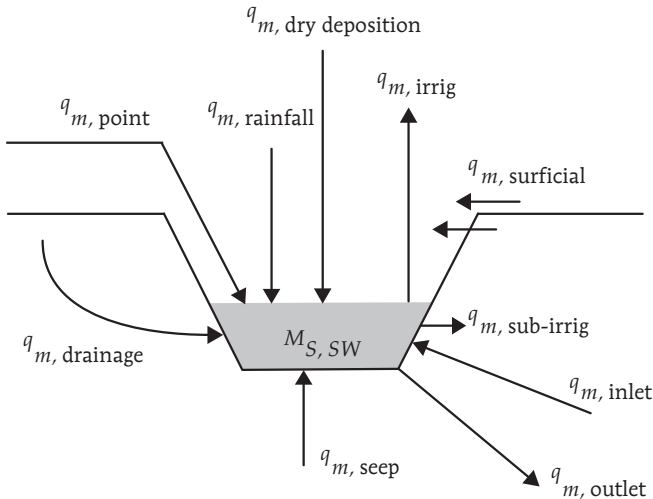
Fig. III.4.2
Regional approach. Solute mass balance terms for the regional surface water system.

After calculating the mass balances of solutes for all sub-regions, mass balances for the regional surface water system are being set up. The solute flux terms for this system are schematically shown in Fig. III.4.2.

The solute mass balance equation is as follows:

$$\Delta M_{S,\text{SW}} = q_{m,\text{rainfall}} + q_{m,\text{dry deposition}} + q_{m,\text{surficial}}$$
$$+ q_{m,\text{point}} + q_{m,\text{inlet}} + q_{m,\text{drainage}} + q_{m,\text{seep}} \qquad \text{[III.14]}$$
$$- q_{m,\text{irrig}} - q_{m,\text{sub-irrig}} - q_{m,\text{outlet}}$$

On an annual basis, $\Delta M_{S,\text{SW}}$ is assumed to be zero. The chloride budget of the surface water system is expected to be in balance due to the inert chemical behavior of chloride. Nitrogen and phosphorus budgets in surface waters are also likely to be in balance, but uptake, storage, and decay processes can conceal this balance. As far as total-N is concerned, the total incoming mass flux is expected to be larger than the outgoing mass flux, and retention and losses of nitrogen within the surface water system itself are likely to occur. Denitrification and biological fixation are also expected to occur. The same balance difference holds for total-P as well, and in this model sorption to sludge may cause net storage of phosphorus within the surface water system.

To implement the model, general information is needed on the area of the region, its possible sub-regions (land area including the small-scale surface water area), and its regional surface water system (area and volume). Long-term average boundary fluxes (water) are needed at the region scale, including information on Q_{seep}, $Q_{\text{surficial}}$, Q_{irrig}, and $Q_{\text{sub-irrig}}$. On the sub-regional level, data on dominant soil type, GTC, and land use also needs to be available. The effective porosity Φ_{eff} and depth d of the local-scale drainage system of a sub-region, combined with meteorological data, will determine the travel time distribution of drainage water. The Ernst-Bruggeman approach is used in this model to give a first estimate of this distribution, then the travel time fractions f_τ ($\tau = 1, 5$) can be manually adjusted.

Additional data that needs to be considered for the regional model includes the following data related to land use including:

- average crop factors and crop uptake mass rates,
- annual application rates of fertilizer and manure, and
- annual rates of sinks and sources as a result of chemical processes within the soil-groundwater system that have an effect on solute mass balances.

Also, the chemical composition of water that originates from deep groundwater seepage and water inlet needs to be provided for. Estimates are needed for long-term values and time series of annual sums of P and ET_r, for the chemical composition of the rain (Cl, total-N, and total-P), and for the total of dry deposition of the indicated solutes. At last, annual water flow and solute mass rates originating from point sources are input data to the regional surface water.

5   Conclusions

In this Chapter, a steady-state approach to calculating the annual water flow and solute loads to a regional surface water system is presented. This approach uses water and nutrient budgets as a means to control mass fluxes. A region consists of a number of sub-regions and a regional surface water system. The regional approach leads to an integration of several solute sources and sinks present within an area, which results in solute loads to the surface water system on an annual basis, taking the travel time distribution of the drainage water into account. The travel times of drainage can vary across a region. Therefore a number of significantly different sub-regions can be defined, therefore, differences in travel times might originate not only from weather conditions, from soil types and hydrology, but also from the type of land use. The regional approach leads to the calculation of a regional travel time distribution of drainage water.

Solute loads to the regional surface water originate from different source types i.e., point and diffuse sources, which are taken into account. Solute loads from the sub-regions to the regional surface water system can be compared to calculated solute loads at the regional outlet or, in a polder area –the pumping station. This comparison leads to conclusions on the effect of processes within the surface water system itself. The annual average residence time of water and solutes within this system can be calculated, as well as the relative contribution of different source types to the total load.

IV

RESULTS OF FIELD EXPERIMENT FLEVOLAND

1   Introduction

General - During the period from June 1992 to June 1994, a field experiment was executed by Groen (1997) in the central part of Flevoland on the hydrology and leaching characteristics of a structured, heavy clay soil (Fig. IV.1.1). The experiment had been set up by the Ministry of Transport, Public Works, and Water Management to study plot-scale pesticide leaching. An extensive report on the experimental setup and analysis of hydrology and pesticide leaching was given by Groen (1997). The scope of the experiment was enlarged to study nutrient leaching as well being a part of the research program of the National Institute of Public Health and the Environment (RIVM).

During two subsequent years field observations on tile drain discharge were performed on two different plots i.e., Plot 1 and Plot 2 (Fig. IV.1.2), and with potatoes being grown on both plots. In addition, field measurements were also performed on the catchment area of the draining and collection ditch defined as 'Ditch'. Reports on the field data were written by Meinardi and Van den Eertwegh (1995), Brongers et al. (1996), and Meinardi and Van den Eertwegh (1997).

Soil and drainage system - Holocene sediments locally confine a sandy aquifer of Pleistocene origin (Ente et al., 1986). The soils consist of clay sediments of IJsselmeer and Zuider Zee deposits. The plough layer runs from the soil surface down to 0.3-0.4 m deep, likely to be followed by a plough pan. From that depth downward to about 1.0-1.5 m below the soil surface, heavy clay deposits are found with permanent and interconnected cracks due to the ripening of the clay soil after reclamation. The crack widths vary between 0.03 and 0.05 m. The basaltic clay columns have a diameter between 0.2 and 0.3 m. From a depth of 1.2 m to 1.5 m below the soil surface, clay deposits, if present, are not ripened, resulting in a low-permeable soil layer (Groen, 1997), hydrologically about closing the soil-water-system at the bottom boundary. In case the total clay layer does not reach deeper than about 1.2 m, the cracks connect the upper soil with the sandy aquifer (Fig. IV.1.3). It is known from geological surveys (Ente et al., 1986) and geo-electrical measurements (Meinardi and Van den Eertwegh, 1995) that the clay layer thickness varies at the site and roughly increases from southwest to northeast. It is likely that at Plot 1, the clay layer is thinner compared to the

Fig. IV.1.1
Flevoland experimental site. Location of experimental site in the Flevopolder area
(by Van Duin and De Kaste, 1989).
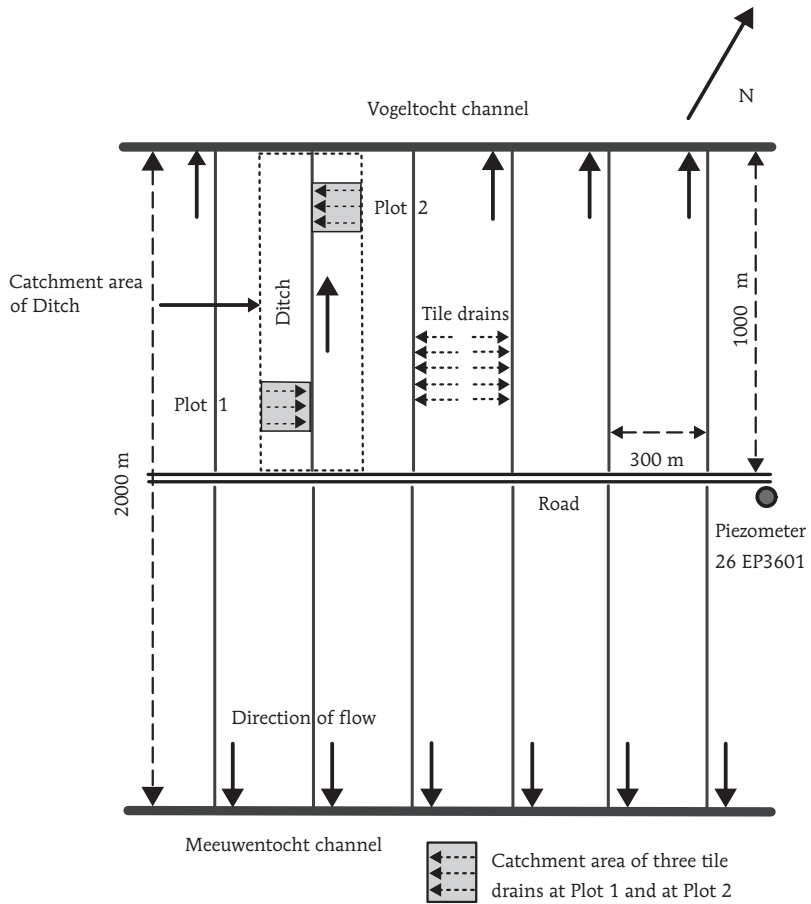
Fig. IV.1.2
Flevoland experimental site. Schematic map shows the locations of Plot 1 and Plot 2 of each 2.16 ha, being the catchment area of three subsurface drains, and the 30 ha catchment area of Ditch, which is indicated between dashed lines.

layer at Plot 2. It is important to note that a different soil profile possibly leads to a different hydrological situation.
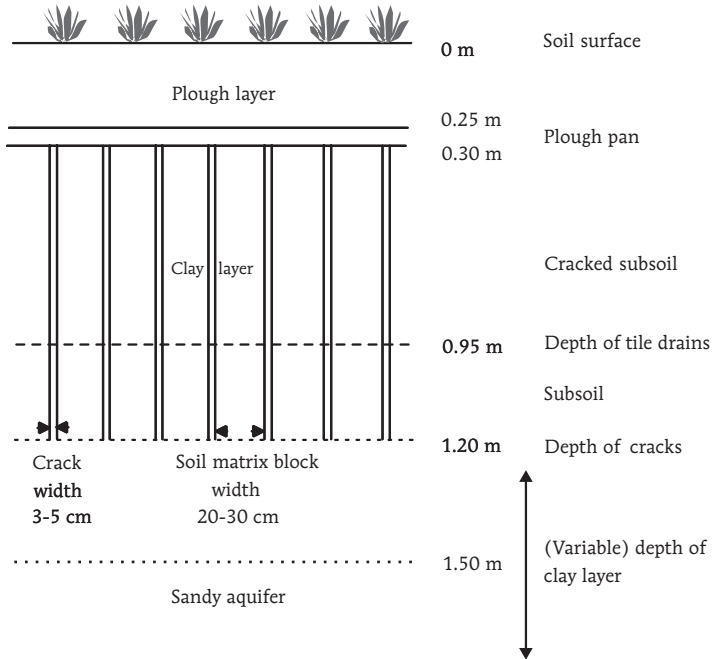
Fig. IV.1.3
Flevoland experimental site. Schematic outline of the general soil profile, showing the plough pan and the *permanently cracked subsoil*. The depth of the cracks is about 1.2 m below the soil surface. If the clay layer is less than 1.2 m deep, the subsoil is fully ripened and the cracks run down to the sandy aquifer. Tile drains are installed at 0.95 m in depth to the soil surface.

The drainage system in the area of the experimental site consists of tile drains, collection ditches, and water-level controlled channels (Fig. IV.1.4). Tile drains are installed at 0.95 m depth at a 48 m spacing. Their slope is about 1‰, and their length is 150 m each. The collection ditches have a length of approximately 1000 m, are 1 to 1.5 m deep, have a 0.5‰ slope and drain freely into the channels. The collection ditches receive outflow from the tile drains, direct drainage from subsurface flow, and any surface runoff from the connected field area. The channel has a fixed and constant water level throughout the year, which is controlled by the regional Zuiderzeeland Water Board. The channel flows into the main channel.
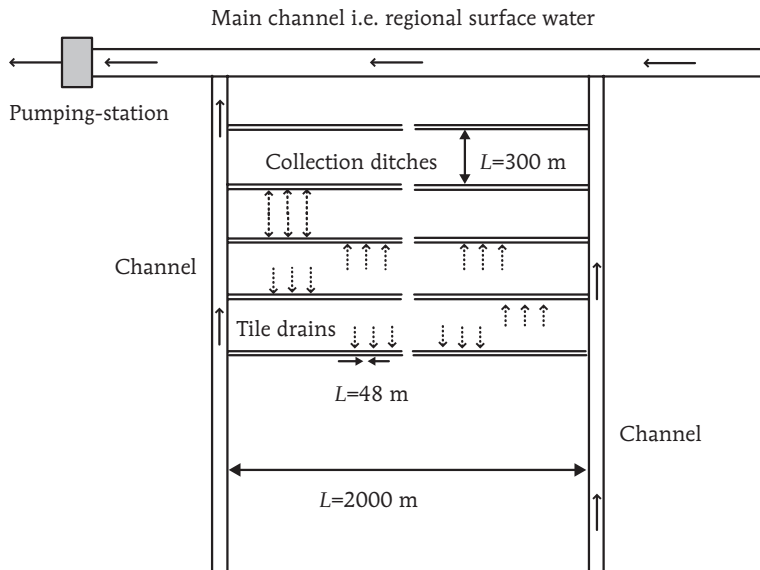
Fig. IV.1.4
Flevoland experimental site. General outline of the drainage system in the area surrounding the experimental site. Drainage system consists of subsurface tile drains, collection ditches, channels, and main channel. Water is transported to pumping stations via the main channel i.e., the regional surface water system.

The soil-physical properties at the experimental site were measured in the laboratory (Alterra Institute, Wageningen). The unsaturated hydraulic conductivity and the largest part of the soil water retention function were measured using the evaporation method (pressure heads from 0 to -800 cm; Wendroth et al., 1993). The pressure membrane method (Klute, 1986) was used to determine the soil water retention function at pressures below -1000 cm. The analytical Mualem-van Genuchten model ([II.18], [II.19]) was used to fit the measurements, and all were duplicated. Table A.1 in Appendix A shows the soil-physical parameters for the soil water retention curve $\theta(h)$ and hydraulic conductivity curve $k(h)$. Parameters were assumed to be valid for the soil at Plot 1 as well as at Plot 2. Table A.1 shows that the k_s values for the fitted curves underestimated the measured k_s values. Underestimation may have occurred due to the presence of macropores in the soil samples, although efforts were made during the selection of the soil sampling locations in the field to avoid visually present cracks in the sample cylinders. Given the efforts it is possible that the macro-porosity in the actual field situation was even larger, leading to higher k_s values as measured.

Crop rotation and nutrient management - The agricultural practices at the arable farm showed a crop rotation, usually in a 1:3 or 1:4 scheme. The average crop rotation was potatoes (1), sugar beet (2), winter wheat (3), and various other crops (4) like grass seeds, onions, peas, or corn. The latter crops were optional in a 1:4 crop rotation. Based on nutrient amounts stored in the soil and available for crop uptake, fertilizer was applied. These applications might have been spread in time, before, after, and during the growing season. If manure was included it was usually applied in autumn before potatoes are planted in the next year's growing season. Manure application is widespread across the polder area and also at the observation farm. Manure mainly originates from nearby dairy farms and areas surrounding the polders in the south and east at intensive animal husbandry farms.

Data on the agricultural nutrient balance mainly originated from the farmer, who used a computer program to support his nutrient management. Using the farmer's data, supplemented by general numbers for nutrient content per unit of crop production, an agricultural nutrient balance was calculated. Annual variation of crop uptake of nutrients was corrected by deviations in actual evapotranspiration rates ET_a during the growing season for a specific year compared to the long-term average ET_p.

The agricultural nutrient balances are the basis for the elaboration of calculated ('measured') nutrient loads for tile drains and the local surface water system. To obtain an overview on nutrient management and losses to the environment, nutrient balances were analyzed over a certain time period to avoid short-term deviations from nutrient equilibrium conditions in the soil-water-system. Additionally, drainage water is a mixture of water from different travel times. Given the 1:3 or 1:4 crop rotation and estimates of travel times of water, a four-year period was chosen in which average nutrient balances are presented. This period includes one full crop rotation, and it was expected to be of major influence on the drainage water composition. Given the field measurements, the period analyzed for Plot 1 is April 1989 through March 1993; for Plot 2 this period runs from April 1990 through March 1994; for the Ditch catchment, both periods were taken into account.

2   Field water balance and hydrology

Field observations - An outline of the experimental site is shown in Fig. IV.2.1. The situation at Plot 2 the Ditch, and the Vogeltocht channel are shown. The measurement equipment setup at Plot 1 was nearly identical. Field observations on Plots 1 and 2 included precipitation, soil water contents, groundwater levels, and drainage fluxes of tile drains and the Ditch. Furthermore drainage water from the drains and Ditch was discharge-dependent and automatically sampled. Water samples have been analyzed on

physical-chemical components such as acidity (pH) and electrical conductivity (EC), nutrients, and pesticides. Bromide was used as a field-scale tracer. In addition during October 1992 to March 1993 (Plot 1 campaign) samples were taken from rainfall and drainage water in order to perform oxygen-18 (^{18}O) measurements. The measurement program at the experimental site has been described in more detail by Groen (1997).
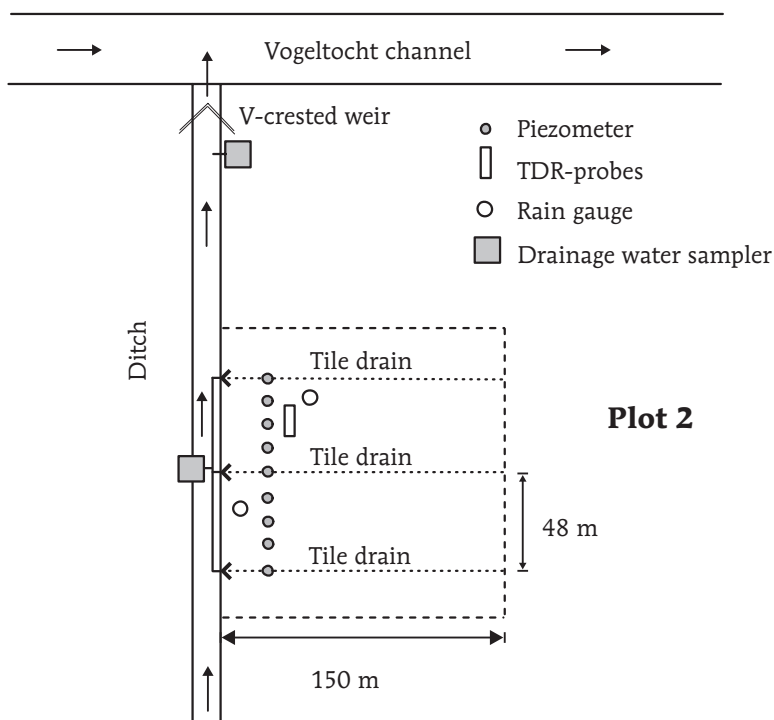
Fig. IV.2.1
Flevoland experimental site. Schematic outline of Plot 2.

Precipitation was measured manually every three days using a standard rain gauge with a funnel catchment of 200 cm^2 and installed at a level of 0.4 m above soil surface.
A measurement height of 0.4 m above the soil surface was chosen to prevent potato leaves from covering the funnel (Fig. IV.2.2). Earlier measurements during the four-year period 1980-1984 nearby the experimental site as reported by Wolters (1996) confirmed the wind effect of the measuring height (Section II.6). On an annual basis, 6% more rainfall was found where the rain gauge was installed at the soil surface. In summer, 4% more rainfall was recorded by the surface-level rain gauge, and in winter 8% more. The three-day sum of precipitation at the site was recorded manually. Additionally,

precipitation was measured continuously and automatically using a tipping bucket rain gauge; each recorded tilt amounted to 0.2 mm of rainfall. The time series of each gauge was checked using the other gauge's time series and found to be consistent.
The precipitation data were not corrected for the measurement height above the soil surface because of the height of the leaves of the potato plants, of the furrows, and because of the soil surface roughness at the site after plough activities in the winter. Reference-crop evapotranspiration ET_r data were retrieved from the KNMI. Daily sums of ET_r were calculated for station Lelystad, located about 2 km northwest of the experimental site.
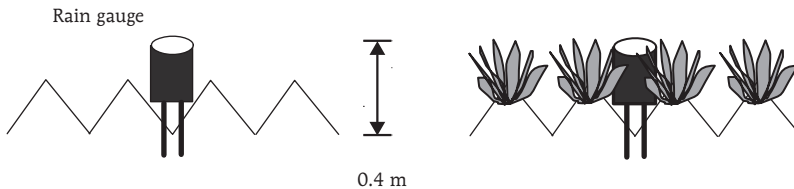
Fig. IV.2.2
Flevoland experimental site. Rain gauge as schematically installed at the site. Measurement height just above the maximum seasonal growth height of the potato leaves. Potatoes were grown in ridges between furrows.

Soil water content profiles were measured using manually-operated, calibrated TDR-probes installed at depths of 0.1, 0.2, 0.3, 0.4, 0.5, 0.8, 1.0, and 1.2 m below the soil surface, with two probes installed at each depth (Groen, 1997). Using nine piezometers, groundwater levels were measured manually three times per week. At one location midway between two tile drains, groundwater levels were automatically recorded on an hourly basis. All piezometers were installed row-wise (Fig. IV.2.1), perpendicular to the tile drains, at a distance of 25 m from the Ditch. The groundwater levels measured at the tile drains were plotted, as well as the groundwater level midway between two subsurface drains. It appeared that the groundwater level rise, midway between tile drains, was limited to a few centimeters only. The groundwater table was quite flat across the plots, indicating a large saturated hydraulic conductivity of the cracked subsoil, estimated at 300 to 500 m d^{-1}. Furthermore, groundwater levels during discharge events were rising to above the tile drains, which were present at a depth of 0.95 m below the soil surface.

Tile drain discharge was measured by connecting three tile drains in a row to a collecting pipe, which discharged freely into a 0.230 m^3 reservoir placed underneath the ditch bottom. When it was full, the reservoir was emptied by a pump, and during pumping the reservoir inlet was closed off. By counting the number of reservoirs filled over time, drainage fluxes were calculated (Groen, 1997). The discharge of the Ditch was measured using a calibrated, sharp-crested 90° V-crested Thomson weir, but around September 20,

1993, the weir was removed due to high water levels in the ditch caused by the high inflows. The backup in water level caused by the weir led to poor drainage conditions in the field, which continued to January 10, 1994. To estimate ditch discharges, a functional relationship was used between tile drains discharge of Plot 2 and ditch discharge, and a non-linear function was fitted ($R^2 = 0.81$) to fill the data gap. During summer periods, tile drainage was rare, but not absent; in winter, drainage response to rainfall events was rapid. The tile drain discharge and ditch discharge was sampled automatically on the basis of drainage rate (Groen and Dekkers, 1990). Sampling resulted in a mixture of discharge-dependent water samples (Groen, 1997).

^{18}O in precipitation and tile drainage - In structured clay soils like the soils under consideration, preferential flow features are expected to occur (Booltink, 1994; Groen, 1997), and experimental evidence for preferential flow is of great help to indicate the phenomenon. Measured groundwater levels rose from the end of the growing season onward to the winter season before reaching the full water storage capacity of the soil; therefore, as soon as groundwater levels exceeded the tile drains depth, tile drains started discharging excess water before the storage capacity was filled. The chemical element oxygen O has three stable isotopes: ^{16}O, ^{17}O, and ^{18}O, with an abundance of 99.76%, 0.035%, and 0.205%, respectively (Mook, 1994). A qualitative measure indicating preferential flow is the observation of quick response to the concentration of the stable, natural isotope ^{18}O, in drainage water, to ^{18}O-concentrations in rainfall events. Isotope techniques can be used to analyze hydrological systems (IAEA, 1991: Gardner et al., 1991), and seasonal variations of ^{18}O-concentrations in drainage water can be used for hydrological analysis purposes. These variations indicate incomplete mixing of drained groundwater, possibly due to preferential flow events (Mook, 1994).

The ^{18}O-concentration is mostly presented by the ratio $^{18}O/^{16}O$ (=$^{18}\delta$) with respect to a reference level called VSMOW (Vienna Standard Mean Ocean Water), set by the IAEA, according to

$$^{18}\delta = \frac{\left(\frac{^{18}O}{^{16}O}\right)_{\text{sample}} - \left(\frac{^{18}O}{^{16}O}\right)_{\text{VSMOW}}}{\left(\frac{^{18}O}{^{16}O}\right)_{\text{VSMOW}}} \times 1000 \qquad \text{[IV.1]}$$

where $^{18}\delta$ is the isotope ratio of $^{18}O/^{16}O$ in the sample relative to the ratio in the VSMOW-standard, in per mil notation (‰). $^{18}\delta$ of rainfall in the Netherlands show more or less sinusoidal seasonal variations, ranging between -9‰ in winter and -6‰ in summer; the annual average was about -7.8‰. It is assumed that these values are representative for Flevoland. The laboratory analysis of the isotope ratio was performed by the Center for Isotope Research (CIO) of Groningen University in the Netherlands. The measurement resolution or accuracy is about 0.1‰.

Fig. IV.2.3 shows $^{18}\delta$ of rainfall and tile drainage water. Both of the phenomena indicated above, fast response of drainage water composition and incomplete mixing, were observed for the example on day 328 (rainfall) and 330 (tile drainage response) as pointed out by circles in Fig. IV.2.3, indicating preferential flow events that were caused mainly by high rainfall events (Nieber et al., 1998). The total rainfall recorded on day 328 was 15.6 mm with $^{18}\delta$=-5.67‰. On that day, $^{18}\delta$ of tile drainage was -6.80‰; two days later, $^{18}\delta$ of tile drainage was -5.78‰. Fig. IV.2.3 shows seasonal variation of $^{18}\delta$ of tile drainage water samples, rising from below -6.5‰ to above -5.5‰ during the drainage season. A seasonal variation can also be observed in $^{18}\delta$ of rainfall water, rising from about -13‰ to -2‰ during the same drainage season. *Drainage water composition responds to the upward trend in rainfall within one drainage season*. Occasions that are less clear and consistent are the occasions when $^{18}\delta$ of tile drainage water is directly influenced by $^{18}\delta$ of precipitation water. It can thus be concluded that some *qualitative field evidence* is given by the ^{18}O-measurements for the occurrence of *preferential flow* events.

Field water balance for tile drains - The field water balance was calculated for Plot 1 (April 1, 1992 through March 31, 1993) and for Plot 2 (April 1, 1993 through March 31, 1994). The area connected to the system for which the water balances were calculated was 144 m wide and 150 m long (2.16 ha). The depth of the water balance was calculated at 1.2 m below the soil surface (system volume 25 920 m^3). Also the field water balance of the Ditch was calculated for the two hydrologic years indicated above. The area related to the water balance system was 300 m wide, 1000 m long (30 ha), and 1.2 m deep (system volume 360 000 m^3). During the two-year field experiment, actual surface runoff $Q_{\mathrm{surficial}}$ to the surface water was not observed, nor were traces of runoff events, like gullies reaching the Ditch. Ponding of water on top of the soil surface might have occurred during heavy rainfall events. However, this ponding would remain detained on the soil surface during infiltration without lateral outflow to the Ditch. At the experimental site, the overall slope of the soil surface is zero; however, on the small scale (1 m) the surface is rough, especially after ploughing activities in autumn. To provide an idea about the potential surface runoff the following argumentation was set up: Suppose that surface runoff can travel a maximum horizontal distance of 25 m, and the 1000 m long ditches at the farm are 300 m apart. Based on the assumed maximum distance of travel for surface runoff, it is concluded that surface runoff *can occur and reach* the surface water across 17% of the soil surface. In practice, surface runoff is not likely to occur during all rainfall events and across the total soil surface at the same time. Reflecting on these field observations, it is then assumed that $Q_{\mathrm{surficial}}$ can be neglected. Hence, the infiltration rate at the experimental site was equal to the rainfall rate P. For the hydrologic year 1992-1993 P was 863 mm a^{-1}, and in 1993-1994 P was 1064 mm a^{-1}.
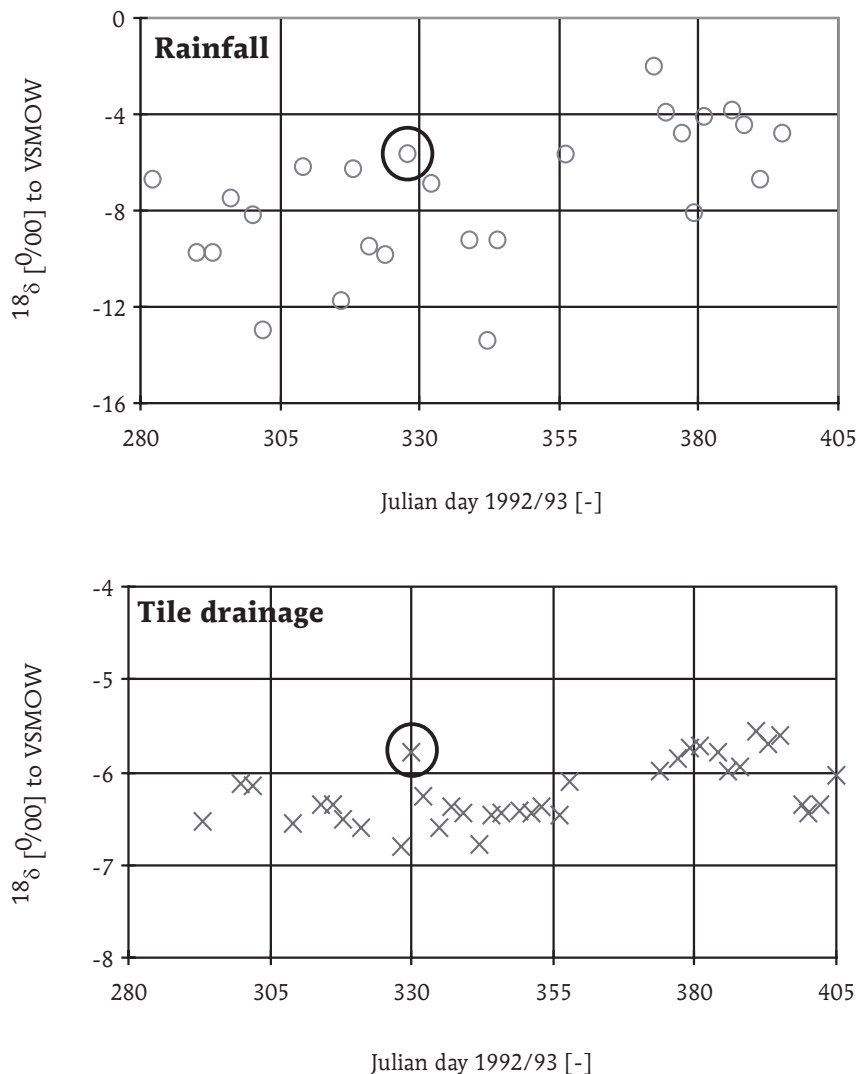
Fig. IV.2.3
Flevoland experimental site. $^{18}\delta$ values [IV.1] in water relative to the Vienna Standard Mean Ocean Water (VSMOW) ratio, of rainfall samples (○ in upper graph), and of tile drainage samples taken at Plot 1 (× in lower graph). The measurement period is from October 6, 1992 (Julian day 280) through February 8, 1993 (Julian day 405).

Actual evapotranspiration - ET_p for potatoes was calculated from ET_r with crop factors f_c from Feddes (1987) using [II.23]. For bare soil, $f_c = 0.4$ (Makkink, 1957, 1960; Meinardi, 1994). ET_p for Plot 1 in 1992-1993 was calculated at 479 mm a^{-1} and at 432 mm a^{-1} in 1993-1994 for Plot 2. ET_a was roughly estimated and used in the field water balance, using an estimated long-term average reduction rate, based on the method presented by Werkgroep HELP-tabel (1987). In this table, reduction rates are given for a combination of soil type, crop, and groundwater level. For arable land on clay soil with groundwater table class (GTC) VI (Werkgroep Herziening Cultuurtechnisch Vademecum, 1988), the reduction rate is estimated at less than 25 mm a^{-1}. For Plot 1 the reduction rate was estimated 20 mm a^{-1}; for Plot 2 reduction was estimated at zero ($ET_a = ET_p$). ET_a for Plot 1 in 1992-1993 was estimated at 463 mm a^{-1}; in 1993-1994 ET_a for Plot 2 was estimated at 412 mm a^{-1}.

Interception evaporation - As far as interception losses are concerned, evaporation of intercepted water (E_i) is not included explicitly, but is assumed to be part of ET_p. E_i can be calculated according to Braden (1985):

$$E_i = a_c \, \text{LAI} \left(1 - \frac{1}{1 + \dfrac{S_c P}{a_c \text{LAI}}} \right)$$

[IV.2]

where a_c is a crop-dependent parameter equal to 0.68 mm d^{-1} (Groen, 1997) and S_c the soil cover [m^2 m^{-2}]. If the precipitation data on an annual basis is corrected for the measuring height, and interception losses from the crop are taken into account using [IV.2], net precipitation is 1% higher on an annual basis –in summer 3 to 4% less– and in winter it is 6% more. Altogether, the combination of both the correction of precipitation and extension with E_i is not of any significant influence on the water balances which will be shown later.

Measured tile drainage - The measured discharge Q_{meas} of the tile drains was measured using a reservoir of known volume and a counter to register the number of reservoirs filled and emptied with time. In 1992-1993 Q_{meas} was 182 mm a^{-1} for Plot 1; in 1993-1994 it was 471 mm a^{-1} for Plot 2.

Combined with the measured soil-water storage change $\Delta V_{w,\text{meas}}$ of 4 mm decreased in 1992-1993 for Plot 1 and increased 80 mm in 1993-1994 for Plot 2 –the field water balance for Plot 1showed a surplus of 185 mm a^{-1}. This surplus was discharged from the plot, by-passing the tile drains. The 1993-1994 field water balance for Plot 2 showed a surplus of 101 mm a^{-1}. As evidenced in Plot 1 in 1992-1993, an unmeasured discharge term was also expected from Plot 2 in 1993-1994.

Unmeasured drainage - An extra drainage term, leaving the balance system as Q_{unmeas}, was present at both plots at the experimental site. To judge whether such a balance term could occur, the vertical groundwater hydraulic head gradient was calculated using groundwater hydraulic heads in the sandy aquifer. These measurements were measured and provided for by the Dutch Institute for Applied Geosciences (NITG TNO) in a nearby piezometer, about 1.2 km east of the experimental site, midway between the Meeuwentocht and Vogeltocht channels, coded 26EP3601 (Fig. IV.1.2). This exercise also led to the conclusion that a net annual Q_{unmeas} term should be introduced to close the water balance. The method presented in Section II.6 was used to calculate the Q_{unmeas} term. Q_{unmeas} in 1992-1993 from Plot 1, which amounted to 165 mm a^{-1}, and in 1993-1994 from Plot 2, it amounted to 92 mm a^{-1}. The field water balance for Plot 1 now closed at 20 mm a^{-1}, for Plot 2 at 9 mm a^{-1}. The field water balances for the two plots as interpreted from the field data are shown in Fig. IV.2.4.

As seen in Fig. IV.2.4, the weather conditions and drainage situations for the two plots were different. At Plot 1, 52% of the total drainage amount was accounted for by tile drains discharge, and 48% was drained by other drainage means. Q_{unmeas} was direct drainage from the water balance system to the Ditch, expected to drain the main part of Q_{unmeas}, and possibly to the water level controlled channel Vogeltocht, by-passing the tile drains. At Plot 2, the percentages were respectively 84% and 16%. The differences in percentages i.e., the division of the total drainage into tile drainage and unmeasured drainage has consequences for travel times and solute transport to the surface water system. In the case of Plot 2, average, shorter travel times of soil water and solutes will occur.

The differences between the two years in recorded rainfall and in the rainfall excess partially cause the difference in the indicated percentages. If higher, and more frequent, high groundwater levels occur, drainage will take place by more shallow drainage means such as tile drains. Another explanation for the differences in drainage events at both plots is the *difference in soil profiles between the two plots*. The thickness of the clay layer at the farm decreases from northeast to southwest, and geophysical measurements (Meinardi and Van den Eertwegh, 1995) at Plot 2 showed a deeper and/or heavier clay layer as compared to the situation at Plot 1. This means that at Plot 1, the clay layer is partially ripened down to the sandy aquifer over a larger part of the plot area compared to Plot 2. This latter plot is likely to have an unripened clay layer between the tile drain level and the sandy aquifer across a large part of its 2.16 ha area. Based on this analysis, the possible flow situation for the two plots is shown schematically in Fig. IV.2.5. These differences will be accounted for in the setup of the numerical model.

Field water balance for the Ditch - The precipitation and infiltration data for the water balance of the Ditch (Fig. IV.1.2) were equal to those shown for the two plots. ET_p was
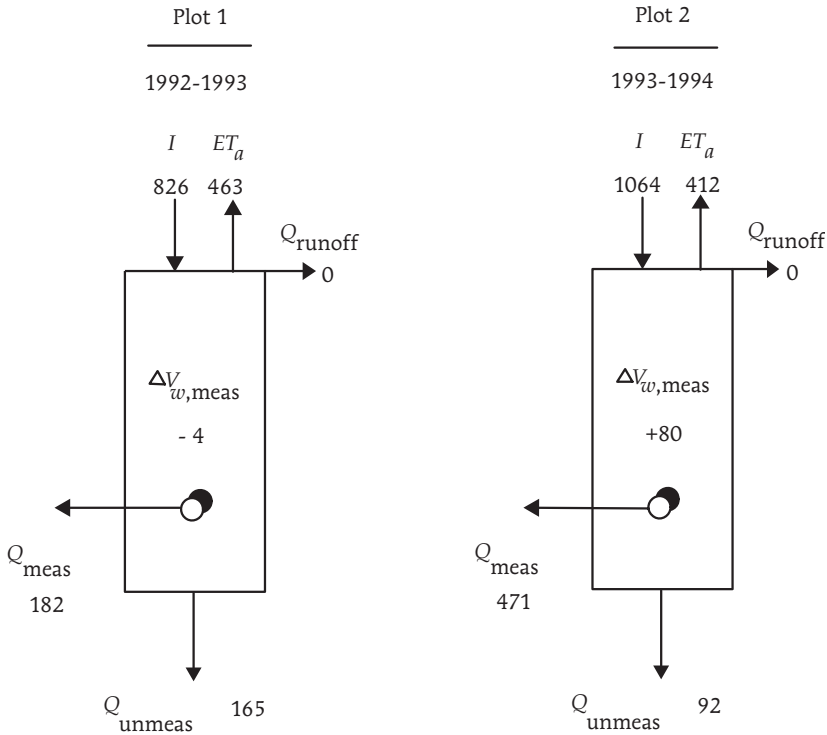
Fig. IV.2.4
Flevoland experimental site. Annual field water balances [mm] for Plot 1 in 1992-1993 (April 1, 1992 through March 31, 1993), and for Plot 2 in 1993-1994 (April 1, 1993 through March 31, 1994).

calculated using the appropriate crop factors for all arable crops present. In 1992-1993 ET_p amounted to 466 mm a^{-1}, and in 1993-1994 to 418 mm a^{-1}. An identical approach as previously stated was used to estimate ET_a. The reduction rate for 1992-1993 was estimated at 20 mm a^{-1}, and in 1993-1994 it was estimated at zero ($ET_a = ET_p$).

Ditch discharge - The discharge Q_{meas} of the Ditch was measured by using a calibrated V-notch weir at the northwest end of the ditch and by continuously measuring ditch water levels. In 1992-1993, Q_{meas} amounted to 212 mm a^{-1}, and in 1993-1994, 253 mm a^{-1}.

The soil water storage change $\Delta V_{w,meas}$ in 1992-1993 was based on measurements at Plot 1, and in 1993-1994 on measurements at Plot 2. It was assumed that the plot measurements were representative for the catchment area of the Ditch. Combined with
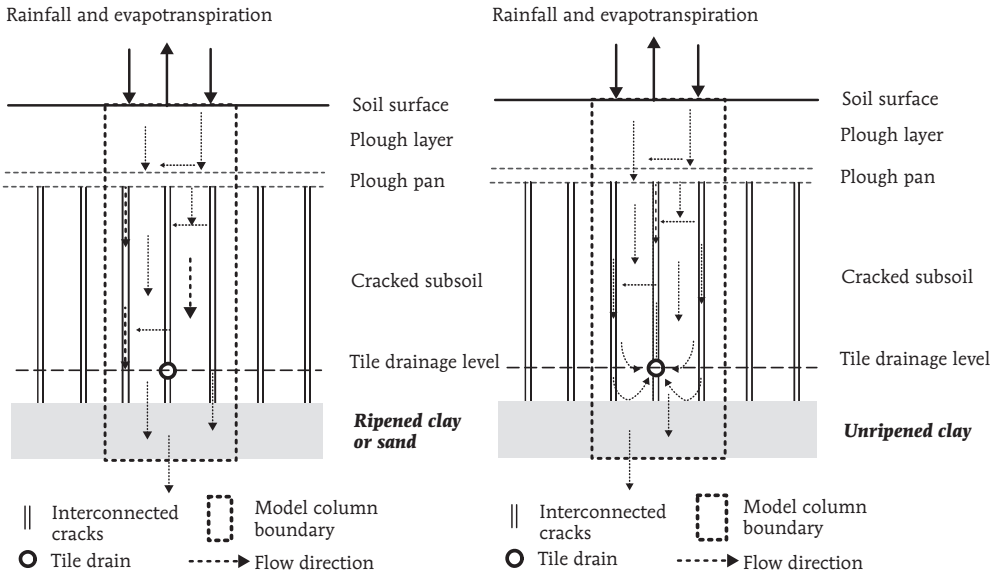
Fig. IV.2.5
Flevoland experimental site. A schematic flow situation across the site area. Plot 1 has a bottom layer of sand, ripened clay, or unripened clay. At this plot, the flow situation is a combination of the situation shown in the left and the right figure. *Plot 2 has mainly a bottom layer of unripened clay*. The flow situation at this plot is comparable to the flow situation shown in the right figure.

$\Delta V_{w,\text{meas}}$ of −4 mm in 1992-1993 and +80 mm in 1993-1994, the field water balance for the Ditch in 1992-1993 showed a surplus of 172 mm a^{-1}. This net surplus was discharged from the catchment area of the Ditch, and the 1993-1994 field water balance for the Ditch showed a surplus of 313 mm a^{-1}. As in the 1992-1993 period, a net unmeasured discharge term was also expected in 1993-1994. This unmeasured discharge was direct drainage from the water balance system of the Ditch to the Vogeltocht channel.

Seepage water - Seepage water from the sandy aquifer was found to enter the Ditch by analyzing the composition of the ditch water. Discharge water of the ditch is a variable mix of excess water, draining from the catchment, and of seepage water. Drainage water and seepage water are likely to have a different chemical composition; hence C_{drainage} does not equal C_{seep}, as far as chloride or nitrate is concerned. The seepage water from the aquifer is brackish with a chloride concentration of about 500 mg l^{-1}, based on measured solute concentrations during periods with low discharge rates. The confining clay layer, a former sea bottom layer, also contains some chloride. The desalinization

process of the topsoil is not in its final stage yet; therefore, the chloride concentration of 'fresh' drainage water, not affected by brackish seepage, is estimated at 75 mg l^{-1}. Taking $C_{drainage} = 75$ mg l^{-1} Cl$^-$ and $C_{seep} = 500$ mg l^{-1} Cl$^-$ as reference concentrations, a calculation was set up to estimate the fraction of seepage water in the total discharge. The calculation is based on ideal mixing of both discharge sources:

$$Q_{meas}\, C_{meas} = Q_{drainage}\, C_{drainage} + Q_{seep}\, C_{seep} \qquad \text{[IV.3]}$$

The seepage water fraction f_s of the measured ditch discharge with concentration C_{meas} is calculated according to

$$f_s = \frac{C_{meas} - C_{drainage}}{C_{seep} - C_{drainage}} \qquad \text{[IV.4]}$$

where

$$f_s = \frac{Q_{seep}}{Q_{meas}} \qquad \text{[IV.5]}$$

Using chloride as a seepage water indicator, Q_{seep} amounted to 77 mm a^{-1} in 1992-1993 and 32 mm a^{-1} in 1993-1994. Chloride is not the only seepage water indicator; nitrate can also be used. The aquifer groundwater hardly contains any nitrate. Using $C_{drainage} = 20$ mg l^{-1} N and $C_{seep} = 0.1$ mg l^{-1} N for NO$_3$-N, Q_{seep} amounted to 45 mm a^{-1} in 1992-1993 and to 22 mm a^{-1} in 1993-1994. Averaging both results for Cl$^-$ and NO$_3$-N, Q_{seep} was estimated at 60 mm a^{-1} in 1992-1993 and at 25 mm a^{-1} for the second year of measurements.

The presence of seepage reaching the Ditch could was also visually illustrated with the groundwater hydraulic heads measured in piezometer 26EP3601 (Fig. IV.1.2), which is located within the Pleistocene sand layer at a depth of 17 m below the soil surface. The average soil surface level at the experimental site was 3.80 m below MSL. The measured groundwater hydraulic heads did not reach the subsurface tile drains level of 4.80 m below MSL, but they did reach the ditch bottom, sloping from 4.80 to 5.30 m below MSL, mainly during winter months (Fig. IV.2.6). The ditch bottom cuts through the confining clay layer from the middle of its course to the northwest end. The water level of the ditch varied as a result of weather influence, and hence drainage processes, due to the fact that the ditch drained freely into the Vogeltocht channel passing the measurement weir.

It can be concluded that the response of the whole ditch drainage system acts differently with variations in meteorological conditions. The first hydrologic year, 1992-1993, is drier than the second year, 1993-1994. Phreatic groundwater levels and hydraulic heads in the aquifer are generally higher in 1993-1994, causing the recharge-seepage situation to be different between the two periods indicated. The draining function of the nearby
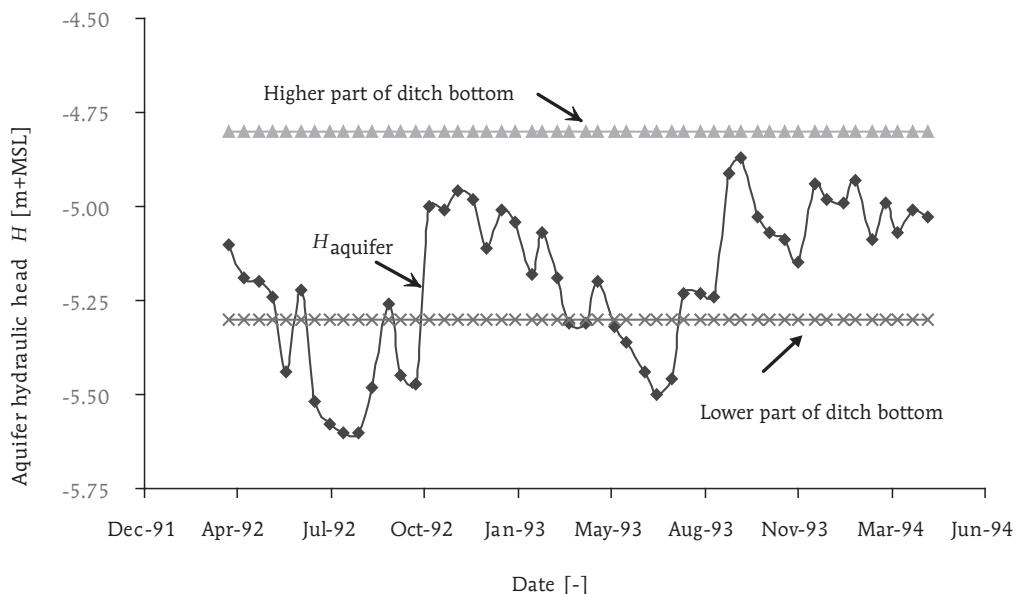
Fig. IV.2.6
Flevoland experimental site. Groundwater hydraulic head H in sandy aquifer measured at piezometer 26EP3601 for the period March 27, 1992 through April 14, 1994. Average tile drains depth, ditch bottom, and controlled-water-level channel, Vogeltocht.

controlled-water-level channel, Vogeltocht, having an approximately constant water level of 5.80 m below MSL, is of importance in this analysis. Given the constant, controlled water level in the channel, hydraulic head gradients from the two plots to the channel are larger during the second year, inducing a larger subsurface flow component directly to the channel and by-passing the Ditch in the second period of measurements.

The field water balances of the Ditch for the two subsequent years are shown in Fig. IV.2.7. The method shown in Section II.6 was used to calculate Q_{unmeas}. The 1992-1993 balance closed at 40 mm a^{-1}, and in the 1993-1994, at -21 mm a^{-1}.

During the first year, 52% of the total drainage was captured and measured by the V-notch weir installed in the ditch, and 48% drained directly to the channel. During the 1993-1994 period, a little over 40% was measured, and somewhat less than 60% drained directly to the channel. A larger precipitation excess resulted more often in higher phreatic groundwater levels and hydraulic heads in the aquifer. The amount of excess water that drained directly to the water-level controlled channel was larger in 1993-1994 as compared to 1992-1993. In these situations, seepage water preferably entered the
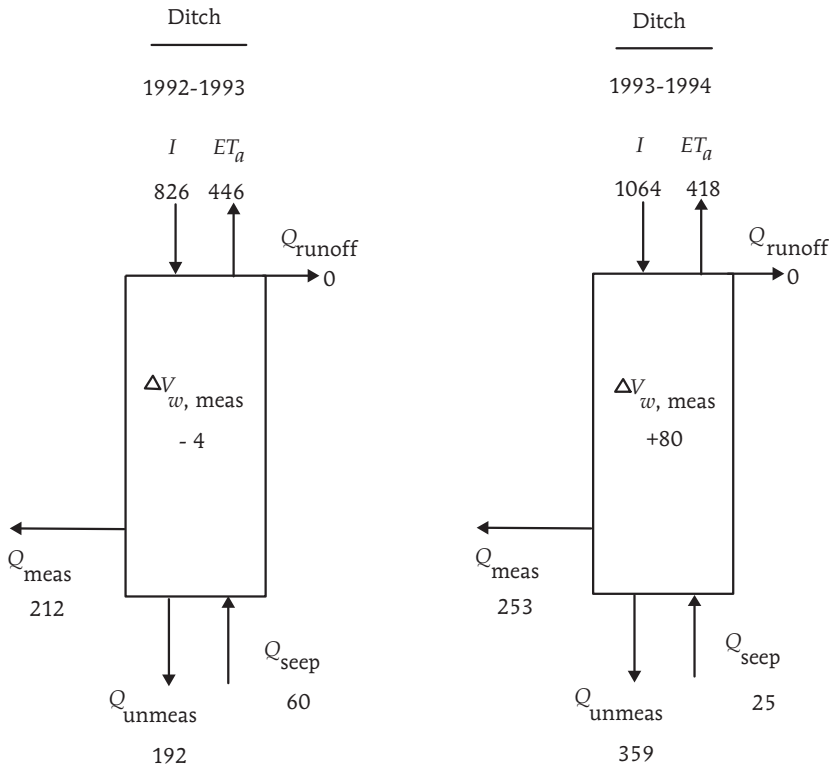
Fig. IV.2.7
Flevoland experimental site. Annual field water balance [mm] of Ditch for the periods April 1, 1992 through March 31, 1993, and April 1, 1993 through March 31, 1994.

channel, not the Ditch. The reasons for this are the larger pressure head differences between the aquifer groundwater hydraulic head and the controlled water level of the channel, on one hand, and the smaller head differences between the hydraulic head in the aquifer and the phreatic groundwater levels at the experimental site.

Another issue concerning the hydrology of the Ditch is the fact that the ditch bottom is sloping at 0.5‰ from southeast to northwest, whereas the local confining clay layer is more or less horizontal, or rather sloping at a smaller rate (Fig. IV.1.2). This leads to the assumption that in the southeastern ditch section, the ditch bottom material is clay. Moving from southeast to northwest, the ditch bottom cuts through the confining clay layer and lies partially within the sandy aquifer. Also going in the northwest direction, approaching the Vogeltocht channel, groundwater hydraulic heads in the aquifer are decreasing due to the draining effect of the controlled-water level channel. It is possible

that the ditch water partially infiltrates the sandy aquifer moving to the northwest direction and is drained by the channel. Infiltration of ditch water is not likely to occur in the southeast section. Somewhere in the middle of the ditch section, groundwater seepage from the aquifer is expected to enter the ditch.

Tracer experiments - Two tracer experiments were conducted at the Flevoland experimental site using a potassium-bromide (KBr) solution. The main goal was to calculate the tracer recovery within one year as time and drainage water production progressed, focusing on timing of the first breakthrough of the tracer. On May 15, 1992 and March 14, 1993, the bromide-solution was applied to the tile drains catchment areas of Plot 1 and Plot 2 respectively. Bromide concentrations of the water originating from the tile drains and the Ditch were measured continuously. Measured background concentrations in water drained by the tile drains were between less than 1 and 2 mg l^{-1} Br$^-$, which hampered the interpretation of the tracer experiment (Groen, 1997). To solve this problem, the following method was used to divide the measured concentration into background and tracer concentration.

In *sea water*, bromide is present in a fixed ratio to chloride. Matthess (1982) mentions a ratio of *Cl-:Br- = 288:1*. The soil-water-system at the experimental site originates mainly from marine sediments, in which sea water influence is still present. In the drainage water of the 30 ha ditch catchment, only a small part of the area was influenced by the tracer experiment at the plot scale, having a 2.16 ha catchment. In the *ditch water*, an average ratio of *Cl-:Br- = 150:1* was found. This ratio was used to divide the measured bromide concentrations in tile drain water into background concentrations and the bromide originating from the tracer experiment. Using the bromide from the tracer experiment, tracer loads of tile drains discharge were calculated and compared with the applied amount of bromide.

Applied and calculated loads of the bromide tracer for the two plots during the first (1992-1993) and second measurement year (1993-1994) respectively are shown in Table IV.2.1.

As can be seen from Table IV.2.1, for Plot 1, *24% of the tracer applied was recovered by drainage within one year; about half of this recovery was found in tile drainage. The total recovery was calculated after 360 mm of drainage after application of the tracer. For Plot 2, *56%* of applied tracer was recovered by drainage within one year and 560 mm of drainage after application of the bromide. When the difference in drainage water production into account, the amount of tracer reaching the tile drains within one year is largest for Plot 2. This indicates *shorter travel times of water and solutes in Plot 2*, compared to the hydrological situation at Plot 1. This is in agreement with the interpreted water balances.

Table IV.2.1

Flevoland experimental site. Bromide tracer loads for Plot 1, during the period April 1, 1992 through March 31, 1993, and for Plot 2, during the period April 1, 1993 through March 31, 1994. Applied tracer amount, calculated tile drains load, background load (Cl^-:Br^-=150:1), unmeasured load, and total tracer load.

Bromide load [kg ha^{-1}a^{-1}]	Plot 1 1992-1993	Plot 2 1993-1994
Tracer applied to the soil surface	7.8	11.7
Calculated tile drainage load	2.9	7.4
Background load in tile drainage	1.9	1.9
Tracer in measured tile drainage	1.0	5.5
Tracer in unmeasured drainage	0.9	1.0
	+	+
Total tracer	*1.9*	*6.5*
Tracer recovery in *tile drainage*, one year after application as fraction [-] of tracer applied	**0.13**	**0.47**
Tracer recovery in *total drainage*, one year after application as fraction [-] of tracer applied	**0.24**	**0.56**

The timing of the first breakthrough of the applied tracer was hard to notice in the drainage water at both plots, and therefore not shown here due to the background concentrations that appeared to be high compared to the amount of tracer applied. It seems that at Plot 1, the first breakthrough occurs around October 26, 1992, i.e., 165 days after application, 31 mm of rainfall excess, and 28 mm of drainage after application of the tracer. At Plot 2, the first breakthrough is likely to occur around September 26, 1993, also 165 days after application, 206 mm of rainfall excess, and 41 mm of drainage after application of the tracer.

3 Transient water flow and solute transport simulations 1992-1994

As stated in the site description in Section IV.2, at the 2.16 ha area, the subsurface drain spacing $L = 48$ m. Thus, the groundwater present in the saturated zone has to travel a maximum of 24 m laterally to reach a tile drain. In the cracked subsoil, the horizontal distance between the permanent cracks is about 0.3 m. The hydraulic conductivity of the cracked subsoil is between 300 and 500 m d^{-1}. A high hydraulic conductivity value is supported by the farmer's experience. Years ago, he used to sub-irrigate the soil and crops in summer by artificially raising the water level of one central ditch after the ditch water infiltrated into the soil through the ditch walls. The subsoil cracks were connected to the ditch walls, and they were also interconnected. In the originally dry ditches at the left and right hand side of the central ditch at 300 m distance, the farmer observed *water beginning to discharge within hours* after raising the central ditch water level. *Hence, it can be concluded that the system under consideration can be modeled by considering 1D vertical flow only*. It can further be concluded that the *travel time –through the subsoil cracks towards a tile drain– is short compared to the time it takes to move downward vertically in the soil profile*.

Using the *dual-porosity computer code* three different plot-scale models were set up. Under field conditions the actual flow situation in the variable saturated flow system was not expected to be exactly 2D in a vertical soil transect at the plot scale because the cracks in the subsoil 'cut off' horizontal flow paths. Due to the presence of the clay columns, flow in the upper 1-1.5 m of the soil is mainly vertical and 1D. As concluded from the field water balance (Fig. IV.2.4), the hydrological situation at Plot 1 differs from that of Plot 2: the bottom layer at 1.05-1.20 m below the soil surface in the Plot 1 model differs from that of Plot 2. Three models were set up, distinguished by three different bottom layers: (A) sand, (B) ripened clay, and (C) unripened clay. Through these models, major differences in hydrology present at the farm can be shown. The bottom layer at the Plot 1 situation is a mix of sand (A), ripened clay (B), and unripened clay (C). The bottom layer at Plot 2 is mainly unripened clay (C). Fig. IV.3.1 shows a schematic of the model columns. The tile drain was treated as a seepage face where water was not able to enter the soil profile by the tile drains. The bottom of the soil profile was treated as a 'far field' boundary condition (Section II.5). Across this boundary both drainage from the soil column and the water supply from the aquifer were allowed. Note that the water from the aquifer was not taken into account in the field water balance.

Model input data on rainfall were measured locally. Reference-crop evapotranspiration data were taken from the meteorological station at Lelystad Airport. Crop factors (f_c) used are for potatoes (Feddes, 1987); for bare soil, $f_c = 0.4$ (Makkink, 1957, 1960;
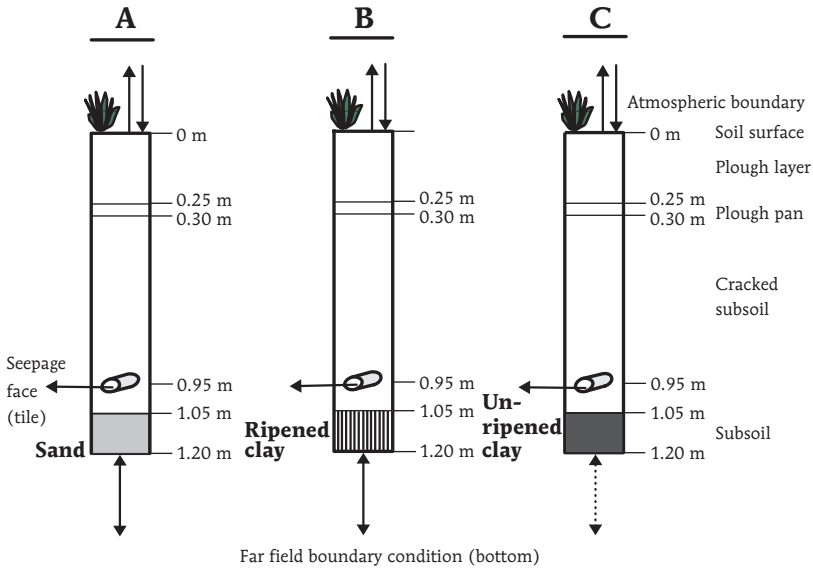
Fig. IV.3.1
Flevoland experimental site. *Schematized models A, B, and C* from left to right. Note differences in bottom layers: (A) sand, (B) ripened clay, and (C) unripened clay. Tile drain is treated as seepage face, and the bottom boundary condition is of a 'far field' seepage face type (Section II.5).

Meinardi, 1994). Daily average air temperature and relative humidity data were taken from meteorological station De Bilt due to the lack of local measurements on these input data. As far as initial conditions were concerned, hydrostatic equilibrium was assumed, and the groundwater level initially was set at 1.20 m below the soil surface.
The simulation period for each model consisted of one year, from April through March of the following year. The parameters used in models A through C are shown in Appendix A. To calculate correct ET_a i.e., any reasonable reduction of ET_p, values for the residual water content θ_r needed to be adjusted. The lab analyses showed $\theta_r = 0.01$, whereas in the models θ_r for the top three layers were used of 0.20, 0.20, and 0.15, respectively. The latter values are interpreted from the θ-values at wilting point as shown in Table IV.3.1.

To illustrate the calculated soil water balances and the division of the total drainage between drainage from the soil matrix and from the macropore domain, the mass balance terms for all models A, B, and C for the 1992-1993 and 1993-1994 measurement periods are graphically shown in Fig. IV.3.2. As stated in Section II.3.1, surface runoff from the matrix domain (Q^*_{runoff} in Fig. IV.3.2) is added to the rainfall

Table IV.3.1
Soil water content θ for major soil types at saturation, at field capacity, and at wilting point.

Soil type	Soil water content θ		
	at saturation	at field capacity	at wilting point
Sand	0.38	0.15	0.08
Sandy loam	0.43	0.21	0.09
Loam	0.47	0.31	0.14
Clay loam	0.49	0.36	0.18
Silty clay	0.51	0.40	0.20
Clay	0.53	0.44	0.21

Source: James (1987).

applied to the macropore domain and may or may not lead to surface runoff from the macropore domain. If the latter occurs, it would be reported as surface runoff from the total flow domain (Fig. IV.3.2). The annual mass rate of water that is transferred below the soil surface, the matrix, and the macropore domain are also shown in Fig. IV.3.2. Table IV.3.2a shows the calculation results for the 1992-1993 period, Table IV.3.2b shows results for the 1993-1994 period.

The annual mass balances for the three models do not differ concerning Q_{runoff}, I, and ET_a. Surface runoff from the total flow domain was calculated at zero. Surface runoff from the matrix did not occur. The reduction of ET_p is about less than 5 mm a^{-1} in both measurement years. ET_a, as calculated by the models, is close to the estimated number shown in the field water balance for 1992-1993, but deviates about 30 mm a^{-1} in 1993-1994. The calculated values of ΔV_w did not deviate much between the three models. The temporal variation shown was close to the field observations and field water balance analysis data in 1992-1993. In the second measurement season, deviations occurred; for example, the temporal variation of the water volume stored in the soil column for the C-model for the 1993-1994 balance period is shown in Fig. IV.3.3. At the start of the season, field water storage was about 100 mm below the calculated water storage. It is likely that the soil profile was at field capacity around April 1, leading to the conclusion that the field data underestimated the actual water storage situation during the first months of the 1993-1994 season. The storage increase in 1993-1994 of 80 mm
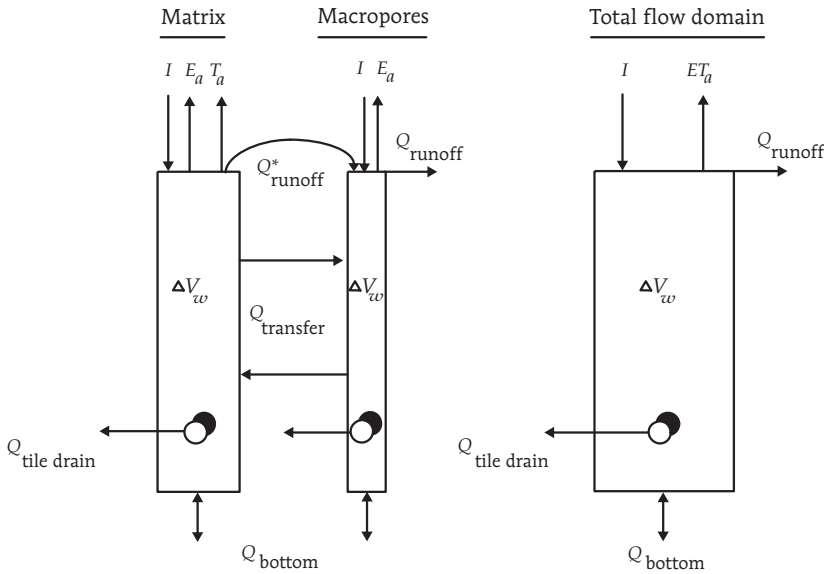
Fig. IV.3.2
Flevoland experimental site. Graphical illustration of annual mass balance terms for water in the soil matrix, the macropore, and the total flow domain for models A through C of Fig. IV.3.1. Q^*_{runoff} is the surface runoff from the matrix domain that is added to the rainfall applied to the macropore domain. Q_{bottom} is the sum of drainage from the soil profile and supply of water from the aquifer to the soil profile.

as shown in the field water balance (Fig. IV.2.4) may thus be incorrect or non-representative for the plot as a whole. The balance differences between the two years appear in ET_a and total $Q_{drainage}$. The 1993-1994 period had a 75% larger rainfall excess compared to 1992-1993, and it has more periods with higher rainfall events. The 1992-1993 period had 192 days where the 1993-1994 period had 237 days with rainfall.

Note the difference between the hydrology of the plots as simulated by the models which was found in the interaction between the sandy aquifer and the 1.20 m soil column. The A-model and B-model had a larger upward flux originating from the sandy aquifer as compared to the C-model. The unripened clay layer in the latter model hampered the upward flow; weather conditions were also a factor. The interaction between aquifer and soil column increased by about 65% (A- and B-model) to 80% (C-model) in 1993-1994 in comparison to the interaction in 1992-1993.

The main differences in the hydrology of the plots at the experimental site represented by the three models were found in the mass transfer of water between the domains, in

Table IV.3.2a

Flevoland experimental site. Computed annual mass balances [mm] for water in the soil matrix, the macropore, and the total flow domain for models A through C of Fig. IV.3.1. *Simulation period: April 1, 1992 through March 31, 1993. P=826 mm a⁻¹* and $ET_p = 479$ mm a⁻¹. Q^*_{runoff} is the surface runoff from the matrix domain that is added to the rainfall applied to the macropore domain. Q_{bottom} is the sum of drainage from the soil profile and supply of water from the aquifer to the soil profile. *Water supply is from aquifer by upward flow through the bottom of the soil profile.

Balance term		A-model			B-model			C-model	
		Matrix	Macropores	Total	Matrix	Macropores	Total	Matrix	Macropores	Total
Q^*_{runoff}		0	-	-	0	-	-	0	-	-
Q_{runoff}		-	0	0	-	0	0	-	0	0
I		791	35	826	791	35	826	791	35	826
E_a		-63	-3	-66	-63	-3	-66	-63	-3	-66
T_a		-413	-	-413	-413	-	-413	-410	-	-410
$Q_{transfer}$	net	-334	+334	-	-338	+338	-	-316	+316	-
	gross	(-386)	(-52)	-	(-382)	(-44)	-	(-382)	(-66)	-
ΔV_w		-1	-2	-3	+1	0	+1	0	-9	-9
$Q_{tile\ drain}$		0	-37	-37	0	-54	-54	-3	-344	-347
Q_{bottom}		-69	-331	-400	-53	-342	-395	-14	-7	-21
$Q^*_{aquifer}$		94	5	99	78	28	106	19	13	32

Table IV.3.2b

Flevoland experimental site. Computed annual mass balances [mm] for water in the soil matrix, the macropore, and the total flow domain for models A through C of Fig. IV.3.1. *Simulation period: April 1, 1993 through March 31, 1994.* $P = 1064$ mm a^{-1} and $ET_p = 432$ mm a^{-1}. Q^*_{runoff} is the surface runoff from the matrix domain that is added to the rainfall applied to the macropore domain. Q_{bottom} is the sum of drainage from the soil profile and supply of water from the aquifer to the soil profile. *Water supply is from aquifer by upward flow through the bottom of the soil profile.

Balance term		A-model			B-model			C-model		
		Matrix	Macropores	Total	Matrix	Macropores	Total	Matrix	Macropores	Total
Q^*_{runoff}		0	-	-	0	-	-	0	-	-
Q_{runoff}		-	0	0	-	0	0	-	0	0
I		1018	46	1064	1018	46	1064	1018	46	1064
E_a		-64	-3	-67	-64	-3	-67	-64	-3	-67
T_a		-362	-	-362	-362	-	-362	-362	-	-362
$Q_{transfer}$	net	-554	+554	-	-557	+557	-	-570	+570	-
	gross	(-610)	(-57)	-	(-612)	(-55)	-	(-633)	(-63)	-
ΔV_w		-15	-8	-23	-12	-12	-24	-12	-10	-22
$Q_{tile\ drain}$		0	-244	-244	-1	-231	-232	-6	-597	-603
Q_{bottom}		-52	-352	-404	-40	-357	-397	-5	-6	-11
$Q^*_{aquifer}$		29	8	37	18	8	26	1	0	1

Fig. IV.3.3
Flevoland experimental site. Temporal variation of water volume V_w stored in the soil column. Results from field measurements at Plot 2 (+, grey) and simulation using the C-model (○, black) of Fig. IV.3.1. Time period: April 1, 1993 (day 92) through March 31, 1994 (day 456).

volume as well as in direction and vertical position within the soil profile, and in the drainage characteristics. The main direction of mass transfer in all models was from matrix to macropore domain. This transfer occurred within the plough layer, primarily directly above the plough pan, and underneath the plough pan in the subsoil, some mass was transferred back from the macropores to the matrix. The third mass 'transfer zone' was around the subsurface drain where transfer occurred from matrix to macropore domain. The interaction between the domains by transfer of water was, thus, not equally spread across the soil column; it was most intensive in potentially stagnant zones in the matrix domain. Examples were, as stated, at the top of the plough pan, at the top of the unripened clay layer, and around the tile drain depth if groundwater levels in the matrix domain rose above the subsurface drain level i.e., above the macropore groundwater level at/near the tile drain. This last 'transfer zone' did appear only in case of the C-model. In the other models, soil water was not stagnant at/near the tile drain. In case of the A-model only, significant mass exchange occurred in the sandy bottom layer of the profile. The 1993-1994 period showed a factor 1.7 as much mass transfer as compared to the first measurement year, which originated from different weather conditions. The exchange of mass will have an effect on the solute transport behavior of the system

modeled. Note that the absolute values of the exchange terms are large. If the mass transfer from the matrix to the macropore domain would have been switched off in case $h_\mu < 0$ (Section II.3), less mass transfer would have been expected.

The division of total drainage into tile drainage and bottom drainage and into the matrix and macropore drainage is shown in Table IV.3.3. It is important to note that in the models, once drainage is passing the bottom layer, this water will not enter the soil profile again. In other words, Q_{bottom} will not reach the tile drains and will enter the local surface water by saturated groundwater flow. It is assumed that the Ditch will catch all drainage water, although, in practice, a portion of it can drain into the channel as shown in Fig. II.6.1. From Table IV.3.3 it can be seen that the travel route and domain of origin of drainage water are quite different for the three models used.

The results of the A-model can be explained by the saturated hydraulic conductivity k_s of the sandy aquifer. A k_s value larger than 13 cm d^{-1} caused the pressure heads at/near the tile drain to be above zero only during peak events. The soil area around the tile drain reached saturation only now and then in 1992-1993; the tile drain did function part of the time in the A-model. In 1993-1994, the tile drain was more often draining excess water; a larger part of Q_{total} was drained by the tile drain compared to the 1992-1993 period. The downward water transport capacity of the fully ripened clay layer in the B-model caused almost the same effect. Most of the water did bypass the tile drain and reached the bottom of the column. Pressure heads at/near the tile drain were rarely above zero. Under wet conditions, the tile drain discharged 40% and 38% of Q_{total} in the A-model and B-model respectively during the 1993-1994 season. Results of the C-model showed that the *unripened clay layer was blocking the bottom outlet for the excess water* in the soil profile. Pressure heads built up, causing the tile drain to often behave as a seepage face; consequentially, the tile drain discharged most of the excess precipitation. The simulation results showed that matrix versus macropore drainage differed as well. The drainage water from the A-model left the flow domain almost solely by the matrix drainage only because of the presence of a single-porosity bottom layer consisting of sand. The B-model showed equal parts of matrix and macropore drainage.

Note that the above analysis does not state that water leaving a specific domain also originates from that same domain. Interaction and exchange of water between the domains will give more insight in this matter. The solute transport behavior gives the extra information necessary to conclude how the hydrological situation and observations should be interpreted.

The modeling exercise was performed to simulate and analyze the hydrology of the experimental site, consisting of two different plots. Based on the computed water balances and drainage components, the appropriate model or models combination for

Table IV.3.3
Flevoland experimental site. Simulations using the dual-porosity model of the division of total drainage into fractions Q_{tile} and Q_{bottom}, and into drainage from the matrix and macropore domain. All fractions were calculated to total drainage. Results shown for model A through C of Fig. IV.3.1. *Drainage water at the bottom leaves by a sandy layer, which is essentially a matrix domain.

Model	Year	Q_{tile}		Q_{bottom}		Q_{total}			
		Matrix	Macropores	Matrix	Macropores	Tile	Bottom	Matrix	Macropores
A	1992-93	0.00	0.09	0.08	0.83*	0.09	0.91	0.08	0.92*
	1993-94	0.00	0.40	0.04	0.56*	0.40	0.60	0.04	0.96*
B	1992-93	0.00	0.07	0.08	0.85	0.07	0.93	0.08	0.92
	1992-93	0.00	0.38	0.04	0.58	0.38	0.62	0.04	0.96
C	1992-93	0.50	0.33	0.08	0.09	0.83	0.17	0.59	0.41
	1993-94	0.47	0.38	0.07	0.08	0.85	0.15	0.55	0.45

each plot could be chosen. A preliminary conclusion was that the C-model best suits Plot 2. The situation at Plot 1 could be best described by a mixture of all three models. To illustrate the performance of the C-model, the measured and calculated tile drainage rates versus time are shown in Fig. IV.3.4.
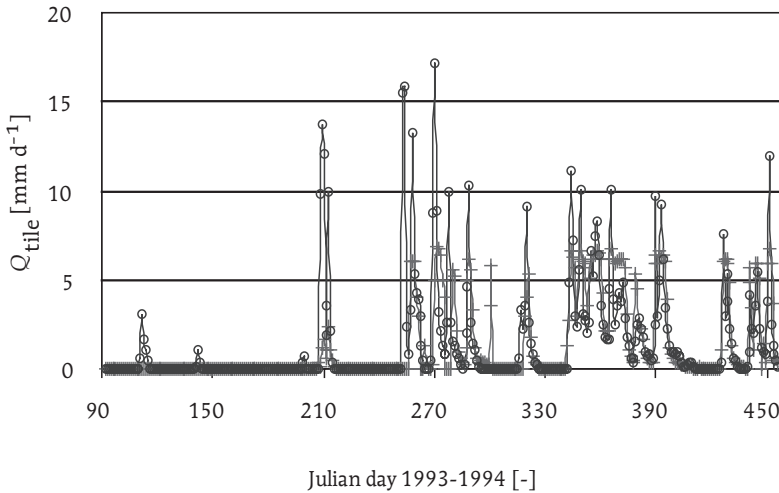
Fig. IV.3.4
Flevoland experimental site. Temporal variation of subsurface drainage rates. Field observations at Plot 2 (+) and simulation results (o) for the C-model. Period shown: April 1, 1993 (day 92) through March 31, 1994 (day 456).

Fig. IV.3.4 shows that the timing of the observed and simulated peaks of the subsurface drainage rate nearly coincides. The calculated total drainage rate is often larger than the measured drainage rates at the experimental field. The field pump capacity was about 8.3 mm d^{-1}, which appeared too small, event-wise, to keep up with the drainage water production (Groen, 1997). Observed drainage water rates were calculated from the pump data, which led to an underestimation of the actual drainage water rates. The dual-porosity model simulations, therefore, are likely to reflect better the actual drainage rates.

As previously stated, the solute transport behavior represented by the models is of great importance to judge which models suit which plot. In the next Section, tracer transport will be modeled and based on those results, the final choice between the combination of hydrology at the two plots and models can be made.

Tracer experiment - At the field site, a KBr-solution was applied by surficial spraying at Plot 1 on May 19, 1992. About 17 kg of bromide was dissolved in 0.4 m^3 of water.

The total tracer load was 7.8 kg ha^{-1}. At Plot 2, a KBr-solution was applied on April 14, 1993, again by spraying, in which about 25 kg of bromide was dissolved in 0.4 m^3 of water. The total tracer load was 11.7 kg ha^{-1} (Table IV.2.1). In the model simulations, the tracer application was represented by an initial concentration $C_{init} = 1.0$ at the matrix top boundary nodes at the start of the simulations, whereas for all other nodes, $C_{init} = 0.0$. Results for the simulations on the tracer transport for Plot 1 and Plot 2 are given in Table IV.3.4.

Table IV.3.4
Flevoland experimental site. Calculated cumulative tracer mass recovery of tile drainage and total drainage. Results for the models A through C are shown in Fig. IV.3.1. Time period: April 1, 1992 through March 31, 1993, and April 1, 1993, through March 31, 1994.

Model	Drainage term	$M_{calculated} / M_{applied}$ 1992-1993	$M_{calculated} / M_{applied}$ 1994-1994
A	tile	0.04	0.18
	total	0.35	0.39
B	tile	0.02	0.14
	total	0.33	0.37
C	tile	0.30	0.52
	total	0.30	0.52
Field data		*Plot 1*	*Plot 2*
	tile	**0.13**	**0.47**
	total	**0.24**	**0.56**

As can be seen from Table IV.3.4, the A-model and B-model did show some tracer loss by Q_{tile}. The main part of the tracer left the soil column by Q_{bottom}. The C-model showed that all calculated tracer losses left the soil column by Q_{tile}, and the tracer recovery results are close to the field data for Plot 2. As compared to Plot 1, the C-model over-predicts the tracer lost through drain tile. The first breakthrough of the tracer as calculated by the models was in 1992-1993 on September 5, 1992 for the A-model and

on October 17, 1992 for the B- and C-model. On September 5, 1992, a rainfall event of 15 mm d^{-1} was recorded. During the three days before October 17, 1992, a total of 44 mm rainfall was recorded. During the 1993-1994 season, all models showed the first tracer breakthrough on July 28, 1993, after three days with a total of 60 mm of rainfall.

The division of the two plots in the typical soil columns represented by the three models can be derived from the data shown in Table IV.3.4. The simulation results of the three models can be combined in such way that the observed tracer recovery in drainage water is well represented by a mixture of the models i.e., typical soil columns.

It is concluded from the dual porosity modeling results that about half of the area of Plot 1 can be represented by the C-model. The other half of the area should be modeled using equal parts of both the A-model and B-model. The hydrology and transport behavior of the soil-water system at Plot 2 can be best described using the C-model for 90% of the area and the B-model for 10% of the area.

4   Travel time distribution of drainage water

Steady-state approach - The Ernst-Bruggeman approach to estimate the travel time of drainage water under steady-state and fully-saturated flow conditions was given by equation [II.5], which is valid for situations with the d/L ratio being larger than 0.1. At the Flevoland experimental site $L = 48$ m. Depth d could not be determined accurately by geophysical measurements at the experimental site due to the combined presence of sandy soil layers with brackish water and of clay layers with fresh water (Meinardi and Van den Eertwegh, 1995, 1997). Both combinations of the present soil layer and water 'type' yielded about the same electrical conductivity or resistance and could not be distinguished from the electrical signal.

Parameter d represents the depth of the local flow system i.e., permanently saturated zone, starting about 0.2 m below the tile drains level. The depth of the local-scale flow system d at Plot 1 was estimated at 5 m; at Plot 2, d was estimated at 3 m due to the presence of an unripened clay layer below the tile drains. In theory, [II.5] is not valid under these conditions of d/L smaller than 0.1 and cannot be applied. But, to roughly estimate the travel time distribution, [II.5] was applied for the long-term case. Parameter estimates on I and Φ_{eff} are still needed.

The long-term precipitation excess (1961-1990) was estimated at 0.425 m a^{-1}, I being equal to this value in cases where surface runoff is absent. The effective porosity Φ_{eff} was estimated as follows: The total porosity of the 1.20 m soil column was between 0.58 and 0.63, dependent on the composition of the bottom layer from 1.00 to 1.20 m depth. The matrix porosity of the clay columns in the cracked subsoil is on the average 58% of

the total porosity of the full column. If water flow and solute transport within these columns are completely neglected and all other column parts fully contribute to transport processes, Φ_{eff} would be around 0.26. However, if some transport occurs within these columns, it is likely that Φ_{eff} can be estimated as 0.30. Table IV.4.1 shows the results for the f_1 to f_3 fractions of the travel time distribution in this example.

Table IV.4.1
Flevoland experimental site. f_1 to f_3 fractions of travel time distribution of drainage water from Plot 1 and Plot 2, based on the Ernst-Bruggeman approach [II.5] with parameters $d = 5$ m at Plot 1, $d = 3$ m at Plot 2, I=0.425 m a^{-1}, and $\Phi_{eff} = 0.30$ for both plots.

Fraction	Plot 1	Plot 2
f_1	0.25	0.38
f_2	0.19	0.23
f_3	0.14	0.15
Total	0.58	0.76

Transient flow conditions - The dual-porosity flow and transport code can be used to calculate the travel time distribution of drainage water in a variably-saturated flow medium *under transient flow conditions*. The model yields the fraction of the recovered versus the applied tracer amount, transported in micropores and macropores in the soil that leave the soil column by drainage.

It is assumed that once water and solutes have left the bottom of the 1.20 m soil column, they do not return to the tile drains. As a result of the model calculations, the tracer that leaves the soil by tile drainage can be translated directly into travel time fractions of drainage water. For bottom drainage, however, the situation is more complex. Fig. IV.2.5 already schematically showed the flow situation at/near the bottom of the soil columns of the two plots.

In general, vertical transport in the soil at the experimental site down to the bottom level of the ripened clay is dominant at both plots. Furthermore, the interconnected ripening cracks break the continuity of the matrix domain; in fact this domain consists of a number of clay columns, separated from each other. Main streamline patterns in the

clay columns are vertical. Horizontal flow leads to mass exchange between matrix and macropore domain. The tile drain cuts through the matrix clay elements and interconnected cracks and receives water and solutes during drainage from both domains in case the pressure head h in any domain exceeds the atmospheric pressure. In case h is smaller than the air pressure at the tile drain, water and solutes will pass the tile drain and flow down to the bottom of the column.

In case a ripened clay or sandy soil layer is present, almost all water and solutes will pass the bottom boundary. If an unripened clay layer exists below the tile drains, such as in Plot 2, further downward movement of water and solutes is hampered. Water pressure will build up, and tile drainage will occur for both domains under the condition that h is larger than or equal to the atmospheric pressure.

For both plots, the travel time distribution of drainage can be estimated from the recovered tracer that has passed the bottom of the model column. Where calculated tile drainage water enters the local surface water system directly, bottom drainage takes a longer travel route and thus a longer travel time. For bottom drainage the travel time distribution that it already took for water and solutes to get to the bottom of the 1.20 m soil profile should be integrated into the remaining travel time distribution to reach the surface water system.

The travel time distribution of drainage water and solutes that pass the unripened bottom layer consists of two parts: the time to pass the remaining part of the unripened clay layer, and the time to pass the sandy aquifer and to reach the surface water system. It is assumed that the unripened clay layer below the level of 1.2 m below the soil surface is not of any significant thickness at Plot 1 and Plot 2. Water and solutes passing the column bottom will have an additional travel time distribution before reaching the surface water. This travel time distribution can be estimated by using the steady-state Ernst-Bruggeman approach [II.5]. The local groundwater flow system below the bottom of the model column has parameters $d = 4$ m (estimate) for both Plots 1 and 2, $I = Q_{bottom}$, and $\Phi_{eff} = 0.35$ for the sandy aquifer. The fractions f_τ ($\tau = 1, \ldots, 3$) of the travel time distribution of water having passed the bottom of the soil column and entering the surface water are 0.21, 0.17, and 0.13.

Using the dual-porosity flow and transport models in combination with the Ernst-Bruggeman approach for Q_{bottom} to reach the surface water, the f_1 fractions were calculated for 1992-1993 and 1993-1994 for the total drainage leaving the 1.20 m soil columns. This fraction counts for all drainage water entering the local surface water system at the Flevoland experimental site within one year, and it is discharge-weighted (Table IV.4.2). Note that for the A- and B-model, only part of the drainage water passing the bottom of the soil column will reach the surface water in the same year. Therefore, the f_1 values for Q_{total} are smaller as compared to for Q_{bottom} for these two models.

Table IV.4.2
Flevoland experimental site. Fraction f_1 of travel time distribution of drainage water for
hydrologic years 1992-1993 and 1993-1994, respectively. Simulation results for models
A through C of Fig. IV.3.1. Fraction f_1 shown for tile drainage Q_{tile}, for bottom drainage
Q_{bottom}, and for total drainage Q_{total} entering the surface water system.

| Model | Fraction f_1 of travel time distribution of drainage water | | | | | |
| | 1992-1993 | | | 1993-1994 | | |
	Q_{tile}	Q_{bottom}	Q_{total}	Q_{tile}	Q_{bottom}	Q_{total}
A	0.04	0.35	0.22	0.18	0.39	0.37
B	0.02	0.33	0.19	0.14	0.37	0.33
C	0.30	0.00	0.30	0.52	0.00	0.52

The f_1 fraction of the travel time distribution of drainage water is just a part of the total
distribution. It is expected that the f_2 and f_3 fractions, together with f_1, are of major
importance to describe the largest part of the total travel time distribution of drainage
water. To see what these f_2 and f_3 fractions represent at the Flevoland experimental site,
drainage water production and applied tracer recovery was calculated using three series of
three different sequential hydrologic years. A selection of meteorological years in the
30-year period 1965-1994 was performed based on ranking of annual sums of P and
ET_r, of five-day sums of rainfall events, and of extreme rainfall events. Overall, the
following three-year periods were chosen: April 1984 – March 1987, a series of *average*
meteorological years, April 1975 – March 1978, a series of *dry* years, and April 1965 –
March 1968, a series of *wet* years. The meteorological data used were taken from stations
Nieuwe Wetering (P) and De Bilt (ET_r) due to lack of local 'old' data and relocations of
measurement stations in the Flevoland area. It is noted that 1967 and 1977 are rather
average weather years, but they complete the three-year time series.

Crop factors f_c to calculate ET_p from ET_r data (Section II.3) were for an average arable
crop, off-season for bare soil $f_c = 0.4$. Factor f_c for an average arable crop was calculated
using crop factors from Feddes (1987) for potatoes, wheat, and sugar beets, representing
a 1:3 crop rotation. Using daily P and ET_p values for these different years, matrix and
macropore drainage rates were simulated using the A, B, and C models with parameters
as presented for the 1992-1994 simulations. In Table IV.4.3 the hydrological results of
the simulations of the three 3-year periods are shown.

Table IV.4.3

Flevoland experimental site. Cumulative annual numbers on P, Q_{runoff}, I, and Q_{tile} and Q_{matrix} as fraction of total drainage Q_{total}, for three sequential hydrologic years 1975-1978 (dry), 1984-1987 (average), and 1965-1968 (wet), respectively. Simulation results are for models A through C of Fig. IV.3.1. Results shown for total flow domain, except for Q^*_{runoff} (matrix domain only; Fig. IV.3.2). *Infiltration rate at the soil surface, equal to $P - Q_{runoff}$.

Model	Period	P [mm]	Q^*_{runoff} [mm]	Q_{runoff} [mm]	I^* [mm]	Q_{tile}/Q_{total} [-]	Q_{matrix}/Q_{total} [-]
A	1975-1978	2027	0	0	2027	0.04	0.18
	1984-1987	2559	0	0	2559	0.16	0.16
	1965-1968	3083	0	0	3083	0.56	0.06
B	1975-1978	2027	0	0	2027	0.03	0.14
	1984-1987	2559	0	0	2559	0.17	0.10
	1965-1968	3083	0	0	3083	0.40	0.06
C	1975-1978	2027	0	0	2027	0.96	0.03
	1984-1987	2559	0	0	2559	0.97	0.02
	1965-1968	3083	0	0	3083	0.98	0.02

From the data shown in Table IV.4.3 it can be seen that all rainfall infiltrated into the soil, also Q^*_{runoff} did not occur. It was, however, expected that some Q^*_{runoff} would occur, especially under wet conditions and/or during high rainfall events. The calculation results show that the more wet the hydrologic years and the more often wet conditions prevailed in the hydrologic years under consideration, the larger the part of Q_{tile} was in Q_{total}, and the larger the part of the drainage that left the soil profile by the macropore domain. The numbers in Table IV.4.3 cannot directly be interpreted in terms of solute transport and travel time of drainage water. Note e.g., that matrix drainage is defined as drainage water leaving the soil profile by the matrix domain. This water could potentially have originated from the macropore domain, transferred to the matrix just before drainage occurred. Therefore, the solute transport behavior as represented by the models will be showed and discussed.

To repeat the tracer experiment numerically, solute mass was initially present in the soil profile only at the top of the matrix flow domain, which was done by setting $C_{initial} = 1.0$ for the top boundary nodes. For all other nodes, $C_{initial} = 0.0$. Plant uptake of solutes was switched off. The travel time distribution fractions f_τ are defined as the solute mass fraction lost by drainage relative to the initial solute mass present, $M_{drainage}/M_{initial}$ i.e., applied tracer mass recovery in drainage water. Results of the simulations are presented by means of f_τ fractions. The year-by-year recovered tracer fraction lost in total drainage by tile drains and bottom drainage was translated into the f_1, f_2, and f_3 fractions. Results are shown in Table IV.4.4.

From Table IV.4.4 can be seen that during dry years, the A- and B-model results show that 33% of the excess rainfall leaves the soil column within three years, whereas for the C-model this number is 68%. Under more average weather conditions, these numbers are 61% and 62% for the A- and B-models, respectively, and 77% for the C-model. During wet years, the models yielded 84% (A-model), 81% (B-model), and 86% (C-model). As the weather conditions were wetter, the differences in the travel time distribution of drainage water between the used models became smaller; the reason for the differences is the soil profile and hence, the hydrological response of the soil-water-system.

The calculated f_τ fractions show similarities as well as some deviations according to the Ernst-Bruggeman approach. Under dry weather conditions, it appeared that f_3 was larger than f_1 and f_2 for the A- and B-models, and that f_2 was larger than f_3 and f_1 for the C-model. Under average weather conditions, f_2 was larger than f_1 for the A- and B-models. Under wet conditions, all models behaved more or less like the Ernst-Bruggeman approach but yielded somewhat larger f_1 fractions.

The local soil profile and the occurrence of preferential flow processes due to macropore flow at the experimental site Flevoland caused deviations in the calculated travel time distribution of drainage water by the dual-porosity model results compared to by the steady-state Ernst-Bruggeman approach (Fig. IV.4.1). The dual-porosity modeling results gained insight in the effect of weather conditions, as well as of the soil profile on the travel time distribution of drainage water. This transient modeling method lead to improved estimates of the f_τ fractions of the travel time distribution at the experimental site. It is concluded that on a larger spatial i.e., regional scale, with the Ditch catchment as a first example, the Ernst-Bruggeman approach is suitable to calculate the travel time distribution of drainage water using $\Phi_{eff} = 0.30$.

It is concluded that the bottom layer from 1.05 to 1.20 m below the soil surface of the soil profile at Plot 1 consists of each of the three bottom layers used in A, B, and C models. The bottom layer at half of Plot 1 consists of unripened clay; the other half consists of almost equal parts of sand and ripened clay. The bottom layer at Plot 2 is

Table IV.4.4

Flevoland experimental site. Fraction f_1 to f_3 of travel time distribution of drainage water for three sequential hydrologic years 1975-1978 (dry), 1984-1987 (average), and 1965-1968 (wet). Simulation results are for models A through C of Fig. IV.3.1. f_τ fractions are shown for tile drainage Q_{tile}, bottom drainage Q_{bottom} and total drainage Q_{total} entering the surface water system.

Model	Fraction	Q_{tile} 1975-1978	Q_{bottom} 1975-1978	Q_{total} 1975-1978	Q_{tile} 1984-1987	Q_{bottom} 1984-1987	Q_{total} 1984-1987	Q_{tile} 1965-1968	Q_{bottom} 1965-1968	Q_{total} 1965-1968
A	f_1	0.02	0.24	**0.10**	0.02	0.35	**0.18**	0.48	0.31	**0.63**
	f_2	0.01	0.25	**0.09**	0.03	0.36	**0.27**	0.03	0.11	**0.14**
	f_3	0.01	0.24	**0.14**	0.01	0.12	**0.16**	0.01	0.03	**0.07**
B	f_1	0.01	0.24	**0.09**	0.03	0.36	**0.20**	0.21	0.33	**0.40**
	f_2	0.01	0.24	**0.09**	0.03	0.34	**0.26**	0.06	0.26	**0.28**
	f_3	0.01	0.26	**0.14**	0.02	0.12	**0.16**	0.02	0.06	**0.13**
C	f_1	0.22	0.00	**0.22**	0.36	0.00	**0.36**	0.52	0.00	**0.52**
	f_2	0.25	0.01	**0.25**	0.28	0.01	**0.28**	0.25	0.01	**0.25**
	f_3	0.21	0.00	**0.21**	0.13	0.01	**0.13**	0.09	0.00	**0.09**
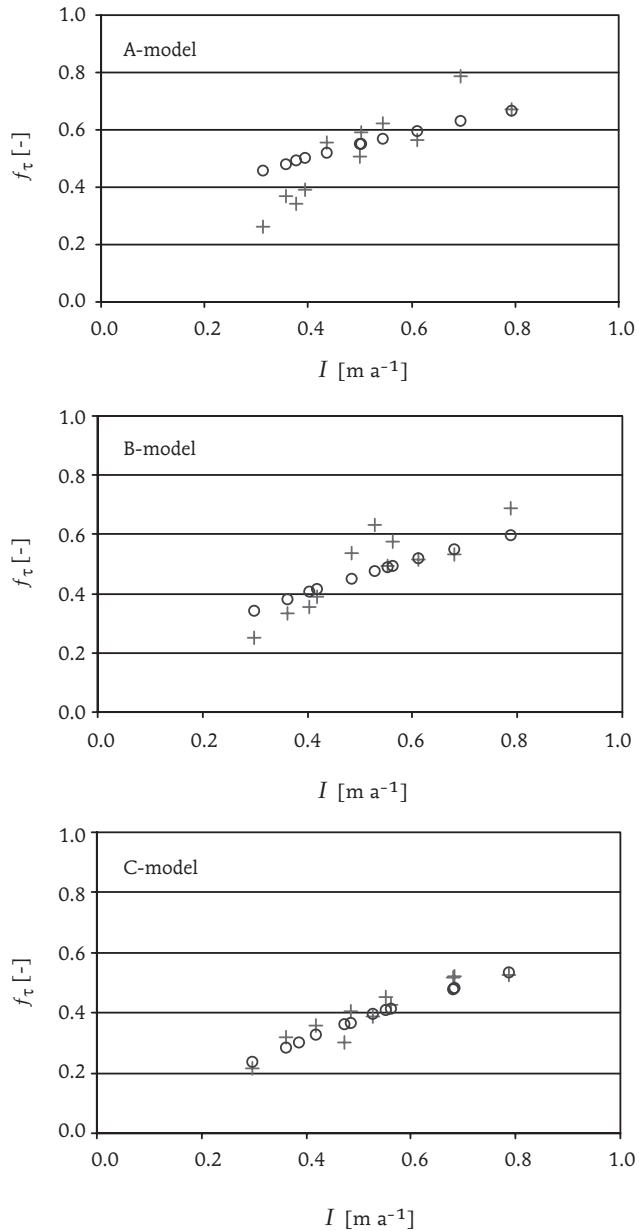
Fig. IV.4.1

Flevoland experimental site. Fractions f_τ of travel time distribution of drainage water, based on calculations of dual-porosity models (A, B, and C) (+) and Ernst-Bruggeman approach [II.5] (o). Parameters used in [II.5] for A-model: $d = 4.50$ m and $\Phi_{eff} = 0.30$; for B-model: $d = 3.75$ m and $\Phi_{eff} = 0.30$; for C-model: $d = 3.25$ m and $\Phi_{eff} = 0.30$.

primarily (90%) an unripened clay layer, at 10% of the area this clay layer is ripened. The bottom layer of the average soil column for the Ditch consists for 66% of unripened clay, for 17% of ripened clay, and for 17% of sand. The average travel time distribution of drainage water from Plot 1, Plot 2, and the Ditch is given in Table IV.4.5.

Table IV.4.5
Flevoland experimental site. Long-term annual average travel time distribution fractions of drainage from Plot 1, Plot 2, and Ditch.

Fraction	Plot 1	Plot 2	Ditch
f_1	0.27	0.34	0.30
f_2	0.26	0.28	0.28
f_3	0.15	0.13	0.14
Total	0.68	0.75	0.72

5   Annual agricultural nutrient budgets and drainage loads

Nutrient budgets - Plot-scale nutrient budgets give insight in the potential losses of nutrients to the environment. Knowledge about the physical and chemical properties of the soil-water-system can provide a relationship between agricultural nutrient losses, as calculated from soil system balances (Section II.6), and nutrient loads to surface water. Therefore, information is needed on the nutrient management practices of the farmer. The hydrology of Plot 1 and 2 was previously described. In this Section, agricultural nutrient budgets are produced and related to the 'measured' nutrient loads in the field of tile drains and ditch drainage, using the travel time distribution of drainage water as the main result of Section IV.4.

Table IV.5.1 shows the nutrient applications and nutrient removal by harvest of the main arable crops as farm averages. Manure applications were generally used in autumn after the harvest of winter wheat, grass seeds, or grassland, and always preceded potatoes in the next year's growing season. From an agricultural point of view, these manure applications served the crop of the next following growing season. As far as nutrient losses by drainage are concerned these applications also added to the surface water load

of nutrients. The data presented were somewhat higher but match the average figures for modern Dutch arable farms (Frank Wijnands, Research Service Arable Farming, personal communication).

Data on the sum of wet and dry deposition of nutrients from the atmosphere were estimated from measurements and calculations made by the Royal Dutch Meteorological Institute and the National Institute of Public Health and Environment (RIVM and KNMI, 1989). The atmospheric deposition is estimated at 30 kg ha^{-1} a^{-1} N and 1 kg ha^{-1} a^{-1} P. No site-specific field measurements were performed on atmospheric deposition, volatilization, denitrification, and internal source or sink terms. Volatilization of ammonia ($NH_3 \uparrow$) was estimated by using [III.8]. N-fixation, and net mineralization were assumed to be negligible. During any particular crop rotation, equilibrium conditions, with respect to soil organic matter, were assumed.
Field measurements on denitrification were not performed. Data from various references (e.g., Aslyng, 1986; Rolston et al., 1984; Van Faassen and Lebbink, 1990; Lotse et al., 1992) for denitrification in arable farming on silt loam and clay soils show a strong variation of denitrification in space and time. Annual N-losses by denitrification for arable land on loam and clay soils vary between 2 and 70 kg ha^{-1} a^{-1}, but they are usually between 20 and 50 kg ha^{-1} a^{-1}. Based on De Klein (1994) and Corré (1995) an estimate was made for denitrification at the Flevoland experimental site. Corré (1995) carried out field measurements at the Rusthoeve experimental farm in the southwestern part of the Netherlands (see also Van den Eertwegh et al., 1999). At this farm, the soils contain less organic matter compared to the Flevoland experimental site and hence Corré (1995) found a denitrification rate of 25 to 30 kg ha^{-1} a^{-1} N only. Also, denitrification might occur in Flevoland under anoxic conditions due to oxidation by nitrate-N of pyrite present in the clay soil matrix. This process occurs particularly if an unripened clay layer is passed by drainage water. Given these factors, the denitrification rate is estimated at 50 kg ha^{-1} a^{-1} N.

The effect of the soil itself on the nutrient balance is more difficult to judge. Soil ripening is not at its final stage yet as can be seen from long-term (1958-1992) soil-surface-level height measurements; the soil subsidence is not yet completed (Van Dooremolen et al., 1996). This process is expected to lead to gain source terms in the nutrient balance sheets. On the other hand, phosphate is expected to adsorb to the solid phase of the clay soil matrix, maybe leading to a net sink for this nutrient. Analysis of the soil system nutrient balance and the relation between nutrient surplus and drainage loads will provide insight on the P-adsorption.

The average soil system nutrient balances are presented in Table IV.5.2. The crop rotation for Plot 1 was grass seeds (1; 1989), sugar beet (2; 1990), winter wheat (3; 1991), and potatoes (4; 1992). The crop rotation for Plot 2 was sugar beet (1; 1991), winter wheat

Table IV.5.1

Flevoland experimental site. Nutrient applications by fertilizer and manure and removal by harvest for main crops as farm averages. *Manure application after harvest of winter wheat. **Potatoes were grown next season after winter wheat.

Crop	Fertilizer		Manure		Removed by harvest	
	N [kg ha^{-1} a^{-1}]	P [kg ha^{-1} a^{-1}]	N [kg ha^{-1} a^{-1}]	P [kg ha^{-1} a^{-1}]	N [kg ha^{-1} a^{-1}]	P [kg ha^{-1} a^{-1}]
Grass seeds	125	44	90	30	35	7
Sugar beet	95	29	0	0	116	34
Winter wheat	175	26	*150-300	*40-80	180	34
Potatoes**	205	52	0	0	200	32

(2; 1992), and potatoes (3; 1993). Note that the plots have different crop rotations, 1:4 for Plot 1, and 1:3 for Plot 2. For the Ditch, nutrient balances for all crops were available for each year, representing the crop rotation on the farm scale of 1:4. The data presented in Table IV.5.2 match the general and average nutrient balances for arable farming in the Netherlands as given by Schröder et al. (1993, 1994). Plot 1 is the most intensively used plot as shown from the data in Table IV.5.2. The difference in N-surplus between the balance systems is caused by differences in crop rotation, and thus by differences in nutrient applications, especially in manure. The P-balance shows a surplus, which will probably be adsorbed into the soil-matrix system on an average annual basis. Depending on the P-sorption capacity of the soil, sooner or later leaching of phosphorus from the soil to tile drains and local surface water will be enlarged in comparison to the present situation. Differences in the P-balance between both plots are caused by differences in crop rotation.

Solute losses by drainage - The solute loads of the drainage water from the tile drains of Plot 1, Plot 2, and of the Ditch were calculated by using measured discharge rates, measured solute concentrations, and an interpolation method to account for solute loads during non-sampled periods. Besides nitrogen and phosphorus, chloride and potassium loads are also given. The field water balance showed that drainage also occurred by routes other than tile drains. Additional solute loads were calculated for this unmeasured drainage Q_{unmeas}. To calculate these loads, solute concentrations were needed. For chloride, phosphorus, and potassium, the measured concentrations in tile drainage were used to calculate the solute load of Q_{unmeas}. To account for denitrification losses, a 50% reduced nitrate-concentration was used to calculate the load by Q_{unmeas}.

The Ditch received and discharged seepage water. To link agricultural practices to solute losses by drainage, the seepage water influence on the solute load of drainage water was corrected by subtracting the seepage water load from the total calculated load. Seepage water concentrations used were 500 mg l^{-1} chloride, 0.1 mg l^{-1} nitrate-N, 1.5 mg l^{-1} Kjeldahl-N, 0.01 mg l^{-1} total-P, and 8 mg l^{-1} K. As a result, solute loads were calculated that originated only from local-scale drainage of precipitation excess and nutrients leaching. This approach enables *coupling of the agricultural nutrient balances with calculated nutrient losses by drainage*. The calculated solute loads of drainage water entering the surface water from Plots 1 and 2 and of the Ditch are shown in Tables IV.5.3 and IV.5.4.

Note that the N-loads exceed the N-surpluses shown in Table IV.5.2 by a factor 1.5 to 2. Reasons for this are that the neglected net mineralization of organic matter was existent, and/or the denitrification rate was overestimated. It is also possible that non-equilibrium conditions in soil-chemical processes occurred, (event-wise) preferential transport of water and solutes took place, and inaccuracies were present in data provided for by the

Table IV.5.2

Flevoland experimental site. Nitrogen (N) and phosphorus (P) budget of Plot 1, of Plot 2, and of Ditch. Data for the average crop rotation as a whole. Plot 1 and Ditch have 1:4 crop rotation, Plot 2 has a 1:3 crop rotation. In: sum of fertilizer, manure, and atmospheric deposition. Out: sum of removal by harvest, volatilization, and denitrification. *P-adsorption is excluded.

| Balance system | | In | | Out | | Surplus | |
| | | N | P | N | P | N | P* |
		[kg ha^{-1} a^{-1}]	[kg ha^{-1} a^{-1}]	[kg ha^{-1} a^{-1}]	[kg ha^{-1} a^{-1}]	[kg ha^{-1} a^{-1}]	[kg ha^{-1} a^{-1}]
Plot 1	1989-1992	256	60	202	29	54	31
Plot 2	1991-1993	243	49	218	32	25	17
Ditch	1989-1992	211	49	203	30	8	19
	1990-1993	221	56	204	29	17	27

Table IV.5.3
Flevoland experimental site. Measured and total solute loads in drainage water from
Plot 1 (April 1, 1992 through March 31, 1993) and from *Plot 2* (April 1, 1993 through
March 31, 1994). For total loads –solute load of unmeasured drainage terms are added.
*50% of this load was discharged during March 1994.

Solute	*Plot 1*, 1992-1993		*Plot 2*, 1993-1994	
	Measured	Total	Measured	Total
Chloride	275	539	250	299
Nitrate-N	54	80	*44	48
Total-N	57	86	51	57
Ortho-P	0.04	0.08	0.09	0.11
Total-P	0.08	0.16	0.18	0.22
Potassium	20	39	38	45

farmer. The first two factors increase the risk of solute losses by drainage from the
structured soils at the site.

The discharge-weighted average Cl-concentration, the corrected load divided by the total
discharge, in drainage from Plot 1 is 210 mg l^{-1}, for Plot 2 about 55 mg l^{-1}.
This difference can be caused by a more intensive agricultural use of Plot 1 in terms of
crop rotation and manure application. This leads to an estimated contribution of
10-20 mg l^{-1} Cl^- extra only. The main reason for the difference is that drainage from
Plot 1 occurs by partially deeper flow paths compared to the situation at Plot 2 as
previously stated.

The upper 1 m soil column of both plots has equal soil layers and is expected to be
comparable as far as Cl-diffusion from soil matrix to soil water is concerned. Differences
are probably caused by the interaction of draining excess water with the brackish water in
the sandy aquifer. Groundwater hydraulic heads in the aquifer are expected to be higher
at Plot 1 as compared to Plot 2, the latter located more toward the Vogeltocht channel.
Also, the clay layer at Plot 1 is more 'leaky' due to the smaller thickness of the confining
layer. It seems that the drainage water composition of Plot 1 is more influenced by the
deeper groundwater composition. This again contributes to the statement that *drainage
routes for Plot 1 are partially deeper compared to those of Plot 2*. This situation matches the
observed differences in nitrogen loads between the plots.

Table IV.5.4
Flevoland experimental site. Measured and total solute loads in drainage water from
Ditch for periods April 1, 1992 through March 31, 1993, and April 1, 1993 through
March 31, 1994. For total loads are the sum of solute load of unmeasured drainage
terms and subtracted seepage water.

| Solute | *Ditch* | | | |
| | 1992-1993 | | 1993-1994 | |
	Measured	Total	Measured	Total
Chloride	450	339	265	249
Nitrate-N	40	65	24	45
Total-N	43	70	28	55
Ortho-P	0.05	0.11	0.09	0.25
Total-P	0.10	0.23	0.18	0.50
Potassium	22	50	18	50

Locally, the aquifer groundwater composition showed nitrate-N concentrations below
1 mg l^{-1}. Given this concentration level, it is likely that almost all nitrate-N found in
tile or ditch drainage is caused by atmospheric deposition and agriculture. The relative
contributions of both sources are 10-15% and 85-90%, respectively. The part of nitrate
in the total-N load is 95% in drainage water from Plot 1, and 85% from Plot 2.
This difference is not large, but it could be caused by differences in denitrification
conditions on the two plots. The unripened clay layer was likely to enhance the
denitrification at Plot 2 compared to Plot 1; in addition the weather conditions were
different. In 1993-1994, more rainfall was recorded and denitrification was larger.
The overall total-N load from Plot 1 is larger than the N-load from Plot 2. Note that
total drainage from Plot 1 was about 350 mm, from Plot 2 about 560 mm. P-loads for
both plots were small; 50% of these loads are loads of dissolved organic phosphate,
which is likely to originate from a background process like the ongoing soil ripening.
Sorption to the clay soil complex is holding the P-surplus in balance and out of the
drainage water. There is no correlation between P-surplus from the nutrient balance and
P-load of drainage water. The potassium losses by drainage are spatially homogeneous at
the farm scale. From the nutrient balance surplus data (not shown) and calculated
loads, the amount of potassium originating from the soil system can be estimated at 75
to 100 kg ha^{-1} a^{-1}. About 50% of this amount did benefit the arable crop production;
the other half was lost by drainage.

The Cl-load of the Ditch was different for the two subsequent hydrologic years. The discharge-weighted average Cl^- concentration in drainage water of the Ditch differed between 100 mg l^{-1} in the first year and 45 mg l^{-1} in the second year. During the second year, a larger part of the total drainage, as compared to the first year, traveled by more shallow flow paths. The main reasons for differences in solute loads from the Ditch between the two measurement years were the almost twice as large precipitation excess in 1993-1994 compared to 1992-1993, which caused dilution effects. This reason is proof that the fraction of drainage water with a travel time of less than one year is of great importance and influence at the Flevoland experimental site. The different local groundwater flow situation was also a factor, especially the influence of seepage water. During wet conditions and ditch discharge events, the groundwater seepage flow entering the ditch was more suppressed compared to dry conditions and low-flow situations. Groundwater seepage rates were smaller during the second year. It is expected that seepage water solute concentrations were constant with time and did not change from year to year. The spatial variation in the contribution of plot drainage to ditch drainage also caused differences. The influence of drainage water from plots at the northeast section of the ditch catchment was larger compared to drainage water from plots at the southwest part. The plots located at the northeast part of the ditch catchment area have a relatively larger area with an unripened clay layer compared to the southwestern plots. Tile drainage from the northeastern plots was a higher percentage of total drainage from those plots compared to the southwestern plots. Tile drainage dominated the ditch water.

Linking agricultural practices to nutrient losses and loads to surface water - To analyze the relationship between agricultural practice and leaching of nutrients from the plots, the surplus of the annual agricultural nutrient budgets will be linked with calculated annual losses of nutrients by drainage, based on field measurements. The 1:4 crop rotation is chosen as the time period. Analysis will be performed on an annual basis, determining the following quantities:

- drainage water flux Q_{drainage},
- f_τ fractions ($\tau = 1,3$) of the travel time of drainage water, where f_4 is taken as the remaining fraction for all drainage with a travel time of more than three years,
- nutrient surplus on soil system balance of the two years preceding the year of analysis, and the crop-rotation average nutrient surplus,
- precipitation excess $P - ET_a$ of the two years preceding the analysis year, and the crop-rotation average annual precipitation excess or long-term average annual precipitation excess.

The nutrient mass flux of drainage water $q_{m,\text{drainage}}$ based on field measurements was shown in the Tables IV.5.3 and IV.5.4. Now, $q_{m,\text{drainage}}$ can be calculated from the nutrient budget surplus, weather data, and travel time distribution. Taking nitrogen (N)

as an example, $q_{m,\text{drainage}}$ is computed as

$$q_{m,\text{drainage,N}} = \sum_{\tau=1}^{4} \left(f_\tau\, Q_{\text{drainage}} \quad \frac{N_{\text{surplus},\tau}}{(P - ET_a)_\tau} \right)$$ [IV.6]

with $\tau = 1$ is year of interest, $\tau = 2$ is preceding year, etc., f_τ the travel time fraction, Q_{drainage} the annual drainage rate, $N_{\text{surplus},\tau}$ the nitrogen surplus mass flux on soil system balance for year τ, and $(P - ET_a)_\tau$ the annual precipitation excess rate. For τ larger than 3, the crop-rotation average nutrient surplus flux and the annual precipitation excess rate were used. The travel time fractions used were based on results presented for f_1 in 1992-1993 and 1993-1994 for all three models used (Table IV.4.2), and for the other f_τ fractions as presented in Table IV.4.5. The crop-rotation average nutrient surplus for N and P and the long-term precipitation excess for Plot 1, Plot 2, and Ditch are given in Table IV.5.5. The results for N and P are given for Plot 1 in Table IV.5.6, for Plot 2 in Table IV.5.7, and for the Ditch in Table IV.5.8.

Table IV.5.5
Flevoland experimental site. Crop-rotation average nutrient surplus for N and P, and rotation-average precipitation excess for *Plot 1*, *Plot 2*, and *Ditch*.

Variable		Plot 1	Plot 2	Ditch	
		1992-1993	1993-1994	1992-1993	1993-1994
$N_{\text{surplus,average}}$	[kg ha^{-1} a^{-1}]	54	25	8	17
$P_{\text{surplus,average}}$	[kg ha^{-1} a^{-1}]	31	17	19	27
$(P - ET_a)_{\text{average}}$	[mm a^{-1}]	270	400	275	390

The calculated loads based on field data and loads calculated by using [IV.6] show deviations for Plot 1 and are both higher as compared to the N-surplus for the nutrient balance for Plot 1. The drainage water composition is not a direct reflection of the four-year average N-concentration leaching from the upper soil, but of the *N-surplus weighted with the travel time distribution of drainage water* as shown in Table IV.4.5. N-load data for Plot 2 are more than two times higher as compared to the four-year average N-balance surplus of 24 kg ha^{-1} a^{-1}. Application of [IV.6] including the travel time distribution of drainage water leads to a better result as compared to a four-year average. The difference between the calculated loads and the N-surplus is mainly caused

Table IV.5.6

Flevoland experimental site, *Plot 1*. Nitrogen N and phosphorus P mass flux of drainage water ($q_{m,\text{drainage}}$) calculated with [IV.6] using the nutrient budget surplus, weather data, and travel time distribution. *Hydrologic year. **Data are from Table IV.5.3, 'total' values. ***P-adsorption is estimated at 43 kg ha^{-1} a^{-1}.

Year*	$P - ET_a$ [mm a^{-1}]	Q_{drainage} [mm a^{-1}]	N_{surplus} [kg ha^{-1} a^{-1}]	P_{surplus} [kg ha^{-1} a^{-1}]	$q_{m,\text{drainage,N}}$ Calculated [kg ha^{-1} a^{-1}]	Field data** [kg ha^{-1} a^{-1}]	$q_{m,\text{drainage,P}}$ Calculated [kg ha^{-1} a^{-1}]	Field data** [kg ha^{-1} a^{-1}]
1989	150		+72	+25				
1990	203		-121	-15				
1991	369		+227	+95				
1992	363	347	+39	+21	77	86	0.92***	0.16

Table IV.5.7

Flevoland experimental site, *Plot 2*. Nitrogen N and phosphorus P mass flux of drainage water ($q_{m,\mathrm{drainage}}$) calculated with [IV.6] using the nutrient budget surplus, weather data, and travel time distribution. *Hydrologic year. **Data are from Table IV.5.3, 'total' values. ***P-adsorption is estimated at 18 kg ha⁻¹ a⁻¹.

Year*	$P - ET_a$ [mm a⁻¹]	Q_{drainage} [mm a⁻¹]	N_{surplus} [kg ha⁻¹ a⁻¹]	P_{surplus} [kg ha⁻¹ a⁻¹]	$q_{m,\mathrm{drainage,N}}$		$q_{m,\mathrm{drainage,P}}$	
					Calculated [kg ha⁻¹ a⁻¹]	Field data** [kg ha⁻¹ a⁻¹]	Calculated [kg ha⁻¹ a⁻¹]	Field data** [kg ha⁻¹ a⁻¹]
1991	329		-22	+7				
1992	431		+86	+21				
1993	652	565	+9	+24	29	57	0.93***	0.22

Table IV.5.8

Flevoland experimental site, *Ditch*. Nitrogen N and phosphorus P mass flux of drainage water ($q_{m,\text{drainage}}$) calculated with [IV.6] using the nutrient budget surplus, weather data, and travel time distribution. *Hydrologic year. **Data are from Table IV.5.4, 'total' values. ***P-adsorption is estimated at 27 kg ha^{-1} a^{-1}.

Year*	$P - ET_a$ [mm a^{-1}]	Q_{drainage} [mm a^{-1}]	N_{surplus} [kg ha^{-1} a^{-1}]	P_{surplus} [kg ha^{-1} a^{-1}]	$q_{m,\text{drainage,N}}$ Calculated [kg ha^{-1} a^{-1}]	$q_{m,\text{drainage,N}}$ Field data** [kg ha^{-1} a^{-1}]	$q_{m,\text{drainage,P}}$ Calculated [kg ha^{-1} a^{-1}]	$q_{m,\text{drainage,P}}$ Field data** [kg ha^{-1} a^{-1}]
1989	183		+28	+11				
1990	196		-87	-3				
1991	349		+61	+44				
1992	380	340	+27	+24	23	70	0.12***	0.23
1993	646	580	+65	+40	46	55	3.94***	0.50

by the 1993-1994 precipitation excess, which is a factor of 1.5 to 1.75 larger than average. Reducing the drainage water production to average levels led to a solid agreement of the calculated N-loads with the N-surplus of the balances. It is also possible that a fertilizer application at Plot 2 in February 1994 causes the difference in the four-year N-surplus and calculated N-load for the tile drains. The fertilizer was surficially applied during a short frost period, after which large amounts of rainfall where recorded. The combination of thaw and rain was likely to cause preferential flow events, whereby the fertilizer-N was partly lost, disturbing the N-balance. After February 1994, a strong rise in nitrate-N concentrations in tile drainage water was observed.
High nitrate-N concentrations were observed during the period February-April 1994 (Brongers et al., 1996).

Comparison of the N-surplus on the agricultural balances for the Ditch catchment and corrected loads shows that the N-loads for each year differ from the N-balance surplus. The two-year average of the N-load of about 60 kg ha^{-1} a^{-1} still reasonably approaches the average N-surplus of 50 kg ha^{-1} a^{-1}. Some differences are expected due to the fact that not all drainage water entering the Ditch will reach the ditch outlet, due to the complex hydrological situation in and around the Ditch as previously indicated.

The data presented on calculated P-loads did not match primarily unless P-adsorption to the solid phase was taken into account. Only a small part of the P-surplus was lost by drainage. No correlation exists between P-loads in drainage water and P-balance surpluses, without taking P-sorption into account. To match measured and calculated P-loads by introducing a P-sorption term in the balance, the estimated P-sorption rate at Plot 1 is 43 kg ha^{-1} a^{-1}, at Plot 2 it is 18 kg ha^{-1} a^{-1}, and at the Ditch it is 27 kg ha^{-1} a^{-1}. Based on the measured P-loads, it can be concluded that the P-sorption capacity of the soil at the experimental site is larger than the largest estimated sorption rate indicated.

6   Conclusions

The field observations at the Flevoland experimental site *generated a set of data of great value on hydrology and nutrient leaching*. The field water balance of both plots and of the Ditch at the Flevoland experimental site showed an unmeasured drainage term. Rainfall excess water left the plots by tile drainage, by direct drainage to the collection ditch, and to the channel. The soil profile was a main factor in this drainage situation, but the drainage system and weather conditions also introduced these drainage discharge routes. Drainage occurred between 50% in Plot 1, and 10% in Plot 2 by means other than the subsurface drains. Surface runoff was not observed at the experimental site, although ponding at the soil surface occurred. The tracer experiment at the field site showed a

recovery of 24%, one year after application and after 360 mm of drainage at Plot 1. The situation at Plot 2 was different; 56% of the tracer applied was recovered after one year and after 560 mm of drainage. At Plot 2, shorter travel times of drainage occurred compared to travel times at Plot 1.

The dual-porosity simulation models with three different bottom soil layers i.e., sand, ripened clay, and unripened clay, were able to reproduce measured and unmeasured drainage terms by introducing appropriate soil profiles and boundary condition types. The tracer recovery was simulated well. A mix of three types of bottom layers i.e., sand (25% of area), ripened clay (25% of area), and unripened clay (50% of area) was used to reproduce the hydrologic situation at Plot 1. The hydrologic situation at Plot 2 was judged having an unripened clay as the bottom layer at 90% of the area and ripened clay at 10% of the area. The bottom layer situation at the Ditch was estimated such that unripened clay was the bottom layer at 66% of the area and ripened clay and sand both at 17% of the area.

The travel time distribution of drainage water at the Flevoland site was calculated using the Ernst-Bruggeman steady-state approach. The simulation models were used to analyze this travel time distribution under transient flow conditions. The model applications yielded some different results compared to the steady-state approach, as shown in Table IV.6.1. However, the steady-state approach was able to reasonably estimate the travel time distribution under average to wet conditions.

It is concluded that the travel time distribution of drainage water at the experimental site is different for the two plots. *The steady-state approach is less suitable to estimate the field-scale travel time distribution as compared to the application of the numerical simulation models, especially under dry circumstances.* Under average to wet conditions, the steady-state is suitable enough. It is expected that on a regional-scale, the steady-state approach will be able to calculate appropriate travel time distribution fractions for all weather conditions. Weather conditions have a large impact on the values of mainly f_1 and f_2.

The arable-crop-rotation average nutrient surpluses and nutrient losses by drainage were linked using the travel time distribution of drainage water, as calculated with the plot-scale models. For phosphorus, a sorption term was introduced to match the calculated with the measured P-losses by drainage. For Plot 1 the average P-sorption was estimated at 43 kg^{-1} ha^{-1} a^{-1} P, for Plot 2 at 18 kg^{-1} ha^{-1} a^{-1} P, and for the Ditch at 27 kg^{-1} ha^{-1} a^{-1} P. Table IV.6.2 shows the results.

The so-called MINAS levy-free surpluses, as mentioned in Section I.1 in 2003 are 100 kg ha^{-1} a^{-1} N and 8.5 kg ha^{-1} a^{-1} P. The N-surplus level was reached each year

Table IV.6.1

Flevoland experimental site. Travel time distribution of drainage water. Calculated fractions f_τ ($\tau = 1,3$) using the Ernst-Bruggeman steady-state approach [II.5] and dual-porosity models for transient flow conditions. Parameters Ernst-Bruggeman approach are $d = 5$ m and $I = 0.360$ m a^{-1} at Plot 1, $d = 3$ m and $I = 0.675$ m a^{-1} at Plot 2. $\Phi_{\text{eff}} = 0.30$ for both plots. Data shown for Plot 1 and Plot 2 for periods 1992-1993 (Plot 1), 1993-1994 (Plot 2), and three-year period of average (1984-1987), dry (1975-1978), and wet years (1965-1968). *One year available only.

| Fraction | Plot 1 | | | | | Plot 2 | | | | |
| | Steady-state | Transient water flow and solute transport | | | | Steady-state | Transient water flow and solute transport | | | |
	1992-1993	1992-1993*	1984-1987 average	1975-1978 dry	1965-1968 wet	1993-1994	1993-1994*	1984-1987 average	1975-1978 dry	1965-1968 wet
f_1	**0.21**	**0.25**	0.27	0.16	0.52	**0.53**	**0.50**	0.34	0.20	0.51
f_2	0.17		0.26	0.17	0.23	0.25		0.28	0.23	0.25
f_3	0.13		0.15	0.18	0.10	0.12		0.13	0.20	0.10
Total	0.51		0.68	0.51	0.85	0.90		0.75	0.63	0.86

Table IV.6.2
Flevoland experimental site. Nitrogen N and phosphorus P mass flux of drainage water ($q_{m,\mathrm{drainage}}$) calculated from the nutrient budget surplus, weather data, and travel time distribution of drainage water. *P-adsorption is excluded.

Location	Period	N_{surplus} [kg ha^{-1} a^{-1}]	P_{surplus}* [kg ha^{-1} a^{-1}]	$P_{\mathrm{adsorption}}$ [kg ha^{-1} a^{-1}]	$q_{m,\mathrm{drainage,N}}$ [kg ha^{-1} a^{-1}] Measured	$q_{m,\mathrm{drainage,N}}$ [kg ha^{-1} a^{-1}] Calculated	$q_{m,\mathrm{drainage,P}}$ [kg ha^{-1} a^{-1}] Measured	$q_{m,\mathrm{drainage,P}}$ [kg ha^{-1} a^{-1}] Calculated
Plot 1	1989-1992	54	31	43	86	77	0.16	0.92
Plot 2	1991-1993	25	17	18	57	29	0.22	0.93
Ditch	1989-1992	8	19	27	70	23	0.23	0.12
	1990-1993	17	27	27	55	46	0.50	3.94

during the crop rotation period, except for one year due to a manure application. Although the crop-rotation average N-surplus was already lower than the levy-free surplus in 2003, N-losses by drainage were significant. The levy-free, P-surplus level was not reached at the time of the experiment. P-losses by drainage were small due to P-sorption to the solid phase of the clay soil.

In case of the Flevoland experimental site, calculated N-loads of the drainage water did partly fit the field data. The level was off by a factor of 1.1 to 3.0; the field data on N-losses was larger in all cases. Preferential flow and transport processes are possible reasons, leading to N-losses that do not match annual average balance surpluses. Due to the non-uniform transport processes, it is likely that the denitrification rate was overestimated, which led to an underestimation of drainage N-losses. It is also possible that an extra N-source was present due to net mineralization of organic matter. Calculated P-loads were in most cases close to measured P-losses after introduction of a P-adsorption term. The adsorption process strongly interfered with the interpretation of the observed P-loads.

Without using a travel time distribution of drainage water, the nutrient loads of the drainage water could not be reproduced. Using average soil system nutrient balance surplus data, larger deviations would have occurred between calculated and measured nutrient loads. The travel time distribution given in Table IV.6.1 suited the field situation at the experimental site for most cases reasonably well. The reason why calculated solute loads did not well match may have found its origin in other factors than the travel time distribution.

The soils under consideration at the Flevoland experimental site show an enhanced leaching risk. Consequentially, N-losses by drainage were larger than expected, based on N-surpluses from agricultural balances. P-losses by drainage did not seem to be influenced by a larger leaching risk. The sorption process caught possibly leaching P on its way to the tile drains.

V

RESULTS OF FIELD EXPERIMENT
HUPSEL-ASSINK

1   Introduction

General - The Hupsel-Assink experimental site (Fig. V.1.1) was located in the Hupsel brook catchment area in the eastern part of the Netherlands (Section I.3). This site has been used for meteorological and hydrological research purposes, as reported by e.g., Studiegroep Hupselse Beek (1971), Stricker (1981), Van Drecht (1985), Van Ommen (1988), and Van Dam et al. (1996). The research presented in this thesis is for the measurement period from October 1992 through March 1994. Due to equipment failure, mass balance calculations were performed only for the period of January 1, 1993 through March 19, 1994. The field study was a cooperative effort between the farmer involved, Wageningen University, National Institute of Public Health and the Environment (RIVM), and the Rijn & IJssel Water Board, formerly Zuiveringschap Oostelijk Gelderland.

At the site and its surrounding area, studies on preferential flow due to water repellency were performed by Ritsema (1998) and by Dekker (1998). Van Dam et al., (1996) reported on studies of measured soil water contents in relation to numerical modeling, using a combination of hysteresis and a mobile-immobile flow concept. Van Ommen (1988) measured the breakthrough curve of a bromide tracer in a subsurface drain of a nearby parcel. He found bromide to appear faster in the drainage water as compared to predicted by uniform soil matrix flow and transport processes. Staining patterns of iodide confirmed the non-uniform infiltration of water and solutes.

Soil and drainage system - The soil surface level of the southeastern part of the experimental site is between 28.35 and 28.55 m above mean sea level (MSL). The northwestern part is somewhat higher; soil surface levels vary between 28.75 and 28.90 m above MSL. The soil at the experimental site was classified as loamy sand, siliceous, and mesic Typic Haplaquods (Wösten et al., 1983). Van Dam et al., (1996) and Van Dam (2000) distinguished four main soil layers, which start at depths of 0, 0.15, 0.35, and 0.90 m below the soil surface, respectively. Soil characteristics and soil-physical parameters are listed in Table V.1.1 and Appendix B.
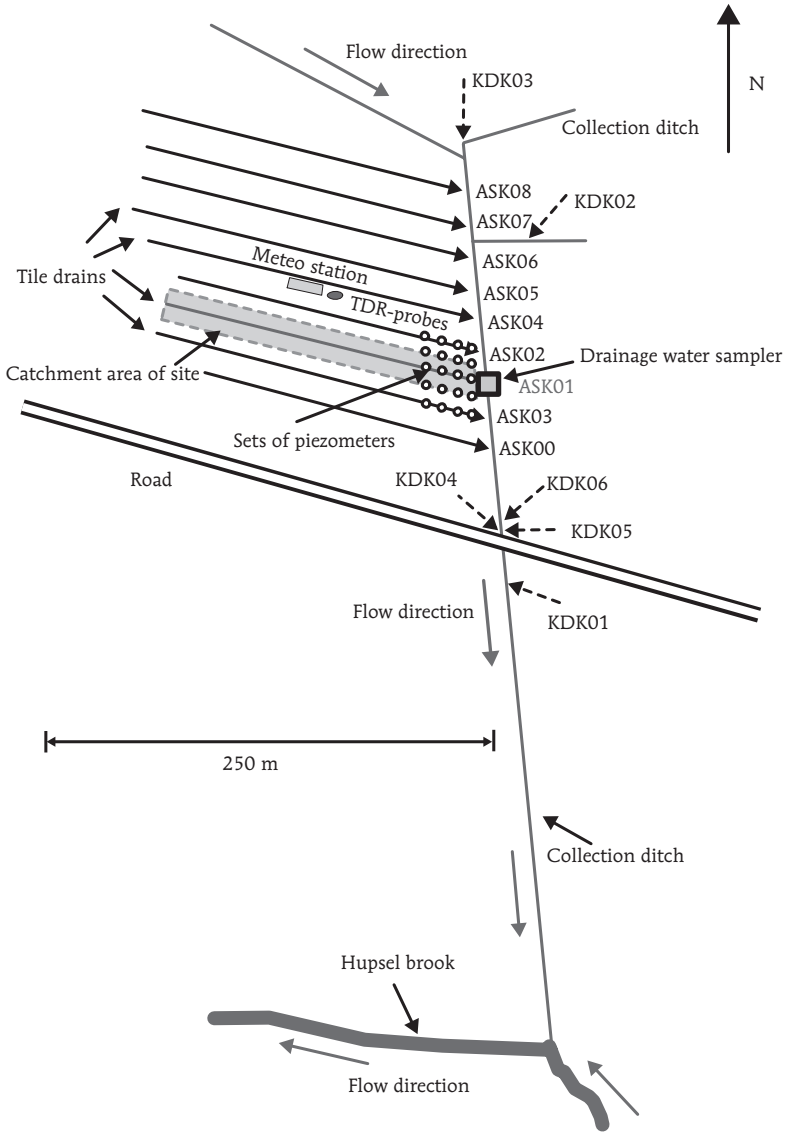
Fig. V.1.1
Hupsel-Assink experimental site. Local drainage situation showing tile drains,
collection ditch, and the Hupsel brook. Catchment area of experimental site shows
locations of tile drain ASK01, the meteorological station, TDR-probes, sets of
piezometers, and drainage water sampler. Sample locations are coded ASK (tile drainage
water) and KDK (ditch water).

Table V.1.1
Hupsel-Assink experimental site. Soil characteristics by Wösten et al. (1983). *Local measurements on phreatic aquifer properties (Dijksma, Wageningen University, personal communication).

Parameter	Depth to soil surface [m]			
	0 - 0.15	0.15-0.35	0.35-0.90	> 0.90
Clay [%]$< 2\mu$m	2	3	3	2
Silt [%]$< 50\mu$m	13	13	4	6
Sand [%]	82	80	92	92
Organic matter [%]	2.9	3.4	0.2	0.1
ρ [kg m^{-3}]	1345	1450	1620	1650
Φ_{tot} [-]	0.41	0.37	0.28	0.34
k_s [m d^{-1}]	2.5	2.5	1.2	0.28 (1.0*)

The sandy phreatic aquifer is about 3 m deep and overlies a low-permeable clay layer of the Miocene Age, which is more than 30 m thick. Boulder clay may be present within the aquifer but has not been indicated by borings. The groundwater levels vary between 0.4 and 0.8 m below the soil surface in winter and are deeper than 1.2 m during dry summer periods (GTC VI). The local drainage system consists of subsurface drains at 0.8 to 0.9 m depth and at 14 m spacing. The subsurface drains distance $L = 14$ m, with the length of the catchment area of the subsurface drains being about 177 m. A 1.2 m deep collection ditch drain is present at the eastern border of the site. During time periods with discharge events, the water levels of the ditch might have temporarily risen above the subsurface drain outlets. The main course of the Hupsel brook is located 400 m south of the experimental site (Fig. V.1.1).

Grassland and agricultural nutrient management - The Hupsel-Assink experimental site was covered with permanent grassland. Data on management practices by the farmer were available from the 1990 growing season and later. It is assumed that in the period before 1990, the agricultural use was more intensive compared to the 1990-1993 period where nutrient applications were concerned. Generally, the grass was cut three times per year, and grazing took place mainly by cattle during most days of the year, while in the first months of winter grazing mainly took place by a few sheep.

2   Field water balance and hydrology

To set up the field water balance, information is needed on all incoming and outgoing water fluxes across the defined balance volume or system. The field water balance was analyzed for the 0.25 ha (2478 m^2) and 3 m deep soil volume (7434 m^3) in which subsurface drain, coded ASK01, is located. The balance period ran from January 1, 1993 through March 19, 1994.

Rainfall and evapotranspiration - Rainfall was measured using a KNMI-standard rain gauge that was installed at the soil surface. This gauge was installed in the center of a 1 m^2 iron grid across a 0.4 m deep pit with a gravel layer on the bottom (Fig. V.2.1). The grid prevented the water from splashing into the gauge; the gravel allowed easier infiltration of water to the pit bottom. Dekker (1979) showed that in the Hupsel brook catchment area the measurement error due to wind effects was between 2% and 3% in spring, summer, and fall, and around 6% in winter. Van den Eertwegh and Meinardi (1999) compared data from the rain gauge at the soil surface to the standard rain gauge at 0.4 m above the soil surface in the period from April 1985 through March 1994. They found that on an annual basis, the soil surface rain gauge caught 3-4% more compared to the standard rain gauge. Total rainfall during the balance period from January 1, 1993 through March 19, 1994 was 1255 mm.
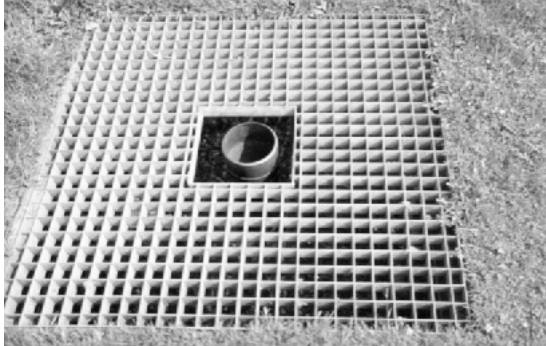
Fig. V.2.1
Hupsel-Assink experimental site. Picture of rain gauge at the soil surface in the field situation (picture taken by Dommerholt, Wageningen University).

Data on ET_r were retrieved from the Royal Dutch Meteorological Institute (KNMI) weather station next to the experimental site (Fig. V.1.1). ET_p for grassland was calculated from ET_r and crop factor f_c for grassland from Feddes (1987) using [II.23], and resulted to 534 mm. During the summer of 1993 a cumulative rainfall deficit of

110 mm occurred. From mid-June to mid-July, an estimated reduction rate of 15 mm has been taken into account to reduce ET_p. The rainfall deficit built up slowly, and the capillary rise was expected to partially keep up with the evaporative demand. ET_a during the balance period was estimated at 519 mm.

Measurements of soil water content - To measure soil water contents at the meteorological site, a neutron probe was used 55 times between October 1992 and March 1994. Measurements were performed from just below down to 2.1 m below the soil surface. No specific field calibration of the neutron probe was performed. Back in 1984, an old neutron probe broke down and was replaced by a new probe. An extensive field calibration for the old probe was implemented in 1984; however by the time the old probe was most likely already malfunctioning (1986-1987), the new probe was calibrated using the combined old and new probe data (Supèr, 1990).

Time Domain Reflectometry (TDR)-probes were installed in August 1993 to provide more information on shallow soil water contents and on their local-scale spatial variation. The TDR-probes had 2 rods of 0.1 m length, and they were installed at four trenches at depths of 0.07, 0.20, 0.40, and 0.65 m below the soil surface. In each trench ten probes were placed 0.2 m apart (Fig. V.2.2). Measurements were performed between August 1993 and December 1994. A cable tester was used as a pulse generator, and software developed by Heimovaara and Bouten (1990) was applied to analyze the wave signal.
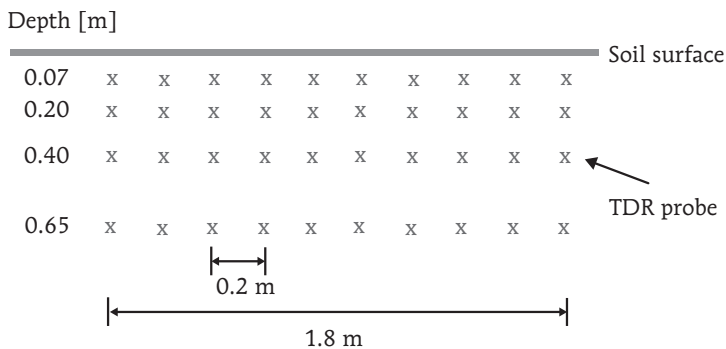
Fig. V.2.2
Hupsel-Assink experimental site. Outline of TDR-probes (marked with x) installed at the site. In total 40 TDR-probes were installed in four horizontal trenches at depths of 0.07, 0.20, 0.40, and 0.65 m below the soil surface. Each trench contained 10 TDR-probes, and each probe was placed 0.20 m apart.

To describe the relationship between soil relative dielectric constant ϵ and the volumetric soil water content θ, the equation as proposed by Topp et al. (1980) was used:

$$\epsilon = a + b\theta + c\theta^2 + d\theta^3 \qquad \text{[V.1]}$$

with coefficients a=3.03, b=9.3, c=146, and d=-76.7 C V^{-1}m^{-1}. The local soil contained organic matter and iron particles, which may have adversely affected the measurements. A field calibration of the TDR-probes was performed in June and August of 1995. The calibration coefficients per layer were used to calculate ϵ for each soil layer (Table B.3, Appendix B). The change in the soil water storage during the balance period was +30 mm; at the end of the period, the soil showed a higher soil water content.

Measurements of groundwater table - The locations of the piezometer sets were concentrated in an area between the collection ditch and 35 m away from the ditch as shown in Fig. V.1.1. All the 41 piezometers had filters of 1.0 m in length, which were at 0.5 to 1.5 m in depth below the soil surface. At five locations, recorders were installed during winter to register the groundwater hydraulic heads every 15 minutes. At the other locations, measurements were manually performed once or twice per week, leading to 85 total observations. Groundwater hydraulic heads never dropped below 1.6 m below the soil surface during the experimental period.

Tile drain discharge measurements - The discharge of a single subsurface drain, coded ASK01 (Fig. V.1.1) was measured by using a linear, so-called Sutro weir (Bos, 1989; Fig. V.2.3). A recorder was installed to register the water level height upstream of the weir by using a float. The linear stage-discharge relationship of the weir is in the following form:

$$Q = aw + b \qquad \text{[V.2]}$$

where Q the discharge rate, w is the stage, and a and b are coefficients. The relationship was calibrated in the laboratory as well as in the field situation. The field calibration data were used to fit the stage-discharge relationship. Drain discharge measurements from April 14 through July 2, 1993 were missing. Q_{meas} for the balance period amounted to 424 mm.

Before the start of the experiment, all subsurface drains at the experimental site were internally cleaned using a high-pressure jet spray device. During cleaning the effluent water was orange colored, indicating iron deposits present in and/or around the drains. These deposits might have hampered the functioning of the drains and probably will do so again as time progresses and deposits accumulate, increasingly clogging the small drain entrance holes.

In order to take water samples from the drainage water, a portable effluent sampler was used. The sampling strategy was planned so that a grab sample of drainage water would
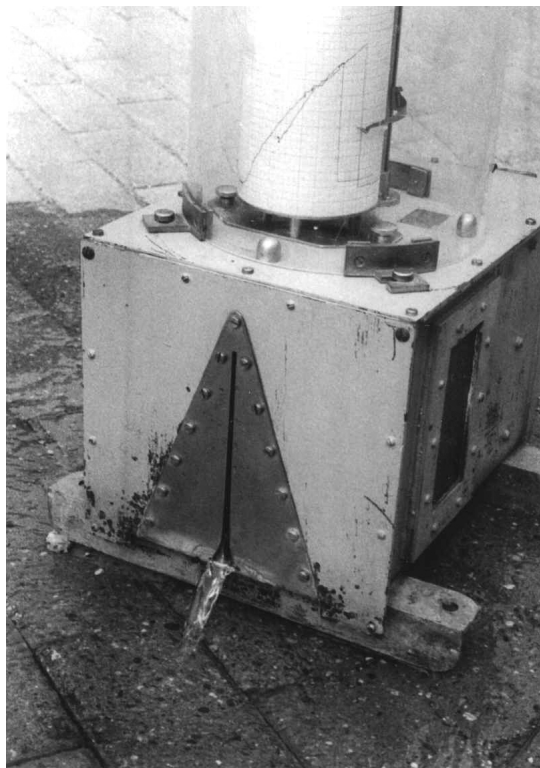
Fig. V.2.3
Hupsel-Assink experimental site. Sutro proportional weir used to measure tile drainage
rates of subsurface drain coded ASK01 (Fig. V.1.1.; picture taken by Dommerholt,
Wageningen University).

be taken every 1 mm of discharge i.e., equal to one sample per 2.5 m^3 of drainage
volume. In practice, however, the actual sampling was somewhat different due to
equipment failures; the equipment was malfunctioning in the second half of November
1992, and in the first half of December 1992; between March 23 and April 8, 1993;
between mid November 1993 through mid December 1993, and between mid January
and mid February 1994. During equipment failure periods, grab samples were taken.
On the whole, 238 samples were taken from a total drained volume of 1143 m^3 of water
–on the average one sample per 4.8 m^3 of water. The field samples were taken to the lab
at least twice a week and analyzed by the lab of the Rijn & IJssel Water Board. If more
than five grab samples were available for one day, samples were manually mixed in the
lab. The outlet of the subsurface drain, coded ASK01, in Fig. V.1.1 was never submerged
by ditch water levels during the experiment. In case of submersion, a different drainage
water sampling strategy needs to be applied (e.g., De Vos, 2001).

Field water balance tile drains - During the experiment, *no surface runoff was observed* from the field; although local-scale ponding occurred frequently. At the field site, surface irrigation was not performed, and sub-irrigation from the ditch was absent. The ditch was usually dry during dry periods in the summer. The field water balance was set up in two steps (Section II.6) to analyze possible unmeasured drainage components. The results for step one showed a water balance surplus of 282 mm.

The conclusion was that either the water balance was inaccurate or a drainage term is missing. An extra amount of water could have left the field in a means other than by tile drains. Rainfall was measured accurately, and the data from several local rain gauges were compared to each other. Extra losses by a larger ET_a term are possible, but not likely. The estimated ET_p reduction was 15 mm. The missing subsurface drainage data for the time period April 14 through July 2, 1993, were reconstructed. Q_{meas} was increased by 10 mm to 434 mm. Unmeasured subsurface drainage routes were likely to have occurred both to the ditch and to the Hupsel brook, which was also visible from the water storage term in the field water balance versus time. At full saturation, the 3 m deep sandy aquifer contains about 1030 mm of water. The storage term shows increasingly larger values as time progressed from October 1993 and later. The only conclusion could be that *a drainage term was missing in the balance, i.e. directed to the ditch and Hupsel brook* (Fig. V.2.4). Part of the reason for this was the groundwater hydraulic head gradients were directed toward other drainage devices, such as the collection ditch and the Hupsel Brook. Another reason was that the subsurface drain, coded ASK01, was increasingly clogged by particles.

Unmeasured drainage to ditch - The collection ditch is one possible unmeasured drainage route. The influence of the ditch on the drainage process can be shown by a 3D view of the groundwater table across the part of the experimental site that was less than 24 m from the ditch. This 3D view for July 28, 1993, is shown in Fig. V.2.5. Hydraulic head differences were directed toward the tile drains and the ditch at the same time. It is concluded that the collection ditch also has a draining function.

Fig. V.2.6 shows the measured groundwater hydraulic heads in two transects almost perpendicularly to the ditch on November 15, 1993, to illustrate the draining function of the ditch. The influence of the ditch on the groundwater table reaches more than 35 m from the ditch. With a total length of the tile drain catchment of 177 m, the extension of the zone of influence of the draining ditch is 20%. No piezometer data were available beyond the 35 m distance. It is expected that the zone does not extend far beyond this distance.

At low discharge rates, the groundwater hydraulic head difference towards the ditch (ΔH) is about 0.2 m of a 35 m distance. At high discharge rates, ΔH is about 0.7 m
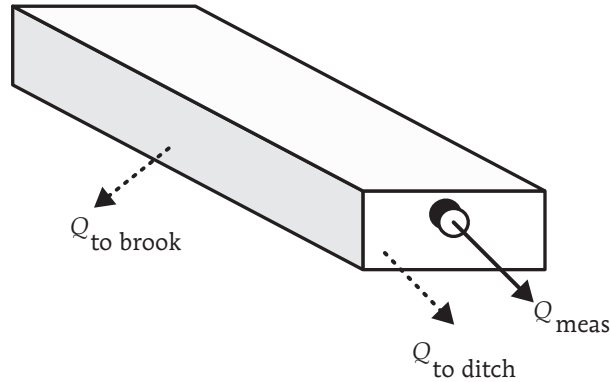
Fig. V.2.4
Hupsel-Assink experimental site. Visualized possible unmeasured drainage routes to the ditch $Q_{\text{to ditch}}$ and $Q_{\text{to brook}}$ derived from the schematic 3D catchment area of the tile drain ASK01.

within 35 m distance. The groundwater discharge directly to the ditch $Q_{\text{to ditch}}$ can be estimated as

$$Q_{\text{to ditch}} = d\,k_s\,L\frac{\Delta H}{\Delta x} \qquad\qquad \text{[V.3]}$$

with $d = 3$ m, $k_s = 0.28$ m d^{-1} (Table V.1.1), $L = 14$ m, $\Delta H = 0.2$ to 0.7 m, and $\Delta x = 35$ m. Application of [V.3] leads to $Q_{\text{to ditch}}$ ranging from 0.0672 m^3 d^{-1} using $\Delta H = 0.2$ m to 0.2352 m^3 d^{-1} using $\Delta H = 0.7$ m. On an annual basis, these values are equal to 10 and 35 mm a^{-1} for the tile drain catchment. An annual average value of $Q_{\text{to ditch}}$ is estimated at 20 mm a^{-1} (365 days). The conclusion is that in the field water balance for the experimental site, $Q_{\text{to ditch}} = 25$ mm should appear for the 443 days period. Adding this drainage term, the water balance still does not close.

Unmeasured drainage to brook - During the water balance period January 1, 1993 through March 19, 1994, the total discharge volume of the Hupsel brook was 651 mm. The water balance of the Hupsel brook will probably match the water balance for the experimental site because the aquifer depth, the soil type, groundwater table class, drainage system, and land use of the experimental site represent the whole basin area quite well. *It is likely that drainage occurred from the experimental site toward the main course of the brook*. After correction of Q_{meas} and the addition of $Q_{\text{to ditch}}$, the water balance surplus is still 247 mm.

The side of the tile drain catchment across where $Q_{\text{to brook}}$ may occur is 177 m long. The mean water level of the Hupsel brook 400 m south from the site is about 25.50 m
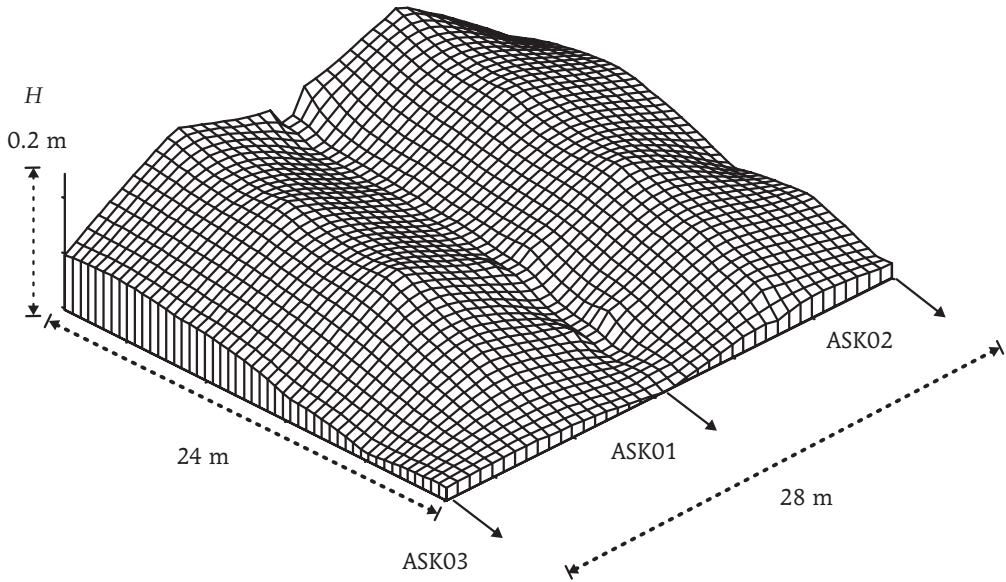
Fig. V.2.5
Hupsel-Assink experimental site. 3D-view of groundwater hydraulic head H at site. Measurement date is July 28, 1993. Subsurface drains are located at 0 m (ASK03), 14 m (ASK01), and 28 m (ASK02) on the x-axis (Fig. V.1.1). The ditch runs parallel to the x-axis; hydraulic head differences were observed toward the tile drains and the ditch, the latter showing the draining function of the ditch.

above MSL. The mean groundwater hydraulic heads at the site were around 28 m above MSL. Application of [V.3] with $d = 3$ m, $k_s = 0.28$ m d^{-1}, L=177 m, $\Delta H = 2.5$ m, and $\Delta x = 400$ m leads to $Q_{\text{to brook}} = 137$ mm on an annual basis. The balance period was 443 days and $Q_{\text{to brook}}$ was increased to 166 mm. To decrease the field water balance surplus, this term was incorporated in the water balance. Fig. V.2.7 shows the final field water balance for the experimental site:

$$I - ET_a - \Delta V_w - Q_{\text{meas}} - Q_{\text{to ditch}} - Q_{\text{to brook}} = \text{balance}$$

or:

$$1255 - 519 - 30 - 434 - 25 - 166 = 81 \text{ mm}$$

The field water balance thus closes at 81 mm. This newly estimated surplus is likely to better represent the errors in all balance terms, and therefore was not analyzed any further. It should be noted that when using $k_s = 1.0$ m d^{-1} instead of 0.28 m d^{-1} (Table V.1.1) to calculate $Q_{\text{to ditch}}$ and $Q_{\text{to brook}}$, the water balance can be closed.
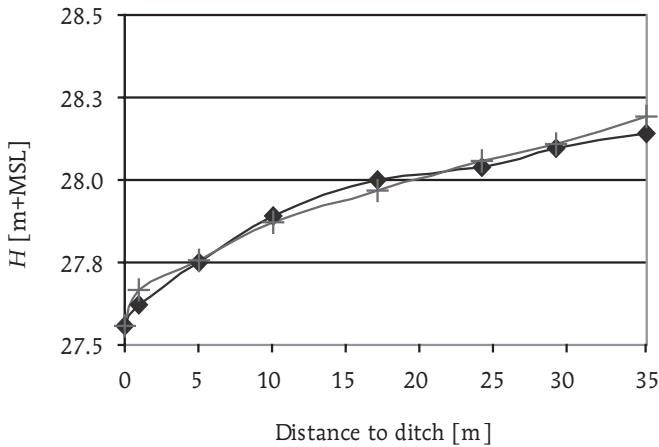
Fig. V.2.6
Hupsel-Assink experimental site. Groundwater hydraulic head *H* measured in two transects of piezometers almost perpendicularly to the ditch. Locations of piezometers are midway between subsurface drains. Measurement date: November 15, 1993. The hydraulic head differences observed in the two transects were toward the ditch, *showing the draining function of the ditch within a zone up to more than 35 m away from the ditch.*

Given the water balance in Fig. V.2.7, 69% of the total drainage left the site by the tile drain. The drainage situation at the experimental site needs to be taken into account in the analysis of the solute mass losses by drainage. It is expected that the travel time of drainage water to the subsurface drain is comparable to that of water drained directly by the ditch.

3   Transient water flow and solute transport simulations 1993-1994

The flow medium at the Hupsel-Assink site was treated as a single porosity medium due to the absence of any soil structure. Subsurface flow of water and solutes was assumed to be symmetrical at both sides of the subsurface drain; therefore, only half of the catchment or flow system was modeled. As concluded from the field water balance shown in Fig. V.2.7, *the excess rainfall from the field was drained by the tile drains, the ditch, and the brook. The last two discharge routes were combined when introduced to the model.* The model side boundary below the subsurface drain was defined as a far field drainage boundary (Section II.5). According to this model boundary unmeasured drainage had taken place. Fig. V.3.1 shows the schematic model of the experimental site.
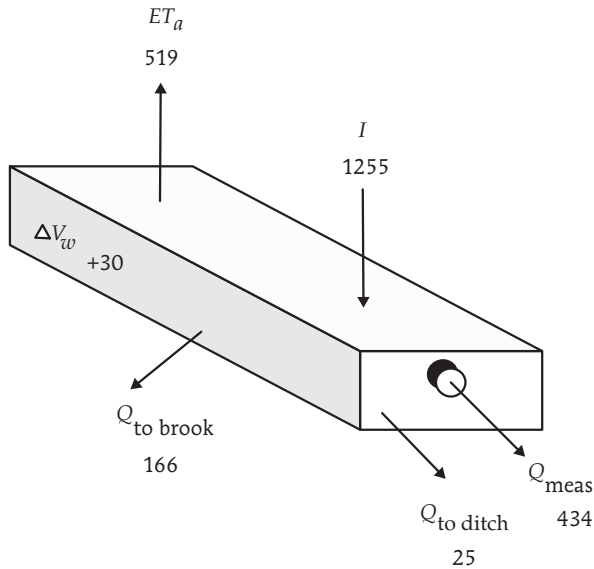
Fig. V.2.7
Hupsel-Assink experimental site. Field water balance [mm] for catchment area of subsurface drain coded ASK01 (Fig. V.1.1). Balance period: January 1, 1993 through March 19, 1993. Three drainage terms are shown: Q_{meas} (tile drain), $Q_{to\ ditch}$, and $Q_{to\ brook}$. The field water balance shows a surplus of 81 mm.

P is split between I and Q_{runoff}. P and ET_r were taken from the meteorological station next to the experimental site, as well as air temperature and relative air humidity; Crop factors (f_c) for permanent grassland were from Feddes (1987). Details on the model parameters and setup can be found in Appendix B. The simulation period ran from January 1, 1993 through March 19, 1994.

Simulation results - The computed mass balance for water during the period of January 1, 1993, through March 19, 1994, is shown in Fig. V.3.2. During the 1993-1994 measurement period, surface runoff was not observed at the site; all precipitation infiltrated into the sandy soil. However, the simulation results show 6 mm of surface runoff. This runoff occurred during two storm events due to which the soil water storage capacity was exceeded. In the field situation, soil surface ponding was likely to have occurred, followed by delayed infiltration.

Starting the simulations with ET_p equal to 548 mm, ET_a was calculated at 533 mm. Of all the drainage water, 66% left the flow domain by tile drainage, which is about the quantity that was found in the field water balance. The overall water balance and
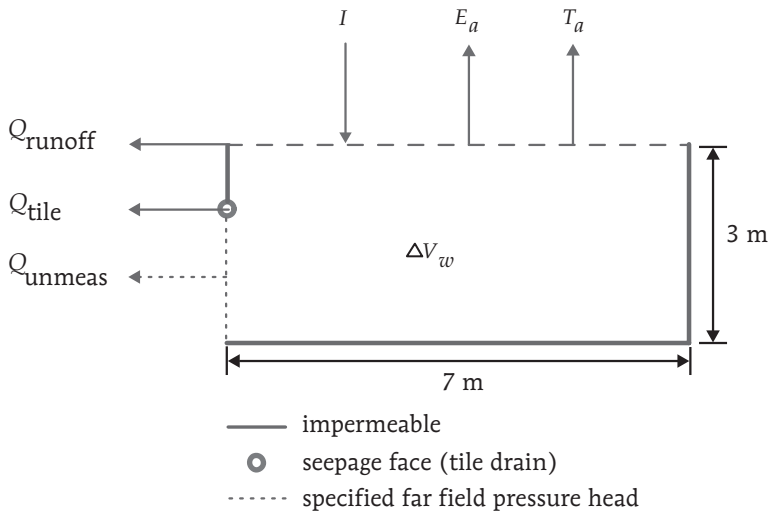
Fig. V.3.1
Hupsel-Assink experimental site. Schematic 2D single-porosity model of half of the catchment of tile drain, coded ASK01 (Fig. V.1.1), and boundary conditions (Section II.5). The soil surface is an atmospheric boundary, the tile drain is represented by a seepage face boundary condition, and the left side below the tile drain has a far field boundary condition to enable drainage across this flow boundary.
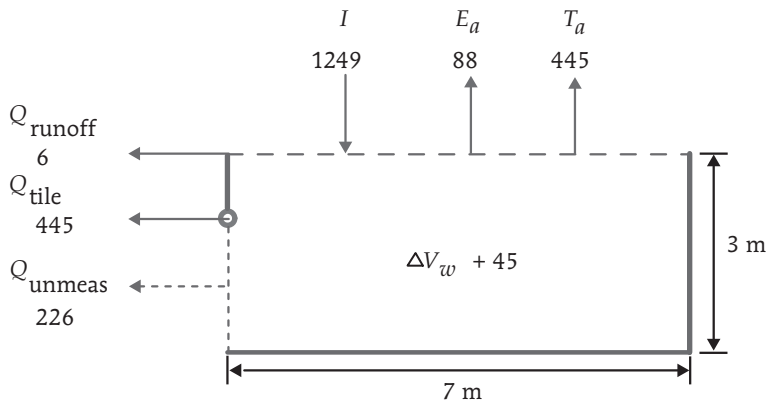
Fig. V.3.2
Hupsel-Assink experimental site. Computed water balance terms [mm] in the single-porosity flow domain for the period of January 1, 1993, through March 19, 1994.

drainage flux was well reproduced by the model. The temporal variation of V_w of the flow domain within the simulation period is shown in Fig. V.3.3. The field water balance data, based on field measurements of soil water content are also shown. In Fig. V.3.4 the measured and calculated tile drainage rates are shown. Both Fig. V.3.3 and Fig. V.3.4 show that the simulated V_w and Q_{tile} do not generally coincide with the measurements.
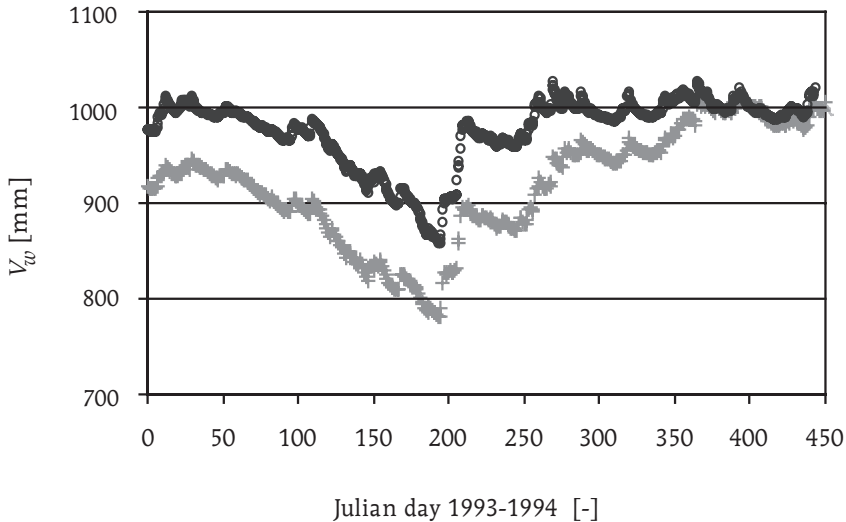
Fig. V.3.3
Hupsel-Assink experimental site. Temporal variation of water storage V_w in the flow domain. Data from field water balance (+, grey) and simulation results (○, black). Time period: January 1, 1993 (day 1) through March 19, 1994 (day 443).

The calculated V_w usually exceeded the field observations. During the spring, late autumn, and winter periods, simulated drainage rates are larger as compared to measured rates. The observed drainage in July 1993 was not reproduced by the simulation model. From summer 1993 until November 1993 Q_{tile} observed was larger compared to Q_{tile} calculated. The deviations of the model calculations from the field observations are explained as follows: as stated by other researchers (e.g., Van Ommen, 1988; Van Dam et al., 1996; Ritsema, 1998; Dekker 1998), the flow process in the unsaturated at the site can be unstable during heavy rainfall events during and after dry periods. The summer of 1993 was dry until July 24, then between July 25 and 28 about 82 mm of rainfall was recorded. The second rainfall event during the latter period caused drainage to occur from the experimental site, and also from the whole Hupsel brook catchment. Responding to the rainfall events, the groundwater level rose and drainage occurred when the soil water storage in the unsaturated zone was not fully replenished.
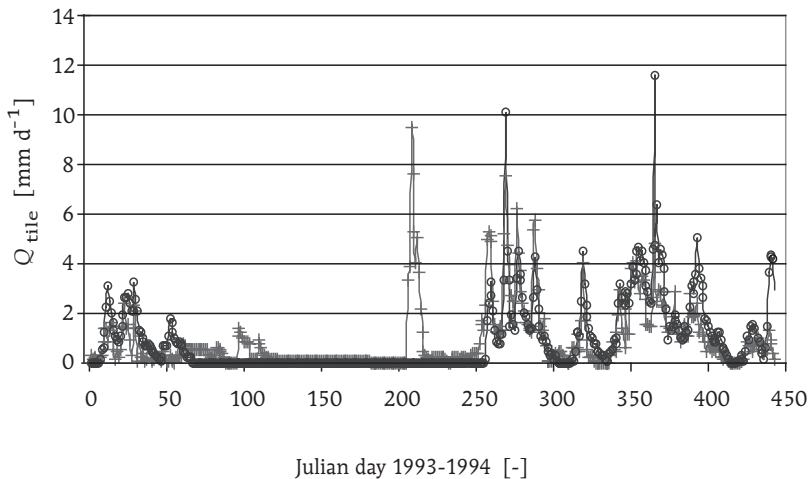
Fig. V.3.4
Hupsel-Assink experimental site. Temporal variation of calculated tile drainage rate Q_{tile}. Field observations (+) and simulation results (o). Time period: January 1, 1993 (day 1) through March 19, 1994 (day 443).

The field observations on the soil water storage amount and the drainage event were such that preferential flow is expected to have occurred.

The loamy sand was not known to show any soil structure or macropores. In the unsaturated zone at the field and basin scale, another type of preferential flow may have occurred in the unsaturated zone: unstable flow. In practice, it appeared that in early autumn and winter, the rainfall excess water was increasingly used to fill the water storage in the vadose zone, while continuing to lead to larger drainage rates as computed by the numerical code. Analyzing the model results, soil water storage was filled first, then drainage occurred at smaller rates compared to the field situation. The unstable flow process slowly dissipated and this situation prevailed until November 1993. As the drainage process progressed and unstable flow mechanisms disappeared, the measured drainage rates were smaller than simulated. *It appeared that subsurface drain clogging increasingly hampered drainage at the experimental site.* The clogging caused the entrance holes of the subsurface drain to be blocked, and calculated drainage rates exceeded the measured rates during the months of November-March. The unstable flow concept was not accounted for by the numerical dual-porosity code. The field data set did not provide any evidence on this type of preferential flow, hence unstable flow as an explanation of the field observation remains hypothetical.

Spatial and temporal variations in soil water content - The soil water contents measured by the TDR-probes (Fig. V.1.1) showed a variability as a function of the saturation degree θ/θ_s, as shown in Fig. V.3.5. The measurements illustrate the existence of circumstances at which preferential flow processes may occur in the unsaturated zone: a heterogeneous spatial distribution of soil water content within a certain range of θ/θ_s. For each trench, at all measurement depths of 0.07 m, 0.20 m, 0.40 m, and 0.65 m below the soil surface, the standard deviation of the soil water content (y-axis) versus the average θ/θ_s (x-axis) is shown.
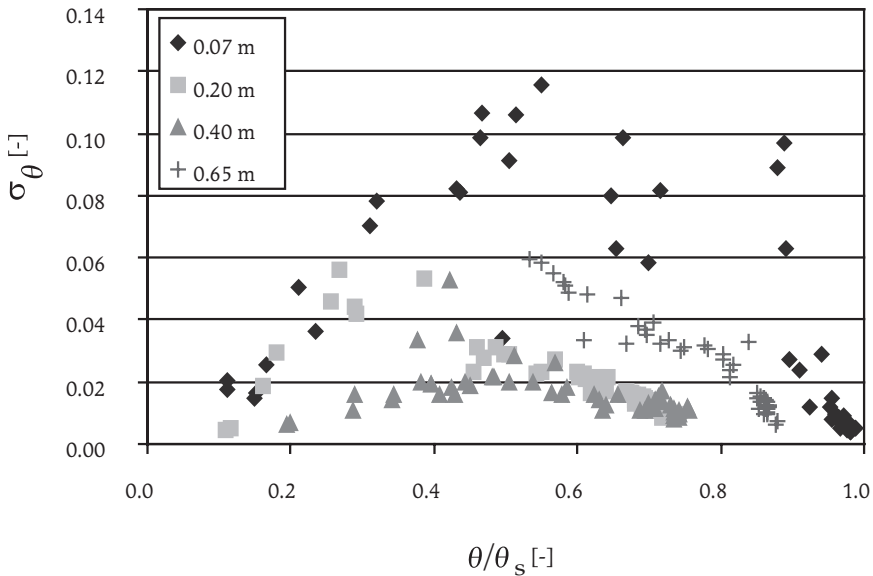
Fig. V.3.5
Hupsel-Assink experimental site. Standard deviations σ_θ of soil water content versus average saturation degree θ/θ_s. Data is shown for each trench at depths 0.07, 0.20, 0.40, and 0.65 m below the soil surface. Measurement period: August 16, 1993 through December 9, 1994. 51 measurements are shown.

σ_θ decreases with depth from 0.07 to 0.40 m as expected, but then increases again for the 0.65 m depth. The reason for this probably lies in the soil layer characteristics (Table V.1.1). The probes at 0.65 m depth are located in a soil layer different in percentage sand, M50, and k_s as compared to the layers above. The finer sands, in combination with a smaller value for k_s, may lead to larger spatial variations in θ. It can also be seen from Fig. V.3.5 that the spatial variation is relatively small under dry as well as under wet conditions. σ_θ reaches its maximum during times showing an average of θ,

which holds for each trench, although no data on this can be shown for the deepest trench because there dry conditions did not occur during the measurement period, while dry conditions did occur for the shallower trenches. Under dry and wet conditions, θ is likely to smooth out: all parts of the soil are about equally dry and wet, respectively. Spatial variation occurs during wetting and drying sequences, as shown in Fig. V.3.6.
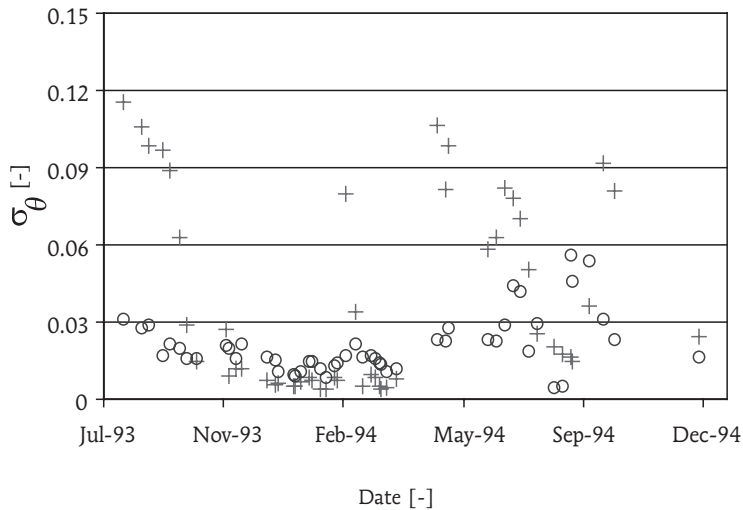
Fig. V.3.6
Hupsel-Assink experimental site. Standard deviation σ_θ of soil water content versus time. Data shown at depths of 0.07 (+) and 0.20 m (o) below the soil surface. Measurement period: August 16, 1993 through December 9, 1994. 51 measurements were used.

As can be seen in Fig. V.3.6, from August 1993 to February 1994, the soil became wetter and standard deviations dropped. During the second half of February 1994, a short-term drying period occurred in combination with frost. The standard deviations rose again toward the summer of 1994 but dropped after rainfall events in July and August 1994.

Hysteresis in groundwater level-subsurface drain discharge relationship - Hysteresis in the relationship between the groundwater level midway between two subsurface drains; the subsurface drain discharge is illustrated by data from a discharge event in January 1993 as shown in Fig. V.3.7. As groundwater hydraulic heads were on the rise (right side of loop), drain discharges were up to 20-50% higher compared to discharges at the same groundwater level but on the falling limb (left side of loop). *This phenomenon is of importance in case conceptual stage-discharge relationships are used to model and predict subsurface drain discharge, especially high (extreme) discharge rates.* Under field conditions

it is expected that Q_{unmeas} also shows hysteresis. Using the dual porosity flow code, the simulation results showed hysteresis of the kind discussed above, but less pronounced, which was caused by the fact that the calculated maximum groundwater hydraulic heads under wet conditions were smaller compared to measured groundwater hydraulic heads.
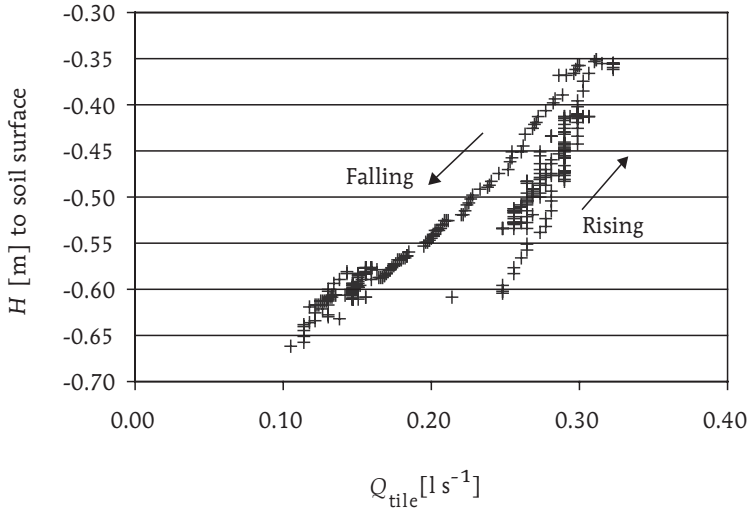
Fig. V.3.7
Hupsel-Assink experimental site. Hysteresis in groundwater hydraulic head H - subsurface drain discharge Q_{tile} relationship. Measurement location of groundwater level: C4 transect, midway between two subsurface drains and 24 m from the ditch. Time period: January 9, 1993 through January 13, 1993.

The field water balance and discharge components for the Hupsel-Assink site during the 1993-1994 period were reproduced well by the 2D single-porosity model. The temporal variation in simulated drainage rates showed deviations, which were possibly caused by a preferential flow process during and after dry periods and by an increase in clogged subsurface drain during the drainage season. Hypothetically, unstable flow may have occurred in the unsaturated zone. Unstable flow in the unsaturated zone causes preferential transport of water and solutes, and it enhances vertical movement. This type of flow will usually lead to shorter travel times of drainage water as compared to homogeneous flow patterns, due to by-passing part of the unsaturated zone. Clogging of subsurface drains leads to smaller tile drainage rates and to a larger part of the rainfall excess water, discharged by means other than subsurface drains. The latter discharge components are likely to follow equally long or longer flow paths, thus resulting in longer travel times of drainage water. Both reasons for the deviations between measured and

calculated drainage rates, if combined, may have no effect on the overall travel time of drainage water as computed by the model and as discussed in the next section.

4   Travel time distribution of drainage water

Steady-state approach - The Ernst-Bruggeman approach to estimate the travel time of drainage water for a steady-state flow situation under fully saturated flow conditions yielded [II.5]. This equation was used to calculate the fractions of the travel time distribution of drainage water. Application of [II.5] to the Hupsel-Assink experimental site yielded travel time fractions f_τ ($\tau = 1,3$) as shown in Table V.4.1 for the 1985-1993 average and the January 1, 1993 through March 19, 1994 period. The annual data are based on hydrologic years.

Table V.4.1
Hupsel-Assink experimental site. Fractions f_1 to f_3 of travel time distribution of drainage water, based on Ernst-Bruggeman approach [II.5]. Parameters: $d = 2.5$ m, $I = 0.330$ m a^{-1} (1985-1993), $I = 0.550$ m a^{-1} (365/443 part of 1993-1994 measurement period), and $\Phi_{\text{eff}} = 0.35$.

Fraction	1985-1993 average $I = 0.330$ m a^{-1}	1993-1994 $I = 0.550$ m a^{-1}
f_1	0.31	0.47
f_2	0.22	0.25
f_3	0.15	0.13
Total	0.68	0.85

The field water balance for the 1993-1994 period (Fig. V.2.7), however, showed that discharge components other than tile drainage existed. On an annual basis, the division of Q_{total} of 517 mm a^{-1} into discharge components at the experimental site was such that 69% was Q_{tile}, and 31% was the sum of $Q_{\text{to ditch}}$ and $Q_{\text{to brook}}$. $Q_{\text{to ditch}}$ occurred in the zone next to the ditch to an extent of 35 m away from the ditch; this distance was of the same order of magnitude as L. It is assumed that the travel time of direct drainage to the ditch was about equal to that of subsurface tile drainage. It is concluded that 73% of

Q_{total} has an identical travel time distribution, and as far as the travel time distribution is concerned, $Q_{\text{to ditch}}$ is incorporated into Q_{tile}. According to [II.6], I was reduced to I^* and consequently, d was reduced to d^* for the tile drain system [II.7]. I^* for the drainage directly to the brook was also reduced to $I^{**} = I - I^*$. Table V.4.2 shows the travel time distribution fractions for Q_{tile}, $Q_{\text{to brook}}$, and Q_{total} for the hydrologic year 1993-1994 within the measurement period, based on the Ernst-Bruggeman approach.

Table V.4.2
Hupsel-Assink experimental site. Hydrologic year 1993-1994, within measurement period of January 1, 1993, through March 19, 1994. Fractions f_1 to f_3 of travel time distribution of drainage water, based on Ernst-Bruggeman approach [II.5].
Parameters: $d^* = 1.5$ m (tile), $d = 2.5$ m (brook), $I^* = 0.385$ m a^{-1} (tile), $I^{**} = 0.165$ m a^{-1} (brook), and $\Phi_{\text{eff}} = 0.35$. *Discharge-weighted average values of f_τ.

Fraction	Drainage		
	Tile	Brook	Total*
f_1	0.52	0.17	0.42
f_2	0.25	0.14	0.22
f_3	0.12	0.10	0.12
Total	0.89	0.41	0.76

Based on steady state flow analysis, it can be concluded that at the experimental site in 1993-1994, *41% of the water and dissolved solutes leave the soil-water-system and enter the surface water within one year after infiltration.* This matches the results of Van den Eertwegh and Meinardi (1999) for the Hupsel brook catchment as a whole. The analysis showed that the average travel time of drainage water at the Hupsel-Assink experimental site was two years. About 25% of the drainage water remains in the soil-water system for more than four years. Hence, to correctly interpret solute concentrations and loads of drainage water, data on the weather conditions and the soil system balance need to be available *at least three to four years before an observation period, preferably five to six years. A longer data period is not needed.*

Transient flow conditions - The 2D single-porosity flow and transport model for the Hupsel-Assink experimental site was used to estimate the travel time of tile drainage and

drainage to the Hupsel brook from the 2D flow domain. During the measurement period in 1993-1994, the f_1 fraction for the total drainage leaving the flow domain was calculated; then it was split into a fraction connected to Q_{tile} and connected to $Q_{to\ brook}$, The f_1 fraction accounts for the solute mass fraction discharged by all drainage water, entering the local surface water system at the experimental site within one year, and is discharge-weighted (Table V.4.3). This solute mass fraction is defined as $M_{drainage}/M_{initial}$ i.e., applied tracer recovery in drainage water. The solute mass was initially present in the soil profile only at the top of the flow domain, which was done by setting $C_{initial} = 1.0$ for the top boundary nodes. For all other nodes, $C_{initial} = 0.0$. Solutes uptake by plant roots was switched off.

Table V.4.3
Hupsel-Assink experimental site. Fraction f_1 of travel time distribution of drainage water for the *hydrologic year 1993-1994*, based on simulation results of the 2D single-porosity model for the period January 1, 1993 through March 19, 1994. Fraction f_1 is shown for tile drainage Q_{tile}, for drainage to the Hupsel brook $Q_{to\ brook}$, and for total drainage Q_{total} entering the surface water system. No solute uptake by plant roots.

Fraction	Q_{tile} 445 mm	$Q_{to\ brook}$ 226 mm	Q_{total} 671 mm
f_1	0.43	0.04	0.47

From Table V.4.3 it can be seen that Q_{tile} counts for 66% of Q_{total} and carries 91% of the solute mass recovered in drainage water. The initially present solute was preferably transported to the tile drain. Q_{unmeas} contained a small fraction of the total solute mass drained. The flow paths of drainage water were apparently shallow and were concentrated in the upper part of the soil profile; if solute uptake by plant roots was fully accounted for, the f_1 fraction was 0.18, 0.02, and 0.20 for Q_{tile}, $Q_{to\ brook}$, and Q_{total}, respectively. These fractions are smaller as compared to the fractions shown in Table V.4.3 due to the competition between solute uptake by plants and solute removal by drainage. The solute mass fraction of the initially present mass removed by plants was 0.64.

It is expected that the f_2 and f_3 fractions, combined with f_1, were of major importance in describing the largest part of the total travel time distribution of drainage water. To determine f_2 and f_3 fractions at the Hupsel-Assink experimental site, drainage water

production and applied tracer recovery was calculated using the same three series of three different sequential hydrologic years as used for the Flevoland experimental site. Again, the solute mass was initially present only at the top of the flow domain. The results of the simulations are presented by means of f_τ fractions. The year by year recovered tracer fraction lost by total drainage by tile drains and bottom drainage was translated into the f_1, f_2, and f_3 fractions. In Table V.4.4 some relevant hydrological data for the three 3-year periods are shown. Results for the f_τ fractions are shown in Table V.4.5.

Table V.4.4
Hupsel-Assink experimental site. Numbers on cumulative P, Q_{runoff}, I, and Q_{tile} as a fraction of Q_{total} for three sequential hydrologic years *1975-1978* (dry), *1984-1987* (average), and *1965-1968* (wet) respectively. Simulation results for the 2D single-porosity model.

Period	P [mm]	Q_{runoff} [mm]	I [mm]	Q_{tile}/Q_{total} [-]
1975-1978	2026	0	2026	0.15
1984-1987	2558	0	2558	0.46
1965-1968	3083	21	3062	0.64

The data in Table V.4.4 show that as the cumulative infiltration increases, the relative fraction of total Q_{tile} drainage also increases. The increasingly larger rainfall excess will leave the flow domain by more shallow flow paths ending up in the subsurface drain. Under wet conditions, surface runoff occurred because the soil water storage capacity was exceeded due to full-saturation of the aquifer.

To generate the results shown in Table V.4.5 and to calculate any reasonable numbers on ET_a, values of θ_r for the two top layers of the sandy soil were increased from 0.01 i.e., the lab analysis results to 0.20. Smaller values of θ_r did not generate any significant drop in ET_p resulting into ET_a as should occur according to Stricker and Brutsaert (1978), especially in 1976. On the basin scale, Q_{brook} during the hydrologic year 1976 was 86 mm a^{-1} with $P = 573$ mm a^{-1} and $ET_p = 589$ mm a^{-1}. Assuming a storage change of -25 mm a^{-1} for the catchment as a whole, ET_a was estimated at 512 mm a^{-1}; the ET_p reduction was then *77* mm a^{-1}. The 2D single-porosity model results showed an ET_p reduction of less than 10 mm a^{-1}. In general, the model calculated smaller ET_p

Table V.4.5

Hupsel-Assink experimental site. Fractions f_1 to f_3 of travel time distribution of drainage water for three sequential hydrologic years 1975-1978 (dry), 1984-1987 (average), and 1965-1968 (wet) respectively, based on the simulation results for the 2D single-porosity model. All f_τ shown for tile drainage Q_{tile}, for drainage to the Hupsel brook $Q_{to\ brook}$ and for total drainage Q_{total} entering the surface water system.

Fraction	Q_{tile} 54 mm	$Q_{to\ brook}$ 310 mm	Q_{total} 364 mm	Q_{tile} 472 mm	$Q_{to\ brook}$ 555 mm	Q_{total} 1027 mm	Q_{tile} 993 mm	$Q_{to\ brook}$ 552 mm	Q_{total} 1545 mm
		1975-1978, dry			1984-1987, average			1965-1968, wet	
f_1	0.00	0.02	0.02	0.26	0.03	0.29	0.46	0.03	0.49
f_2	0.00	0.00	0.00	0.07	0.18	0.25	0.08	0.16	0.21
f_3	0.02	0.28	0.30	0.01	0.11	0.12	0.02	0.05	0.07
Total			0.32			0.66			0.77

reductions than expected, based on water balance data for the Hupsel brook basin. After the adjustment of θ_r, a reduction of k_s for the root zone as shown in Table V.1.1 by a factor of 10 would lead to reasonable ET_p reductions. This was not elaborated any further. It would imply that, given the root water uptake concept used (Section II.3.2), either k_s values and/or the parameters for the soil hydraulic conductivity function used (Appendix B, Table B.1) would be subject to study and improvement.

The f_τ fractions are a function of I as the data in Table V.4.5 show according to the Ernst-Bruggeman approach [II.5]. All 2D single-porosity modeling results for the Hupsel-Assink experimental site, solute uptake by plant roots excluded, and using the Ernst-Bruggeman approach [II.5], were plotted against I. The parameters used in [II.5] were $d = 2.75$ m and $\Phi_{\text{eff}} = 0.35$. Note that this latter value for Φ_{eff} is slightly larger than the value used before. Fig. V.4.1 shows that the results of both methods match well.
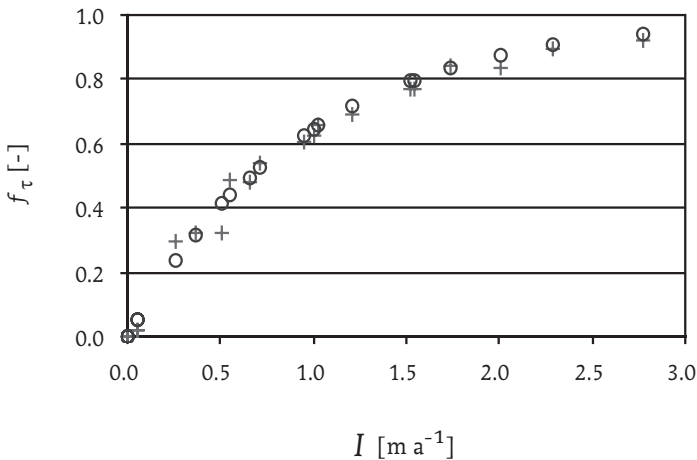
Fig. V.4.1
Hupsel-Assink experimental site. Fractions f_τ of travel time distribution of drainage water, based on calculations of 2D single-porosity model (+) and Ernst-Bruggeman approach [II.5] (o). Parameters used in [II.5]: $d = 2.75$ m and $\Phi_{\text{eff}} = 0.35$.

It can be concluded that for the Hupsel-Assink site, both the 2D numerical model and the analytical Ernst-Bruggeman approach [II.5] can be used to describe the travel times of drainage water. For simplicity reasons, the use of [II.5] is recommended to generate annual f_τ fractions. Application of the 2D single-porosity model yields, of course, more information on the dynamics of flow and transport processes within the porous medium modeled, including evapotranspiration effects. The long-term annual average travel time distribution of drainage water leaving the Hupsel-Assink experimental site under long-term average infiltration situations is shown in Table V.4.6.

Table V.4.6
Hupsel-Assink experimental site. Fractions f_τ of travel time distribution of drainage water, based on Ernst-Bruggeman approach [II.5]. Fractions f_τ are shown for an average hydrologic year, and more specifically for 1993-1994. Parameters: $d = 2.75$ m and $\Phi_{\text{eff}} = 0.35$.

Fraction	Average $I = 0.330$ m a^{-1}	1993-1994 $I = 0.550$ m a^{-1}
f_1	0.29	0.44
f_2	0.21	0.25
f_3	0.15	0.14
Total	0.65	0.83

5 Annual agricultural nutrient budgets and drainage loads

Nutrient budgets - Data on nutrient applications and removal by grazing and harvest of grass were based on the farmer's information. The data available were chemical analyses on manure composition, fertilizer, and manure application rates, as well as lab analyses on soil samples to determine optimal nutrient application rates. No field measurements were performed on soil chemical processes. The solute balance terms influenced and induced by these processes, like denitrification, were taken from Van den Eertwegh and Meinardi (1999), as the soil-hydrological situation at the experimental site is representative of the general situation in the Hupsel brook catchment.

A diffusion term was introduced in the soil system balance. This term does not reflect the diffusion of solutes from the solid phase of the sandy aquifer, but from the solid phase of the impermeable Miocene Age clay layer below it. This clay layer is of marine origin, and the water in it is still likely to contain salts, nutrients (P mainly), and pyrite.
The estimated average annual soil-system balances are shown in Table V.5.1. It was assumed that during the period 1990-1993, the soil organic matter was at an equilibrium and annual net mineralization was zero. P-sorption to the solid phase is estimated. If the resulting P-surplus shown was fully discharged by drainage, annual average P-concentrations in subsurface drainage water entering the Hupsel brook would be between 0.4 and 0.5 mg l^{-1}. In practice, observed P-concentrations were on the

average 0.21 mg l^{-1} (Van den Eertwegh and Meinardi, 1999). The soil-system balances will be used in the regional model for the Hupsel brook basin (Chapter VII).

Table V.5.1
Hupsel-Assink experimental site. Estimated soil system balances for Cl$^-$, total-N, and total-P. Average annual data is for the 1990-1993 period. Net adsorption of P to soil matrix and solute losses by drainage are excluded.

Balance term	Cl$^-$ [kg ha^{-1} a^{-1}]	Total-N [kg ha^{-1} a^{-1}]	Total-P [kg ha^{-1} a^{-1}]
Rainfall	20	25	0.9
Dry deposition	1	15	0.1
Surficial runoff	0	0	0.0
Fertilizer	64	150	0.0
Manure (incl. grazing)	113	283	89.6
Fixation	-	0	0.0
Diffusion	50	1	< 0.1
Net mineralization	0	0	0.0
Denitrification	-	-50	-
Volatilization (NH$_3$ ↑)	-	-31	-
Removal by harvest and grazing	-96	-297	-32.5
Average surplus 1990-1993: available to drainage and adsorption (P only)	153	96	58.2

Data on the annual surpluses for Cl$^-$, total, and total-P are needed to link the soil system balance to observed solute loads of drainage water as shown in Table V.5.2. As can be seen from the data shown, total-N and total-P surpluses decreased sharply in 1992 and 1993 as compared to prior years. It is expected that such a decrease will appear in lower total-N concentrations in drainage water within one or two years, based on the travel time distribution concluded on in Section V.4. For total-P, the effect of this decrease is expected to appear less rapidly in drainage water due to the high P-storage in the soil profile resulting from the sorption process.

Table V.5.2
Hupsel-Assink experimental site. Estimated annual surpluses for the years 1990, 1991, 1992, and 1993 of soil system balances for Cl^-, total-N, and total-P. Solute losses by drainage are excluded. *P-adsorption to solid phase is not included.

Year	Cl^- $[kg\ ha^{-1}\ a^{-1}]$	Total-N $[kg\ ha^{-1}\ a^{-1}]$	Total-P* $[kg\ ha^{-1}\ a^{-1}]$
Before 1990 (average)	200	159	75
1990	98	118	69
1991	148	199	109
1992	159	61	21
1993	207	5	33
Average surplus 1990-1993: available to drainage and adsorption (P only)	153	96	58

Composition of shallow groundwater - During March 23 and 24, 1993, samples were taken from the shallow groundwater in 37 piezometers (Fig. V.1.1). In all water samples, electrical conductivity EC, pH, and temperature were measured in the field, and NO_3-N concentrations were measured using the Nitracheck method (Vissenberg, 1995). Based on EC measurements, 37 samples were combined to yield a total of 15 samples and analyzed in the lab. The field NO_3^- measurements closely agreed with the laboratory results ($R^2 > 0.99$). Table V.5.3 shows the results on the lab analyses.

It can be observed that *the drainage water composition was about the same as the groundwater composition* at the experimental site. The annual total drainage was equal to the annual rainfall excess. Long-term average annual drainage loads can be estimated based on the field average groundwater composition and rainfall excess, which is about 330 mm a^{-1}. The combination of the rainfall excess and the groundwater composition data leads to annual average drainage loads of about 140, 88, and 0.4 kg ha^{-1} a^{-1} Cl^-, total-N, and total-P, respectively. Compared to the annual average soil system balance surplus for the 1990-1993 period (Table V.5.1), these loads are 8% lower for Cl^-, 8% lower for total-N, and 71% lower for total-P. It is highly possible that given the travel time distribution of drainage water, the precipitation excess in 1993-1994 in combination with the decreased solute surpluses (Table V.5.2) led to lower solute concentrations in the shallow groundwater in 1993.

Composition of subsurface drainage water - The time series for the main measured solute concentrations in the drainage water of the subsurface drain, coded ASK01 (Fig. V.1.1), are shown in Fig. V.5.1. N-Kjeldahl concentrations varied between 2 and 4 mg l^{-1} and did not show any significant variation with time, nor did the NH_4^+ concentrations (below 0.5 mg l^{-1}). *All temporal variation in total-N was caused by temporal variation of* $NO_3 - N$. The SO_4^{2-} concentrations were only measured incidentally, and concentration levels were between 120 and 200 mg l^{-1}.

Table V.5.3
Hupsel-Assink experimental site. Composition of shallow groundwater is between 0.5 and 1.5 m below the soil surface. Field measurements were taken on March 23 and 24, 1993. Laboratory measurements are given by Rijn & IJssel Water Board (formerly Zuiveringschap Oostelijk Gelderland).

Mixed samples from piezometers no.	Cl^- [mg l^{-1}]	NO_3-N [mg l^{-1}]	total-N [mg l^{-1}]	ortho-P [mg l^{-1}]	total-P [mg l^{-1}]	SO_4^{2-} [mg l^{-1}]
3,4,30	50	0.5	2.6	0.06	0.06	170
15,29,31,32	41	23.0	25.1	0.04	0.07	155
2,18,21	54	8.2	13.7	0.20	0.48	230
9,27	28	4.6	7.2	0.07	0.08	78
8,26	41	14.0	15.4	0.05	0.08	120
11,13	34	22.0	23.5	0.03	0.06	110
16,17,22,33	40	25.0	27.1	0.04	0.07	155
6,7,23,24,25	32	29.0	31.4	0.10	0.15	87
1,28	42	14.0	15.9	0.03	0.07	145
35,36	48	0.5	1.3	0.03	0.15	185
34,37	38	51.0	54.1	0.02	0.06	120
10,12	50	26.0	27.4	0.02	0.05	195
14	23	35.0	37.6	0.05	0.09	53
20	53	2.5	4.1	0.04	0.09	320
5,19	49	110.0	112.1	0.02	0.16	160
Field average	42	24.4	26.6	0.05	0.11	152
ASK01 drainage water, *March 1993*	50	28.9	30.7	0.02	0.06	*no data*
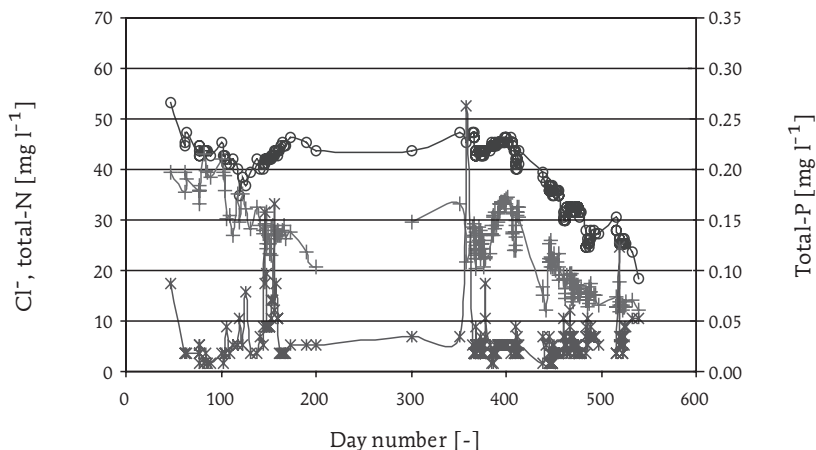
Fig. V.5.1
Hupsel-Assink experimental site. Concentrations in drainage water of subsurface drain ASK01 of Cl⁻ (o), total-N (+), and total-P (*). Period: November 16, 1992 through March 23, 1994. Day one is October 1, 1992.

Nitrogen and chloride - Total-N and Cl⁻ concentrations show a decreasing trend as the drainage season progresses. This phenomenon is not so clear for Cl⁻ during the winter of 1992/93. The ratio NO_3^-/Cl^- shows the same decreasing trend. It may be concluded that breakthrough of a solute front occurs with lower concentrations within the drainage season due to dilution effects, and that an increased degradation of NO_3-N by denitrification occurred under wet conditions in 1993/94. It is also possible that the decreased total-N surplus of the soil system balance in 1992 and 1993 (Table V.5.2) resulted in a decreasing NO_3-N concentration and NO_3^-/Cl^- ratio in drainage water. All conclusions indicate lower than average travel times of drainage water.

Phosphorus - During field visits it was often observed that during and after drainage events, orange to reddish flocks floated in the ditch at and around the subsurface drain outlets. A lab analysis of a sample of water with these flocks indicated high Fe and P-concentrations. As stated before, iron particles were seen in the discharge during the cleaning of the subsurface drains. Phosphate concentrations did not show any trend within a drainage season or throughout the measurement period. Ortho-P concentrations all were below 0.05 mg l⁻¹ P, and total-P concentrations showed peak levels of 0.1 to 0.3 mg l⁻¹ P, which were once above 1 mg l⁻¹ P.

After excavating part of the subsurface drain at the site, it was also observed that an iron-rich zone had been formed directly around the drain tube, causing an

orange-colored 'ring' of soil around the subsurface drain. *The accumulation of P around the subsurface drain* was shown by a simple soil sample program of soil in and around the drain trench (Fig. V.5.2). The soil fertility P-level was measured using a water extraction method (P-w) and a non-water extraction method (P-AL). Average P-w and P-AL numbers of the soil within the trench were two to three times higher compared to soil samples taken just outside the trench at the same depth.
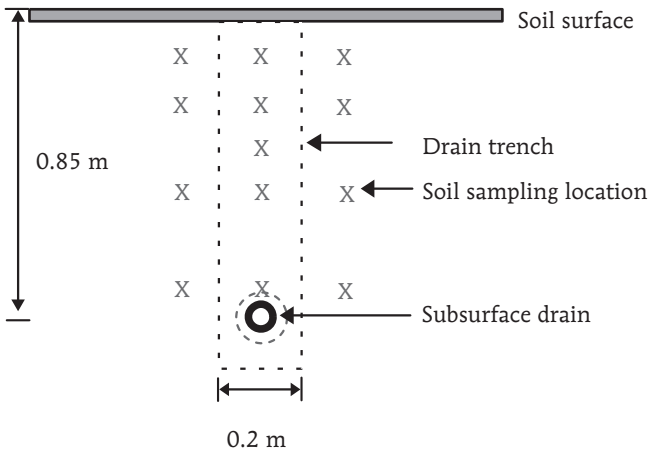
Fig. V.5.2
Hupsel-Assink experimental site. Soil sampling locations (X) in and around the subsurface drain trench.

The explanation of the field observations is as follows: Dissolved reduced iron and phosphate were transported in the soil-water system to the subsurface drain. In the vicinity of the subsurface drain, oxygen was present during certain times of the year, enabling precipitation of Fe-P aggregates. The transported iron and phosphate concentrated, accumulated around the drain, and partially entered the tile, forming flocks in the vicinity of the subsurface drain wall. These flocks were discharged during events with a high drainage rate; hence, the discharge of flocks was not a continuous, smooth process, but there was a stepwise release of iron flocks. There was a fairly large chance that drainage water with these flocks was missed and, thus, not sampled by the automatic sampling equipment. Hence, the measured drainage P-concentrations in drainage water were not representative of the P-loss by drainage. Due to this phenomenon, it was expected that the calculated P-loads of the drainage water underestimate the actual P-load.

Representation of drainage water - The subsurface drain, coded ASK01 (Fig. V.1.1), was not the only drain at the field site; a total of nine subsurface drains are present across four parcels, all of which are grassland. A spatial sampling program was set up and carried out to analyze discharge water from all subsurface drains. *The aim was to see whether the composition of drainage water across the field and neighboring parcels would be comparable to the continuously monitored drainage water of the ASK01 drain.* If comparable, this would make subsurface drain ASK01 a more or less representative sampling location. The spatial sampling program also consisted of other subsurface drainage and ditch water, the latter locations were coded KDK (Fig. V.1.1). Fig. V.5.3 shows the variation of solute concentrations from all locations sampled during the full measurement period from November 16, 1992 through April 15, 1994. Data on Cl^-, total-N, and total-P are shown.

The grassland parcel at the experimental site was provided with three subsurface drains, coded ASK01, ASK02, and ASK03 (Fig. V.1.1). The solute concentrations measured in drainage water from the ASK01-coded drain and in water from the other subsurface drains, coded ASK02 and ASK03, at the experimental site are well matched, which also accounts for the other ASK-coded subsurface drains. It is concluded that the ASK01 drainage water composition was representative of drainage water from the local parcel.

Differences were observed between the composition of water from the ASK-coded drains and other subsurface drains in the area (locations not shown in Fig. V.1.1). Although the land use at the time of the experiment and soil type were identical, average drainage water from 14 other subsurface drains showed 50% lower Cl^-, 20% lower total-N, and 4 times higher total-P concentrations. Lower Cl^- and total-N concentrations indicate a generally lower nutrient application level as compared to parcels drained by the ASK subsurface drains during a few years preceding the experiment, although data on nutrient applications were not available. Higher total-P concentrations might have originated from a more agriculturally-intensive land use in the past, when the soil in the vicinity was loaded with phosphate.

Differences also occurred between the composition of surficial discharge i.e., surface runoff and drainage from shallow open trenches and of subsurface drainage water. Very little data on surficial discharge components were available, so it is not possible to draw conclusions from these data. An indicative analysis showed that surficial discharge components contained 3 to 4 times less Cl^- and total-N, and up to 10 times more total-P as compared to subsurface drainage. The surficial flow components have passed shallow parts of the soil only when, on one hand, the rainfall water influence on dissolved solutes in soil water is high, leading to low Cl^- and total-N concentrations. On the other hand, adsorbed phosphate in the solid phase is likely to be very pronounced at the top of the soil as the P-front moved down from the soil surface. This possibly
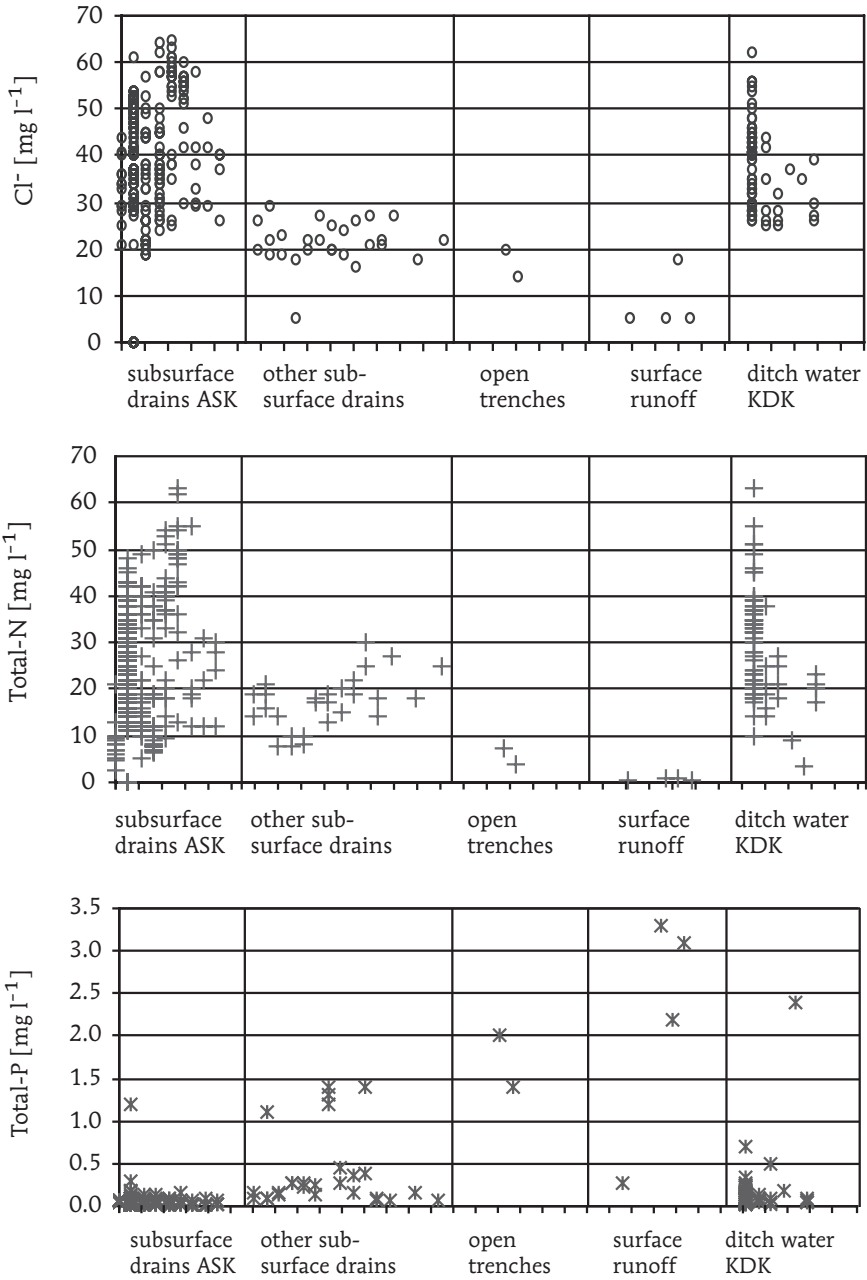
Fig. V.5.3
Hupsel-Assink experimental site. Variation of solute concentrations in different 'types' of drainage water from November 16, 1992 through April 15, 1994. Data shown: Cl⁻ (o), total-N (+), and total-P (*).

caused high total-P concentrations in the soil water at the top of the soil profile, which were picked up by shallow flow components.

Differences between surface water in the collection ditch and subsurface drainage water from the ASK-coded drains were small for Cl^- and total-N. Although the ditch water contained 3 times more total-P, it is concluded that the ditch received total-P from subsurface drainage. As previously stated, total-P was particularly missed from the ASK01 drain due to the sampling strategy and the erratic process of release of the accumulated particles within the subsurface drain. Based on data from the ASK01 drain, one could conclude that total-P in drainage water was low. Fig. V.5.3 shows, however, that P-concentrations in the water discharged by several subsurface drains was above 1 mg l^{-1} P, indicating the increasing influence of a downward moving P-sorption front in the soil on drainage water composition. In the case that these observed P-concentration levels indicated a breakthrough of the P-front down to the subsurface drainage level, P-loads to the surface water system are expected to be high and to continue, barely influenced by nutrient application measures at the soil surface level.

During 15 arbitrarily chosen drainage events within the measurement period, samples were taken from three or more subsurface drains at the same time during a single day. Two example dates were chosen: December 16, 1993, and March 18, 1994, and on both dates, the discharge water of eight subsurface drains was sampled. Fig. V.5.4 shows data series for the ASK-coded subsurface drains for the parameters Cl^- and total-N.

The overall conclusion on the composition of drainage water from different locations at the experimental site and the neighboring parcels is that the composition of the drainage water from the ASK01 drain is representative of subsurface drainage water from the experimental site and its surrounding area, except for phosphate. This conclusion contributes to the earlier statement that calculated P-loads from the ASK01-coded drain were not expected to be reliable. The P-concentrations of water from the ASK01 and other ASK-coded drains are lower compared to drainage from other subsurface drains. The exact reason for this is not known, but two possible reasons can be indicated:

- the agricultural history of the drained ASK parcels is less nutrient rich (lower application levels), and/or
- the solid phase of the soils in the area west of the collection ditch contains more Fe and Al as compared to the surrounding area, and P-sorption capacity is more pronounced, and/or
- measurement errors in the tile drainage water sampling program.

During periods with low discharge rates, also referred to in literature as *'base-flow' periods*, observed Cl^- levels in drainage water are usually high compared to periods of
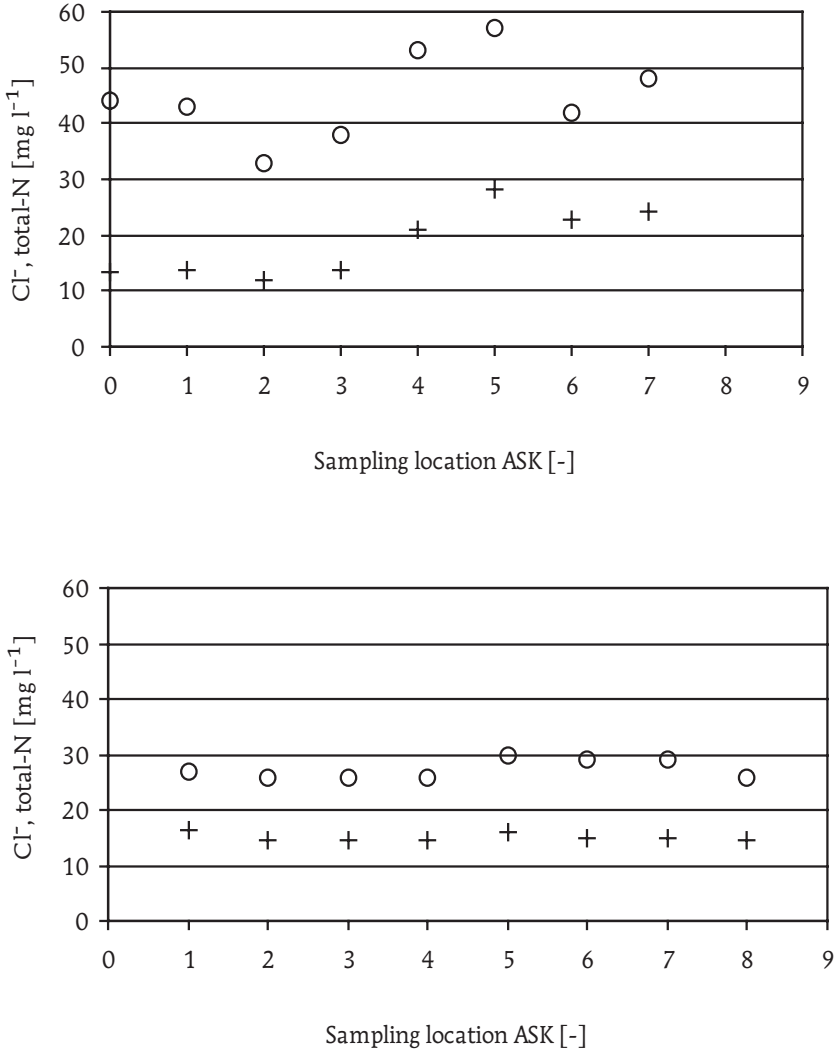
Fig. V.5.4
Hupsel-Assink experimental site. Composition of *subsurface drainage water from ASK-coded drains* (Fig. V.1.1) *during one single day*. Data shown: Cl$^-$ (**o**) and total-N (**+**) on December 16, 1993, in upper graph and on March 18, 1994, in lower graph.

high discharge rates or storm events. It seems as if subsurface drainage and brook water consists of a larger part of 'old' water at low discharge rates and less so at high discharge rates. High Cl^- levels coincide with low NO_3-N and high SO_4^{2-} levels. A possible explanation is that 'old' water has deep and/or long subsurface travel routes. The deeper the travel route and the longer the travel time of drainage, the closer it gets to the bottom of the aquifer and to the Miocene Age clay layer; consequently, a longer time period is available for groundwater to interact with the clay layer. Along deep travel routes, Cl^- is delivered through diffusion from the marine clay layer from the Miocene Age and is picked up by the groundwater; pyrite is oxidized by oxygen, or more likely by NO_3-N through chemical denitrification under anaerobic conditions. As a result, the relatively deep groundwater flow path, the 'base-flow' component, shows high Cl^- and high SO_4^{2-} levels in combination with low NO_3-N levels (Van den Eertwegh and Meinardi, 1999).

Solute losses by drainage - The solute loads of drainage water were calculated for the drainage water leaving the experimental site by the ASK01-coded subsurface drain (Fig. V.1.1). Drain discharge measurements and water sample analyses were available from January 1, 1993 through March 19, 1994; however, during two periods within the total measurement period, data were missing. To complete the time series, the following repair has been performed: During the period April 14, 1993 through July 2, 1993, subsurface drain discharge was estimated at a total of 10 mm (Section V.2). The drainage water composition during this period is interpolated between measurements on April 19, 1993 and July 28, 1993. Between March 20, 1994 and March 31, 1994, subsurface drain discharge was estimated at a total of 20 mm. This number is equal to the precipitation excess as the soil water storage remained filled as it was measured. The drainage water composition during the latter period is assumed to be equal to measurements on March 23, 1994. Table V.5.4 summarizes the solute loads of the subsurface drainage water from the experimental site. To calculate the solute loads for the unmeasured drainage, it was assumed that the chemical composition of the unmeasured drainage was equal to the subsurface drainage water composition. As previously stated, calculated P-loads were not reliable.

Linking agricultural practices to nutrient losses to surface water - The solute loads in Table V.5.4 do not match the surpluses from the soil system balances in Table V.5.1. The reasons for this are related to the travel time distribution of drainage water, soil chemical processes, and abnormal weather conditions during the measurement period. To correctly link soil system balance surpluses to observed solute losses by drainage, information is needed on the weather conditions and the travel time distribution of drainage water, as discussed in Section IV.5. The fractions of the travel time distribution of drainage water at the experimental site were given in Table V.4.6. The average soil system balance surplus for Cl^-, total-N, total-P was shown in Table V.5.1. The long-term

Table V.5.4

Hupsel-Assink experimental site. Calculated solute loads in drainage water. Total loads include the drainage load by unmeasured drainage. *January 1, 1993 through March 31, 1994, subsurface drainage load. **April 1, 1993 through March 31, 1994, estimated total solute load of drainage by subsurface drain, by the ditch, and by the Hupsel brook.

Solute	Measured * [kg ha^{-1}]	Total** [kg ha^{-1} a^{-1}]
Cl$^-$	202	268
NO$_3$-N	114	146
Total-N	126	161
Ortho-P	0.08	0.11
Total-P	0.22	0.30

annual average precipitation excess for the Hupsel-Assink experimental site was estimated at 350 mm a^{-1}. The calculation results are given in Table V.5.5.

The conclusion on the nutrient loads is that the data in Table V.5.5 show that the calculated solute loads in drainage water of Cl$^-$ and total-N nearly match the measured loads of the total subsurface drainage water. The calculated P-load did not match the field data on losses by drainage due to the P-sorption term. The annual solute loads as predicted by using the shallow groundwater composition and the 1993-1994 rainfall excess did not match the observed solute loads, but when the travel time distribution calculation was used, it was successful. The travel time distribution given in Table V.4.6 well suits the field situation at the experimental site.

6   Conclusions

The field observations at the Hupsel-Assink experimental site resulted in a set of data of great value on hydrology and nutrient leaching. Rainfall observations appeared to be best performed with a rain gauge installed at the soil surface. Hysteresis was observed in the relationship between the groundwater hydraulic head and the tile drainage rate. During the experiment, surface runoff was not observed at the plot, but ponding conditions occurred. Surface runoff was observed in the neighborhood of the experimental site and at other locations within the Hupsel brook basin. A drainage event in the summer of

Table V.5.5
Hupsel-Assink experimental site. Load of drainage water $q_{m,\text{drainage}}$ as calculated [IV.6] from the soil system balance surplus, weather data, and travel time distribution. *Hydrologic year, running from April through March. **Data are from Table V.5.4, total values.

Year*	$P - ET_a$ [mm a^{-1}]	Q_{drainage} [mm a^{-1}]	Cl_{surplus} [kg ha^{-1} a^{-1}]	N_{surplus} [kg ha^{-1} a^{-1}]	P_{surplus} [kg ha^{-1} a^{-1}]	$q_{m,\text{drainage}}$ [kg ha^{-1} a^{-1}] Calculated			Field**		
						Cl$^-$	Total-N	Total-P	Cl$^-$	Total-N	Total-P
<1990	350		200	159	75						
1990	281		98	118	69						
1991	245		148	199	109						
1992	218		159	61	21						
1993	664	572	207	5	33	256	166	52	268	161	0.30

1993, as observed at the plot as well as at the basin scale, was induced by preferential flow, hypothetically unstable flow, in the unsaturated zone.

The field water balance of the plot at the experimental site from January 1, 1993 through March 19, 1994 showed an incomplete registration of the subsurface discharge i.e., an unmeasured drainage term. Rainfall excess water left the plot by tile drainage, by direct drainage to the collection ditch, and to the Hupsel brook. Hydraulic head gradients were observed that would favor drainage to occur through other routes than through the subsurface drain. The soil profile, the slightly sloping catchment area of the tile drain monitored, and the increased clogging of the tile drain possibly led to less drainage through the tile drain, hence to more drainage through other, unmeasured routes. *Around 30% of the total drainage was not discharged by the tile drain: 5% was discharged by the ditch, and 25% was discharged by the Hupsel brook.* Reduction of potential evapotranspiration was around 15 mm.

The 2D single-porosity model could reproduce the field water balance with measured and unmeasured drainage terms by introducing appropriate soil profiles and boundary condition types. The unmeasured drainage was well represented by allowing water to drain from the side of the flow domain from a zone below the tile drain. The overall temporal variation of drainage was calculated reasonably well; however, some measured drainage events during dry periods were missed. These events were possibly caused by preferential flow, hypothetically unstable flow in the unsaturated zone. This type of flow was conceptually not accounted for by the computer code. Calculated drainage rates were higher compared to measured rates as the drainage season progressed, due to clogging of the subsurface drain at the experimental site. In order to calculate any reduction of ET_p, values of θ_r for soil layers present within the root zone were increased from 0.01 (laboratory results) to 0.20. Using this latter value, the ET_p reduction was still small. Only major changes in k_s values and/or in parameters for the Mualem-Van Genuchten soil hydraulic conductivity function could generate any significant ET_p reduction.

The travel time distribution of drainage water at the Hupsel-Assink site was calculated using the Ernst-Bruggeman steady-state approach. A simulation model was used to analyze this distribution under transient flow conditions. For the 1993-1994 period, the *2D single-porosity model yielded about equal results compared to the steady-state approach*, as shown in Table V.6.1. Some deviations occur in f_τ values between the data shown for the single-porosity model and in Table V.4.6. These deviations, e.g., for average weather situations are due to the fact that when using the 2D model, actual weather data were used. These might differ slightly from long-term average weather data as used in Table V.4.6. It is concluded that the steady-state approach is suitable to estimate the travel time distribution on an annual basis.

Table V.6.1
Hupsel-Assink experimental site. Travel time distribution of drainage water. Calculated fractions f_τ ($\tau = 1,3$) using the Ernst-Bruggeman steady-state approach [II.5] and 2D single-porosity model for transient flow conditions. Data shown for hydrologic year 1993-1994, and three subsequent average (1984-1987), dry (1975-1978), and wet years (1965-1968).

Fraction	Steady- state	Transient flow modeling			
	1993-94	1993-94	Average	Dry	Wet
f_1	**0.42**	**0.47**	0.29	0.02	0.49
f_2	-	-	0.25	0.00	0.21
f_3	-	-	0.12	0.30	0.07
Total	-	-	0.66	0.32	0.77

The MINAS levy-free surpluses as mentioned in Section I.1 in 2003 are 180 kg ha^{-1} a^{-1} N and 8.5 kg ha^{-1} a^{-1} P. MINAS balance data were not available for the farm at the experimental site. The N and P-surpluses were decreasing in 1992 and 1993, but the effect of the decreasing surpluses on the drainage water composition were visible for N only. The large P-mass stored in the soil profile masked out any effect from the decreasing surpluses. The composition of the drainage water from the ASK01-coded drain matched the shallow groundwater composition. The ASK01 drainage water represented all drainage water from the area surrounding the experimental site, except for phosphate. The measured P-concentrations were therefore not suitable to calculate reliable P-losses by drainage; however, observations at other subsurface drains showed that P-losses by drainage actually occurred. P-concentrations in water discharged by several subsurface drains exceeded 1 mg l^{-1} P and possibly indicated the breakthrough of a P-front in the soil down to the subsurface drains level. The observed solute losses by drainage were calculated after correction of the unmeasured drainage terms which resulted from the field water balance.

The annual nutrient surpluses and nutrient losses by drainage were linked by using the travel time distribution of drainage water, as calculated with the plot-scale model. For phosphorus, a P-sorption term was introduced to match the calculated with the measured P-losses by drainage. For the plot at the experimental site, the average P-sorption was estimated at 57 kg^{-1} ha^{-1} a^{-1} P. Table V.6.2 shows the results.

Table V.6.2

Hupsel-Assink experimental site. Nitrogen N and phosphorus P mass flux of drainage water ($q_{m,\text{drainage}}$) calculated from the nutrient budget surplus, weather data, and travel time distribution of drainage water. *P-adsorption is not included. **Less reliable value.

Period	N_{surplus} [kg ha^{-1} a^{-1}]	P_{surplus}* [kg ha^{-1} a^{-1}]	P_{sorption} [kg ha^{-1} a^{-1}]	$q_{m,\text{drainage,N}}$ [kg ha^{-1} a^{-1}] Measured	Calculated	$q_{m,\text{drainage,P}}$ [kg ha^{-1} a^{-1}] Measured	Calculated
1990	+118	+69	68				
1991	+199	+109	108				
1992	+61	+21	20				
1993	+5	+33	31	161	164	0.30**	2.30
1990-1993	+96	+58	56.8				

The calculated N-load of the drainage water matched the field data. Due to the unreliable field data on P-losses by drainage it is hard to tell whether the calculated P-loads were good estimates. The calculated P-loads were higher compared to the measured load, caused by an underestimation of the P-adsorption.

The annual solute loads predicted by the shallow groundwater composition and the 1993-1994 rainfall excess did not match the observed solute loads. Using the travel time distribution given in Table V.6.1, the calculation was successful.

VI

APPLICATION OF REGIONAL APPROACH TO FLEVOLAND

1   Description of Flevoland polder area

General - The Flevoland polder area consists of two areas, which are each drained by a main channel i.e., regional surface water system. The Hoge Afdeling (HA) area drains into the Hoge Vaart (HV) main channel. The Lage Afdeling drainage area drains into the Lage Vaart main channel. The regional model as presented in Chapter III was applied to the HA drainage area (Fig. VI.1.1). The HV main channel is about 80 km long; its area is 95 ha, and it has a volume of 4 734 000 m^3 (Verbrugge, Zuiderzeeland Water Board, personal communication). The HV main channel has a controlled constant water level of 5.2 m below MSL, while the Lage Vaart main channel has a level of 6.2 m below MSL. The draining area to the HV main channel is 40 250 ha. The channel receives regional-scale groundwater seepage as well. The water and solutes present in the main channels is discharged by three pumping-stations for each channel, and each station has three pumps. The total pumping capacity is 11-12 mm d^{-1}. The response time of the system to rainfall excess in winter is less than 6 h. In summer, regional-scale drainage usually starts after 60 mm of rainfall excess. The mean residence time of water t_r in the main channels is about one week (Verbrugge, Zuiderzeeland Water Board, personal communication).

Geohydrology - The geohydrology of the Flevoland polder can be generally described by a confining layer of Holocene origin, overlying a sandy aquifer deposited in the Pleistocene Age (Meinardi et al., 1978; Ente et al., 1986). The area belongs to a tectonically subsiding basin, filled in by marine sediments, and in the Pleistocene Age it was filled mainly by fluviatile sediments. The practically impervious hydrological basis is formed by the top of the Maassluis formation at a depth of 190-260 m below MSL. Above this formation, aquifers can be defined, which consists of the gravel and sand part of the formations of Harderwijk, Enschede, Sterksel, and Urk. The regional-scale groundwater flow direction is mainly from southeast to west-northwest. The top soils are mainly of Holocene parent materials deposited in lakes, surrounded by bog peat. Wave erosion of this peat caused high organic matter contents in the sediments. After the main part of the bog peat was eroded, material predominantly of mineral composition was deposited on top. The sedimentation took place under fresh water conditions and afterwards under

increasing brackish conditions. In 1932 the brackish Zuyder Zee was closed off from the North Sea and within a few years turned into the freshwater Lake IJssel. Reworked sediments by storms were again deposited (after Groen, 1997). The thickness of the confining layer is less than 1 m in the southeastern part of the polder area and increases towards the northwest to over 10 m near the city of Lelystad. This layer consists of loamy sand, some peat layers, loamy clay, and clay. It generally contains between 3% and 5% organic matter contents (Groen, 1997).
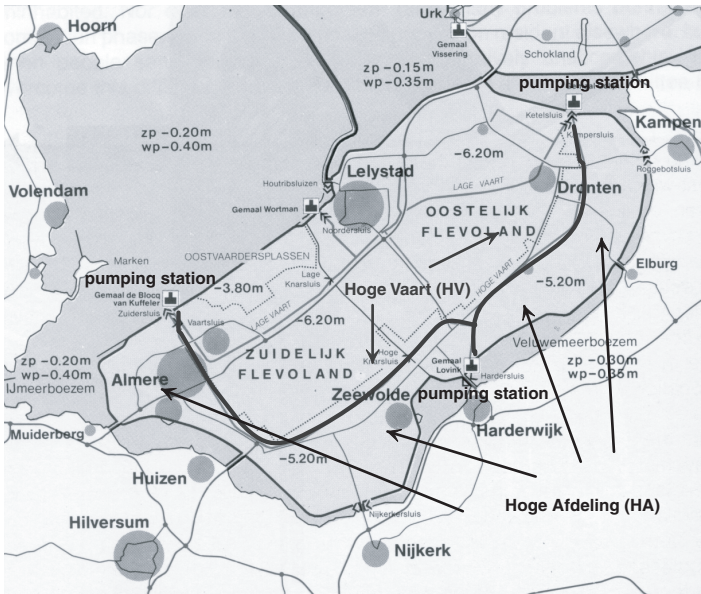
Fig. VI.1.1
Flevoland polder area. Hoge Vaart (HV) main channel with three pumping stations and the Hoge Afdeling (HA) drainage area, and the cities of Almere, Lelystad, Dronten, and Zeewolde (by Van Duin and De Kaste, 1989).

Soil types - The Flevoland polder area consists for 50% of clay soils, for 39% of silty clay loam, for 7% of loamy sand, and for 4% of sandy soils. The clay soils of the type kaolinite and illite are permanently cracked due to physical and chemical ripening. These clay types cover 80% of the clay soil area in the Flevopolder. Montmorillonite clay type soils show shrinking and swelling, which covers 20% of the clay soil area in the Flevopolder (Groen, 1997). The shrinkage cracks in the plough layer have been removed by tillage activities, but are permanently present in the subsoil down to 1.2 m below the soil surface. Soil ripening has induced soil subsidence in the Flevoland polder area, which has been reported by Van Dooremolen et al. (1996). Since the reclamation of 41 locations in

eastern Flevoland and 49 locations in the south, soil surface measurements have been performed. The average soil subsidence from the beginning of the reclamation to 1996 in eastern Flevoland and in southern Flevoland is about 0.9 m. The soil ripening process in southern Flevoland did not yet reach its final stage.

Drainage system - One separate system of subsurface tile drains, collection ditches, and channels, constitutes the discharge region, and these discharge regions drain into the main channels. The drainage area of the HV main channel consists of 13 discharge regions; the Lage Vaart main channel consists of 15 discharge regions. The channels within in these discharge regions have controlled and constant water levels and they drain into the main channels (Section IV.1, Fig. IV.1.4). The subsurface drains and collection ditches drain by gravity into the channels. The subsurface drain spacing varies from less than 12 to 24 and 48 m, mainly dependent on the soil hydraulic conductivity and groundwater seepage rate. The plot dimensions in eastern Flevoland are typically 300 m by 1000 m. In southern Flevoland the plots are 450 by 1000 m. The land use includes arable land (40% of area), grassland (10%), fruit trees (5%), recreation areas and woodlands (15%), dry and wet infrastructure (10%), and urban areas (20%). The arable farms have a typical crop rotation period of three to four years, combining potatoes, sugar beets, cereals, and other crops like onions, carrots, peas, and beans. The urban areas are mainly the city or town areas of Almere, Lelystad, and Dronten (Fig. VI.1.1).

Regional water balance - The long-term annual average P and ET_r rates were estimated by Schultz (1992) at 775 mm a^{-1} and 525 mm a^{-1} respectively. Rainfall at present is measured at eight stations. Compared to the polder-average rainfall, the average spatial variation is about 5% on a monthly basis. At time periods shorter than one month, the spatial variation can be larger. Due to its low ground surface levels and controlled water levels, groundwater seepage is a well-known phenomenon in the Flevoland polder. This seepage originates from deep groundwater for more than 90% (Oostra, 1996). The regional-scale seepage rate of deep groundwater originates mainly from the Veluwe, Utrechtse Heuvelrug, and lake IJssel regions. The major part of this seepage flows directly into the channels because it usually cuts through the confining Holocene layer and has a direct hydrological contact with the Pleistocene aquifer, although a small part of the seepage appears in subsurface drains and/or collection ditches. Besides regional-scale seepage of deep groundwater, local-scale seepage below the dikes also occurs, which is mainly discharged directly by the ditches to the vicinity of the dikes. The annual average discharge by the six pumping-stations amounts to 650 mm a^{-1} (Verbrugge, Zuiderzeeland Water Board, personal communication). The annual average water balance for the Flevoland polder area for the hydrologic years of the 1988-1998 period is shown in Table VI.1.1.

Table VI.1.1
Flevoland polder area. Average annual water balance for the period April 1988 –
March 1999.

Quantity	$[\mathrm{mm\ a^{-1}}]$
P	825
ET_a	489
Q_{seep}	320
Q_{outlet}	656

Surface water composition - The chemical composition of the surface waters in the
Flevoland polder is monitored by the Zuiderzeeland Water Board, formerly
heemraadschap Fleverwaard. Since December 1987 this organization ran a surface water
grab-sample monitoring program across approximately 100 locations in the channel
system. The routine monitoring frequency is usually one month. The sampling scheme of
surface water at the three HV pumping-stations was as follows:

– December 1987 through mid-June 1992: manual sampling if one or more
  pumping-stations were in operation,
– mid-June 1992 through December 1997: time-proportional sampling. If one or
  more pumping-stations were in operation; a grab sample was taken automatically
  every ten minutes and placed in a vessel. A mixed sample was taken from the vessel
  every Friday, and
– from January 1998 onward: the grab sampling program was used, taking one
  sample every two weeks whether or not the pumping-stations were in operation.

The time-proportional sampling method relatively yields the most accurate solute load
estimates because it is nearly flow-proportional due to the fact that pumps while
operated run at almost constant capacities.

For the HV main channel, all data were available for the hydrologic years 1988-1990 and
1997-1998, and partially for 1991 and 1994. During 1992-1993 and 1995-1996, part of
the time series of water quality data is missing. Missing data on the composition of
surface water at the pumping-stations were added by interpolation between months
and/or between available data at other locations per channel. Fig. VI.1.2 shows annual
average solute loads at the outlets of the HV main channel versus the discharge rate of
the pumps at all HV pumping-stations for the 1988-1998 period.
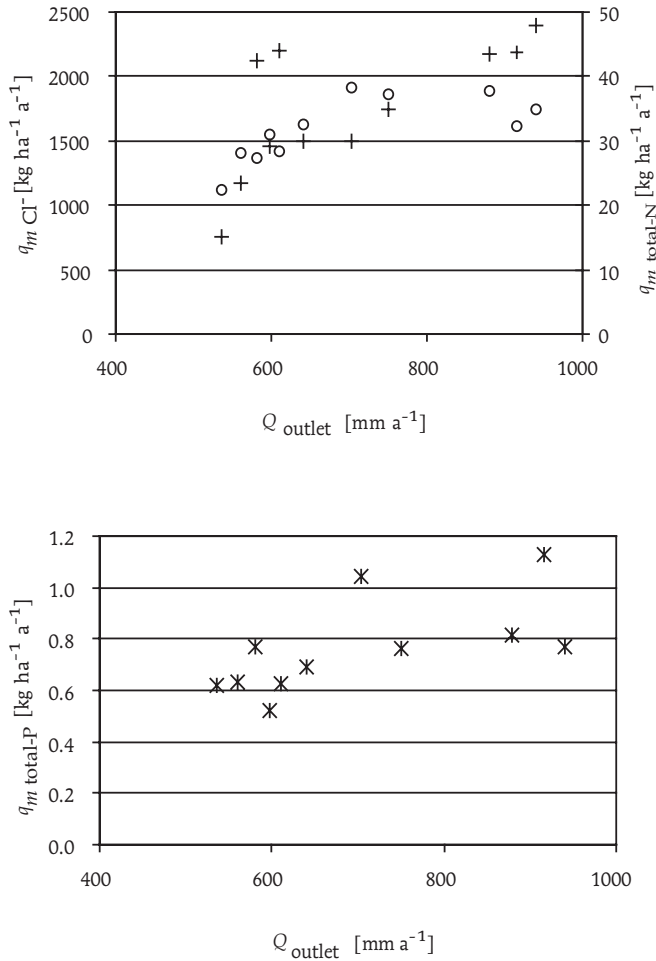
Fig. VI.1.2
Flevoland polder, Hoge Vaart (HV) main channel. Annual average discharge rates of the pumps at HV outlet pumping-stations in [mm a^{-1}] versus solute loads of Cl$^-$ (o), total-N (+), and total-P (*) in [kg ha^{-1} a^{-1}] for the hydrologic years 1988-1998.

Total-N and total-P are both parameters subject to chemical processes in and around the surface water system. Main processes in the surface water system are net retention of N and P by sorption, by plant uptake, and losses to the atmosphere by denitrification of NO_3-N. These processes lead to a net loss and/or retention of nutrients. The regional surface water quality is determined by the sources loading the surface water system with solutes and by processes in the surface water system itself. Main sources are deposition from the atmosphere, discharge of effluent from industries, wastewater treatment plants, and by other point sources, runoff and leaching from agricultural soils, and other point and diffuse sources in rural areas. In urban areas, it is assumed that there are no point source contributions to the surface water except from the effluent of wastewater treatment plants. This assumption will usually meet practical situations, but not always. Some point source contributions to the surface water will be present such as storm water overflows. In rural areas, small-scale direct loads of wastewater occur, but the main part of the wastewater is treated first or discharged, for example, through reed fields. The effluent of the wastewater treatment plants is a point source to the main channels.

Review of regional-scale field data - The first reports on the composition of subsurface drainage and ditch water in the Flevoland polder originated from De Jong (1972, 1980, 1983). De Jong (1980) found a positive correlation between the application of manure and fertilizer and with leaching of NO_3-N from grassland plots (field data from 1976-1978). Phosphate concentration levels in subsurface drainage water were generally below 0.1 mg l^{-1} P. No correlation was found with P-application levels. De Jong (1983) reported on drainage water composition on three arable farms and on a regional monitoring program on 40 locations. Leaching of nutrients correlated strongly with high discharge events. Chloride and sulfate concentrations in drainage water in eastern Flevoland were lower as compared to southern Flevoland, possibly indicating the more progressive ripening in the eastern Flevoland polder, which is nine years older.

Meinardi and Van den Eertwegh (1995, 1997) ran a monitoring program during 1992-1995 on the subsurface drainage water composition from loam and clay soils across 28 locations in the Netherlands, of which 14 locations were located in the Flevoland polder. Meinardi et al. (1998b) reported more generally about the depth of the flow system and hydrology of clay soils in the Netherlands. The conclusion on the Flevoland polder locations was that chloride and sulfate mainly originated from the solid phase of the ripening polder. Influence of deep groundwater seepage was found to be present in high Cl^- and P-concentrations measured. Denitrification due to pyrite oxidation did not appear to play an important role, although measured sulfate concentrations indicated a strong oxidation of sulfide components. The NO_3-N concentrations found were negatively correlated with the clay contents of the soils unless the soils were structured, which is often the case in the Flevoland polder.

If N-leaching was calculated as a percentage of total-N amounts applied, arable land values were between 10% and 25%, grassland was between 5% and 15%, and fruit-orchards were between 15% and 25%. Grassland seemed to appear to be more efficient in N-use as compared to other land use forms. *No site or region-specific field data are available for the Flevoland polder itself on hydrology and nutrient leaching from arable land on loamy soils.* The data presented by De Vos (1997) for the Lovinkhoeve experimental farm in the Noordoostpolder region and by Van den Eertwegh et al. (1999) for the Rusthoeve experimental farm in the southwest of the Netherlands provide insight into N-losses by drainage from arable land.

2 Results of regional model application

Model setup - The Hoge Afdeling (HA) region has features and characteristics that are representative of other parts of the polder area. These include soil type, land use, and travel time distribution of drainage water. Hydrologically, two needed assumptions were made:

- surface water in the HV main channel does not flow to the Lage Vaart main channel vice versa, and
- no subsurface flow occurs from the HA to the Lage Afdeling (LA) drainage region of the Flevoland polder.

Characteristics of the region modeled were partially based on the work of Hoogvliet (1994), Oostra (1996), and Bosdijk (1997). Data on point sources of water and solutes and on surface water composition were the courtesy of the Zuiderzeeland Water Board. Extra data were taken from Kuiper (1996), and data on the use of fertilizer and manure were taken from RIVM (2001). The HA drainage area, or region, and its 13 discharge regions (number 16 to 28) are shown in Fig. VI.2.1.

The subdivision of the land area of the HA region into sub-regions was mainly based on soil type, land use, and estimated depth of the local-scale groundwater flow system. The total HA region has 2% local-scale surface water area. This part of the surface water area is neglected; all area is seen as land area. It is assumed that t_r of water in the local-scale surface water system is negligible. Table VI.2.1 shows the overall characteristics of the six sub-regions.

The seepage water composition is based on solute concentrations in the upper sandy aquifer. Cl^- and total-N concentrations are assumed not to change while groundwater flows upward from the aquifer into the regional surface water. Nitrogen in seepage water is mainly in the form of ammonium (NH_4^+). Of total-P, 90% of the solute is assumed to adsorb and/or precipitate at/near the channel bottom before it reaches the surface water

Table VI.2.1

Flevoland polder, HA region. Overall characteristics of the six sub-regions. *All sub-regions use station Lelystad for ET_r data. **Dominant.

Sub-region	Area [ha]	Discharge regions	Meteo-station*	Soil type**	GTC**	Land use**
1	15 250	16,17,19-22	Dronten, Biddinghuizen, Harderwijk	Loam	6	Grassland
2	2750	18	Biddinghuizen	Clay	6	Arable land
3	1500	23	Harderwijk, Zeewolde SW	Clay	6	Orchard
4	10 500	24-25	Zeewolde SW	Sand	6	Rural area (woodlands mainly)
5	1500	26	Zeewolde, Zeewolde SW	Clay	6	Grassland
6	7750	27-28	Oostvaardersdiep	Clay	6	Urban area
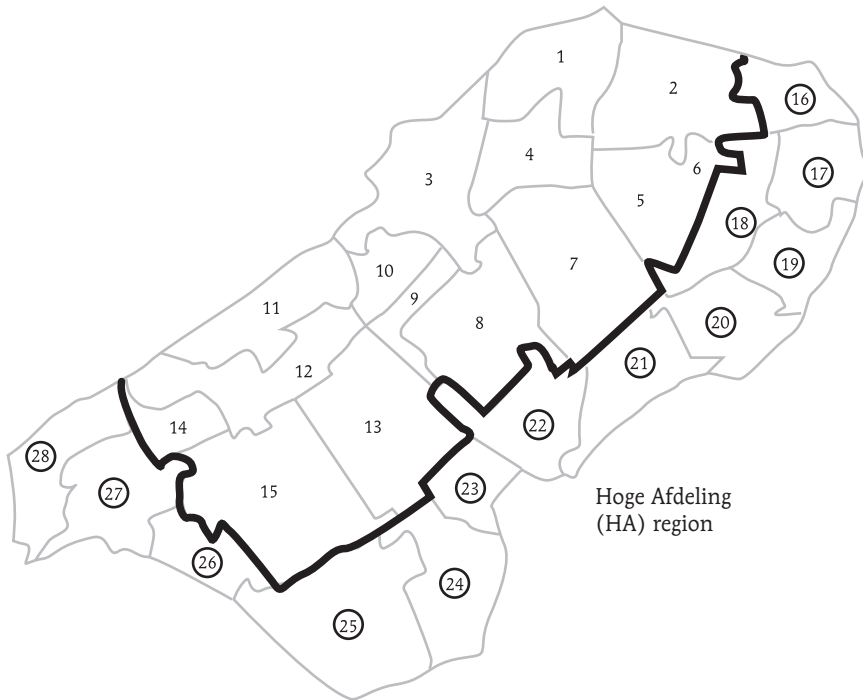
Fig. VI.2.1
Flevoland polder, HA region. HA region east and south of the wide line. Its discharge
regions are numbered 16 through 28 and marked by circles.

itself due to the expected presence of iron and oxygen. As a consequence, the P-mass
stored in the channel bottom sediment increases. All seepage is assumed to enter the
regional surface water system on an annual basis. The seepage rate was kept constant
and estimated at 370 mm a^{-1}, based on the average 1988-1998 regional water balance
for the HA region. The solute concentrations in groundwater seepage, in rainfall, and the
annual average rates of dry deposition are shown in Table VI.2.2. The results are shown
and judged for the hydrologic years April 1988 through March 1999.
General information on model parameters and variables is shown in Appendix C. More
information on model parameters, data on land use, and on mass balance terms related
to soil-chemical processes is given in Appendix D.

Regional-scale travel times - Each of the six sub-regions has its own specific travel time
distribution of drainage water as shown in Table D.1 of Appendix D. The overall annual
regional travel time distribution can be calculated as a discharge-weighted average of f_τ
originating from the sub-regions. The overall travel time distribution from the HA region

Table VI.2.2
Flevoland polder, HA region. Average composition of deep groundwater seepage
(Oostra, 1996) of rainfall and dry deposition numbers (RIVM and KNMI, 1989).

Parameter	Seepage $[\text{mg l}^{-1}]$	Rainfall $[\text{mg l}^{-1}]$	Dry deposition $[\text{kg ha}^{-1}\,\text{a}^{-1}]$
Cl^-	375	5	0.5
Total-N	2	2	10
Total-P	0.15	0.125	0.1

shows 1988-1998 mean values for travel time fractions f_1 to f_3 respectively of 0.41,
0.19, and 0.11; hence, *71% of the drainage water left the area within three years.*
These numbers varied from year to year as a result of variable weather conditions. The
standard deviation of the fraction f_2 and f_3 ranged from 0.02 to 0.03. The standard
deviation of the fraction f_1 was 0.17. The weather conditions have mainly influenced the
youngest fraction and consequentially, the oldest fractions as well.

Residence time in surface water - The calculated mean annual residence time of water
within the regional surface water system $t_r = 6.6$ days for the 1988-1998 period, varying
between 4 days during a wet year like 1998, to 10-11 days during a dry year e.g., 1995.
The numbers are in concurrence with actual practice (Verbrugge, Zuiderzeeland Water
Board, personal communication).

Calculated discharge - The calculated and measured annual discharge rates of the pumps
at all HV pumping-stations are shown in Fig. VI.2.2. Calculated and measured values are
in agreement; the calculated drainage during dry and wet years show some deviations to
measured drainage rates, especially for dry and wet years. These deviations could be
caused by Q_{seep}, which was kept constant throughout the years. If Q_{seep} would vary with
time, the calculated discharge rates would increase during dry years and decrease during
wet years.

Calculated solute loads - The dissolved Cl^-, total-N, and total-P contents in the regional
surface water have different sources. The solutes in the HA region originated from the
atmosphere i.e., wet and dry deposition, point sources i.e., effluent of wastewater
treatment plants, seepage water, and solute losses by drainage. The relative contribution
of each source to the total solute loads is important for the determination of measures to
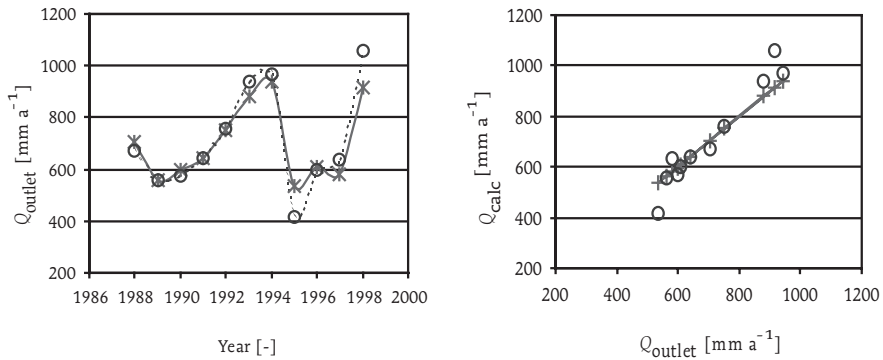
Fig. VI.2.2
Flevoland polder, HA region. Measured (+) and calculated discharge rates Q_{outlet} (o) of
HV pumping-stations for 1988-1998 period. A: discharge rates versus time. B:
measured versus calculated discharge rates.

improve surface water quality. Based on the solute mass balance (Section III.4) computed
for the HV regional surface water system, the contribution of each source to the total
load to the surface water was calculated. Table VI.2.3 shows the calculated relative
contribution of the sources mentioned for all solutes as average percentage of the total
load in the 1988-1998 period.

Table VI.2.3
Flevoland polder, HA region. Average relative contribution of water and solute sources
to HV regional surface water in [%] of the total load in the April 1988 – March 1999
period. *Average number for full period: from 1996 onwards the relative contribution
decreased to less than 2%.

Source	Water [%]	Cl⁻ [%]	Total-N [%]	Total-P [%]
Atmosphere	< 1	< 1	< 1	< 1
Point sources	< 1	< 1	4	30*
Groundwater seepage	56	86	19	55
Drainage	43	13	76	14

The relative contribution to water of groundwater seepage and precipitation excess transformed into drainage water is about equal. The Cl-loads are mainly determined by seepage water. The relative contribution of drainage water is 13%, including salt diffusion from the solid phase in the shallow groundwater flow system. Drainage water has the largest relative contribution to total-N loads, mainly originating from N-losses from agricultural land. *It is stressed that the relative contribution of point P-sources decreased with time from over 35% (1988-1994) to less than 2% (1997-1998) in the 1988-1998 period due to better operation and re-allocation of sewage water treatment plants.* Seepage water dominates the annual P-load to the HV regional surface water system.

Note that the analysis provided is based on average annual situations. However, as far as the surface water composition, quality, and ecological effect in the region are concerned, one has to focus on seasons and seasonal situations. During the summer months, drainage is almost absent, but seepage water and point sources are still present. These sources will dominate the surface water composition in summer. Looking at the relative contributions shown for seepage and point sources on an annual basis, all relative contributions of all solutes from these sources will be larger in summer months. As far as solute loads to regional surface water and the composition of the surface waters surrounding the modeled region as a whole are concerned, winter months with all contributing sources are also of interest.

The solute loads calculated by the model were loads to the surface water system. They were compared to calculated solute loads pumped out at the outer ends of the main channel by the three pumping-stations. The solute loads calculated at the outlet of the region, and by the regional model, are shown in Fig. VI.2.3 for Cl^-, in Fig. VI.2.4 for total-N, and in Fig. VI.2.5 for total-P.

The calculated Cl-loads to the regional surface water do not match the Cl-loads discharged by the pumping-stations very well. The average load of about 1600 kg ha^{-1} a^{-1} agrees, but the calculated temporal variation is too small. Seepage water is a relatively large contributor to the total Cl-loads as indicated above (Table VI.2.4). In the regional model, Q_{seep} as well as C_{seep} are assumed to be time independent throughout all the years. Any temporal variation within years, or between years, will largely influence the Cl-loads. The modeling result shows that it is very likely that the regional-scale average seepage rate varies with time, about 10% annually, which is caused by a fluctuation in the groundwater flow entering the model region and by variations in the hydrological response within the polder area. During dry years, larger seepage rates are expected as compared to rates during wet years. It is not expected that C_{seep} will vary significantly from year to year.
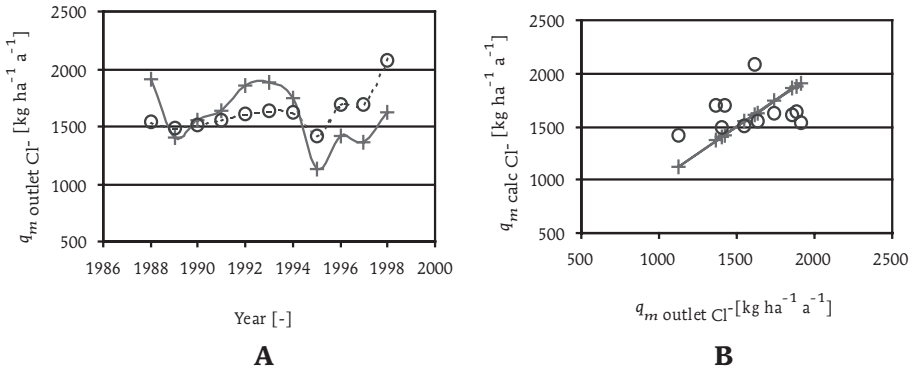
Fig. VI.2.3
Flevoland polder, HA region. Cl-loads discharged by pumping-stations at outlet $q_{m \text{ outlet Cl}}$ (+) versus calculated Cl-loads $q_{m \text{ calc Cl}}$ (o) to HV regional surface water system for the1988-1998 period. A: $q_{m \text{ outlet Cl}}$ and $q_{m \text{ calc Cl}}$ versus time. B: $q_{m \text{ outlet Cl}}$ versus $q_{m \text{ calc Cl}}$.
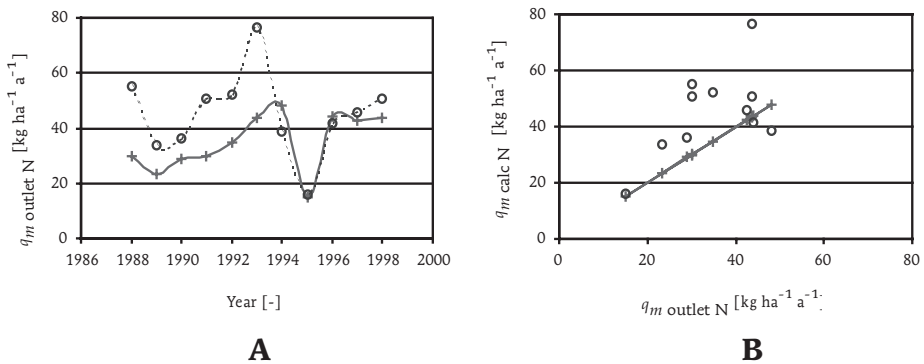
Fig. VI.2.4
Flevoland polder, HA region. Total-N loads discharged by pumping-stations at outlet $q_{m \text{ outlet N}}$ (+) versus calculated total-N loads $q_{m \text{ calc N}}$ (o) to HV regional surface water system for 1988-1998 period. A: $q_{m \text{ outlet N}}$ and $q_{m \text{ calc N}}$ versus time. B: $q_{m \text{ outlet N}}$ versus $q_{m \text{ calc N}}$.

The calculated total-N loads deviate from the loads pumped out of the HV regional surface water system in two ways: the absolute level is a factor of 1.3 higher (45 to 35 kg ha^{-1} a^{-1} N), and the timing before 1995 is off. Beginning with the timing, it was already indicated that during 1992 and 1993, data were missing on surface water composition and calculated loads were not very reliable; therefore, these periods have to be left out of consideration. So, the timing may not be off, but it may only seem off. Looking at the data, 1991 could also have been a suspicious year with regard to the field data available. The absolute difference between the loads shown is probably due to

- an overestimation of the N-losses by drainage,
- effects of net N-retention and N-losses by denitrification, for example, within the surface water system itself, and/or
- an overestimation of C_{seep} for total-N.

A factor of some influence is the denitrification rate within the sub-regions, either within the local-scale surface waters as well as in the soil-water-systems. Using the regional model, the denitrification rates in the soil system were estimated between 80 and 100 kg ha^{-1} a^{-1}. These numbers are somewhat larger as compared to references analyzed in Section IV.5. Of the total-N loads to the surface water, 29% is net retained and/or lost –note that t_r=6.6 days. Oostra (1996) calculated a net retention and/or loss percentage for N of around 35%. If C_{seep} would be decreased to 1 mg l^{-1} N, the calculated N-loads would be 10% higher as the N-loads were pumped out. After this adjustment, the total-N calculated load to the surface water system would get close to matching the N-loads that were pumped out.

The absolute average level of the regional model calculations on the P-load is a factor of about 1.2 higher as compared to field data. The timing is also different; the calculated results are showing more short-term fluctuations, but they generally follow the trend in the outlet data. The reasons for the observed differences are

- inaccurately calculated total-P loads at the outlet of the HV regional surface water system,
- underestimation of sorption of P in soils and local-scale surface water in sub-regions,
- an overestimation of C_{seep} for total-P, and/or
- net P-retention within the surface water system itself.

Foppen and Griffioen (1995), Hetterschijt et al. (1995), Hetterschijt et al. (1997), and De Louw et al. (1997) reported on phosphate transport from deep groundwater to the surface water in several Dutch polder areas. They found P-retention during the upward transport of seepage water. The P-sorption to the solid phase of the soils and P-retention
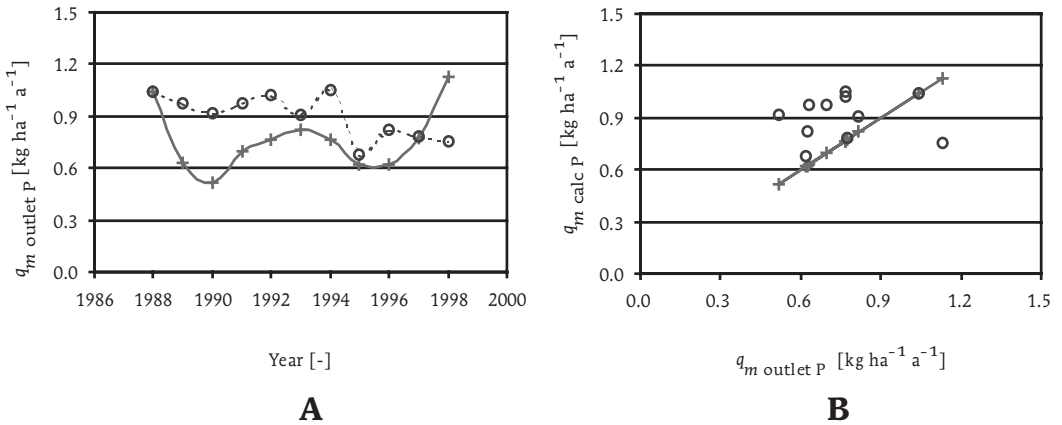
Fig. VI.2.5
Flevoland polder, HA region. Total-P loads discharged by pumping-stations at outlet $q_{m\ outlet\ P}$ (+) versus calculated total-P loads $q_{m\ calc\ P}$ (o) to HV regional surface water system for 1988-1998 period. A: $q_{m\ outlet\ P}$ and $q_{m\ calc\ P}$ versus time. B: $q_{m\ outlet\ P}$ versus $q_{m\ calc\ P}$.

in the local-scale surface water within the sub-regions is calculated at 4-7 kg ha^{-1} a^{-1} P for agricultural sub-regions. These numbers originate from the assumption that for soils with GTC VI, 99% of the P-surplus for the soil surface balance is assumed to adsorb to the solid phase. Increasing the percentage to 100% leads to a decrease of the calculated P-load from 3.7 to 2.6 kg ha^{-1} a^{-1} P. C_{seep} for total-P was already decreased to 0.15 mg l^{-1} P as previously stated. A further decrease of the seepage water total-P concentration to 0.12 mg l^{-1} leads to a match with calculated P-loads with P-loads pumped out. It can be concluded that net P-retention occurs in the HA region, roughly between 0.1 and 0.2 kg ha^{-1} a^{-1} P in the channel bottom sediment present in the HA regional surface water system. This surface-water-system is the most likely compartment for P to accumulate.

Regional approach and experimental site - To compare the agricultural data and nutrient balances of the Flevoland experimental site (Section IV.5), the average soil-system-balance for total-N and total-P for arable land on clay with GTC VI of sub-region 2 will be presented for the data period 1988 through 1998. Results are shown in Table VI.2.4. The region-average agricultural data show more intensively-used arable land with respect to nutrient applications. On the contrary, the losses of nutrients by drainage are higher at the experimental site. Note that where the losses by drainage are concerned, the site-specific data were independently calculated solute loads of drainage water. The nutrient losses by drainage as calculated by the regional approach originated from balance sheets and a travel time distribution of drainage water.

Table VI.2.4
Flevoland polder, HA region. Soil system balance for arable land on clay soil with
GTC VI of sub-region 2. Crop rotation 1:3 i.e., sugar beets, winter wheat, and potatoes.
Annual average data. *No contribution by seepage.

Balance term	Regional approach, 1988–1999		Experimental site, 1989–1993	
	N	P	N	P
	[kg ha^{-1} a^{-1}]	[kg ha^{-1} a^{-1}]	[kg ha^{-1} a^{-1}]	[kg ha^{-1} a^{-1}]
Atmospheric deposition	26	1	30	1
Fertilizer	144	29	154	36
Manure	106	26	87	21
Mineralization	30	2	0	0
Diffusion	2	< 0.1	0	0
Denitrification	-80	-	-50	-
Volatilization	-14	-	-11	-
Sorption	-	-27	-	-24
Removed by harvest	-189	-30	-164	-32
Balance surplus	25	1	46	2
Losses by drainage*	20-25	1.0-1.5	60-70	0.2-0.5

The data shown in Table VI.2.4 are comparable to the site-specific data of the farm.
Fertilizer application rates used in the regional model are smaller, and manure
application rates are higher in comparison to the experimental site situation.
The soil-surface-balance surplus is 25 kg ha^{-1} a^{-1} N and 1 kg ha^{-1} a^{-1} P for the
sub-region, whereas the site-specific data showed surpluses of 46 kg ha^{-1} a^{-1} N and
2 kg ha^{-1} a^{-1} P. The higher N-surpluses at the site led to higher N-losses by drainage.
P-losses by drainage are lower and show the opposite phenomenon. If the N-losses by
drainage are included in the mass balances, the site-specific mass balances show a deficit.
To explain this deficit, either a larger or an extra nutrient source should be found, or the
data provided for by the farmer were not completely correct. Other reasons are that at
the experimental site:

– non-equilibrium conditions as far as soil-chemical processes occurred, and
– event-wise preferential transport of water and solutes took place, increasing the
  risk of solute losses by drainage.

3 Conclusions

It is concluded that the regional approach for the Hoge Afdeling (HA) drainage area of the Flevoland polder area yielded good results on annual water balances. Both the draining rainfall excess and the groundwater seepage had an equal part in the water balance for the total region. Average groundwater seepage rates varied spatially. It appeared that the annual seepage rate, which was taken here as a constant value, also varied from year to year. Wet years had larger seepage rates than average, dry years, which showed smaller rates.

The sources of Cl^-, total-N, and total-P in the Hoge Vaart (HV) main channel were the atmosphere, point sources, groundwater seepage, and drainage. *Seepage water was the largest Cl-source* (86%), followed by drainage (13%). *Drainage water was the largest N-source* (76%), followed by seepage (19%). For phosphorus, point sources such as the effluent of wastewater treatment plants contributed to an average of 30% to the total P-load to the HV main channel until 1994-1995. Currently, the relative contribution of point sources to the total P-load has decreased to less than 2%. *Seepage water relatively contributes four times as much to the total P-load as compared to drainage water.*

The regional average travel time distribution showed fractions f_1 to f_3 equal to 0.41, 0.19, and 0.11. This distribution resulted in a timing of Cl^- and total-N loads to the HV main channel i.e., regional surface water that was not always correct. Part of the deviations in timing was due to the availability and quality of field data on surface water quality. The P-loads to the HV regional surface water were not correctly timed due to temporal variation of the seepage rate.

The calculated solute loads to the regional surface water of the Hoge Afdeling region were 1625 kg ha^{-1} a^{-1} Cl^-, 45 kg ha^{-1} a^{-1} N, and 0.9 kg ha^{-1} a^{-1} P. The average N-load was a factor 1.3 larger in comparison to the N-load measured at the outlet of the region, mainly due to retention and degradation processes. The absolute level of the P-load to the regional surface water was larger than the P-load at the outlet by a factor of 1.2 due to retention processes in and around the regional surface water system itself. Hence, retention and degradation processes in and around the regional surface water system itself were important factors in the N and P-budget of the surface water.

To make accurate estimates of solute loads from field data, analyses clarified the importance of well-designed, water quality monitoring programs. These programs should not only aim at an appropriate description of the surface water quality, but they should also provide good estimates of solute loads leaving the area.

VII

APPLICATION OF REGIONAL APPROACH TO HUPSEL BROOK BASIN

1 Description of Hupsel brook basin

General - The 650 ha basin of the Hupsel brook is located in the eastern sand district of the Netherlands, mainly east of the line between the centers of Groenlo and Eibergen. The basin is unique in the country in a way that it is hydrologically isolated from the surrounding area. The geographical and (geo)hydrological situation is positioned so that the basin can be seen as a large lysimeter, an advantage for studying hydrological characteristics and response of sandy areas. Water only enters the area by rainfall and leaves it only by evapotranspiration and brook discharge, which occurs by passing the H-flume 10A weir at the outlet of the catchment. Therefore, the basin has been used earlier for studies on evapotranspiration (Stricker, 1981) and to verify hydrological models, e.g., reported by Ruygh et al. (1990) or Querner (1993).

The soils in the basin are mainly sandy, but old clay layers and boulder clay appear locally at shallow depths (Wösten et al., 1983). Grassland covers about 70% of the land area, and the next largest crop is corn, which covers 20% of the land area. The Pleistocene phreatic aquifer is 1 to 10 m deep, overlying an impermeable clay layer of Miocene age origin that is greater than 30 m thick (Wösten et al., 1983). The catchment is extensively drained by subsurface and ditch drains. The surface water system consists of the main watercourse of the Hupsel brook, which has seven branches. The total length of the watercourses is about 11 km (Fig. VII.1.1). The surface area of the surface water system is about 2.1 ha in the winter and 0.9 ha in the summer, in which some watercourses run dry. Four measurement structures are installed in the area designated as weirs 10A, 19, 22, and 23, and another seventeen fixed weirs were installed to bridge brook bottom elevations and ground surface level differences and to enhance surface water storage. The position of the Hupsel brook region is special in that the travel time of drainage water is relatively small compared to the travel time of drainage water from other areas, making the Hupsel brook basin unique and very suitable for field studies on the impact of land use changes on the composition of shallow groundwater and of surface water.

Regional water balance - Werkman (1995) used the MOGROW model based on the work by Querner (1993). However, he found that the catchment is not completely
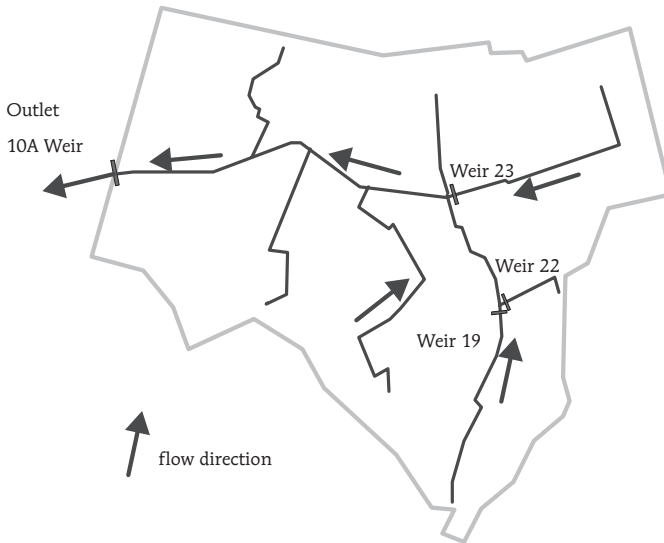
Fig. VII.1.1
Hupsel brook basin, HB region. Schematic outline of the 650 ha Hupsel brook and its branches, measurement weirs, and outlet at 10A Weir.

isolated hydrologically: leakage of water by groundwater flow across the western border may lead to a water loss of about 35 mm a^{-1}. Van den Eertwegh and Meinardi (1999) studied the hydrologic years 1985 through 1993; the average annual water balance for this time period is shown in Table VII.1.1 with $Q_{\mathrm{irrig}} = 0$ and $Q_{\mathrm{sub\text{-}irrig}} = 0$. The ET_a value they found is somewhat high, and if the analysis of Werkman (1995) is taken into account, ET_a should be decreased to 480 mm a^{-1}. Given this number, the reduction of ET_p would become 50 mm a^{-1}, which seems too large. It is not proof that the basin is isolated completely, but the opposite is also hard to prove. Therefore, it is assumed here that the basin area is hydrologically isolated.

The discharge route of the rainfall surplus water can be divided into three components (Van den Eertwegh and Meinardi, 1999), (1) surficial discharge by overland flow, interflow, and trench discharge (2) shallow groundwater drainage by subsurface and open drains and (3) deep groundwater drainage by main water courses. Van den Eertwegh and Meinardi (1999) showed that in 1985-1993, 3-4% of the discharge at the catchment outlet was of surficial origin, 55-75% of shallow groundwater, and 20-40% of deep groundwater. It was estimated that 40% of the outlet discharge has a maximum travel time of one year. About 90% of all surplus rainfall water present in the catchment area left the basin within five years.

Table VII.1.1
Hupsel brook basin. Average water balance for hydrologic years 1985 – 1993.

Quantity	[mm a^{-1}]
P	843
ET_a	516
Q_{brook}	328

Sources of solutes - Neither towns, wastewater treatment plants, nor industry are located within the basin. Although some farms drain their wastewater to the surface water system, the area is very suitable to study the impact of diffuse sources of solutes on surface water quality, as long as the point sources are known. In 1972, an investigation by Kolenbrander and Van Dijk (1972) showed the eutrophication problem in this rural area. Water, salt, and nutrient budgets of the Hupsel brook catchment area for the 1985-1993 period are described in Van den Eertwegh and Meinardi (1999), showing that high nutrient loads leave the catchment. Surficial runoff was also specified as a separate source. Note, however, that this source is mainly from agricultural land and thus relates to agricultural practices. The drainage and surface water composition across the HB region is illustrated by Fig. VII.1.2, which shows the results of a sampling strategy in November 1996 that was performed by RIVM across the catchment area. Water samples were taken from the Hupsel brook and its branches, from subsurface drainage water, and from drainage water in shallow trenches. The average solute concentrations in all three types of sampling locations appeared to be the same. The subsurface drainage water shows the largest variation, followed by the trench water, and finally the Hupsel brook water, where all incoming fluxes are somewhat mixed.

Surface water composition - During April 1985 through March 1994 about 1900 water samples were taken from the brook water at the 10A weir outlet of the basin. The sampling program was mainly discharge-dependent. With the use of automated equipment a sample was taken every 1 mm of discharge, which is equivalent to 6500 m^3 of volume. From May 1987 through September 1988, water sampling equipment failure occurred, and a grab sample was taken only once a month. The calculated solute loads at the outlet for the hydrologic year 1987 are, therefore, unreliable. Table VII.1.2 shows calculated annual loads in terms of solute concentrations. Fig. VII.1.3 shows the annual water discharge rates versus the solute loads that left the area by the 10A weir during April 1985 through March 1994.
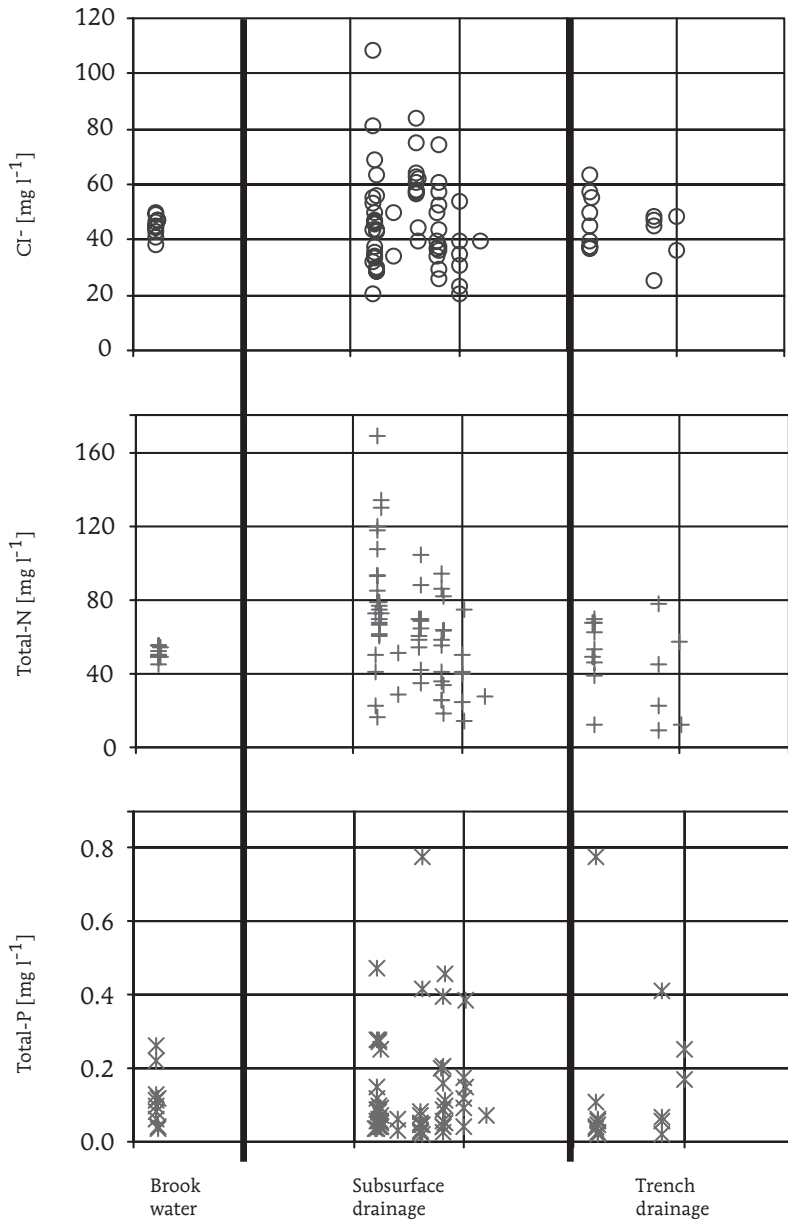
Fig. VII.1.2
Hupsel brook basin, HB region. Spatial variation of Cl- (**o**), total-N (**+**), and total-P concentrations (*****) in drainage and surface water of the Hupsel brook region, November 1996. Sampling and lab analyses were performed by RIVM. Water samples are of surface water of the Hupsel brook, of subsurface drainage water, and of open trench drainage water.

Table VII.1.2

Hupsel brook basin, HB region. Annual average calculated loads in terms of solute concentrations at the outlet of the Hupsel brook at 10A weir (Fig. VII.1.1), April 1985 through March 1994.

Parameter	Solute concentration $[\text{mg l}^{-1}]$	Solute mass flux $[\text{kg ha}^{-1} \text{ a}^{-1}]$
Cl	43	142
Total-N	34	112
Total-P	0.25	0.83

About 90-95% of total-N consisted of nitrate-N, and total-P consisted for 70% of organic P-components in the brook water. Cl and total-N concentrations were usually high during the beginning of the drainage season, around October-November, and showed a declining trend as the drainage season proceeded. The temporal variations of total-P were more erratic. The annual mass rates of salt and total-N that left the area showed an almost linear relationship with the annual drainage rates, thus indicating a full dilution process, except for years with a high rainfall surplus, so for those years relatively smaller mass fluxes were calculated. A possible explanation for this effect is that during wet years a relatively large part of the drainage water is of shallow, hence, young origin, and is more diluted than older water. A supplementary explanation considering total-N is that denitrification of nitrate is greater during wet years.

During the hydrologic years 1985-1993, the salt budget of the land area within the catchment was approximately in balance, although a slightly decreasing salt storage in the soil-groundwater system was observed due to manure export out of the area. The N-budget of the land area still showed net accumulation of N in the soil, although the accumulation itself was declining. The P-budget also showed a sustained surplus, Consequently, P-sorption to the solid phase was likely to continue, and the P-front within the soil was expected to move further downward.
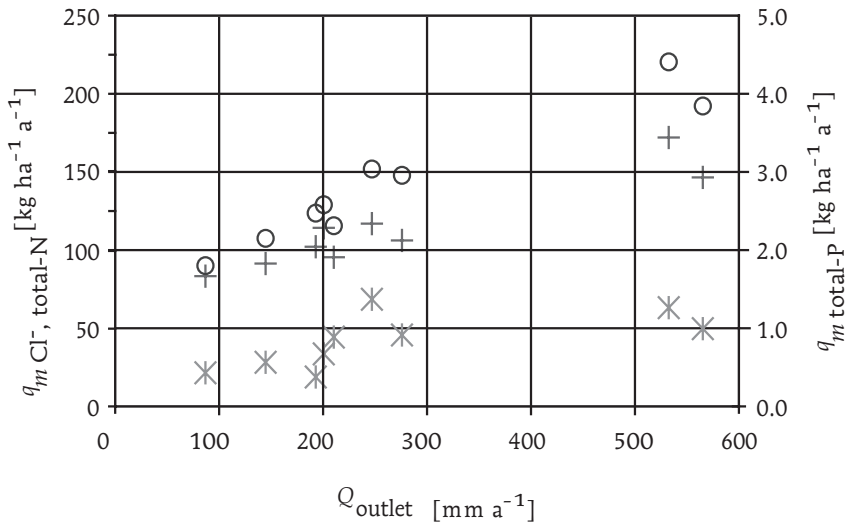
Fig. VII.1.3
Hupsel brook basin, HB region. Annual brook discharge rates at outlet Q_{outlet} and solute loads q_m for Cl^- (**o**), total-N (**+**), and total-P ($*$) as measured and calculated at 10A weir outlet of Hupsel brook, April 1985 through March 1994.

2   Results of regional model application

Model setup - In the regional modeling approach, information is required on soil type, drainage situation, and data related to land use, and data on mass rates related to soil chemical processes. The calculations began in April 1980 with estimated input data, but results are shown and judged for the period of April 1985 through March 1994. For the latter period, all relevant input data time series were available. At the outlet of the basin at the 10A weir, accurate calculated solute loads were available for the total period.

The HB region is divided into five sub-regions and one regional surface water system, constituting the Hupsel brook and its seven branches. The sub-regions consist of land area –in total 648.5 ha– including small-scale collection ditches. The regional surface water system has an area of 1.5 ha and an average volume of 7530 m^3. The subdivision into sub-regions was performed by looking at the depth of the sandy aquifer to the hydrological base i.e., the Miocene clay layer, the land use, and Groundwater Table Classes (GTC). The choice of the sub-regions reflects the overall characteristics of the basin area, which are not necessarily geographical sub-regions. Van den Eertwegh and Meinardi (1999) gave an overview of these factors. Table VII.2.1 gives an overview of the overall characteristics of the five sub-regions.

Table VII.2.1
Hupsel brook basin, HB region. Area and dominant soil type, GTC, and land use of sub-regions. *All sub-regions use station Hupsel for P and ET_r data. **Dominant.

Sub-region*	Area [ha]	Soil type**	GTC**	Land use**
1	130	Sand	V	Corn
2	190	Sand	IV	Grassland
3	50	Loam	III	Grassland
4	70	Sand	II	Rural area
5	208.5	Sand	V	Grassland

The solute concentrations in rainfall and the annual average of dry deposition rates are shown in Table VII.2.2. More information on model parameters, data on land use, and on mass balance terms related to soil-chemical processes is given in Appendix E.

Table VII.2.2
Hupsel brook basin, HB region. Average composition of rainfall and dry deposition numbers.

Parameter	Rainfall [mg l^{-1}]	Dry deposition [kg ha^{-1} a^{-1}]
Cl$^-$	2	0.5
Total-N	3	15
Total-P	0.125	0.1

Source: RIVM and KNMI (1989).

Regional-scale travel times - Each of the 5 sub-regions has its own specific travel time distribution of drainage water as shown in Table E.1. The overall annual regional travel time distribution can be calculated as a discharge-weighted average of f_τ originating from the sub-regions. The overall travel time distribution from the HB region shows

1985-1993 mean values for travel time fractions f_1 to f_3, respectively of 0.29, 0.18, and 0.12; *hence, 59% of the drainage water left the area within three years*. These numbers varied from year to year as a result of variable weather conditions. The standard deviation of the fraction f_2 and f_3 ranged from 0.01 to 0.03. The standard deviation of the fraction f_1 was 0.12. The weather conditions mainly influenced the youngest fraction and, consequentially, the oldest fractions ($\tau > 3$) as well.

Residence time in surface water - The calculated mean of annual residence time of water within the regional surface water system, $t_r = 1.6$ days for the 1985-1993 period, varying between 0.6-0.7 days during a wet year (e.g., 1987, 1993) to over three days during a dry year (e.g., 1989).

Calculated discharge - The calculated and measured annual discharge rates of the HB region at the 10A weir outlet are shown in Fig. VII.2.1. A strong agreement between calculated discharge at the outlet of the basin and by the regional model; the calculated drainage rates during dry and wet years show small differences with the measured drainage rates.

A   **B**
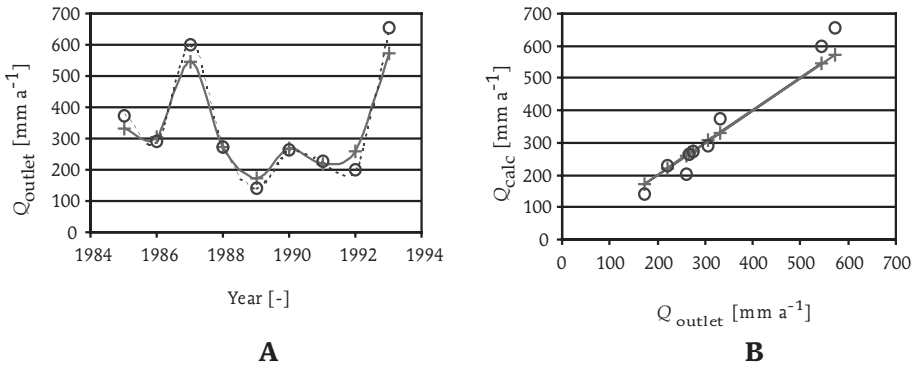
Fig. VII.2.1
Hupsel brook basin, HB region. Measured (+) and calculated discharge rates (o) at outlet of basin 10A weir for 1985-1993 period. A: discharge rates versus time. B: measured versus calculated discharge rates.

Calculated solute loads - The dissolved Cl^-, total-N, and total-P contents in the regional surface water have different sources. The relative contribution of each source to the total loads is important for the determination of measures to reduce solute losses to the surface water system and improve surface water quality. Based on the solute mass balance computed for the regional surface water system as shown in Section III.4 the contribution of each source to the total load to the surface water was calculated.

Table VII.2.3 shows the relative contribution of the sources indicated for all solutes as average fractions of the total load in the 1985-1993 period. For water and all solutes, the precipitation excess transformed into drainage water is the largest source. The main source of P is subsurface drainage water. Point sources and surficial flow components play some role in the total-P loads to the surface water. *This indicates that measures to improve surface water quality by emission reductions have to aim at both subsurface flow paths as well as surficial flow mechanisms.*

Table VII.2.3
Hupsel brook basin, HB region. Relative contribution of water and solute sources to regional surface water. Average percentages of the total load in the 1985-1993 period.

Source	Water [%]	Cl^- [%]	Total-N [%]	Total-P [%]
Atmosphere	<1	<1	<1	<1
Point sources	<1	<1	<1	6
Surficial runoff	3	<1	<1	10
Subsurface drainage	96	98	98	83

The solute loads calculated by the model are loads to the surface water system. They will be compared to calculated solute loads at the outlet of the catchment. The solute loads calculated at the outlet of the region and by the regional model are shown in Fig. VII.2.2 (Cl^-), in Fig. VII.2.3 (total-N), and in Fig. VII.2.4 (total-P).

The calculated Cl-loads to the surface water match the Cl-loads at the outlet very well. The average calculated load of 143 kg ha^{-1} a^{-1} approximately agrees with the measured load of 142 kg ha^{-1} a^{-1}. The temporal variation of the calculated Cl-loads is slightly larger. Note that the Cl-load at the outlet for 1987 was not reliable.

The calculated average total-N loads are 6 kg ha^{-1} a^{-1} higher compared to the average measured total-N load of 112 kg ha^{-1} a^{-1}, and the timing of the calculated total-N loads is correct. For 1987 and 1993 the total-N loads were overestimated by the regional approach. Note that the total-N load at the outlet of the basin for 1987 was not reliable. Although the residence time of water t_r in the Hupsel brook is limited to a few days at the most, some denitrification is likely to occur within the regional surface water. On the other hand, if the measured 1987 total-N load would have been corrected from 151 to
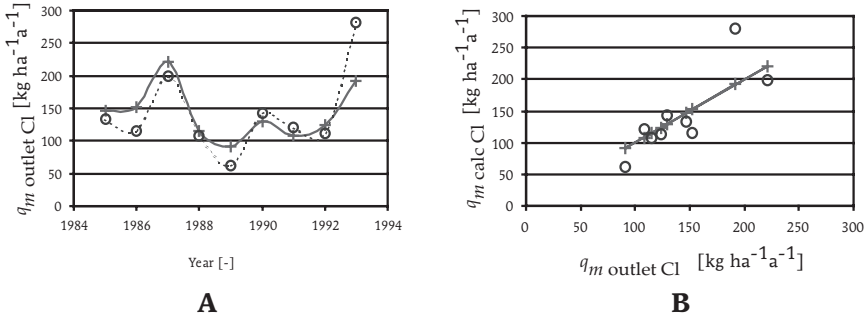
Fig. VII.2.2
Hupsel brook basin, HB region. Cl-loads discharged by 10A weir at outlet $q_{m \text{ outlet Cl}}$ (+) versus calculated Cl-loads $q_{m \text{ calc Cl}}$ (o) to regional surface water system for the 1985-1993 period. A: $q_{m \text{ outlet Cl}}$ and $q_{m \text{ calc Cl}}$ versus time. B: $q_{m \text{ outlet Cl}}$ versus $q_{m \text{ calc Cl}}$.
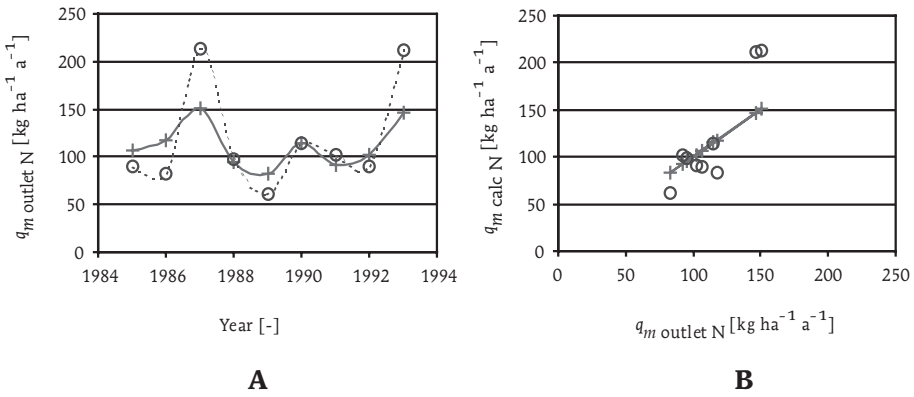
Fig. VII.2.3
Hupsel brook basin, HB region. Total-N loads discharged by 10A weir at outlet $q_{m \text{ outlet N}}$ (+) versus calculated total-N loads $q_{m \text{ calc N}}$ (o) to regional surface water system for the 1985-1993 period. A: $q_{m \text{ outlet N}}$ and $q_{m \text{ calc N}}$ versus time. B: $q_{m \text{ outlet N}}$ versus $q_{m \text{ calc N}}$.
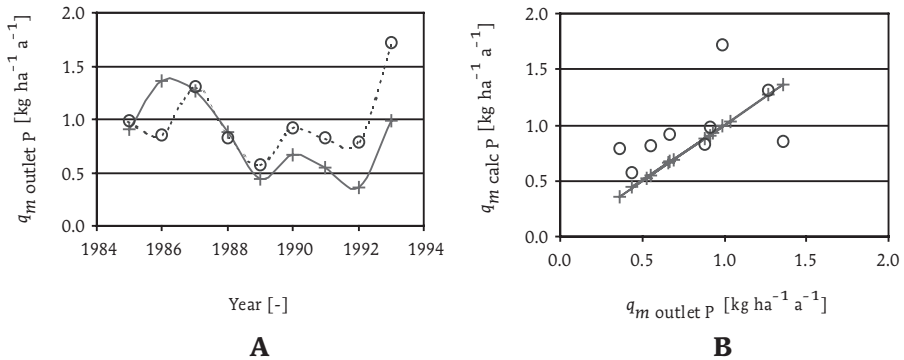
Fig. VII.2.4
Hupsel brook basin, HB region. Total-P loads discharged by 10A weir at outlet $q_{m\ \text{outlet P}}$ (+) versus calculated total-P loads $q_{m\ \text{calc P}}$ (o) to regional surface water system for the 1985-1993 period. A: $q_{m\ \text{outlet P}}$ and $q_{m\ \text{calc P}}$ versus time. B: $q_{m\ \text{outlet P}}$ versus $q_{m\ \text{calc P}}$.

220 kg ha^{-1} a^{-1} based on the model results, the annual average measured total-N load would be around 120 kg ha^{-1} a^{-1} i.e., quite close to the calculated average. A more important factor of influence is denitrification within the sub-regions i.e., the soils. The denitrification rates in the soil system are constant with time and estimated between 80 and 115 kg ha^{-1} a^{-1} N (Van den Eertwegh and Meinardi, 1999). Under wet circumstances, these rates might have been too small, leading to an overestimation of N-losses by drainage in wet years like 1987 and 1993.

The absolute level of the calculated P-load of 0.98 kg ha^{-1} a^{-1} is by a factor of about 1.2 higher in the estimation of the P-load as compared to the measured P-load. The timing of the calculated P-load is in general agreement with the overall measured values. Note that the total-P load at the outlet for 1987 was not reliable. The reason for the observed difference is probably a net P-retention within the surface water system itself. The P-sorption to the solid phase of the soils and P-retention in the local-scale surface water within the sub-regions is calculated at 40-45 kg ha^{-1} a^{-1} P for agricultural sub-regions. Van den Eertwegh and Meinardi (1999) found a value of 33 kg ha^{-1} a^{-1} P for the basin as a whole. A further increase of the net sorption within the sub-regions is unlikely. Apparently, net P-retention occurs in the regional surface water of the HB region, roughly 0.15 kg ha^{-1} a^{-1} P in the surface water bottom sediment present in the HB regional surface water system.

Regional approach and experimental site - To compare the agricultural data and nutrient balances of the Hupsel-Assink experimental site (Section V.5), the average soil system balance for total-N and total-P for grassland on sand with GTC V of sub-region 5 will be

presented; the results are shown in Table VII.2.4. The region-average agricultural data show more intensively used grassland with respect to nutrient applications. On the contrary, the losses of nutrients by drainage are higher at the experimental site. Note that where the losses by drainage are concerned, the site-specific data were independently calculated solute loads of drainage water, based on field data. The solute losses by drainage in the HB region model were calculated solute losses by drainage through the use of balance sheets and with a travel time distribution.

Table VII.2.4
Hupsel brook basin, HB region. Soil system balance for grassland on sand with GTC V of sub-region 5. Annual average data. *Differences originate from the composition of manure at the average basin scale as compared to of manure from one single farm.

| Balance term | Regional model, 1985–1994 | | Experimental site, 1990–1993 | |
	N $[kg\ ha^{-1}\ a^{-1}]$	P $[kg\ ha^{-1}\ a^{-1}]$	N $[kg\ ha^{-1}\ a^{-1}]$	P $[kg\ ha^{-1}\ a^{-1}]$
Atmospheric deposition	40	1	36	1
Fertilizer	256	8	150	0
Manure*	342	65	283	90
Mineralization	10	2	0	0
Diffusion	1	<0.1	1	<0.1
Denitrification	-115	-	-50	-
Volatilization	-36	-	-31	-
Sorption	-	-39	-	-57
Removed by harvest	-350	-35	-297	-33
Balance surplus	148	2	92	1
Losses by drainage	145-150	1.0-1.5	140-160	1.0-1.5

The data shown in Table VII.2.4 for P are comparable to the site-specific data of the farm. Fertilizer application rates are smaller at the site, compensated by higher manure application rates. The soil surface balance surplus is 288 $kg\ ha^{-1}\ a^{-1}$ N and 38 $kg\ ha^{-1}\ a^{-1}$ P for the sub-region, whereas the site-specific data showed surpluses of 172 $kg\ ha^{-1}\ a^{-1}$ N and 58 $kg\ ha^{-1}\ a^{-1}$ P. The lower N-surpluses at the site lead to lower N-losses by drainage. P-losses by drainage for both systems are about equal.

The differences between the systems occur in the N-balance, not in the P-balance, which is caused by two reasons: 1) the experimental site is less intensively used as far as N applications are concerned, and 2) differences that occur in the composition of manure, where a different N:P-ratio can be seen.

3 Conclusions

It is concluded that the regional approach yielded good results on annual water balances for the Hupsel brook basin (HB region). For the hydrologic years 1985-1993, surface runoff amounted to 1% to 5% of the water entering the Hupsel brook where 94% to 98% entered the brook by subsurface drainage.

The sources of Cl^-, total-N, and total-P in the Hupsel brook were the atmosphere, point sources, surface runoff, and drainage. On the average drainage water was the largest Cl-source (98%), the largest N-source (98%), and the largest P-source (83%). For phosphorus, point sources like the effluent of untreated wastewater contributed 6% to the total P-load to the brook. Surface runoff contributed 10% to the total-P load of the brook. The relative contribution of point sources and surface runoff to the total-P load decreased with time from 17% to 12%.

The regional average travel time distribution showed fractions f_1 to f_3 equal to 0.29, 0.18, and 0.12. This distribution resulted in a correct timing of Cl^- and total-N loads to the Hupsel brook i.e., regional surface water. The P-loads to the regional surface water were timed less correctly due to sorption processes.

The calculated average solute loads to the Hupsel brook were 143 kg ha^{-1} a^{-1} Cl^-, 118 kg ha^{-1} a^{-1} N, and 0.98 kg ha^{-1} a^{-1} P. The average N-load to the brook water was larger by a factor of 1.1 as compared to the N-loads measured at the outlet of the catchment, mainly due to degradation processes. The denitrification of NO_3-N in the regional surface water system itself was not significant. The absolute level of the P-load to the regional surface water was larger than the P-load at the outlet by a factor of 1.2 due to retention processes in and around the regional surface water system itself from source to outlet. Hence, P-retention in and around the brook surface water system itself was an important factor in the P-budget of the surface water.

To accurately estimate the solute loads from field data, analyses clarified that it remains important to have well-designed water quality monitoring programs. These programs should not only aim at an appropriate description of the surface water quality, but also provide good estimates of solute loads leaving the area.

Due to the absence of other major sources of salt and nutrients as compared to agriculture, the basin was highly suitable for providing regional-scale field data on the

relationship between agricultural nutrient budgets and drainage losses of nutrients to the regional surface water system. Based on the average travel time distribution of drainage water, the possible effects of significantly different nutrient application rates should be visible in surface water quality data and solute loads at the 10A weir outlet within three years.

SUMMARY AND CONCLUSIONS

The main sources of nutrients in surface water in the Netherlands are losses through point sources from industry and from wastewater treatment plants, and through non-point sources like groundwater seepage, losses by drainage from agricultural land, and atmospheric deposition. Policy measures have been undertaken since the 1970s that have reduced the nutrient loads to surface waters. The effluent concentrations in wastewater from industries and from wastewater treatment plants have decreased significantly. Emission reductions from other point sources of nutrients have also been realized. While the emissions of nutrients from point sources have decreased considerably, those from non-point sources have not; as a result, the relative contribution of non-point sources has steadily increased. Surface water quality often does not meet the specific reference levels, and to meet these levels in the future, nutrient loads from non-point sources need to be further reduced. In an attempt to reduce the non-point sources, mandatory nutrient management measures have been issued for farmers in the Netherlands.

This research

Nutrients applied to the land surface find their way as solutes to groundwater and surface water. The flow of water in the soil and in surface water systems is the main transport mechanism for nutrients. Travel routes of excess rainfall water, flow velocities, and the travel time of drainage water are the key factors to understand and interpret solute loads of drainage water. In this thesis, the *travel time of drainage water* is defined as the time that it takes for net precipitation to discharge into the surface water from the moment it reaches the land surface combined with subsequent subsurface flow.

The objectives used for this study were as follows:

1. To distinguish and quantify different discharge components of the precipitation excess, drained by *local-scale* drainage systems such as subsurface tile drains and collection ditches.
2. To present a procedure to estimate the amount of nutrients transported from the soil surface to surface-water systems at the *regional scale*, which is based on water and nutrient budgets. This procedure must be able to account for differences in soil

types, hydrology, and soil surface loads of nutrients, and it should be applicable to different hydrological regions in the Netherlands.

The research objectives have been achieved by these methods:

- collecting and analyzing field data on hydrology and nutrient budgets for specific field situations, and
- presenting the travel time distribution of drainage water for different experimental sites and regions across the Netherlands.

Theoretical framework

Steady-state approach travel time - The *Ernst-Bruggeman approach* (Ernst, 1973; Bruggeman, 1999) to estimate the travel time distribution of drainage water is based on the assumptions of steady-state, saturated flow conditions and Piston-type solute transport on an annual basis. This approach can be used in situations with subsurface drains and regional-scale groundwater recharge or seepage. It is not applicable to situations where the local-scale depth of the groundwater flow system is large compared to the drain distance and/or when the unsaturated zone plays an important role in the flow process.

Travel time under transient flow conditions - The *dual-porosity flow and transport concept* to model water flow and solute transport in variably saturated and structured flow media (Gerke and Van Genuchten, 1993a, 1993b; Nieber and Misra, 1995) is a useful instrument to support plot-scale hydrological research and analysis of travel times of drainage water. Two flow domains are defined in the dual-porosity medium: the matrix domain and the macropore domain respectively. In both domains, flow and transport interact through pressure head and solute concentration gradients that determine the exchange of mass between the domains. The governing equation for flow in both domains is based on the Richards equation, and while this equation is suitable to predict the flow in the matrix domain, it offers some challenges to model the flow in the macropore domain. When using a numerical method to solve the equation, the dominance of gravity in water flow in this domain increases convergence difficulties. Although some difficulties arose with the dual-porosity code, it ran efficiently. Convergence problems were encountered when rain fell on initially dry soil, which were reduced by the implementation of a mixed implicit-explicit method to solve the coupled equations. The method was implemented by using an automatic switch, which is dependent on the nodal degree of saturation to determine whether an implicit or an explicit method is used for a particular node. Determining the appropriate switch point to use for a particular field site was discovered by trial and error. Retardation, as a result

of sorption processes was accounted for by the code, but other soil-chemical processes were not. The main reason to omit the soil-chemical processes in transient and field-scale modeling is that the focus of this thesis is on the *physical transport process* and on the effect of *travel times of drainage water* on drainage water composition. The information on the physical transport process, as generated by the numerical models, has been used to construct annual solute budgets at both the field scale and the regional scale.

Regional approach - The regional approach determines annual budgets for water, salt (Cl^-), nitrogen (total-N), and phosphorus (total-P) for the land area and regional surface water, as well as for solute loads to the regional surface water. The approach assumes equilibrium conditions, and it neglects possible variations in soil-physical and soil-chemical conditions that affect the budgets for water and solutes. A region consists of a number of sub-regions, which represent the land and small-scale surface water area, and of a regional surface water system. Each sub-region has a dominant land use, soil type, groundwater table regime, and specified travel time distribution of drainage water. This distribution, initially based on the Ernst-Bruggeman approach, may vary from year to year, depending on annual averages of weather conditions. Manual corrections of the travel time fractions can be applied, e.g., after analysis of field data or more detailed modeling. All drainage water from the sub-regions enters the regional surface water system. If present, groundwater seepage is assumed to directly enter the regional surface water.

For model input, point sources need to be provided. In addition, the approach needs agricultural data on annual fertilizer and manure applications, as well as on long-term averages of solute removal by the harvest of crops. As far as chemical processes and their influences on solute budgets and solute transport are concerned, denitrification of NO_3-N, both by bacteria and by oxidation of pyrite, and P-sorption to the solid phase is of major importance. These processes are incorporated in the nutrient budget and loads calculations by the regional approach. The regional approach keeps track of the water and solute budgets as well as of the residence time of water and solutes in the regional surface water.

Field-scale experiments

Experimental site Flevoland - The experimental site Flevoland is located in the central marine clay area of the Netherlands in the Flevoland polder area. The clay soil in this area was structured, and the land use at the site was arable land. The experimental site consisted of two sequentially-monitored measurement plots. Field observations were performed at Plot 1 from April 1992 through March 1993, and at Plot 2 from April 1993 through June 1994. Surface runoff was not observed at the site, but ponding did occur.

Excess rainfall left the two plots not only by tile drainage as measured, but also by direct flow to the collection ditch and to the regional surface water system. The field water balances were calculated from April 1992 through March 1993 for Plot 1, and from April 1993 through March 1994 for Plot 2. The field water balances yielded an unmeasured drainage term of 48% and 16% of total drainage from Plot 1 and from Plot 2, respectively. For the collection ditch catchment, these percentages amounted to 48% in 1992-1993 and 59% in 1993-1994. The division of total drainage into several discharge components found its origin mainly in the soil profile. A tracer experiment yielded a tracer recovery after one year of application of 24% and 56% for Plot 1 and Plot 2, respectively. Hydrology was found to be different at each plot.

The Ernst-Bruggeman steady-state approach was initially used to estimate the travel time of drainage water at the site. The dual-porosity approach for water flow, and solute transport was used to set up plot-scale models and to analyze the travel time of drainage water under transient flow conditions. Calculated water balances by the simulation models matched the field water balances well. *The models could reproduce measured, as well as unmeasured, drainage terms by introducing appropriate soil profiles and boundary condition types.* Not only did flow and transport within the matrix and macropore domain appear to be important in judging the solute transport behavior of plots, but the mass exchange between the two flow domains also appeared to be a factor. Deviations occurred between the calculated travel times by the steady-state and transient modeling approaches, and these deviations grew larger with dry and more wet weather conditions. At the experimental site, numerical transient modeling showed better results as compared to the steady-state approach, however, the steady-state approach yielded reasonable results. The long-term average travel time distribution of drainage water at the Flevoland experimental site is shown in Table S.1. *The travel time fractions shown in Table S.1 indicate that any significant change in management practices i.e., nutrient applications at the soil surface will be effective toward influencing drainage water quality for 70-75% within three years.*

At the Flevoland experimental site, potatoes were grown at the two measurement plots, where a 1:3 crop rotation consisted of potatoes, sugar beets, and winter wheat. Fertilizer was applied to every crop, and manure was applied only after the harvest of winter wheat. In autumn, the applications of manure were not meant to fertilize winter wheat; they were meant to fertilize potatoes, which are grown in the year following the harvest of the wheat. The surpluses of the N and P balances and nutrient loads of drainage were linked by using the travel time distribution of drainage water. *The measured N-loads of drainage were 55 to 86 kg ha^{-1} a^{-1} N.* Calculated N-loads loads did partly not match these field data well. They underestimated the measured loads by 10% and 49% for Plot 1 and Plot 2, respectively, and by 67% and 16% for the Ditch during the first and second

Table S.1
Flevoland experimental site. Long-term annual average of fractions of travel of time distribution of drainage water.

Fraction	Age-class of travel time [a]	f_τ [-] Plot 1	Plot 2	Ditch
f_1	$t \leq 1$	0.27	0.34	0.30
f_2	$1 < t \leq 2$	0.26	0.28	0.28
f_3	$2 < t \leq 3$	0.15	0.13	0.14
Total	$t \leq 3$	0.68	0.75	0.72

measurement year. Possible reasons for this are non-uniform flow and transport processes, which would result in N-losses that did not fit into the annual average of balance methods. In addition, field data on manure applications were most likely not accurate enough. Due to P-adsorption to the solid phase, calculated P-loads exceeded the measured loads by a factor of 10. *The measured P-load of drainage was about 0.2-0.5 kg ha^{-1} a^{-1}, and the annual P-mass adsorbed 20-40 kg ha^{-1} a^{-1}*, which enriched the soil system. The soils at the Flevoland experimental site showed an enhanced leaching risk due to the presence of soil structure.

Experimental site Hupsel-Assink - The experimental site Hupsel-Assink was located in the eastern sand district of the Netherlands within the Hupsel brook basin; its land use was permanent grassland. The field experiment ran from the period of November 1992 through March 1994, and it consisted of one plot. Rainfall observations were best performed with a rain gauge installed at the soil surface. Surface runoff was not observed during the measurement period, but occasionally ponding occurred. Excess rainfall water left the Plot not only by tile drainage as measured, but also by direct drainage to the collection ditch and to the Hupsel brook i.e., the regional surface-water system. The field water balance of the Plot for the period of January 1, 1993 through March 19, 1994 yielded an unmeasured drainage term of 31% of total drainage. The characteristics of the soil profile, and the local drainage situation that included an increasingly clogged subsurface drain, contributed to the production of this large unmeasured drainage component.

The Ernst-Bruggeman approach and a numerical 2D single-porosity model were used to estimate the travel time of drainage water under steady-state and transient flow situations, respectively. Calculated water balances were in good agreement with the field water balances. The numerical model was able to reproduce measured, as well as unmeasured, drainage terms, after the introduction of appropriate boundary condition types. The temporal variation of drainage rates was well timed, but some measured drainage events were missed. During the summer of 1993, preferential flow events generated drainage, and the resulting drainage from this flow phenomenon was also observed at the scale of the Hupsel brook basin. Unstable flow in the unsaturated zone, being a possible explanation of the observed drainage event, was not conceptually accounted for by the model used. The travel time distribution fractions of drainage, as calculated with the steady-state approach according to Ernst-Bruggeman, were confirmed by the numerical modeling of water flow and solute transport under transient conditions (Table S.2). *The travel time distribution of drainage water as shown in Table S.2 indicates that any significant change in management practices i.e., nutrient applications at the soil surface, will be 66% effective at influencing the composition of drainage water within three years.*

Table S.2
Hupsel-Assink experimental site. Long-term annual average of fractions of travel time distribution of drainage water.

Fraction	Age-class of travel time [a]	f_τ [-]
f_1	$t \leq 1$	0.29
f_2	$1 < t \leq 2$	0.25
f_3	$2 < t \leq 3$	0.12
Total	$t \leq 3$	0.66

Fertilizer and manure were applied at the grassland plot several times per year. The surpluses of the soil system Cl^- and N balances and loads of drainage were well linked by using the travel time distribution of drainage water. *The field data showed losses by drainage of 160 kg ha^{-1} a^{-1}N and 270 kg ha^{-1} a^{-1}Cl$^-$.* The calculated chloride and nitrogen loads matched the field data. Calculated P-loads exceeded the measured loads by

a factor of 8, due to P-adsorption to the solid phase and unreliable field data. *The P-load of drainage water was less than 1% of the P-surplus on the average of annual agricultural soil-surface balance*. The annual P-adsorption rate, however, was estimated at 55-60 kg ha^{-1} a^{-1}.

General remarks on field-scale experiments - The extensive field-scale observations and the thorough analysis of the field data from the experimental sites proved to be very beneficial. Field data were not only collected on hydrology and nutrient losses by drainage, but the experiments also provided insight on local hydrological situations. *Of major importance was the linking of nutrient budget surpluses to solute loads in drainage water*. Part of the drainage water discharge was measured directly at the plot/field outlet, while the remainder left the area by other pathways and was estimated based on overall water balances. A serious underestimation in solute loss by drainage would have been made if this remaining drainage water had been neglected in the analysis.

If field experiments on solute losses by drainage are setup, either 'historic' data on agricultural practices need to be available, or a certain time period of measurements needs to be taken into account, primarily for several years. The reason for this is that the travel time of drainage water is needed to make correct interpretations of the concentrations found in the drainage water. *The results showed that in the case of the Flevoland and Hupsel-Assink experimental sites, a 'historic' data period of three to five years was sufficient to interpret the drainage water composition*. It also appeared important to have well-designed water quality monitoring programs in order to calculate accurate solute loads from field data.

Application of regional approach

Regional approach, Hoge Afdeling region - The Hoge Afdeling (HA region) of the Flevoland polder area in the central part of the Netherlands is a man-made, 40 250 ha polder area with controlled surface water levels. Excess rainfall water drains freely into ditches, and flows from ditches into channels. The channels discharge their water freely into the Hoge Vaart main channel, defined as the regional surface water system. The regional surface water is pumped out by pumping-stations at the outlet of the main channel. Groundwater seepage is present across the whole area. The calculated regional-scale travel time distribution for the HA region is shown in Table S.3.

The f_1 fraction for the HA region resulted from a *preferential flow component in the unsaturated zone under wet conditions* and small depths of local groundwater flow systems. The mean residence time of water in the HA regional surface water system was six to

Table S.3
Flevoland polder, Hoge Afdeling (HA region). Calculated annual average of fractions of regional-scale travel time distribution of drainage water for the period of April 1988 through March 1999.

Fraction	Age class of travel time [a]	f_τ [-]
f_1	$t \leq 1$	0.41
f_2	$1 < t \leq 2$	0.19
f_3	$2 < t \leq 3$	0.11
Total	$t \leq 3$	0.71

seven days. The annual average of water balance and nutrient loads to the surface water are presented in Table S.4.

For the HA region, the travel time distribution resulted in a reasonable prediction of the timing of Cl- and total-N loads to the regional surface water, whereas the timing of the P-loads was not accurate. The main reason for the inaccuracies in the calculated P-load was most likely the occurrence of sorption processes in the regional surface water system, which was not accounted for in the regional approach, and P-retention during the process of upward groundwater seepage from the aquifer to the surface water system. *The absolute levels of total-N and total-P loads to the regional surface water were 29% and 18% larger, respectively, compared to the solute loads at the outlet of the channel, due to retention and degradation in/around the surface-water system.*

Regional approach, Hupsel brook region - The Hupsel brook basin (HB region) is the 650 ha catchment of the Hupsel brook, located near the Dutch-German border in the east of the country. The soils in the region are sandy and of Pleistocene origin. Grassland and corn cultivation dominate land use in the region. A shallow phreatic aquifer of 1-10 m deep lies on top of a 30-40 m layer of impermeable clay. All land drains freely into the brook and its branches, and the brook discharge is measured continuously at the outlet of the basin. The calculated regional-scale travel time distribution for the region is shown in Table S.5. The mean residence time of water in the regional surface water was

Table S.4
Flevoland polder, Hoge Afdeling (HA region). Calculated average of water balance of the land area [mm a^{-1}] and nutrient loads to the regional surface water [kg ha^{-1} a^{-1}]. Data is for the hydrologic years of April 1988 through March 1999. *At pumping stations.

Flevoland polder, Hoge Afdeling (HA region), 1988-1999		
Water balance	**[mm a^{-1}]**	
	measured	calculated
P	816	-
ET_a	489	465
Q_{seep}	372	-
Q_{outlet}	699	711
Solute load to regional surface water	**[kg ha^{-1} a^{-1}]**	
	measured*	calculated
$q_{m,Cl}$	1592	1625
$q_{m,total\text{-}N}$	35	45
$q_{m,total\text{-}P}$	0.76	0.90

one to two days. The annual average of the water balance and nutrient loads to the surface water are presented in Table S.6.

Application of the regional approach to the HB region yielded good results on annual water balances. High annual drainage rates were slightly overestimated, and low rates were underestimated. *The travel time distribution given in Table S.5 resulted in correct timing of Cl$^-$ and total-N loads to the regional surface water*; in addition, the absolute level of these solute loads was well calculated. Due to retention in and around the surface-water system, the absolute level of the total-N and total-P load to the regional surface water was 5% and 18% larger respectively than the solute load at the outlet of the basin.

General remarks on regional approach - It appeared important to have *well-designed water quality monitoring programs* in order to calculate accurate solute loads from field data. To successfully implement measures in order to reduce solute loads to surface water, it is

Table S.5
Hupsel brook basin (HB region). Calculated annual average of fractions of regional-scale travel time distribution of drainage water for the period of April 1985 through March 1994.

Fraction	Age class of travel time [a]	f_τ [-]
f_1	$t \leq 1$	0.29
f_2	$1 < t \leq 2$	0.18
f_3	$2 < t \leq 3$	0.12
Total	$t \leq 3$	0.59

Table S.6
Hupsel brook basin (HB region). Calculated average of water balance [mm a^{-1}] of the land area and nutrient loads to the regional surface water [kg ha^{-1} a^{-1}]. Data is for hydrologic years in the period of April 1985 through March 1994.

Hupsel brook basin (HB region), 1985-1994

Water balance	[mm a^{-1}]	
	measured	calculated
P	843	-
ET_a	516	510
Q_{brook}	328	336

Solute load to regional surface water	[kg ha^{-1} a^{-1}]	
	measured	calculated
$q_{m,Cl}$	142	143
$q_{m,total-N}$	112	118
$q_{m,total-P}$	0.83	0.98

necessary to know the relative contribution of different sources. Table S.7 shows the relative contribution of the two main sources of chloride, of total-N and of total-P, to the total water flow and nutrient loads to the regional water system in both regions modeled.

Table S.7
Flevoland polder, Hoge Afdeling (HA region), and Hupsel brook basin (HB region). Relative contribution fractions of the total drainage and solute load to the regional surface water of the main sources of water and its solutes. Calculated average of fractions are from the source to the total drainage and total loads. Data for the HA region is for the period of April 1988 through March 1999; data for the HB region is for the period of April 1985 through March 1994.

Parameter	HA region, 1988-1999		HB region, 1985-1994	
	Groundwater seepage	Agriculture drainage	Point sources	Agriculture drainage
Water	0.56	0.43	<0.01	0.96
Chloride	0.86	0.13	<0.01	0.98
Total-N	0.19	0.76	<0.01	0.98
Total-P	0.55	0.14	0.06	0.83

The major point sources in the HA region, the wastewater treatment plants, have been successfully reconstructed and solute loads from them have been reduced. *At present, in the Hoge Afdeling region, groundwater seepage dominates Cl-loads and P-loads to the regional surface water, while agricultural sources dominate the N-loads.* Measures used to reduce the solute loads to surface water need to concurrently focus on water management practices to reduce the seepage water influence and on agricultural practices. To monitor any effect of a possible reduction of one of the two sources, the other main source also has to be monitored. In the HB region, agricultural sources dominate all solute loads due to the absence of other major sources, which makes the basin appropriate for monitoring changes in agricultural practices and their relatively fast response on surface water composition. *The Hupsel brook basin is very suitable to providing regional-scale field data on the relationship between agricultural nutrient budgets and drainage losses of nutrients to the regional surface-water system.* Based on the average of the travel time distribution of

drainage water, the possible effects of significantly different nutrient application rates should be visible in surface water composition data and solute loads at the outlet of the basin within three years.

SAMENVATTING EN CONCLUSIES

Inleiding

De voedselrijkdom van het Nederlandse oppervlaktewater is op veel plekken zo groot dat van eutrofiëring kan worden gesproken. Eutrofiëring is de (over)belasting van het open water met nutriënten zoals stikstof (N) en fosfor (P), met als gevolg een toename van de groei van algen en waterplanten. Eutrofiëring kan leiden tot algenbloei, verminderd doorzicht in open water en zuurstofloosheid. Dit zijn voorbeelden van ongewenste verschijnselen uit het oogpunt van onder andere natuur en recreatie waardoor het gebruik en de functie van het oppervlaktewater in gevaar komen. De belangrijkste soorten bronnen van N en P in het oppervlaktewater in Nederland zijn puntbronnen, diffuse bronnen en interne bronnen. Voorbeelden van puntbronnen zijn industriële lozingen en effluentstromen van zuiveringsinstallaties van afvalwater (a.w.z.i.'s). Voorbeelden van diffuse bronnen zijn kwel van nutriëntrijk grondwater, drainagewater van landbouwgronden en atmosferische depositie. Een voorbeeld van een interne bron is de uitwisseling van fosfaat tussen een (onder)waterbodem richting het bovenstaande open water. Het Nederlandse oppervlaktewater komt uiteindelijk terecht in de Noordzee en draagt zo bij tot een belasting van het zeewater met onder andere nutriënten.

De overheid heeft diverse maatregelen getroffen die tot een reductie hebben geleid van de belasting van het oppervlaktewater met nutriënten. De stofconcentraties in het effluentwater van a.w.z.i.'s en van industriële complexen zijn significant gedaald sinds de invoering van de Wet verontreiniging oppervlaktewater (Wvo) in de 70-er jaren. Reducties van andere puntbronnen dan de a.w.z.i.'s zijn ook gerealiseerd. Terwijl de terugdringing van puntbronnen gestaag vorderde, is de sanering van diffuse bronnen achtergebleven. Deze situatie heeft ertoe geleid dat het relatieve aandeel van diffuse bronnen in het totaal van bronnen van N en P is gegroeid. Streefbeelden en MTR-(Maximaal Toelaatbaar Risico) waarden voor het oppervlaktewater worden vaak niet gehaald. Om deze binnen afzienbare tijd in zicht te krijgen of überhaupt ooit te bereiken, moeten de diffuse bronnen verder gesaneerd worden. In een poging om deze bronnen verder terug te dringen is een aantal beleidsmaatregelen en verplichte regelgeving voor onder andere de Nederlandse agrarische sector tot stand gekomen op het gebied van mest- en mineralengebruik.

Het onderzoek

Meststoffen die op het land gebracht worden, komen voor een deel terecht in de oogst van gewassen en bodem, maar belanden daarnaast als opgeloste stoffen in het grondwater en via drainage in het oppervlaktewater. Om de belasting van het oppervlaktewater te kunnen berekenen moet bekend zijn *hoe* en *wanneer* het neerslagoverschot (neerslag minus verdamping), inclusief de daarin opgeloste meststoffen, het oppervlaktewater bereikt. De stroming van water in de bodem en in het oppervlaktewater is het belangrijkste transportmechanisme voor de in het water aanwezige nutriënten. De afvoerroutes van het neerslagoverschot, de stroomsnelheden van het water en de verblijftijd van drainagewater zijn de sleutelfactoren om de stofvrachten van drainagewater te kunnen interpreteren en analyseren. Deze verblijftijd bepaalt wanneer het neerslagoverschot in het open water tot afvoer komt. Daarmee bepaalt de verblijftijd het moment waarop effecten van het landgebruik zichtbaar worden in de hoeveelheid en samenstelling van het drainagewater. Het landgebruik is een belangrijke factor in de verdamping van water en de toegepaste soort en hoeveelheid meststoffen. Indien het landgebruik significant verandert ten opzichte van een referentiesituatie zullen pas na een bepaalde (verblijf)tijd de effecten ervan op het drainagewater zichtbaar worden. In dit proefschrift is de *verblijftijd van drainagewater* gedefinieerd als de tijdsperiode die het duurt voordat het neerslagoverschot het oppervlaktewater bereikt, gerekend vanaf het moment van infiltratie aan maaiveld, gevolgd door een stroming door de bodem. De verblijftijd is in dit proefschrift meestal gegeven als een discrete verblijftijdverdeling, bestaande uit een aantal fracties behorend bij drainagewater binnen een zekere verblijftijdklasse.

De doelstellingen van het onderzoek waren als volgt:

1. Het onderscheiden en kwantificeren van de verschillende componenten en routes van de afvoer van het neerslagoverschot richting *lokale drainagesystemen*, zoals drainagebuizen en sloten.
2. Het ontwikkelen van een rekenmethode om de belasting van *regionaal oppervlaktewater* met meststoffen te schatten, mede op basis van stofbalansen. Deze methode moet toepasbaar zijn voor verschillende bodemtypes en bij verschillende niveaus van meststoffengebruik. De methode moet bruikpasbaar zijn voor verschillende hydrologische regio's in Nederland.

De doelstellingen van het onderzoek zijn bereikt door:

– data te verzamelen en te interpreteren op het gebied van hydrologie en nutriëntenbalansen voor specifieke situaties op veldschaal, en
– de verblijftijdverdeling van drainagewater te berekenen voor verschillende veldsituaties en regio's binnen Nederland.

De veldexperimenten hebben plaatsgevonden op twee locaties, te weten in de Flevopolder, in oostelijk Flevoland, en in de Achterhoek, binnen het stroomgebied van de Hupselse beek. Voor de uitwerking van de regionale benadering zijn het afwateringsgebied van de Hoge Vaart (Flevopolder) en het stroomgebied van de Hupselse beek gebruikt.

Theoretisch kader

Verblijftijd bij stationaire stromingssituatie - De benadering van *Ernst-Bruggeman* (Ernst, 1973; Bruggeman, 1999) om de verblijftijd van drainagewater te schatten is gebaseerd op jaargemiddelde stationaire, verzadigde stromingssituaties en gaat uit van stoftransport op basis van volledige verdringing (type Piston). Deze benadering is geldig voor situaties met buisdrainage en sloten en er kan rekening gehouden worden met kwel dan wel wegzijging op regionale schaal. De methode kan theoretisch gezien niet toegepast worden onder condities waarin de diepte van de lokale grondwaterstroming naar drainagemiddelen groot is ten opzichte van de drainafstand en/of waarin de onverzadigde zone een belangrijke rol speelt in de stroming van water en stoffen door de bodem.

Verblijftijd bij niet-stationaire stromingssituatie - Het '*dual-porosity*'concept (Gerke en Van Genuchten, 1993a, 1993b; Nieber en Misra, 1995) voor de beschrijving van stroming van water en stoftransport, in een variabel onverzadigd-verzadigd, gestructureerd poreus medium is een geschikte manier om de analyse van verblijftijden van drainagewater te ondersteunen. Bij dit concept wordt het poreuze stromingsmedium onderverdeeld in twee parallelle media met verschillende porositeiten, te weten de bodemmatrix en de macroporiën. De bodemmatrix bestaat uit alleen capillaire poriën; de macroporiën vertegenwoordigen alle niet-capillaire poriën. Water- en stoftransport in beide systemen staan onder invloed van elkaar; interactie tussen de bodemmatrix en de macroporiën vindt plaats op basis van gradiënten in drukhoogte en stofconcentratie. Deze gradiënten bepalen de uitwisseling van water en stoffen tussen de beide media. Indien de eigenschappen van beide media identiek zijn, dan wel in het geval dat elke interactie wordt uitgeschakeld, kunnen ook de waterstroming en het stoftransport in een '*single porosity*' medium berekend worden.

De Richards stromingsvergelijking wordt zowel voor de bodemmatrix als voor de macroporiën gebruikt. Deze vergelijking werkt prima voor de berekening van de stroming van water door een bodemmatrix, maar de toepassing ervan op stroming door macroporiën is een uitdaging. In het geval dat een numerieke methode wordt gebruikt om de stromingsvergelijking voor het macroporiën-medium op te lossen, is het moeilijk om een oplossing te vinden (convergentie) omdat de zwaartekracht de stroming van water domineert. Andere convergentie-problemen zijn opgedoken bij regenval op een droge bodem en deze zijn opgelost door tijdens de simulaties automatisch te schakelen

tussen een impliciete en expliciete numerieke oplossingsmethode. Deze omschakeling is gebaseerd op de verzadigingsgraad van water in een rekenknooppunt. Het moment van omschakeling werd bepaald op basis van 'trial and error', met als maat de fout in de berekende waterbalansen. Op het gebied van stoftransport is alleen retardatie meegenomen als resultante van een bodemchemisch proces (adsorptie aan vaste fase). De belangrijkste reden om niet andere bodemchemische processen te modelleren is dat dit onderzoek zich vooral heeft gericht op *fysische transportverschijnselen van water en stoffen* en op het effect van *verblijftijden van drainagewater* op de samenstelling van het afgevoerde water richting het open water.

Regionale benadering - Met de regionale benadering kunnen balansen worden berekend op jaarbasis voor water, zout (Cl), stikstof (N) en fosfor (P) voor het landoppervlak en het regionale oppervlaktewater. Daarnaast wordt de jaarlijkse stofbelasting richting het regionale oppervlaktewater bepaald. De benadering gaat uit van evenwichtssituaties in bodem en water en verwaarloost hiermee eventuele variaties in bodemfysische en –chemische condities die de water- en stofbalansen zouden kunnen beïnvloeden. Een te modelleren regio wordt onderverdeeld in een regionaal oppervlaktewatersysteem en in een aantal deelgebieden. Deze deelgebieden vormen samen het landoppervlak en lokaal klein open water. Elk deelgebied wordt gekenmerkt door een dominant landgebruik, bodemtype en grondwatertrap en de verblijftijdverdeling van drainagewater. Deze verblijftijdverdeling varieert van jaar tot jaar, afhankelijk van het weer, en is in eerste instantie gebaseerd op de benadering van Ernst-Bruggeman. Aanpassing van de hiermee berekende verblijftijdverdeling is mogelijk op basis van gebiedskennis, velddata of berekeningen met andere modellen. Al het drainagewater van de deelgebieden komt vroeg of laat terecht in het regionale oppervlaktewater. Er wordt aangenomen dat eventueel in een gebied aanwezige grondwaterkwel direct in het regionale oppervlaktewatersysteem uittreedt. De regionale benadering berekent tenslotte een jaargemiddelde regionale verblijftijdverdeling van drainagewater en jaargemiddelde verblijftijden van water in het regionaal oppervlaktewatersysteem.

Puntbronnen van water en stoffen voor het regionale watersysteem moeten als modelinvoer opgegeven worden. Op landbouwkundig gebied vereist de regionale benadering gegevens over het jaarlijks gebruik van kunstmest en dierlijke mest en gegevens over de langjarig gemiddelde afvoer van stoffen met de oogst van gewassen. Denitrificatie van nitraat door zowel bacteriën als door oxidatie van pyriet als ook adsorptie van fosfaat aan de vaste fase in de bodem zijn belangrijke chemische processen die van invloed zijn op de N- en P-balansen. Deze processen worden in de vorm van balanstermen meegenomen in de berekeningen.

Experimenten op veldschaal

Veldexperiment Flevoland - Het veldexperiment Flevoland werd uitgevoerd in het centrale zeekleigebied van Nederland in de Flevopolder. De kleigrond op de locatie was gescheurd en er werden akkerbouwgewassen geteeld. De experimenten en metingen vonden plaats op twee percelen van een akkerbouwbedrijf. Op twee proefvelden zijn elk één jaar en na elkaar intensief metingen verricht aan bodem, hydrologie en meststoffen. De proefvelden bestonden uit de vanggebieden van drie drainagebuizen, zo'n 2,16 hectares groot in omvang. Daarnaast werden er gedurende de gehele campagne metingen verricht aan het vanggebied van de kavelsloot ter grootte van 30 hectares. De waarnemingen op proefveld 1 vonden plaats van april 1992 tot en met maart 1993, op proefveld 2 van april 1993 tot en met juni 1994. Oppervlakte-afvoer werd niet waargenomen tijdens de meetcampagnes, plasvorming wel tijdens sommige buien. Het neerslagoverschot verliet de percelen niet alleen via buisdrainage, maar ook via directe drainage naar de kavelsloot en naar de nabijgelegen tocht. Deze tocht is onderdeel van een netwerk van grotere watergangen, uitmondend in het regionale oppervlaktewatersysteem. Waterbalansen op basis van velddata voor beide percelen zijn uitgerekend voor de hydrologische jaren van april 1992 tot en met maart 1993 (proefveld 1) en van april 1993 tot en met maart 1994 (proefveld 2). Voor het vanggebied van de kavelsloot zijn beide jaren beschouwd.
De waterbalansen voor de proefvelden gaven te zien dat voor proefveld 1 en 2 respectievelijk 48% en 16% van het neerslagoverschot niet via de drainagebuizen werd afgevoerd. Voor de kavelsloot golden percentages van 48% en 59% voor het eerste respectievelijk tweede meetjaar. De reden waarom het neerslagoverschot via andere routes dan via drainagebuizen afgevoerd werd, was gelegen in de opbouw van het bodemprofiel op de proefvelden. Een tracerproef met bromide als merkstof op de beide proefvelden had als resultaat dat binnen één jaar 24% en 56% voor respectievelijk proefveld 1 en 2 van de opgebrachte tracerhoeveelheid het perceel via drainage verliet. *De hydrologische situatie op beide proefvelden bleek behoorlijk verschillend.*

De benadering volgens Ernst-Bruggeman werd in eerste instantie gebruikt om de verblijftijdverdeling van drainagewater van de vanggebieden binnen het veldexperiment Flevoland te schatten. Vervolgens zijn drie verschillende numerieke modellen gebruikt voor drie verschillende bodemprofielen. De met de numerieke modellen berekende waterbalansen kwamen goed overeen met die op basis van de veldgegevens.
De gesimuleerde afvoer van water via zowel de drainagebuizen, zoals in het veld gemeten, als via niet-bemeten andere afvoerroutes kwam goed overeen met de werkelijkheid. Hiertoe moesten geschikte bodemprofielen en randvoorwaarden in de computermodellen verwerkt worden. Water- en stoftransport in zowel de bodemmatrix als de macroporiën was belangrijk voor de nabootsing van de veldsituatie, maar zeker ook de *interactie tussen beide stromingsmedia.* Deze interactie leidde tot uitwisseling van water en stoffen tussen deze

media. Er waren afwijkingen tussen de verblijftijdverdeling van drainagewater, berekend op basis van de Ernst-Bruggeman benadering en met behulp van de numerieke modellen. Deze afwijkingen waren groter naarmate de weersomstandigheden droger of natter waren. De berekeningen met de numerieke modellen gaven betere resultaten, terwijl de eenvoudige en snel toepasbare Ernst-Bruggeman benadering redelijke resultaten opleverde. De langjarig gemiddelde verblijftijdverdeling van drainagewater in de veldsituatie in Flevoland is te zien in Tabel S.1. *De fracties in Tabel S.1 hebben tot gevolg dat een significante wijziging in het landbouwkundig gebruik van de percelen, meer specifiek bijvoorbeeld in de bemestingssituatie, binnen drie jaar tot een verandering leidt van de samenstelling van 70-75% van het drainagewater.*

Tabel S.1
Veldexperiment Flevoland. Langjarig gemiddelde verblijftijdverdeling in fracties f_τ (τ=1,...,3) van drainagewater in de veldsituatie van proefveld 1 en 2 en van de kavelsloot. Het drainagewater bestaat voor een deel ter grootte van fractie f_1 uit water dat minder dan één jaar geleden aan maaiveld geïnfiltreerd is, voor een fractie f_2 uit water dat tussen één en twee jaar geleden infiltreerde etc.

Fractie	Verblijftijdklasse [j]	f_τ [-]		
		Proefveld 1	Proefveld 2	Kavelsloot
f_1	$t \leq 1$	0.27	0.34	0.30
f_2	$1 < t \leq 2$	0.26	0.28	0.28
f_3	$2 < t \leq 3$	0.15	0.13	0.14
Totaal	$t \leq 3$	0.68	0.75	0.72

Tijdens de meetcampagne werden op beide proefvelden aardappels verbouwd binnen een gemiddeld driejarige gewasrotatie van wintertarwe, aardappels en suikerbieten. Elk gewas ontving kunstmestgiften, terwijl dierlijke mest werd toegepast na de oogst van wintertarwe in het najaar, voorafgaand aan het aardappelseizoen van het jaar erna. Voor de proefvelden en het vanggebied van de kavelsloot zijn N- en P-balansen opgesteld voor het bodemsysteem, voor het meetjaar zelf en voor vier jaren daaraan voorafgaand. Het overschot op deze N- en P-balansen is omgerekend naar de stofvracht van het drainagewater door gebruik te maken van de verblijftijdverdeling van het drainagewater. *De gemeten N-vrachten van het drainagewater in de veldsituatie bedroegen 55 tot*

86 kg ha^{-1} j^{-1} N. De berekende N-vrachten kwamen hiermee gedeeltelijk overeen; de berekeningen onderschatten de gemeten vrachten met 10% tot 49% voor respectievelijk proefveld 1 en 2 en met 67% en 16% voor de kavelsloot respectievelijk in het eerste en het tweede meetjaar. Een mogelijke reden voor deze onderschattingen waren niet-uniforme stromingsprocessen in de bodem die tot N-verliezen naar het oppervlaktewater leidden die groter waren dan op basis van N-overschotten op jaarlijkse N-balansen aangenomen werd. Deze processen kunnen er bijvoorbeeld toe geleid hebben dat een balansterm zoals denitrificatie overschat werd omdat het bodemprofiel in de veldsituatie door preferent transport toch feitelijk droger was. Daarnaast is het mogelijk dat de beschikbare veldgegevens over de samenstelling en toepassing van dierlijke mest onvoldoende nauwkeurig waren. De berekende P-vrachten van drainagewater overschatten de gemeten P-vrachten met een factor 10 vanwege adsorptie van fosfaat aan de vaste fase in de kleibodem. *De gemeten P-vrachten in de veldsituatie waren 0,2 tot 0,5 kg ha^{-1} j^{-1} P*, minder dan 1 à 2% van het overschot op de P-balans. De berekende P-adsorptie lag tussen 20 en 40 kg ha^{-1} j^{-1} P en leidde tot een verrijking en oplading van de bodem. *De gestructureerde kleibodems in het veldexperiment te Flevoland hebben een verhoogd risico tot gevolg ten aanzien van de uitspoeling van meststoffen, met name van stikstof, vergeleken met niet-gestructureerde bodems.*

Veldexperiment Hupsel-Assink - Het veldexperiment Hupsel-Assink was gelegen in het oostelijk zandgebied van Nederland en binnen het stroomgebied van de Hupselse beek. Het landgebruik was permanent grasland. De meetperiode liep van november 1992 tot en met maart 1994 en betrof metingen op één proefveld, te weten het vanggebied van één drainagebuis ter grootte van 0,25 hectare. Regenval bleek het beste gemeten te kunnen worden met een regenmeter die ter hoogte van het maaiveld opgesteld was. Oppervlakte-afvoer was niet waargenomen gedurende de veldcampagne, maar incidenteel kwam plasvorming voor op het grasland. Het neerslagoverschot verliet het proefveld niet alleen via de drainagebuis, maar ook via grondwaterstroming direct naar de kavelsloot en naar de Hupselse beek, in het gebied fungerend als regionaal oppervlaktewater. De waterbalans van het proefveld op basis van veldgegevens was opgesteld voor de periode januari 1993 tot en met maart 1994. *Hieruit bleek dat 31% van de totale drainage niet via de drainagebuis tot afvoer kwam.* Het bodemprofiel en het feit dat de drainagebuis in toenemende mate tijdens de meetcampagne verstopt raakte door ijzervlokken, leidden tot deze niet-bemeten drainageroute.

De Ernst-Bruggeman benadering en een twee-dimensionaal '*single-porosity*' numeriek model (macroporiën afwezig) zijn beide gebruikt om een verblijftijdverdeling van het drainagewater te schatten onder stationaire, respectievelijk niet-stationaire stromingssituaties. De met het numerieke model berekende waterbalansen kwamen goed overeen met de waterbalansen die afgeleid waren van de velddata. *Het numerieke model*

was in staat de gemeten en niet-gemeten drainage te simuleren met behulp van geschikte initiële condities en randvoorwaarden. Het verloop van de drainage in de tijd werd goed berekend, hoewel sommige drainage-gebeurtenissen niet door het model berekend werden. In de zomer van 1993 trad preferente stroming van water in de onverzadigde zone op die leidde tot drainage. Dit verschijnsel trad op meerdere plekken op in het stroomgebied van de Hupselse beek, omdat er een vanuit een droge beginsituatie plotseling toenemende beekafvoer waargenomen werd. De vorming van instabiele vochtfronten en dito stroming in de onverzadigde zone is een mogelijke verklaring van de waargenomen verschijnselen. Dit type stroming maakt geen onderdeel uit van de modelconcepten. De verblijftijd-verdeling van het drainagewater volgens de benadering van Ernst-Bruggeman werd bevestigd door de berekeningen met het numerieke model en is te zien in Tabel S.2. *De fracties in Tabel S.2 hebben tot gevolg dat een significante wijziging in het landbouwkundig gebruik van de percelen, meer specifiek bijvoorbeeld in de bemestingssituatie, binnen drie jaar tot een verandering leidt van de samenstelling van 66% van het drainagewater.*

Tabel S.2
Veldexperiment Hupsel-Assink. Langjarig gemiddelde verblijftijdverdeling van drainagewater in fracties f_τ (τ=1,...,3) in de veldsituatie van het proefveld.
Het drainagewater bestaat voor een deel ter grootte van fractie f_1 uit water dat minder dan één jaar geleden aan maaiveld geïnfiltreerd is, voor een fractie f_2 uit water dat tussen één en twee jaar geleden infiltreerde etc.

Fractie	Verblijftijdklasse [j]	f_τ [-]
f_1	$t \leq 1$	0.29
f_2	$1 < t \leq 2$	0.25
f_3	$2 < t \leq 3$	0.12
Totaal	$t \leq 3$	0.66

Zowel kunstmest als dierlijke mest werden diverse keren per jaar toegepast op het grasland. Voor het proefveld zijn Cl-, N- en P-balansen opgesteld voor het bodemsysteem, voor het meetjaar zelf en vier jaar daaraan voorafgaand. De overschotten op de Cl- en N-balans voor het bodemsysteem konden met succes omgerekend worden naar de gemeten stofvrachten van het drainagewater, gebruik makend van de

verblijftijdverdeling van het drainagewater. *De gemeten stofvrachten van het drainagewater in de veldsituatie waren 270 kg ha^{-1} j^{-1}Cl en 160 kg ha^{-1} j^{-1}N.* De berekende Cl- en N-vrachten kwamen hiermee goed overeen. De berekende P-vrachten van drainagewater overschatten de gemeten P-vrachten met een factor 8 door adsorptie van fosfaat aan de vaste fase in de zandbodem enerzijds en door onbetrouwbare velddata aangaande representatieve P-concentraties in het drainagewater anderzijds. *De gemeten P-vracht in de veldsituatie was 0,83 kg ha^{-1} j^{-1}P, minder dan 1% van het gemiddelde overschot op de P-balans. De berekende P-adsorptie lag tussen 55 en 60 kg ha^{-1} j^{-1} P* en leidde tot een verrijking en oplading van de bodem.

Veldexperimenten, algemeen en aanbevelingen - De intensieve meetcampagnes in het veld en de uitvoerige analyse van de datasets bleken zeer waardevol. De veldwaarnemingen leidden niet alleen tot de inzameling van gegevens over water en meststoffen, maar gaven inzicht in de lokale hydrologische situatie. Een gedeelte van het drainagewater werd gemeten op de proefvelden door de afvoer van drainagebuizen te monitoren, maar een ander deel van het neerslagoverschot bleek de proefvelden via andere drainageroutes te verlaten, gebaseerd op waterbalansen. *De stofvracht van drainagewater zou duidelijk onderschat zijn indien de niet-gemeten afvoer van drainagewater verwaarloosd zou zijn in de gehele analyse.* Daarnaast bleek het *van groot belang te zijn, de verblijftijdverdeling van drainagewater te betrekken bij de vertaling van de overschotten van stofbalansen voor de bodemsystemen van de proefvelden naar de gemeten stofvrachten van het drainagewater.*

Wanneer veldexperimenten ter bestudering van de samenstelling van drainagewater opgezet worden, is informatie nodig over het 'historische' (landbouwkundig) gebruik van een perceel ten aanzien van bijvoorbeeld meststoffen. Indien deze informatie ontbreekt is een lange meetperiode nodig teneinde de samenstelling van het drainagewater te kunnen koppelen aan bodem en landgebruik. Een belangrijke reden hiervoor is de verblijftijdverdeling van het drainagewater. Enerzijds laat deze verdeling zien dat de afvoer in een bepaald jaar maar voor een deel bestaat uit het neerslagoverschot van datzelfde jaar, anderzijds toont deze aan dat het een aantal jaren duurt voordat de invloed van bemesting merkbaar en meetbaar is in de samenstelling van drainagewater. Kennis over de verblijftijdverdeling van drainagewater is noodzakelijk om de stofvrachten van drainagewater te kunnen interpreteren. *De resultaten voor zowel de proefvelden in Flevoland als in Hupsel laten zien dat een 'historische' dataperiode van drie tot vijf jaar voldoende lang is om de samenstelling van drainagewater met succes te kunnen interpreteren.* Daarnaast is het van wezenlijk belang gebleken om over een goed opgezet meetprogramma aangaande de samenstelling van drainage- en oppervlaktewater te beschikken, dat geschikt is om nauwkeurige vrachtberekeningen uit te voeren.

Regionale benadering

Regionale benadering, Flevopolder, Hoge Afdeling - De Hoge Afdeling (HA regio) van de Flevopolder in het centrale zeekleigebied van Nederland is een 40.250 hectares groot afwateringsgebied binnen de diepe droogmakerij met vrijwel constante waterpeilen. Het neerslagoverschot in het gebied komt mede via drainagebuizen terecht in kavelsloten die vrij afwateren op tochten, en deze tochten wateren weer af op de Hoge Vaart. De Hoge Vaart is gedefinieerd als het regionaal oppervlaktewatersysteem. Het water uit dit systeem verlaat de Flevopolder via gemalen, die het water uitslaan op de randmeren en het IJsselmeer. Overal in het gebied komt grondwaterkwel voor, maar deze is niet-uniform ruimtelijk verdeeld over de regio. De verblijftijdverdeling van drainagewater op regionale schaal zoals berekend met de regionale benadering is te zien in Tabel S.3. *Te zien is dat 71% van het regionale drainagewater qua chemische samenstelling binnen drie jaar reageert op een significant veranderend landgebruik c.q. gebruik van meststoffen.* De gemiddelde verblijftijd van water in het regionaal oppervlaktewater zelf bedraagt gemiddeld ongeveer 7 dagen (1988-1999).

Tabel S.3
Flevopolder, Hoge Afdeling (HA regio). Langjarig gemiddelde verblijftijdverdeling van drainagewater in fracties f_τ (τ=1,...,3) voor de HA regio voor de periode april 1988 tot en met maart 1999. Het drainagewater bestaat voor een deel ter grootte van fractie f_1 uit water dat minder dan één jaar geleden aan maaiveld geïnfiltreerd is, voor een fractie f_2 uit water dat tussen één en twee jaar geleden infiltreerde etc.

Fractie	Verblijftijdklasse [j]	f_τ [-]
f_1	$t \leq 1$	0.41
f_2	$1 < t \leq 2$	0.19
f_3	$2 < t \leq 3$	0.11
Totaal	$t \leq 3$	0.71

De grootte van de f_1 fractie van de verblijftijdverdeling van het drainagewater is met name veroorzaakt door *preferent transport van water en stoffen in de onverzadigde zone* onder natte omstandigheden en daarnaast door de *geringe diepte van het lokale*

stromingssysteem van het grondwater. De jaarlijks gemiddelde waterbalans en stofvrachten naar het regionale oppervlaktewater voor de periode 1988-1999 zijn te zien in Tabel S.4.

Tabel S.4
Flevopolder, Hoge Afdeling (HA regio). Berekende gemiddelde waterbalansen voor het landoppervlak van alle deelgebieden in de HA regio [mm j^{-1}] en stofvrachten naar het regionale oppervlaktewater, de Hoge Vaart [kg ha^{-1} j^{-1}]. De gegevens gelden voor de hydrologische jaren april 1988 tot en met maart 1999. *Bij de gemalen van de Hoge Vaart.

Flevopolder, Hoge Afdeling (HA regio), 1988-1999

Waterbalans	[mm j^{-1}]	
	gemeten	berekend
P	816	-
ET_a	489	465
Q_{kwel}	372	-
Q_{gemaal}	699	711

Stofvracht naar regionaal oppervlaktewater	[kg ha^{-1} j^{-1}]	
	gemeten*	berekend
$q_{m,Cl}$	1592	1625
$q_{m,totaal - N}$	35	45
$q_{m,totaal - P}$	0.76	0.90

De actuele verdamping werd door de regionale benadering met 5% onderschat, en hierdoor de afvoer van water bij de gemalen 2% overschat. De jaargemiddelde kwelhoeveelheid werd door de jaren heen constant verondersteld, maar het leek meer waarschijnlijk dat deze van jaar tot jaar varieerde. De toegepaste verblijftijdverdelingen van drainagewater uit de deelgebieden van de Hoge Afdeling leidden ertoe dat het berekende verloop in de tijd van de Cl- en N-vrachten naar het regionale oppervlaktewater redelijk overeenkwam met dat van de metingen. Afwijkingen waren te zien in het tijdsverloop van de gemeten ten opzichte van de berekende P-vrachten. *De berekende belasting van het oppervlaktewater met N en P was respectievelijk 29% en 18%*

hoger dan de door de gemalen uitgeslagen stofvracht van de Hoge Vaart richting de randmeren en het IJsselmeer. De in vergelijking met de stofbelasting naar het open water lagere stofvrachten zoals gemeten bij de gemalen is veroorzaakt door een combinatie van retentie en omzetting van N en P in en om het regionale oppervlaktewater. De belangrijkste reden met betrekking tot P is waarschijnlijk de adsorptie van P in en om het regionale oppervlaktewatersysteem en de retentie van P in de bodem tijdens het opwaarts transport van kwel uit het diepe grondwater in de richting van het open water. Voor N is denitrificatie in en om het open water waarschijnlijk een belangrijk proces. Genoemde processen zijn niet meegenomen in de regionale benadering.

Regionale benadering, Hupselse beek - Het stroomgebied van de Hupselse beek is 650 hectares groot en gelegen in Oost-Gelderland tegen de Duitse grens. De zandige bodems in het gebied stammen uit het Pleistoceen. Grasland en snijmaïs domineren het landgebruik. Een watervoerend pakket van 1 tot 10 m dikte wordt aan de onderzijde hydrologisch begrensd door een 30 tot 40 m dikke kleilaag uit het Mioceen. Het drainagewater uit het gehele gebied komt al dan niet direct tot afvoer in de beek en deze beekafvoer wordt continu gemeten bij het afvoerpunt van het stroomgebied. De berekende verblijftijdverdeling van het drainagewater op regionale schaal is te zien in Tabel S.5. *Bijna 60% van het regionale drainagewater reageert qua chemische samenstelling binnen drie jaar op een significant veranderend landgebruik c.q. gebruik van meststoffen.* De gemiddelde verblijftijd van water in het regionaal oppervlaktewater bedraagt 1 tot 2 dagen (1985-1994).

De jaarlijks gemiddelde waterbalans en stofvrachten naar het regionale oppervlaktewater zijn te zien in Tabel S.6. De toepassing van de regionale benadering op het stroomgebied van de Hupselse beek gaf goede resultaten te zien voor de waterbalans. Hoge afvoeren tijdens natte jaren werden echter iets overschat, lage afvoeren tijdens droge jaren enigszins onderschat. *De verblijftijdverdeling van drainagewater zoals in Tabel S.5 leverde een correct verloop in de tijd op van Cl- en N-vrachten naar het regionale oppervlaktewater.* Daarnaast werden de absolute vrachten van deze stoffen goed berekend. De resultaten voor de P-vrachten waren redelijk. *Door retentie van N en P in en om het oppervlaktewatersysteem was de berekende N- en P-belasting respectievelijk 5% en 18% groter dan de desbetreffende vracht bij het afvoermeetpunt van het stroomgebied.*

Regionale benadering, algemeen en aanbevelingen - Om met succes maatregelen te nemen die tot vermindering van de stofbelasting van het oppervlaktewater leiden is het relevant te weten welke bronnen welk aandeel in de totale belasting hebben. Tabel S.7 laat voor de beide beschouwde regio's de relatieve bijdrage aan het totaal zien van de twee grootste bronnen van wateraanvoer en van de stofbelasting naar het regionale open water.

De belangrijkste puntbronnen naar het water van de Hoge Vaart in de Hoge Afdeling zijn de effluentlozingen van a.w.z.i.'s, die met succes qua stofbelasting van het ontvangende oppervlaktewater zijn gesaneerd in de 90-er jaren. *In de huidige situatie binnen de Hoge Afdeling is de kwel vanuit het grondwater de belangrijkste bron van Cl en P in het regionale oppervlaktewater. De afvoer van drainagewater uit landbouwpercelen is de belangrijkste N-bron voor de Hoge Vaart.* Maatregelen om succesvol de stofbelasting van het oppervlaktewater te reduceren moeten zowel op het vlak van peilbeheer als op de sanering van landbouwkundige bronnen gericht zijn.

Tabel S.5

Hupselse beek (HB regio). Langjarig gemiddelde verblijftijdverdeling van drainagewater in fracties f_τ (τ=1,...,3) voor de HB regio voor de periode april 1985 tot en met maart 1994. Het drainagewater bestaat voor een deel ter grootte van fractie f_1 uit water dat minder dan één jaar geleden aan maaiveld geïnfiltreerd is, voor een fractie f_2 uit water dat tussen één en twee jaar geleden infiltreerde etc.

Fractie	Verblijftijdklasse [j]	f_τ [-]
f_1	$t \leq 1$	0.29
f_2	$1 < t \leq 2$	0.18
f_3	$2 < t \leq 3$	0.12
Totaal	$t \leq 3$	0.59

In het stroomgebied van de Hupselse beek wordt de stofbelasting van het oppervlaktewater gedomineerd door landbouwkundige bronnen door de afwezigheid van andere belangrijke bronnen. De bepalende factor die de landbouw speelt als bron van zout en meststoffen maakt het *stroomgebied uitermate geschikt om de effecten te onderzoeken van veranderingen in landgebruik en landbouwkundig handelen op de samenstelling van oppervlaktewater op regionale schaal.* In het stroomgebied kan de relatie tussen overschotten op stofbalansen voor het bodemsysteem en de stofbelasting van het open water goed onderzocht worden.

Net zoals bij de veldexperimenten bleek dat bij de toepassing van de regionale benadering het van essentieel belang was, om te kunnen beschikken over *goed ontworpen*

Tabel S.6
Hupselse beek (HB regio). Berekende gemiddelde waterbalansen voor het landoppervlak van alle deelgebieden in de HB regio [mm j^{-1}] en stofvrachten naar het regionale oppervlaktewater, de Hupselse beek [kg ha^{-1} j^{-1}]. De gegevens gelden voor de hydrologische jaren april 1985 tot en met maart 1994.

Hupselse beek (HB regio), 1985-1994		
Waterbalans	[mm j^{-1}]	
	gemeten	berekend
P	843	-
ET_a	516	510
Q_{beek}	328	336
Stofvracht naar regionaal oppervlaktewater	[kg ha^{-1} j^{-1}]	
	gemeten	berekend
$q_{m,\text{Cl}}$	142	143
$q_{m,\text{totaal - N}}$	112	118
$q_{m,\text{totaal - P}}$	0.83	0.98

meetprogramma's op het gebied van de samenstelling van drainage- en oppervlaktewater teneinde betrouwbare stofvrachten te kunnen berekenen. Een in de tijd continue en afvoer-afhankelijke monstername van het te onderzoeken water zijn kenmerken van een geschikt meetprogramma.

Een gedegen herkomst- en bronnenanalyse aangaande de nutriënten in het oppervlaktewater is een vereiste om gericht kansrijke te kunnen nemen maatregelen ter vermindering van de belasting van het oppervlaktewater met meststoffen. Om eventuele effecten van maatregelen, die gericht zijn op de reductie van bepaalde bronnen, te kunnen meten en analyseren moeten andere relevante en belangrijke bronnen altijd mee in beeld worden gebracht. Voor zover maatregelen effecten hebben op de samenstelling van drainagewater, bepaalt de verblijftijd van het drainagewater het moment waarop deze effecten tot uiting komen in de belasting van het oppervlaktewater.

Tabel S.7
Flevopolder, Hoge Afdeling (HA regio) en Hupselse beek (HB regio). Relatieve bijdrage (fractie) aan de totale wateraanvoer en stofbelasting naar het regionale oppervlaktewater van de twee belangrijkste bronnen van water en stoffen. De berekende gemiddelde bijdrage is relatief ten opzichte van het totaal van wateraanvoer en stofbelasting naar het regionale open water. De gegevens voor de Hoge Afdeling zijn geldig voor de periode april 1988 tot en met maart 1999; de gegevens voor de Hupselse beek gelden voor de periode april 1985 tot en met maart 1994.

Stof	Flevopolder, Hoge Afdeling, 1988-1999		Hupselse beek, 1985-1994	
	Grondwater-kwel	Drainagewater landbouw	Puntbronnen	Drainagewater landbouw
Water	0.56	0.43	<0.01	0.96
Chloride	0.86	0.13	<0.01	0.98
Totaal-N	0.19	0.76	<0.01	0.98
Totaal-P	0.55	0.14	0.06	0.83

A

FLEVOLAND EXPERIMENTAL SITE

Model setup, general:

- Mesh: grid of 125 nodes and 164 triangular elements. Minimum average grid length: 0.02 m.
- $\alpha_L = 0.5$ times the smallest grid cell length, and $\alpha_T = 0.1\,\alpha_L$. These values are equal for all layers for both domains.
- $D_0 = 2.3 \times 10^{-9}$ m^2 s^{-1}.
- Retardation factor: $R = 1.0$.
- Initial pressure head h_{init} condition: hydrostatic equilibrium. The groundwater level is initially at 1.50 m below the soil surface.
- Conductance factor subsurface drain: 0.75 d^{-1}.
- Conductance factor 'far field' boundary: 0.01 d^{-1}.
- Switch from implicit to explicit scheme at saturation degree of 0.001.

Table A.1
Flevoland experimental site. Soil-physical parameters for Plot 1 and Plot 2 soil water retention curve $\theta(h)$ and hydraulic conductivity curve $k(h)$ as determined in laboratory. *Groen (1997) used k_s at plough pan between 0.5 and 0.7 cm d^{-1}.

Sampling depth	Parameters of fitting curves							Measured
	θ_r	θ_s	α	n	m	l	k_s	k_s
[m]	[-]	[-]	[cm^{-1}]	[-]	[-]	[-]	[cm d^{-1}]	[cm d^{-1}]
0.15-0.23	0.01	0.47	0.0091	1.155	0.134	-5.0	0.261	14.72
0.30-0.38*	0.01	0.51	0.0106	1.144	0.126	-2.756	0.893	7.19
0.45-0.53	0.01	0.58	0.0021	1.168	0.144	-5.0	0.050	5.31
1.00-1.20	0.01	0.74	0.0028	1.189	0.159	-5.0	0.050	-
1.20-1.70	0.01	0.36	0.0224	1.507	0.336	-0.140	13.21	-

Source: Groen (1997)

Table A.2
Flevoland experimental site. Soil physical properties used in A, B, and C dual porosity models for layers 1 to 3. Anisotropy factors according to Groen (1997), plough layer (1) assumed isotropic. *Unit of k_s is [cm d^{-1}]. **$n = n_{\text{fitting curve}} + 1.0$. ***$f(k_s)_{\text{interface}}$ -factor to determine k_s of soil matrix at the matrix-macropore interface.

Parameter	Layer 1: 0.00-0.25 m		Layer 2: 0.25-0.30 m		Layer 3: 0.30-1.05 m	
	Matrix	Macropores	Matrix	Macropores	Matrix	Macropores
θ_s	0.45	0.02	0.50	0.01	0.58	0.05
θ_r	0.20	0.001	0.20	0.001	0.15	0.001
k_s*	0.10	14.72	0.893	7.19	0.05	147.2
α	0.0091	0.1	0.0106	0.1	0.0021	0.1
n**	1.155	10.0	1.144	10.0	1.168	10.0
m	0.134	0.95	0.126	0.95	0.144	0.95
l	-5.0	0.5	0.5	0.5	-5.0	0.5
$f(k_s)_{\text{interface}}$***	1.0	-	2.0	-	2.0	-
a	1.0	-	2.0	-	15.0	-
k_h/k_v	1.0	1.0	0.2	1.0	0.2	1.0

Table A.3

Flevoland experimental site. Soil physical properties used in A, B, and C dual porosity models for layer 4. Anisotropy factors according to Groen (1997). *Unit of k_s is [cm d^{-1}]. **$n = n_{\text{fitting curve}} + 1.0$. ***$f(k_s)_{\text{interface}}$ -factor to determine k_s of soil matrix at the matrix-macropore interface.

Parameter	Layer 4: 1.05-1.20 m Sand		Layer 4: 1.05-1.20 m Ripened clay		Layer 4: 1.05-1.20 m Unripened clay	
	Matrix	Macropores	Matrix	Macropores	Matrix	Macropores
θ_s	0.18	0.18	0.58	0.05	0.37	0.37
θ_r	0.005	0.005	0.12	0.001	0.10	0.10
k_s^*	13.21	13.21	2.5	147.2	0.05	0.05
α	0.0224	0.0224	0.0021	0.1	0.0028	0.0028
n^{**}	1.507	1.507	1.168	10.0	1.189	1.189
m	0.336	0.336	0.144	0.95	0.159	0.159
l	-0.14	-0.14	-5.0	0.5	-2.5	-2.5
$f(k_s)_{\text{interface}}^{***}$	1.0	-	2.0	-	1.0	-
a	1000000.	-	15.0	-	1000000.	-
k_h/k_v	1.0	1.0	0.2	1.0	0.2	0.2

Table A.4

Flevoland experimental site. Crop-related parameters used in A, B, and C dual-porosity models. *Non-existing 'average' arable crop, for 1:3 crop rotation with winter wheat, potatoes, and sugar beet.

Parameter	Explanation	Crop			
		winter wheat	sugar beet	potatoes	arable crop*
$d_{root,init}$	initial root depth [cm]	10	10	10	10
$d_{root,max}$	maximum root depth [cm]	100-150	120	40-60	80-100
h_1		100	100	100	100
h_2		25	25	25	25
$h_{3,H}$		-500	-320	-320	-400
$h_{3,L}$		-900	-600	-600	-700
h_4		-16000	-16000	-16000	-16000
LAI_{min}		0.05	no data	0.0	0.0
LAI_{max}		6.8	no data	6.1	6.0
Harvest period		August	October	September	September
IRDIS	root depth distribution function (2=linear decrease with depth)	2	2	2	2

B

HUPSEL-ASSINK EXPERIMENTAL SITE

Model setup, general:

- Mesh: grid of 2301 nodes and 4300 triangular elements. Minimum average grid length: 0.06 m.
- Layer 4, m-parameter: estimates, based on layer 3 data.
- Values for k_s are curve-fitted values.
- α_L = 0.5 times the smallest grid cell length, and α_T = 0.1 α_L. These values are equal for all layers for both domains.
- D_0 = 1 x 10^{-9} m^2 s^{-1}.
- Retardation factor: $R = 1.0$.
- LAI is constant at 3.0 m^2 m^{-2}.
- Average root depth: 0.15 m. Sine variation between 0.1 m during the beginning of February and 0.2 m during the beginning of August each year. Root distribution function: linear decrease with depth.
- Initial pressure head h_{init} condition: hydrostatic equilibrium. The groundwater level is initially at 1.05 m below the soil surface.
- Conductance factor subsurface drain: 10 d^{-1}.
- Conductance factor 'far field' boundary: 0.025 d^{-1}.
- Switch from implicit to explicit scheme at saturation degree of 0.20.

Table B.1

Hupsel-Assink experimental site. Soil physical parameters for soil water retention function and hydraulic conductivity function for Mualem-Van Genuchten model. Note: matrix domain only shown, single-porosity flow domain. $*k_s$: fitted value, unit is [cm d^{-1}]. $** f(k_s)_{interface}$ -factor to determine k_s of soil matrix at the matrix-macropore interface. ***Hysteresis was not considered.

Parameter	a1 layer 0-0.15 m		b2 layer 0.15-0.35 m		c11 layer 0.35-0.90 m		c12 layer 0.90-3.00 m	
	Matrix drying	wetting***	Matrix drying	wetting***	Matrix drying	wetting***	Matrix drying	wetting***
θ_s	0.41	0.41	0.37	0.37	0.31	0.31	0.34	0.34
θ_r	0.20	0.20	0.20	0.20	0.15	0.15	0.01	0.01
k_s*	250.	250.	250.	250.	120.	120.	100.	100.
α	0.0470	0.1691	0.0544	0.2694	0.0434	0.0634	0.0168	0.0261
n	1.2405	1.2405	1.2420	1.2420	1.5615	1.5615	1.8110	1.8110
m	0.19	0.19	0.19	0.19	0.36	0.36	0.36	0.36
l	2.50	2.50	2.50	2.50	0.20	0.20	0.50	0.50
$f(k_s)_{interface}$ **	1.0	-	1.0	-	1.0	-	1.0	-
a	-	-	-	-	-	-	-	-
k_h/k_v	0.5		0.5		0.5		0.5	

Source: Van Dam et al. (1996).

Table B.2
Hupsel-Assink experimental site. Crop-related parameters used in single porosity model.

Parameter	Explanation	Grassland
$d_{\text{root,init}}$	initial root depth [cm]	10
$d_{\text{root,max}}$	maximum root depth [cm]	20
h_1		-10
h_2		-25
$h_{3,\text{H}}$		-200
$h_{3,\text{L}}$		-800
h_4		-8000
LAI_{min}		3.0
LAI_{max}		3.0
Harvest period		-
IRDIS	root depth distribution function (2=linear decrease with depth)	2

Table B.3
Hupsel-Assink experimental site. Calibrated coefficients for the relationship between soil relative dielectric constant ϵ and the volumetric water content θ [V.1].
*After Topp et al. (1980).

Depth to soil surface [m]	Coefficient			
	a	b	c	d
	3.03*	9.3*	146*	-76.7*
0.07	3.25	0.12	0.0015	0.0
0.20	3.00	0.50	0.0020	0.0
0.40	3.00	0.05	0.0155	0.0
0.65	3.00	0.15	0.0080	0.0

C

REGIONAL APPROACH, GENERAL

Table C.1
Regional approach: model options. Soil type, Groundwater Table Class (GTC), and land use options. *MHG: mean highest groundwater level. **MLG: mean lowest groundwater level, both in [m] below the soil surface.

Soil type	GTC	MLG* [m] - soil surface	MHG** [m] - soil surface	Land use
Clay	I	< 0.50	(< 0.20)	Grassland
Loam	II	0.50 - 0.80	(< 0.40)	Corn
Sand	III	0.80 - 1.20	< 0.40	Arable land
Peat	IV	0.80 - 1.20	> 0.40	Orchard (fruit trees)
	V	> 1.20	< 0.40	Rural area
	VI	> 1.20	0.40 - 0.80	Urban area
	VII	(> 1.60)	> 0.80	

Table C.2
Regional approach. Long-term average reduction rates (R) to ET_p. Units in [mm a^{-1}].

| Soil type | GTC | Land use | | | | | |
		Grass	Corn	Arable	Orchard	Rural	Urban
Clay	I	0	0	0	0	0	0
	II	0	0	0	5	0	0
	III	5	10	10	10	4	5
	IV	10	15	15	15	8	9
	V	15	25	25	20	11	14
	VI	20	35	35	25	15	18
	VII	40	50	50	45	30	36
Loam	I	0	0	0	0	0	0
	II	5	0	0	10	4	5
	III	5	15	15	10	4	5
	IV	10	20	20	15	8	9
	V	20	30	30	25	15	18
	VI	50	40	40	55	38	45
	VII	60	55	55	65	45	54
Sand	I	0	0	0	0	0	0
	II	5	0	0	10	4	5
	III	5	5	10	10	4	5
	IV	15	15	20	20	11	14
	V	30	30	35	35	23	27
	VI	65	55	60	70	49	59
	VII	90	80	85	95	68	81
Peat	I	0	0	0	0	0	0
	II	11	0	0	16	8	10
	III	27	10	10	32	20	24
	IV	32	20	20	37	24	29
	V	63	35	35	68	47	57
	VI	72	60	60	77	54	65
	VII	98	95	95	103	74	88

Source: Werkgroep HELP-Tabel (1987).

D

FLEVOLAND POLDER AREA, HOGE AFDELING (HA REGION)

Table D.1
Flevoland polder, HA region. Parameters of sub-regions for Ernst-Bruggeman approach [II.5] and travel time distribution fractions f_τ. *Note that the actual value of I varies from year to year in model calculations.

Sub-region	$I_{\text{long term}}$* [mm a^{-1}]	d [m]	Φ_{eff} [-]	f_1 [-]	f_2 [-]	f_3 [-]	f_4 [-]	f_5 [-]
1	343	4	0.32	0.50	0.25	0.13	0.06	0.06
2	417	4	0.30	0.42	0.24	0.14	0.08	0.12
3	277	4	0.30	0.46	0.25	0.13	0.07	0.09
4	353	4	0.35	0.36	0.23	0.15	0.09	0.17
5	333	3	0.30	0.85	0.13	0.02	0.00	0.00
6	277	5	0.30	0.19	0.15	0.12	0.10	0.44

Table D.2
Flevoland polder, HA region. Sub-regions, dominant soil type, GTC, annual average
seepage rates [mm a^{-1}] and solute concentrations in seepage water C_{seep} in [mg l^{-1}].
*Total of deep seepage, seepage caught by subsurface drains and ditches, and seepage
pass below dikes.

Sub-region	Soil type	GTC	Q_{seep}	C_{seep}*		
				Cl$^-$	Total-N	Total-P
1	Loam	VI	525	175	0.5	0.2
2	Clay	VI	200	525	1.5	0.8
3	Clay	VI	455	60	2.0	0.4
4	Sand	VI	250	1330	3.0	2.0
5	Clay	VI	790	1190	2.5	1.5
6	Clay	VI	75	770	1.0	0.3

Source: Oostra (1996).

Table D.3

Flevoland polder, HA region. Average annual land-use related data. Units of Cl^-, total-N, and total–P in [kg ha^{-1} a^{-1}].

*Combined with corn cultivation on 10% of the area grassland.

Land use	Sub-region	f_c [-]	Fertilizer			Manure			Removed (harvest)		
			Cl^-	N	P	Cl^-	N	P	Cl^-	N	P
Grassland*	1,5	0.90	0	300	27	130	325	50	125	460	46
Arable	2	0.75	0	145	30	43	105	30	25	165	33
Orchard	3	1.00	0	100	20	0	0	0	5	75	8
Rural	4	1.00	0	0	0	0	0	0	2	25	1
(woodlands mainly)											
Urban	6	1.00	0	5	1	0	0	0	0	0	0

Table D.4

Flevoland polder, HA region. Estimated annual solute mass rates q_m by diffusion, mineralization, and denitrification. Units in [kg ha^{-1} a^{-1}]. *Negative numbers indicate net immobilization. **P-adsorption is expressed as the fraction of the P-balance surplus.

| Sub-region | $q_{m,\text{diffusion}}$ | | | $q^*_{m,\text{mineralization}}$ | | | $q_{m,\text{denitrification}}$ | P-adsorption** |
	Cl^-	Total-N	Total-P	Cl^-	Total-N	Total-P		[-]
1	150	2	0.001	2	-50	-5.0	85	0.995
2	150	2	0.001	3	30	3.0	65	0.995
3	150	2	0.001	3	15	1.5	30	0.995
4	5	1	0.0005	1	8	0.8	10	0.995
5	150	2	0.001	3	-50	-5.0	100	0.995
6	150	2	0.001	0	15	1.5	30	0.995

E

HUPSEL BROOK BASIN (HB REGION)

Table E.1

Hupsel brook basin, HB region. Parameters of sub-regions for Ernst-Bruggeman approach [II.5] and travel time distribution fractions f_τ. *Note that the actual value of I varies from year to year in model calculations.

Sub-region	$I_{\text{long term}}$* [mm a^{-1}]	d [m]	Φ_{eff} [-]	f_1 [-]	f_2 [-]	f_3 [-]	f_4 [-]	f_5 [-]
1	387	6	0.35	0.17	0.14	0.12	0.10	0.47
2	325	3	0.35	0.27	0.20	0.14	0.11	0.28
3	315	2	0.35	0.39	0.24	0.15	0.09	0.13
4	224	1	0.32	0.47	0.25	0.13	0.07	0.08
5	338	2	0.35	0.38	0.24	0.15	0.09	0.14

Table E.2
Hupsel brook basin, HB region. Sub-regions, dominant soil type and GTC, and long-term annual average surficial runoff rate $Q_{\text{surficial}}$ [mm a^{-1}].

Sub-region	Soil type	GTC	$Q_{\text{surficial}}$
1	Sand	V	7
2	Sand	IV	5
3	Loam	III	5
4	Sand	II	15
5	Sand	V	7

Table E.3
Hupsel brook basin, HB region. Average annual land-use related data used. Units of Cl$^-$, total-N, and total–P in [kg ha^{-1} a^{-1}].

Land use	Sub-region	f_c [-]	Fertilizer			Manure			Removed (harvest)		
			Cl$^-$	N	P	Cl$^-$	N	P	Cl$^-$	N	P
Grass	2,3,5	0.99	80	270	8	135	340	65	120	370	37
Corn	1	0.90	0	65	14	140	355	67	70	220	28
Arable	-	-	-	-	-	-	-	-	-	-	-
Orchard	-	-	-	-	-	-	-	-	-	-	-
Rural	4	1.00	0	0	0	0	0	0	2	25	1
Urban	-	-	-	-	-	-	-	-	-	-	-

Table E.4

Hupsel brook basin, HB region. Estimated annual solute mass rates q_m by diffusion, mineralization, and denitrification. Units in [kg ha^{-1} a^{-1}]. *Negative numbers indicate net immobilization. **P-adsorption is expressed as the fraction of the P-balance surplus.

Sub-region	$q_{m,\text{diffusion}}$			$q^*_{m,\text{mineralization}}$			$q_{m,\text{denitrification}}$	P-adsorption**
	Cl⁻	Total-N	Total-P	Cl⁻	Total-N	Total-P	[-]	
1	15	1	0.0001	1	5	0.5	100	0.980
2	15	1	0.0001	1	-2	-0.2	105	0.985
3	25	2	0.0001	2	0	0.0	115	0.960
4	25	1	0.0001	1	3	0.3	35	0.955
5	15	1	0.0001	1	-5	-0.5	110	0.980

BIBLIOGRAPHY

Allen, R.G., L.S. Pereira, D. Raes, and M. Smith, 1998
  Crop evapotranspiration. Guidelines for computing crop water requirements. Food and
  Agriculture Organization of the United Nations (FAO), FAO Irrigation and Drainage
  Paper No. 56.

Appelo, C.A.J., and D. Postma, 1993
  Geochemistry, groundwater and pollution. Published by:
  A.A. Balkema/Rotterdam/Boston, 1999. ISBN 90 5410 106 7.

Aslyng, H.C., 1986
  Nitrogen balance in crop production and groundwater quality. Agricultural Water
  Management, pp. 291-301. Editor: A.L.M. van Wijk and J. Wesseling. Published by:
  A.A. Balkema/Rotterdam/Boston, 1986.

Bach, M., and H.-G. Frede, 1998
  Agricultural nitrogen, phosphorus, and potassium balances in Germany: Methodology
  and Trends, 1970 to 1995. Zeitschrift für Pflanzenernährung und Bodenkunde,
  Vol. 161, pp. 385-393.

Bakker, H. de, 1979
  Major soils and soil regions in the Netherlands. Publisher: dr. W. Junk B.V. Publishers
  (The Hague, Boston, London), and Centre for Agricultural Publishing and
  Documentation (Wageningen).

Bear, J., and A. Verruijt, 1987
  Modeling groundwater flow and pollution. Theory and Applications of Transport in
  Porous Media Series. Published by: D. Reidel Publishing Company, 1987.

Beek, C.L. van, and O. Oenema, 2002
  Nutriëntenbalansen in de Vlietpolder in het jaar 1999. Alterra Report No. 482 (2002).

Bently, W.J., and R.W. Skaggs, 1993
  Changes in entrance resistance of subsurface drains. Journal of Irrigation and Drainage
  Engineering, Vol. 119, pp. 584-599.

Berkowitz, B., 1994
  Modeling flow and contaminant transport in fractured media. Advances in Porous
  Media Series, Vol. 2. Published by: Elsevier, 1994. Chapter 6, pp. 397-451.

Beven, K., and P.F. Germann, 1982
  Macropores and water flow in soils. Water Resources Research 18 (5), pp. 1311-1325
  (1982).

Boers, P.C.M., W.E.M. Laane, and L. van Liere, 1995
  Regionaal omgaan met landelijke normen. Landschap No. 6, pp. 15-21 (1995).

Boers, P.C.M., P.A. Finke, J.J.M. Van Grinsven, and P. Groenendijk, 1996
Definitie en haalbaarheid van een interdepartementaal model voor de berekening van nutrientenemissie naar grond- en oppervlaktewater. RIZA, Lelystad, RIVM, Bilthoven, SC-DLO, Wageningen, the Netherlands. SC-DLO, Interne mededeling No. 414.

Booltink, H.W.G., 1994
Field-scale distributed modeling of bypass flow in a heavily textured clay soil. Journal of Hydrology 163, pp. 65-84 (1994).

Boons-Prins, E.R., G.H.J. de Koning, C.A. van Diepen, and F.W.T. Penning de Vries, 1993
Crop specific simulation parameters for yield forecasting across the European Community, No. 32, CABO-DLO. Simulation Reports.

Bos, J.F.F.P., 2002
Specialised and mixed farming systems on marine silt loam soils in the Netherlands. An analysis of environmental and economic performance under current and future policy scenarios using linear programming. PhD Thesis, to be submitted to Wageningen University.

Bos, M.G. (ed.), 1989
Discharge measurement structures. Third revised edition. ILRI Publication, 20, 1989. ISBN 90 7075 415 0.

Bosdijk, T., 1997
GIS als instrument voor milieubeheer. MSc Thesis, Wageningen University, Dept. of Geographic Information Management and Remote Sensing.

Bouma, J., 1981
Soil morphology and preferential flow along macropores. Agricultural Water Management 3, pp. 235-250 (1981).

Boumans, L.J.M., C.R. Meinardi, and G.J.W. Krajenbrink, 1989
Nitraatgehalten en kwaliteit van het grondwater onder grasland in de zandgebieden. RIVM Report No. 728472013.

Bouten, W., 1992
Monitoring and modelling forest hydrological processes in support of acidification research. PhD Thesis, University of Amsterdam.

Bowman, R.S., J.L. Wilson, and P. Hu, 2001
Diffusion coefficients of hydrologic tracers measured by a Taylor dispersion technique. Department of Earth and Environmental Science, New Mexico Institute of Mining and Technology.

Braak, C., 1945
Influence of the wind on rainfall measurements. Royal Dutch Meteorological Institute (KNMI), Mededeelingen en Verhandelingen No. 48.

Braden, H., 1985
Energiehaushalts- und Verdünstungsmodell für Wasser- und Stoffhaushaltuntersuchungen landwirtschaftlich genutzter Einzugsgebiete. Mitteilungen der Deutschen Bodenkundlichen Gesellschaft, Vol. 42, pp. 254-299.

Brongers, I., K.P. Groen, G.A.P.H. van den Eertwegh, and C.R. Meinardi, 1996
Emissie van bestrijdingsmiddelen en nutrienten naar het oppervlaktewater via drainage. Ministry of Transport, Public Works and Water Management, Flevobericht No. 384.

Bronswijk, J.J.B., 1991
> Magnitude, modeling and significance of swelling and shrinkage processes in clay soils. PhD Thesis, Wageningen Agricultural University.

Bronswijk, J.J.B., W. Hamminga, and K. Oostindie, 1995
> Field-scale solute transport in a heavy clay soil. Water Resources Research 31 (3), pp. 517-526 (1995).

Bruggeman, G.A., 1999
> Analytical solutions of geohydrological problems. Elsevier Scientific Publishers, Amsterdam.

Brusseau, M.L., Z. Gerstl, D. Augustijn, and P.S.C. Rao, 1994
> Simulating solute transport in an aggregated soil with the dual-porosity model: measured and optimized parameter values. Journal of Hydrology 163, pp. 187-193 (1994).

Buishand, T.A., and C.A. Velds, 1980
> Neerslag en verdamping. Royal Dutch Meteorological Institute (KNMI), Series Klimaat van Nederland, No. 1.

Bruin, H.A.R. de, 1981
> The determination of (reference-crop) evapotranspiration from routine weather data. CHO-TNO, the Netherlands. Proceedings and Information No. 28, pp. 25-37 (1981).

Bruin, H.A.R. de, 1987
> From Penman to Makkink. In: Evaporation and Weather, pp. 5-31. CHO-TNO, the Netherlands.

CBS, 1991
> Milieufacetten, cijfers bij de tweede nationale milieuverkenning, 1991. CBS-publicaties, 1991.

CBS, 1996
> Milieustatistieken voor Nederland, 1994. CBS-publicaties, 1996.

Celia, M.A., E.T. Bouloutas, and R.L. Zarba, 1990
> A general mass-conservative numerical solution for the unsaturated flow equation. Water Resources Research 26 (7), pp. 1483-1496 (1990).

CHO-TNO, 1987
> Evaporation and weather. Proceedings and Information No. 39. Netherlands Organization for Applied Scientific Research, Committee on Hydrological Research.

Colenbrander, H.J., and Ph.Th. Stol, 1970
> Neerslag en neerslagverdeling naar plaats en tijd. Deelrapport 5 van het Hydrologisch Onderzoek in het Leerinkbeekgebied. Provincie Gelderland, Arnhem.

Corré, W.J., 1995
> Denitrificatie in poldergronden. Verslag van een onderzoek naar het belang van denitrificatie in de stikstofhuishouding van poldergronden en het mogelijke effect van peilverhoging op de denitrificatie, uitgevoerd in opdracht van de provincie Zeeland. Rapport 41, AB-DLO.

Dagan, G., 1989
> Flow and transport in porous formations. Publisher: Springer Verlag, Berlin. ISBN 3-540-51098-2.

Dam, J.C. van, 2000
> Field-scale water flow and solute transport. PhD Thesis, Wageningen University.

Dam, J.C. van, J.H.M. Wösten, and A. Nemes, 1996
> Unsaturated soil water movement in hysteretic and water repellent field soils. Journal of Hydrology, Vol. 184, pp. 153-173 (1996).

Dam, J.C. van, J. Huygen, J.G. Wesseling, R.A. Feddes, P. Kabat, P.E.V. van Walsum, P. Groenendijk, and C.A. van Diepen, 1997
> Theory of SWAP Version 2.0. Simulation of water flow, solute transport and plant growth in the soil-water-atmosphere-plant environment. Wageningen Agricultural University, Dept. of Water Resources. Report 71.

Dekker, C.G., 1979
> Een onderzoek naar de grootte van de systematische windfout van de standaard regenmeter. Royal Dutch Meteorological Institute (KNMI), Verslagen V-317.

Dekker, L.W., 1998
> Moisture variability resulting from water repellency in Dutch soils. PhD Thesis, Wageningen Agricultural University.

Dooremolen, W.A. van, A. van der Scheer, and H.J. Swinkels, 1996
> Waarnemingen en prognoses van de maaiveldsdaling in Flevoland. Rijkswaterstaat, Directie IJsselmeergebied. Flevobericht No. 388.

Drecht, G. van, 1985
> Toetsing van model ONZAT m.b.v. meetgegevens uit het hydrologisch proefgebied Hupselse beek. RIVM Report No. 847211001.

Dufour, F.C., 1998
> Grondwater in Nederland. Onzichtbaar water waarop wij lopen. In the series: Geologie van Nederland, deel 3. Published by: NITG TNO, Delft, 1998.

Duin, R.H.A. van, and G. de Kaste, 1989
> The pocket guide to the Zuyder Zee project. Ministry of Transport and Public Works. ISBN 90 6914 012 8.

Duin, E.H.S. van, and A.H. Dijkhuis, 1992
> De belasting van grond- en oppervlaktewater met nutriënten in Flevoland. Report, Wageningen University, Department of Water Quality Management and Aquatic Ecology.

Eertwegh, G.A.P.H. van den, and C.R. Meinardi, 1999
> Water- en nutriëntenhuishouding van het stroomgebied van de Hupselse beek. RIVM, National Institute of Public Health and the Environment, Report No. 714901005.

Eertwegh, G.A.P.H. van den, J.R. Hoekstra, and C.R. Meinardi, 1999
> Praktijkproef Nutrientenbalans: nutrientenbelasting oppervlaktewater via drainage van akkerbouwpercelen op zavel. Wageningen Agricultural University, Dept. of Water Resources. Report 75.

Eertwegh, G.A.P.H. van den, J.L. Nieber, and R.A. Feddes, 2001
> Multidimensional flow and transport in a drained, dual-porosity soil. ASAE 2nd International Symposium and Exhibition on Preferential Flow, Hawaï, 2001.

Ente, P.J., J. Koning, and R. Koopstra, 1986
> De bodem van oostelijk Flevoland. Ministry of Transport, Public Works and Water Management, Flevobericht No. 258.

Ernst, L.F., 1973
> De bepaling van de transporttijd van het grondwater bij stroming in de verzadigde zone. ICW Wageningen, ICW Nota No. 755.

European Community, 1991
> Richtlijn 1991/676/EC van de Raad van 12 december 1991 inzake de bescherming van water tegen verontreiniging door nitraten uit agrarische bronnen. Nitrates Directive (91/676/EC).

European Community, 2000
> Directive 2000/60/EC of the European Parliament and of the Council of 23 October 2000 establishing a framework for Community action in the field of water policy.

Faassen, H.G. van, and G. Lebbink, 1990
> Nitrogen cycling in high-input versus reduced-input arable farming. Netherlands Journal of Agricultural Science 38, pp. 265-282 (1990).

FAO, 1999
> Yearbook on Fertilizers. FAO, Rome.

Feddes, R.A., P.J. Kowalik, and H. Zaradny, 1978
> Simulation of field water use and crop yield. In the series Simulation Monographs. Published by: Pudoc Wageningen, 1978.

Feddes, R.A., 1987
> Crop factors in relation to Makkink reference-crop evapotranspiration. Evaporation and Weather, pp. 33-45. CHO-TNO, the Netherlands. Proceedings and Information No. 39.

Foppen, J.W., and J. Griffioen, 1995
> Contribution of groundwater outflow to the phosphate balance of ditch water in a Dutch polder. Man's Influence on Freshwater Ecosystems and Water Use, pp. 177-184. IAHS, Proceedings No. 230.

Frouws, J., 1993
> Mes en Macht. Een politiek-sociologische studie naar belangenbehartiging en beleidsvorming inzake de mestproblematiek in Nederland vanaf, 1970. Published by Wageningen Agricultural University. Studies van Landbouw en Platteland 11. ISBN 90 6754 309 8.

Gardner, C.M.K., J.P. Bell, J.D. Cooper, W.G. Darling, and C.E. Reeve, 1991
> Groundwater recharge and water movement in the unsaturated zone. Applied Groundwater Hydrology: A British Perspective. Ch. 5, pp. 54-76. Clarendon Press, Oxford

Gelhar, L.W., C. Welty, and K.R. Rehfeldt, 1992
> A critical review of data on field-scale dispersion in aquifers. Water Resources Research 28 (7), pp. 1955-1974 (1992).

Gerke, H.H., and M.Th. van Genuchten, 1993a
> A dual-porosity model for simulating the preferential movement of water and solutes in structured porous media. Water Resources Research 29 (2), pp. 305-319 (1993).

Gerke, H.H., and M.Th. van Genuchten, 1993b
Evaluation of a first-order water transfer term for variably saturated dual-porosity flow models. Water Resources Research 29 (4), pp. 1225-1238 (1993).

Germann, P.J., and L. DiPietro, 1996
When is porous-media flow preferential? A hydromechanical perspective. Geoderma 74, pp. 1-21 (1996).

Golub, G.H., and Ch.F. van Loan, 1989
Matrix Computations. Second Edition. Series: John Hopkins Series in the Mathematical Sciences (3). Published by: The John Hopkins University Press, Baltimore and London, 1989.

Groen, K.P., and H.G. Dekkers, 1990
Een installatie voor de bemonstering van verontreinigd drainwater. Rijkswaterstaat Directie Flevoland. Intern rapport No., 1990-28 liw.

Groen, K.P., 1997
Pesticide leaching in polders. Field and model studies on cracked clays and loamy sand. PhD Thesis, Wageningen Agricultural University.

Hassink, J., and J.J. Neeteson, 1991
Effect of grassland management on the amounts of soil organic N and C. Netherlands Journal of Agricultural Science, Vol. 39, pp. 225-236 (1991).

Hassink, J., 1995
Organic matter dynamics and N mineralization in grassland Soils. PhD Thesis, Wageningen Agricultural University.

Heimovaara, T.J., and W. Bouten, 1990
A computer-controlled 36-channel time domain reflectometry system for monitoring soil water contents. Water Resources Research 26 (3), pp. 2311-2316 (1990).

Hetterschijt, R.A.A., J. Griffioen, J.W.A. Foppen, and E.A. Buijs, 1995
Hydrogeochemie van fosfaat bij kwel van grondwater in polders. Deelrapport III: Hydrogeochemische processen rondom vier slootbodems in laag-Nederland. TNO-GG (NITG) Rapport No. GG-R-95-69(A)

Hetterschijt, R.A.A., P.G.B. de Louw, J.W.A. Foppen, J. Griffioen, and R.J. Stuurman, 1997
Fosfaatbelasting van oppervlaktewater door grondwaterkwel. Deel II: Methoden voor de bepaling van de fosfaatbelasting. H_2O (30) No. 12, pp. 602-605 (1997).

Hoogvliet, M., 1994
Water- en stikstofhuishouding Flevoland. MSc thesis, Utrecht University, Dept. of Physical Geography.

IAEA, Editorial Staff, 1991
Isotope techniques in water resources development. IAEA, Vienna, Austria, 1991.

James, L.G., 1987
Principles of farm irrigation system design. John Wiley and Sons, New York (USA).

Jong, S. de, 1972
Over de uitspoeling van fosfaten van landbouwgronden in oostelijk Flevoland. Interne mededeling 289, Rijkswaterstaat, Rijksdienst voor de IJsselmeerpolders (RIJP).

Jong, S. de, 1980

De samenstelling van het drain- en slootwater in relatie tot de mestgift op twee weidebedrijven in sectie W in oostelijk Flevoland. Werkdocument No. 1980-297 Abw. Rijkswaterstaat, Rijksdienst voor de IJsselmeerpolders (RIJP).

Jong, S. de, 1983

De kwaliteit van het drain- en slootwater in Flevoland. RIJP Rapport No. 1983-5 Abw. Rijkswaterstaat, Rijksdienst voor de IJsselmeerpolders (RIJP).

Jury, W.A., 1975a

Solute travel-time estimates for tile-drained fields: I. Theory. Soil Science Society of America Proceedings 39, pp. 1020-1024 (1975).

Jury, W.A., 1975b

Solute travel-time estimates for tile-drained fields: II. Application to experimental studies. Soil Science Society of America Proceedings 39, pp. 1024-1028 (1975).

Jury, W.A., W.R. Gardner, and W.H. Gardner, 1991

Soil Physics. Fifth edition. John Wiley & Sons, Inc.

Jury, W.A., and H. Flühler, 1992

Transport of chemicals through soil: mechanisms, models, and field application. Advances in Agronomy, Vol. 47, pp. 141-201. Academic Press, Inc.

Kirkham, D., 1949

Flow of ponded water into drain tubes in soil overlying an impervious layer. Transactions of the American Geophysical Union 30 (3), pp. 369-385 (1949).

Kirkham, D., 1958

Seepage of steady rainfall through soil into drains. Transactions of the American Geophysical Union 39 (5), pp. 892-908 (1958).

Klapwijk, Sj.P., 1988

Eutrophication of surface waters in the Dutch polder landscape. PhD Thesis, Delft University of Technology, the Netherlands.

Klavers, H., and A. de Vries, 1993

Vrachtberekeningsmethoden, een casestudy voor Maas en Rijn. Ministry of Transport, Public Works, and Water Management, RIZA Werkdocument 93.021X.

Klein, C.A.M. de, 1994

Denitrification in grazed grasslands in the Netherlands. PhD Thesis, Utrecht University.

Klute, A., 1986

Water retention: laboratory methods. Methods of soil analysis: part 1; Physical and mineralogical methods. A. Klute (ed.), ASA and SSSA Agronomy Series No. 9, Madison, Wisconsin, pp. 635-662.

Kolenbrander, G.J., 1971

De eutrofiering van oppervlaktewater door de landbouw en de stedelijke bevolking. Stikstof, pp. 384-395 (1971).

Kolenbrander, G.J., and T.A. van Dijk, 1972

Eutrofiëring van oppervlaktewater door de landbouw in het stroomgebied van de Hupselse Beek. Report No. 12, Institute for Soil Fertility (currently PRI).

Kolenbrander, G.J., 1981
 Leaching of nitrogen in agriculture. Nitrogen losses and surface run-off, pp. 199-221.
 Editor: Brogan, J.C., published by ECSC, EEC, EAEC, Brussels – Luxembourg.

Kroon, T., P. Finke, I. Peereboom, and A. Beusen, 2001
 Redesign STONE. De nieuwe schematisatie voor STONE: de ruimtelijke indeling en
 toekenning van hydrologische en bodemchemische aspecten. Ministry of Public Works
 and Water Management RIZA, Alterra, and RIVM, the Netherlands. RIZA, Report No.
 2001.017.

Kuiper, P.J.C., 1996
 Gewasbeschermingsmiddelen en nutriënten in het uitslagwater van oostelijk en
 zuidelijk Flevoland. Rijkswaterstaat RIZA, Nota No. 96.029.

López, E., A. Núñez, and F. Díaz-Fierros, 1992
 Utilizacion del cloruro como medida de la capacidad dispersante de continaminantes en
 suelos. Conferencias Plenarias Comunicaciones, pp. 51-56. Sociedad Española de la
 Ciencia del Suelo, Departamento de Edafologia, Universidad de Navarra, Navarra,
 España.

Lotse, E.G., J.D. Jabro, K.E. Simmons, and D.E. Baker, 1992
 Simulation of nitrogen dynamics and leaching from arable soils. Journal of
 Contaminant Hydrology 10, pp. 183-196 (1992).

Louw, P.G.B. de, R.A.A. Hetterschijt, J.W.A. Foppen, J. Griffioen, and R.J. Stuurman, 1997
 Fosfaatbelasting van oppervlaktewater door grondwaterkwel. Deel I: Geohydrologische
 en geochemische processen. H_2O (30) No. 20, pp. 598-601 (1997).

Makkink, G.F., 1957
 Testing the Penman formula by means of lysimeters. Journal of the Institution of Water
 Engineers 11, pp. 277-288 (1957).

Makkink, G.F., 1960
 De verdamping uit vegetaties in verband met de formule van Penman. CHO-TNO
 Verslagen en Mededelingen No. 4, pp. 90-115 (1960).

Matthess, G., 1982
 The properties of groundwater. Published by: John Wiley and Sons, Inc., 1982.

Meer, H.G. van der, 1991
 Stikstofbalansen. Stikstofbenutting en -verliezen van gras- en maisland. Stand van
 zaken in het onderzoek naar de stikstofproblematiek van gras- en maisland. Editor:
 H.G. van der Meer. Published by: Ministerie van Landbouw, Natuurbeheer, en Visserij,
 DLO, 1991.

Meinardi, C.R., C. van den Akker, C.J. Dekker, G.J. Heij, and J.W. Kieft, 1978
 Geohydrologische gegevens van zuidelijk Flevoland en de Gelderse Vallei. RID,
 mededeling 784.

Meinardi, C.R., 1985
 Groundwater in the Netherlands. RIVM Report LBG 85-192.

Meinardi, C.R., 1991
 De stroom van voedingsstoffen (stikstof, fosfor, kalium) van de bodem naar het kleine
 open water. RIVM Report No. 724903004.

Meinardi, C.R., 1994
> Groundwater recharge and travel times in the sandy regions of the Netherlands. PhD Thesis, Free University Amsterdam. RIVM Report No. 715501004.

Meinardi, C.R., and G.A.P.H. van den Eertwegh, 1995
> Onderzoek aan drainwater in de kleigebieden van Nederland. Deel I: Resultaten van het veldonderzoek. RIVM Report No. 714901007.

Meinardi, C.R., and G.A.P.H. van den Eertwegh, 1997
> Onderzoek aan drainwater in de kleigebieden van Nederland. Deel II: Gegevens van het oriënterend onderzoek. RIVM Report No. 714801013.

Meinardi, C.R., C.G.J. Schotten, and J.J. de Vries, 1998a
> Grondwateraanvulling en oppervlakkige afstroming in Nederland. Langjaarlijkse gemiddelden voor de zand- en leemgebieden. In : Stromingen No. 3, pp. 27-41 (1998).

Meinardi, C.R., G.A.P.H. van den Eertwegh, and C.G.J. Schotten, 1998b
> Grondwateraanvulling en oppervlakkige afstroming in Nederland. Deel 2: De ontwatering van kleigronden. Stromingen No. 4, pp. 5-19 (1998).

Meurs, E.J.J., and R. Booij, 1999
> Variatie in afvoer van stikstof en fosfaat bij aardappel, suikerbiet en prei. AB-DLO, Wageningen, Report No. 158.

Mook, W.G., 1994
> Principles of Isotope Hydrology. Lecture Notes Free University, Amsterdam.

Mualem, Y., 1974
> A conceptual model of hysteresis. Water Resources Research Vol. 10, pp. 514-520.

Neff, E.L., 1977
> How much rain does a rain gage gage? Journal of Hydrology 35, pp. 213-220 (1977).

NHV, 1998
> Water in the Netherlands. Netherlands Hydrological Society (NHV)- special 3.

Nieber, J.L., and D. Misra, 1995
> Modeling flow and transport in heterogeneous, dual-porosity drained soils. Irrigation and Drainage Systems 9, pp. 217-237 (1995).

Nieber, J.L., G.A.P.H. van den Eertwegh, and R.A. Feddes, 1998
> Modeling multidimensional water flow and solute transport in dual-porosity soils. ASAE 7th Drainage Symposium, Proceedings 'Drainage in the 21st Century: Food Production and the Environment', Florida, 1998.

Nijland, G.O., and J. Schouls, 1997
> The relation between crop yield, nutrient uptake, nutrient surplus, and nutrient application. Wageningen Agricultural University Papers 97-3.

Oenema, O., and C.W.J. Roest, 1997
> Nitrogen and phosphorus losses from agriculture into surface waters. Eutrophication Research, Vol. 2, pp. 13-25.

Oenema, O., P.C.M. Boers, M.M. van Eerdt, B. Fraters, H.G. van der Meer, C.W.J. Roest, J.J. Schröder, and W.J. Willems, 1997
> The nitrate problem and nitrate policy in the Netherlands. AB-DLO Nota 88.

Oenema, O., and M. Heinen, 1999
Uncertainties in nutrient budgets due to biases and errors. Nutrient disequilibria in Agroecosystems, pp. 75-97.

Oenema, O., H. Kros, and W. de Vries, 2001
Approaches and uncertainties in nutrient budgets: implications for nutrient management and environmental policies. European Journal of Soil Science (in press).

Ommen, H.C. van, 1988
Transport from diffuse sources of contamination and its application to a coupled unsaturated-saturated system. PhD Thesis, Wageningen Agricultural University.

Oostindie, K., and J.J.B. Bronswijk, 1995
Consequences of preferential flow in cracking clay soils for contamination-risk of shallow aquifers. Journal of Environmental Management 43, pp. 359-373 (1995).

Oostra, J.W.J., 1996
De water- en stofbalansen voor stikstof, fosfor en chloride in de Flevopolder. MSc Thesis, Utrecht University, Dept. of Geochemistry.

Philip, J.R. and D.A. de Vries, 1957
Moisture movement in soils under temperature gradients. Transactions of the American Geophysical Union No. 38, pp. 222-228.

Ploeg, J.D. van der, 1999
De virtuele boer. Van Gorcum & Comp. B.V. ISBN 90 2323 496 0.

Ray, C., C.W. Boast, T.R. Ellsworth, and A.J. Valocchi, 1996
Simulation of the impact of agricultural management practices on chemical transport in macroporous soils. Transactions of the ASAE 39 (5), pp. 1697-1707 (1996).

Ray, C., T.R. Ellsworth, A.J. Valocchi, and C.W. Boast, 1997
An improved dual porosity model for chemical transport in macroporous soils. Journal of Hydrology, 193, pp. 270-292 (1997).

Ridder, N.A. de, and G. Zijlstra, 1994
Seepage and groundwater flow. Drainage principles and applications, 2nd edition, ILRI-Publications 16, published by: International Institute for Land Reclamation and Improvement (ILRI), 1994. Chapter 9, pp. 305-340.

Riemsdijk, W.H. van, 1990
Phosphate saturation of dutch sandy soils. In book 'Dierlijke mest, problemen en oplossingen', edited by P. del Castilho, W.H. Rulkens, and W. Salomons, pp. 223-245.

Ritsema, C.J., 1998
Flow and transport in water repellent sandy soils. PhD Thesis, Wageningen Agricultural University.

RIVM, 1995
Milieubalans, 1995. National Institute for Public Health and Environment. Published by: Samson H.D. Tjeenk Willink B.V., Alphen aan den Rijn (NL), 1995.

RIVM, 2001
Milieubalans, 2001. National Institute for Public Health and Environment. Published by: Kluwer B.V., Alphen aan den Rijn (NL), 2001.

RIVM and KNMI, 1989
    Netherlands precipitation chemistry network. Monitoring results, 1988. Report
    No. 228703012, RIVM, National Institute for Public Health and Environment and
    KNMI, Royal Dutch Meteorological Service, 1989.

Rolston, D.E., P.S.C. Rao, J.M. Davidson, and R.E. Jessup, 1984
    Simulation of denitrification losses of nitrate fertilizer applied to uncropped, cropped,
    and manure-amended field plots. Soil Science 137 (4), pp. 270-279 (1984).

Rooij, G.H. de, 1996
    Preferential flow in water-repellent sandy soils. PhD Thesis, Wageningen Agricultural
    University.

Ruygh, E.F.W., P.S. Grashoff, C.F. Hopstaken, and J.P.M. Witte, 1990
    Verification of DEMNIP on data from the Hupselse beek research basin. Hydrological
    Research Basins and the Environment, pp. 261-270. Editors: Hooghart, J.C., C.W.S.
    Posthumus, and P.M.M. Warmerdam. Published by NITG TNO Delft, the Netherlands.

Querner, E.P., 1993
    Aquatic weed control within an integrated water management framework. PhD Thesis,
    Wageningen Agricultural University.

Saad, Y., 1996
    Iterative methods for sparse linear systems. PWS Publishing Co., Boston.

Salm, C. van der, A. Breeuwsma, J.G.A. Reijerink, R.F.A. Hendriks, and J.G. Wesseling, 1995
    Fosfaatverliezen door uitspoeling in relatie tot het fosfaatoverschot en de
    bemestingstoestand. Een onderzoek in het kader van de P-desk studie. SC-DLO, Report
    No. 389.

Schils, R.L.M., 1994
    Nitrate losses from grazed grass and grass/clover pastures on clay soil. Meststoffen,
    1994, pp. 78-84.

Schoumans, O.F., A. Breeuwsma, A. El Bachrioui-Louwerse, and R. Zwijnen, 1991
    De relatie tussen de bodemvruchtbaarheidsparameters Pw- en P-AL-getal en
    fosfaatverzadiging bij zandgronden. SC DLO, Wageningen, Report No. 112.

Schoumans, O.F., 1997
    Relation between phosphate accumulation, soil P levels, and P leaching in agricultural
    land. SC-DLO, Wageningen, the Netherlands. Report No. 146.

Schoumans, O.F. and P. Groenendijk, 2000
    Modeling soil phosphorus levels and phosphorus leaching from agricultural land in the
    Netherlands. Journal of Environmental Quality, Vol. 29, pp. 111-116.

Schröder, J.J., P. van Asperen, G.J.M. van Dongen, and F.G. Wijnands, 1993
    Nutrientenbenutting en -verlies bij akkerbouwgewassen: een theoretische verkenning.
    Deelstudie voor het project 'Introductie geïntegreerde akkerbouw'. Verslag 186,
    AB-DLO, 1993.

Schröder, J.J., P. van Asperen, G.J.M. van Dongen, and F.G. Wijnands, 1994
    Nutrientenbenutting en -verlies op de innovatiebedrijven geïntegreerde akkerbouw:
    Resultaten, 1990-1993. Deelstudie voor het project 'Introductie geïntegereerde
    akkerbouw'. Rapport 26, AB-DLO, 1994.

Schröder, J.J., 1999
    Mineralenbalansen in relatie tot bouwplan en bemestingsstrategie: een voorverkenning
    voor aangepaste bedrijfsopzetten voor akkerbouw en vollegrondsgroenteteelt op
    zandgrond. AB-DLO, Wageningen, Report No. 154.
Schröder, J.J., and W.J Corré (eds.), 2000
    Actualisering stikstof- en fosfaat- desk-studies. Plant Research International (PRI) B.V.,
    Wageningen, the Netherlands. Report 22.
Schultz, E., 1992
    Waterbeheersing van de Nederlandse droogmakerijen. PhD Thesis, Delft University of
    Technology.
Stouthart, F., and J. Leferink, 1992
    Mineralenboekhouding, inclusief werkboeken voor begeleider en deelnemer. CLM,
    Utrecht.
Stricker, J.N.M., 1981
    Methods of estimating evapotranspiration from meteorological data and their
    applicability in hydrology. Evaporation in Relation to Hydrology, pp. 59-77. CHO-TNO,
    the Netherlands.
Stricker, J.N.M., and W. Brutsaert, 1978
    Actual evapotranspiration over a summer period in the Hupsel catchment. Journal of
    Hydrology 39, pp. 139-157 (1978).
Studiegroep Hupselse beek, 1971
    Hydrologic research in the catchment of the Hupselse Beek, the Netherlands.
    Studiegroep Hupselse beek. Biannual Report 1,1971.
Supèr, J., 1990
    IJking CP versus NEA neutronensonde. DBW-RIZA, Werkdocument 90.077X.
Thunnissen, H.A.M., 1987a
    Oppervlakte-afvoer: hoeveelheid en samenstelling. RIVM Report No. 728472003.
Thunnissen, H.A.M., 1987b
    Eenvoudige methode voor de schatting van verblijftijden van grondwater in de
    verzadigde zone. RIVM Report No. 728472002.
Topp, G.C., J.L. Davis, and A.P. Annan, 1980
    Electromagnetic determination of soil water content: measurement in coaxial
    transmission lines. Water Resources Research 16 (1), pp. 574-582 (1980).
Ven, F.H.M. van de, 1989
    Waterbeheersing stedelijke gebieden. Lecture notes Delft University of Technology.
Ven, G.P. van de, 1993
    Leefbaar laagland. Geschiedenis van de waterbeheersing en landaanwinning in
    Nederland. Published by Uitgeverij Matrijs (NL).
Vissenberg, H.A., 1995
    Bepaling van een aantal kenmerken voor de nitraatbepaling in grondwater met de
    Nitracheck. RIVM Bilthoven, Report No. 712601001.
Volker, A. and W.H. van der Molen, 1991
    The influence of groundwater currents on diffusion processes in a lake bottom: an old
    report reviewed. Journal of Hydrology, Vol. 126, pp. 159-169 (1991).

Vos, J.A. de, 1997
Water Flow and nutrient transport in a layered silt loam soil. PhD Thesis, Wageningen Agricultural University.

Vos, J.A. de, 2001
Monitoring nitrate leaching from submerged drains. Journal of Environmental Quality, Vol. 30, No. 3, pp. 1092-1096 (2001).

Watson, C., and D. Atkinson, 1999
Using nitrogen budgets to indicate nitrogen use efficiency and losses from whole farm systems: a comparison of three methodological approaches. Nutrient Cycling in Agroecosystems 53, pp. 259-267.

Wendroth, O., W. Ehlers, J.W. Hopmans, H. Kage, J. Halbertsma, and J.H.M. Wösten, 1993
Reevaluation of the evaporation method for determining hydraulic functions in unsaturated soils. Soil Science Society of America Journal 57, pp. 1426-1443 (1993).

Werkgroep HELP-Tabel, 1987
De invloed van de waterhuishouding op de landbouwkundige produktie. Mededelingen Landinrichtingdienst No. 176.

Werkgroep Herziening Cultuurtechnisch Vademecum, 1988
Cultuurtechnisch Vademecum. Cultuurtechnische Vereniging.

Werkman, W.J., 1995
Lage afvoeren in het stroomgebied van de Hupselse Beek. Een analyse met het geintegreerde grond- en oppervlaktewaterstromingsmodel MOGROW. Scriptie Vakgroep Waterhuishouding/Interne mededeling 378, Staring Centrum.

Wessel, W., 1987
Measurement of total and denitrifying biomass in soil and the improvement of a model of denitrification in soil. Dept. of Theoretical Production Ecology, Wageningen Agricultural University, the Netherlands, Report, 1987-11.

Willems, W.J., and B. Fraters, 1995
Naar afgestemde kwaliteitsdoelstellingen voor nutriënten in grondwater en oppervlaktewater. Discussienotitie. RIVM Report No. 714901003.

Wolters, H.A., 1996
Neerslag en afvoer in het landelijk gebied van Flevoland. Ministry of Transport, Public Works and Water Management. Flevobericht No. 357.

Wösten, J.H.M., G.H. Stoffelsen, J.W.M. Jeurissen, A.F. van Holst, and J. Bouma, 1983
Proefgebied Hupselse Beek: regionaal bodemkundig en bodemfysisch onderzoek. Stichting voor Bodemkartering, Report No. 1706.

Wunderink, S.E., 1996
De belasting van het Nederlandse oppervlaktewater met fosfaat en stikstof. Het Waterschap, Vol. 9, pp. 304-311 (1996).

Zee, S.E.A.T.M. van der, 1988
Transport of reactive contaminants in heterogeneous soil systems. PhD Thesis, Wageningen Agricultural University.

LIST OF PUBLICATIONS

Luft, G., G.A.P.H. van den Eertwegh, and H.-J. Vieser, 1990
Veränderung der Bodemsee-Wasserstände von 1887 bis 1987 (in German). LfU Baden-Württemberg, Karlsruhe. Handbuch Hydrologie Baden-Württemberg, Teil 6, 6.2 Berichte, 1990.

Luft, G., and G.A.P.H. van den Eertwegh, 1990
Long-term changes in water level of Lake Constance and possible causes. Annex to Proceedings and Information No. 44, pp. 21-40 (1990). CHO TNO Committee on Hydrological Research, the Netherlands.

Luft, G., and G.A.P.H. van den Eertwegh, 1991
Long-term changes in the water level of Lake Constance and possible causes. IAHS Symposium Hydrology of Natural and Man-made Lakes, Vienna, 1991. IAHS Publication No. 206, 1991.

Eertwegh, G.A.P.H. van den, 1992
Voorspellingen waterstand en afvoer Rijn. Ministry of Public Works and Water Management, RIZA, Lelystad, the Netherlands. RIZA Report No. 92.006.

Eertwegh, G.A.P.H. van den, and P.M.M. Warmerdam, 1993
Storm runoff and nutrient transport from a drained plot in the Hupsel catchment. Second International Conference on Friend, Braunschweig,1993. Editor: A. Herrmann, TU Braunschweig, Germany.

Eertwegh, G.A.P.H. van den, 1994
Transport of nutrients to small surface waters through drainage. IAHR Symposium Transport and Reactive Processes in Aquifers, Switserland, 1994, Proceedings, pp. 255-261.

Eertwegh, G.A.P.H. van den, and A.L. Mugie, 1994
Korte termijn voorspellingen waterstand en afvoer Bovenrijn te Lobith. H_2O (27) 1994, No. 5.

Meinardi, C.R., and G.A.P.H. van den Eertwegh, 1995
Onderzoek aan drainwater in de kleigebieden van Nederland. Deel I: Resultaten van het veldonderzoek. RIVM Report No. 714901007.

Brongers, I., K.P. Groen, G.A.P.H. van den Eertwegh, and C.R. Meinardi, 1996
Emissie van bestrijdingsmiddelen en nutrienten naar het oppervlaktewater via drainage. Ministry of Transport, Public Works and Water Management, Flevobericht No. 384.

Meinardi, C.R., and G.A.P.H. van den Eertwegh, 1997
Onderzoek aan drainwater in de kleigebieden van Nederland. Deel II: Gegevens van het oriënterend onderzoek. RIVM Report No. 714801013.

Meinardi, C.R., G.A.P.H. van den Eertwegh, and C.G.J. Schotten, 1998
Grondwateraanvulling en pppervlakkige afstroming in Nederland. Deel 2: De ontwatering van kleigronden. In: Stromingen 4, pp. 5-19 (1998).

Nieber, J.L., G.A.P.H. van den Eertwegh, and R.A. Feddes, 1998
> Modeling multidimensional water flow and solute transport in dual-porosity soils. ASAE 7th Drainage Symposium Proceedings 'Drainage in the 21st Century: Food Production and the Environment', Florida, 1998.

Eertwegh, G.A.P.H. van den, and C.R. Meinardi, 1999
> Water- en nutriëntenhuishouding van het stroomgebied van de Hupselse Beek. RIVM, National Institute of Public Health and the Environment, report Number: 714901005. Wageningen Agricultural University, Dept. of Water Resources. Report 74.

Eertwegh, G.A.P.H. van den, J.R. Hoekstra, and C.R. Meinardi, 1999
> Praktijkproef Nutrientenbalans: Nutrientenbelasting oppervlaktewater via drainage van akkerbouwpercelen op zavel. Wageningen Agricultural University, Dept. of Water Resources. Report 75.

Louw, P.G.B. de, G.A.P.H. van den Eertwegh, and J. Griffioen, 2000
> High nutrient and chloride loads to surface waters in polder areas due to groundwater seepage. Proceedings of the XXX IAH Congress on Groundwater: Past achievements and future challenges. Cape Town, South Africa, 2000. A.A. Balkema Publishers, Rotterdam-Brookfield.

Eertwegh, G.A.P.H. van den, J.L. Nieber, and R.A. Feddes, 2001
> Multidimensional flow and transport in a drained, dual-porosity soil. ASAE 2nd International Symposium and Exhibition on Preferential Flow, Hawaï, 2001.

Louw, P.G.B. de, J. Griffioen, G.A.P.H. van den Eertwegh, and B. Calf, 2002
> High nutrient and chloride loads in polder areas due to groundwater exfiltration. 2nd International Conference on New Trends in Water and Environmental Engineering for Safety and Life: Eco-compatible Solutions for Aquatic Environments, Capri, Italy, June 24-28, 2002.

CURRICULUM VITAE

Gé van den Eertwegh werd op 1 april 1966 geboren te Helden-Panningen. Op zijn zevende verhuisde hij naar Baarlo waar hij de lagere school vervolgde. In 1978 trok hij naar het Collegium Marianum te Venlo, waar hij 6 jaar later het Gymnasium-β diploma behaalde. Een studie aan de Landbouwuniversiteit te Wageningen (LUW) volgde, Cultuurtechniek werd de studierichting, met als specialisatie Hydrologie en Waterbeheer. Hij liep stage bij de Landesanstalt für Umweltschutz te Karlsruhe, Baden-Württemberg (BRD), later bij Grontmij NV te De Bilt. Zijn afstudeervakken betroffen de afvoerhydrologie, de herkomst van meststoffen in het watermilieu, en de geohydrologie. In augustus 1990 studeerde hij af en eind 1990 kwam er werk in zicht bij het RIZA te Lelystad. Een tijdelijke klus viel hem ten deel, meewerken aan de verbetering van de korte-termijn voorspellingen van de waterstand en afvoer van de Bovenrijn te Lobith. (Gelukkig werd later met de gemaakte computermodellen de hoogwatergolf van 1995 aardig goed voorspeld, al kon hij dat vanuit de VS niet goed meemaken, terwijl zijn thuishaven te Tiel ontruimd werd.) Tegen de afloop van het kontrakt bij het RIZA kwam er begin 1992 een AIO-plaats beschikbaar bij de LUW, gefinancierd door het RIVM, met de toevoeging dat vrouwelijke kandidaten de voorkeur zouden krijgen. Toch geschreven en toch gekregen, en de werkweek werd verdeeld over de standplaatsen Wageningen en Bilthoven. De AIO-termijn werd verlengd met één jaar omdat er een extra veldexperiment in Zeeland bij kwam. Eind 1996 kwam de functie van projectleider integraal waterbeheer bij het hoogheemraadschap van Rijnland in beeld. Een mooie combinatie van theorie en praktijk in de echte wereld van het waterbeheer.
Het proefschrift was nog niet af, maar dat zou niet lang duren (...). De sollicitatie was succesvol. In de zomer van 1999 werd de sector Waterbeheer gereorganiseerd. Hij ging de functie van coördinator van het team Landelijk Gebied van de afdeling Integrale Plannen en Projecten bekleden, hetgeen hij tot op heden met veel plezier doet.

ACKNOWLEDGEMENTS

G. A. P. H. van den Eertwegh,

Herenstraat 120,
2313 AN   Leiden.